LITHUANIAN UNIVERSITY OF HEALTH SCIENCES

Daiva Galinytė

C-PHYCOCYANIN ISOLATED FROM CYANOBACTERIAL BIOMASS: DEVELOPMENT OF TOPICAL DELIVERY SYSTEMS AND EVALUATION OF BIOLOGICAL ACTIVITY

Doctoral Dissertation
Medical and Health Sciences,
Pharmacy (M 003)

Kaunas, 2026

Dissertation has been prepared at the Department of Pharmacognosy, Faculty of Pharmacy, Lithuanian University of Health Sciences during the period of 2021–2025.

Scientific Supervisor

Prof. Dr. Nijolė Savickienė (Lithuanian University of Health Sciences, Medical and Health Sciences, Pharmacy – M 003).

Consultant

Prof. Dr. Jurga Bernatonienė (Lithuanian University of Health Sciences, Medical and Health Sciences, Pharmacy – M 003).

The dissertation is defended at the Pharmacy Research Council of the Lithuanian University of Health Sciences:

Chairperson

Prof. Dr. Vacis Tatarūnas (Lithuanian University of Health Sciences, Medical and Health Sciences, Pharmacy – M 003).

Members:

Dr. Kristina Zymonė (Lithuanian University of Health Sciences, Medical and Health Sciences, Pharmacy – M 003);
Prof. Dr. Elvyra Jarienė (Vytautas Magnus University, Agricultural Sciences, Agronomy – A 001);
Prof. Dr. Ramunė Rutkaitė (Kaunas University of Technology, Technological Sciences, Chemical Engineering – T 005);
Dr. Rezarta Shkreli (Aldent University (Albania), Medical and Health Sciences, Pharmacy – M 003).

Dissertation will be defended at the open session of the Pharmacy Research Council of the Lithuanian University of Health Sciences at 11 a.m. on 4th September 2026 at the Museum of the History of Lithuanian Medicine and Pharmacy.
Address: Rotušės 28, LT-44279 Kaunas, Lithuania.

LIETUVOS SVEIKATOS MOKSLŲ UNIVERSITETAS

Daiva Galinytė

IŠ MELSVABAKTERIŲ BIOMASĖS IŠSKIRTAS C-FIKOCIANININAS: VIETINIO POVEIKIO PERNAŠOS SISTEMŲ KŪRIMAS IR BIOLOGINIO AKTYVUMO VERTINIMAS

Daktaro disertacija
Medicinos ir sveikatos mokslai,
farmacija (M 003)

Kaunas, 2026

Disertacija rengta 2021–2025 metais Lietuvos sveikatos mokslų universiteto Farmacijos fakulteto Farmakognozijos katedroje.

Mokslinė vadovė

prof. dr. Nijolė Savickienė (Lietuvos sveikatos mokslų universitetas, medicinos ir sveikatos mokslai, farmacija – M 003).

Konsultantė

prof. dr. Jurga Bernatonienė (Lietuvos sveikatos mokslų universitetas, medicinos ir sveikatos mokslai, farmacija – M 003).

Disertacija ginama Lietuvos sveikatos mokslų universiteto Farmacijos mokslo krypties taryboje:

Pirmininkas

prof. dr. Vacis Tatarūnas (Lietuvos sveikatos mokslų universitetas, medicinos ir sveikatos mokslai, farmacija – M 003).

Nariai:

dr. Kristina Zymonė (Lietuvos sveikatos mokslų universitetas, medicinos ir sveikatos mokslai, farmacija – M 003);
prof. dr. Elvyra Jarienė (Vytauto Didžiojo universitetas, žemės ūkio mokslai, agronomija – A 001);
prof. dr. Ramunė Rutkaitė (Kauno technologijos universitetas, technologijos mokslai, chemijos inžinerija – T 005);
dr. Rezarta Shkreli (Aldento universitetas (Albanija), medicinos ir sveikatos mokslai, farmacija – M 003).

Disertacija bus ginama viešajame Farmacijos mokslo krypties tarybos posėdyje 2026 m. rugsėjo 4 d. 11 val. Lietuvos medicinos ir farmacijos istorijos muziejuje.
Disertacijos gynimo vietos adresas: Rotušės a. 28, LT-44279 Kaunas, Lietuva.

CONTENTS

ACKNOWLEDGEMENTS

First of all, I would like to thank my *Alma Mater*, the Lithuanian University of Health Sciences, where my interest in pharmaceutical science first began. I am grateful for the opportunity to return to the Faculty of Pharmacy more than ten years later and continue my scientific journey. These four years have been filled with learning, discoveries, challenges, disappointments, new experiences, and continuous personal and scientific growth. None of this would have been possible without the people who supported me along the way.

My sincere thanks go to my supervisor, Prof. Dr. Nijolė Savickienė, for guiding me throughout my doctoral studies, for many scientific and personal discussions, for her constant support, encouragement, and belief in me. Thank you for always being an inspiring example, both as a scientist and as a person.

I would like to express my sincere gratitude to my scientific consultant, Prof. Dr. Jurga Bernatonienė, for her advice on pharmaceutical technology, valuable discussions, kind encouragement, and for inspiring me to look for innovative solutions in research.

I am very grateful to Dr. Judita Koreivienė, Dr. Jūratė Karosienė, and Dmitrij Morudov from the Laboratory of Algology and Microorganism Ecology at the Nature Research Centre. Thank you for introducing me to cyanobacteria research, teaching me the methods used for C-PC isolation, warmly welcoming me to your laboratory, sharing your knowledge and experience, providing the biological material for this research, and for our successful collaboration throughout the project.

My sincere thanks also go to Prof. Dr. Rima Naginienė, Dr. Dalia Baranauskienė, and Dr. Jurgita Šulinskienė from the Laboratory of Toxicology, Neuroscience Institute, for their help with heavy metal analysis and for making this part of the research much easier than I had expected.

I would like to thank Prof. Dr. Vitalis Briedis for giving me the opportunity to perform the skin permeation studies, and Dr. Modestas Žilius for introducing me to the experimental methods, coordinating the studies, sharing his experience, and for many useful discussions, advice, and support.

I am also grateful to Prof. Dr. Dainius Haroldas Pauža and Dr. Kristina Rysevaitė-Kyguolienė for introducing me to the fascinating microscopic world through confocal microscopy.

My sincere thanks go to Prof. Dr. Maria Letizia Manca from the University of Cagliari for supervising my research internship and coordinating the work on transfersomal formulations. I would also like to thank her research team, especially Dr. Matteo Aroffu, for generously sharing their knowledge and experience and, of course, for teaching me to enjoy a good espresso.

I would like to thank Prof. Dr. Elvira Escribano Ferrer from the University of Barcelona for performing the cryogenic transmission electron microscopy analysis, which allowed us to visualize the developed transfersomes.

My sincere gratitude goes to Dr. Vilma Zigmantaitė and the whole team of the Biological Research Centre at the Lithuanian University of Health Sciences for their help in planning and carrying out the *in vivo* study, for solving the challenges we faced during the research, and for delicious matcha we enjoyed together after experiments.

I would also like to thank Prof. Dr. Ingrida Balnytė for her valuable help with the immunohistochemical analyses.

My sincere thanks go to Prof. Dr. Nomeda Juodžiukynienė for her professionalism, patience, and for introducing me to the fascinating field of histopathology, as well as for her support in planning and carrying out the *in vivo* study.

I would also like to thank Prof. Dr. Arūnas Savickas for his advice on pharmaceutical technology, and Prof. Dr. Nataliia Hudz, Dr. Rima Jūratė Gerbutavičienė, and Dr. Ieva Kudlinskienė for their helpful comments and advice during manuscript preparation.

I would like to thank everyone at the Department of Pharmacognosy for creating such a friendly and supportive environment. Thank you for always being ready to answer my questions, discuss ideas, and share your experience. It has been a pleasure to be part of the department and to celebrate special occasions and enjoy the many moments we shared along the way.

I am grateful to UAB Eurovaistinė and to all my colleagues at the pharmacy for their understanding and support, which allowed me to successfully combine my work and doctoral studies.

To my friends, thank you for continuing to invite me to meet, for telling me that you missed me, and for always being there. Thank you for your friendship, support, advice, and for every moment we have shared together.

I would also like to thank my godfather, whose quiet wisdom has inspired me since childhood, for his valuable linguistic comments on the Lithuanian summary of this dissertation.

Finally, I would like to thank my family.

To my children, Dorotėja and Jokūbas, thank you for making my world brighter and more colourful.

To my mother, thank you for always reminding me that health is the most important thing.

To my father, thank you for our scientific discussions and for your constant reminders of what needed to be done and when during my doctoral studies.

To my sister, thank you for always improving the quality of my life and for bringing moments of art into my scientific journey.

To my cousin, thank you for always listening to every success and every disappointment I experienced throughout my doctoral journey.

To my dog, Tylia Kadabra, thank you for reminding me to take breaks and for making sure I went for a walk, even during the busiest days.

To my cat, Mica, thank you for your affection, for getting enough sleep for both of us when I could not, and for reminding me, in your own cat-like way, that even the gentlest touch may hide sharp claws.

LIST OF ABBREVIATIONS

Akt (PKB)	–	protein kinase B
C-PC	–	c-phycocyanin
CLSM	–	confocal laser scanning microscopy
COX-2	–	cyclooxygenase-2
Cryo-TEM	–	cryogenic transmission electron microscopy
DMBA	–	7,12-dimethylbenz[a]anthracene
DPPH	–	2,2-diphenyl-1-picrylhydrazyl
EE	–	encapsulation efficiency
ELISA	–	enzyme-linked immunosorbent assay
ERK	–	extracellular signal-regulated kinase
Gly-T	–	glycerol-containing C-PC-loaded transfersomes
Gly-Chol-T	–	glycerol and cholesterol-containing C-PC-loaded transfersomes
HaCaT	–	human keratinocyte cell line
HEC	–	hydroxyethyl cellulose
HEMC	–	hydroxyethyl methylcellulose
HPMC	–	hydroxypropyl methylcellulose
Hyal-T	–	sodium hyaluronate-containing C-PC-loaded transfersomes
Hyal-Chol-T	–	sodium hyaluronate and cholesterol-containing C-PC-loaded transfersomes
Hyal-Gly-T	–	sodium hyaluronate and glycerol-containing C-PC-loaded transfersomes
Hyal-Gly-Chol-T	–	sodium hyaluronate, glycerol, and cholesterol-containing C-PC-loaded transfersomes
ICP-MS	–	inductively coupled plasma mass spectrometry
IL	–	interleukin
MAPK	–	mitogen-activated protein kinase
MD	–	mean particle diameter
mTOR	–	mechanistic target of rapamycin
MTT	–	3-(4,5-dimethylthiazol-2-yl)-2,5-diphenyltetrazolium bromide
NaCMC	–	sodium carboxymethylcellulose
NRC	–	State Scientific Research Institute Nature Research Centre
PBS	–	phosphate-buffered saline
PG	–	propylene glycol
PI	–	polydispersity index

PI3K	–	phosphoinositide 3-kinase
ROS	–	reactive oxygen species
S75	–	lipoid S75 phospholipid
TE	–	trolox equivalents
TEAC	–	trolox equivalent antioxidant capacity
TPA	–	12-O-tetradecanoylphorbol-13-acetate
TNF-α	–	tumour necrosis factor alpha

INTRODUCTION

Cyanobacteria, also referred to as blue-green algae, are among the earliest life forms on Earth, dating back more than 3.5 billion years, and have played a fundamental role in the development of the planet's oxygen-rich atmosphere [1, 2]. Their long-term persistence under continuously changing environmental conditions highlights that survival is not determined solely by strength, but by the ability to adapt. This remarkable adaptability is largely attributed to their capacity to produce a wide range of bioactive molecules, with cytotoxic, antifungal, antibacterial, and antiviral properties, which support defence, competition, and survival [1]. Cyanobacteria are a natural and integral component of aquatic ecosystems; however, increasing levels of CO_2, global warming, and eutrophication have contributed to a rise in the frequency, intensity, duration, and geographic distribution of cyanobacterial blooms [3-5]. This phenomenon poses significant ecological and public health concerns. Cyanobacterial blooms can disrupt ecosystem balance by intensifying competition among aquatic organisms for essential resources, including nutrients, dissolved oxygen, and light [6]. Furthermore, these blooms may pose risks to human health by producing bioactive, potentially toxic compounds [7]. As the global occurrence of cyanobacterial blooms continues to increase, there is a growing need for effective mitigation strategies [3]. Mechanical removal of excessive cyanobacterial biomass has been proposed as an urgent intervention during bloom events [5]. Notably, such biomass can also be considered a valuable resource for the recovery of bioactive compounds, supporting sustainable and circular bioeconomy approaches while minimizing negative environmental impact [8].

Among the bioactive compounds identified in cyanobacteria, c-phycocyanin (C-PC) has attracted particular attention. It is a water-soluble pigment belonging to the phycobiliprotein family, functioning as a key component of the photosynthetic apparatus by capturing light energy and facilitating its transfer [9]. Beyond this role, C-PC exhibits a wide range of biological activities, particularly due to its pronounced antioxidant and anti-inflammatory properties [10, 11]. Its antioxidant activity primarily involves its ability to scavenge reactive oxygen species (ROS) and modulate oxidative stress-related pathways, thereby reducing cellular damage [12, 13]. In addition, C-PC enhances endogenous antioxidant defence systems by increasing the activity of key enzymes such as superoxide dismutase, catalase, and glutathione peroxidase, while reducing lipid peroxidation [14]. Beyond its antioxidant effects, C-PC also exhibits significant anti-inflammatory activity, including the inhibition of cyclooxygenase-2 (COX-2) and the suppression of

proinflammatory cytokines, such as IL-1, IL-6, and TNF-α [9, 15, 16]. Moreover, C-PC has demonstrated protective effects against ultraviolet (UV)-induced skin damage by reducing ROS levels, inhibiting matrix metalloproteinases, and preserving collagen integrity, thereby exhibiting anti-photoaging potential [14, 17]. It has also been shown to promote tissue regeneration and wound healing [10, 16, 18]. Additionally, C-PC modulates key cellular processes, including apoptosis and cellular senescence, through signalling pathways such as PI3K/AKT/mTOR, and influences melanogenesis via p38/MAPK and ERK pathways [19, 20]. Importantly, C-PC exhibits antitumor activity against melanoma by inhibiting cell proliferation and migration and modulating key oncogenic signalling pathways, including MAPK and cell cycle regulators. It may also inhibit angiogenesis and tumour progression, while demonstrating selective activity toward tumour cells [21]. Furthermore, C-PC has been shown to modulate the tumour microenvironment by enhancing immune responses, including increased infiltration of CD4+ and CD8+ T lymphocytes and B cells [22]. Collectively, these findings highlight C-PC as a multifunctional bioactive compound capable of targeting oxidative stress, inflammation, extracellular matrix degradation, cellular senescence, and melanogenesis – key processes involved in skin aging and carcinogenesis. Nevertheless, its potential for preventive application in topical systems targeting early-stage cutaneous squamous cell carcinoma (cSCC) remains insufficiently explored, particularly in *in vivo* studies.

Approximately one-third of all cancers diagnosed worldwide are skin cancers. Despite ongoing prevention efforts, the global incidence of these malignancies has continued to increase, with some forms becoming more aggressive [23]. This increase is largely associated with population aging and improvements in diagnostic and screening methods [24]. Among these malignancies, cSCC is one of the most common malignant skin tumours and develops through a multistep process involving well-defined precancerous and early pathological stages. Disease progression typically occurs from actinic keratosis (AK) and intraepidermal dysplasia to invasive carcinoma, and is accompanied by progressive alterations in epidermal architecture, increased keratinocyte proliferation, and impaired differentiation [24]. The development of cSCC is influenced by multiple risk factors, including cumulative ultraviolet (UV) exposure, advanced age, fair skin, immunosuppression, smoking, and genetic susceptibility [25]. To better understand skin aging as a risk factor, it can be classified into intrinsic (chronological) aging, representing the natural biological progression over time, and extrinsic aging, also known as photoaging, which is primarily induced by environmental stressors, particularly ultraviolet (UV) radiation [26]. UV exposure promotes the generation of ROS, leading to oxidative stress and disruption of the skin's

antioxidant defence system [17]. Skin aging is characterized by a progressive decline in regenerative capacity and structural integrity, resulting in impaired barrier function, delayed wound healing, and dysregulation of water and thermal homeostasis. Moreover, cellular senescence is increasingly recognized as a key contributor to skin aging and associated pathological processes. Senescent cells are characterized by irreversible cell cycle arrest and the development of a senescence-associated secretory phenotype, which includes the release of proinflammatory cytokines, matrix-degrading enzymes, and growth factors [27]. These age- and UV-associated alterations in the skin, together with sustained inflammatory processes, contribute to a microenvironment that may promote tumour development [26]. At the molecular level, early stages of cSCC are driven by genetic and epigenetic alterations, including loss of TP53 function, dysregulation of cell cycle control, and activation of pro-inflammatory signalling pathways. Chronic inflammation and tumour microenvironment remodelling, mediated by factors such as COX-2 and inflammatory cytokines, play a crucial role in tumour initiation and progression [24].

Considering these mechanisms involved in skin aging, UV-induced damage, and tumour development, preventive strategies that target early molecular events such as oxidative stress, inflammation, and extracellular matrix remodelling are of particular importance. In this context, C-PC may be considered a promising compound with the potential to prevent early-stage cSCC [28].

However, when developing topical technological formulations containing C-PC, it is essential to ensure its adequate purity, stability, and skin permeability. The purity of C-PC is evaluated using the spectrophotometrically determined absorbance ratio (A_{620}/A_{280}) and is directly related to its biological effectiveness and application potential [29]. Furthermore, when C-PC is isolated from naturally occurring cyanobacterial biomass, it is important to assess potential contamination with cyanotoxins and heavy metals, as this may pose safety concerns and limit its application potential.

Another major challenge in formulation development is the stability of C-PC. Specifically, C-PC derived from mesophilic cyanobacteria is generally thermally unstable and may denature at elevated temperatures (above 40 °C). In addition, its stability is strongly influenced by pH, with optimal stability at near-neutral pH and reduced stability in acidic or alkaline environments [12]. More broadly, C-PC is highly sensitive to environmental stressors such as light and pressure, and its stability may also be affected by interactions with other formulation components [16, 30]. Therefore, all these factors must be carefully considered during the development of technological formulations

containing C-PC, as they may compromise its structural integrity and biological activity.

Another important aspect in the development of topical formulations is skin permeability. The stratum corneum, the outermost layer of the skin, consists of 10–15 layers of dead, keratin-rich cells (keratinocytes) and represents the primary barrier to the penetration of topically and transdermally applied compounds [31]. Successful passive permeation through the stratum corneum requires that compounds possess specific physicochemical properties, including a relatively low molecular weight, moderate lipophilicity, and balanced solubility in both aqueous and lipid environments [26]. In contrast, C-PC is a hydrophilic macromolecule with a relatively high molecular weight. Its α- and β-polypeptide chains have molecular masses of approximately 10–19 kDa and 14–21 kDa, respectively, and each subunit is covalently linked to phycocyanobilin chromophores responsible for its characteristic colour and light-absorbing properties [11, 32]. These subunits can assemble into higher-order structures, forming trimers $(\alpha\beta)_3$ (~120 kDa) and hexamers $(\alpha\beta)_6$ (~240 kDa), which further limit their ability to penetrate the skin barrier [11]. Therefore, improving the skin permeability of C-PC remains a major challenge and an important focus in the development of effective topical delivery systems.

To overcome the barrier properties of the stratum corneum, various strategies have been developed to enhance skin permeability. These approaches can be broadly classified into chemical and physical methods. Chemical penetration enhancers, such as glycols, ethanol, terpenes, and azone derivatives, are widely used to increase drug permeation by disrupting the lipid organization of the stratum corneum and enhancing diffusional pathways. However, their use may be associated with skin irritation and potential long-term damage [16, 33]. Among chemical approaches, penetration enhancers such as propylene glycol (PG) are commonly used in topical formulations to improve drug permeation by altering the diffusional pathways within the skin. However, despite its widespread use, limited information remains on its effectiveness in enhancing the skin penetration of C-PC. Physical techniques, including iontophoresis, sonophoresis, electroporation, microneedles, and thermal or mechanical ablation, have also been explored to improve transdermal delivery. Although effective, these methods are often associated with discomfort, high cost, and reduced patient compliance, limiting their routine application in topical therapy [31, 33]. In contrast, nanotechnology-based delivery systems have emerged as a promising alternative for enhancing dermal drug delivery. Nanocarriers can improve drug penetration, protect bioactive compounds from degradation, and partially overcome the barrier function of the stratum corneum [31, 34]. Previous studies have demonstrated

that nanodispersion systems can enhance the skin delivery of protein-based compounds, including C-PC, by improving their penetration through the stratum corneum [14]. Various phospholipid-based vesicular systems, including liposomes, ethosomes, and penetration enhancer-containing vesicles, have been investigated for the delivery of bioactive compounds, including C-PC [35–37]. Among these, transfersomes represent a particularly promising approach. Transfersomes are highly deformable phospholipid vesicles containing edge activators that enhance membrane flexibility, allowing them to penetrate through the intercellular lipid pathways of the stratum corneum [38]. Previous studies have demonstrated successful delivery of protein-based therapeutics using transfersomes, resulting in improved skin deposition and biological activity [40, 41]. Moreover, these systems have been shown to improve drug stability, enhance solubility, promote skin partitioning, and facilitate the delivery of hydrophilic biomolecules, including proteins and peptides [33, 41]. In this context, the present study aimed to develop and evaluate C-PC-containing technological formulations to improve C-PC's stability and skin permeability, and to assess their potential protective effects on early-stage skin carcinogenesis.

The dissertation aimed to isolate and characterize C-PC from naturally derived cyanobacterial biomass, to develop and evaluate advanced technological formulations for improving its stability and skin permeability, and to investigate the effects of C-PC on inflammatory, proliferative, and dysplastic changes in the skin during the early stages of skin carcinogenesis.

Objectives of the dissertation

1. To isolate C-PC samples from naturally occurring cyanobacterial biomass and determine the purity of C-PC samples and quantify heavy metal content.
2. To develop technological formulations containing C-PC samples and evaluate their physicochemical properties and the stability of C-PC within these systems.
3. To investigate the skin permeation of C-PC from the developed formulations under *ex vivo* conditions.
4. To investigate the effects of C-PC on inflammatory, proliferative, and dysplastic changes in the skin during the early-stages of skin carcinogenesis in a DMBA/TPA-induced mouse model.

SCIENTIFIC NOVELTY

This dissertation presents a comprehensive, integrative approach that combines extraction, safety evaluation, and the development of topical delivery systems of C-PC samples derived from naturally occurring cyanobacterial biomass, with a focus on their potential application in targeting the early-stages of skin carcinogenesis.

To the best of our knowledge, this study provides the first investigation of heavy metal content in C-PC samples isolated from cyanobacterial biomass collected in the Kaunas Lagoon (Lithuania), contributing to the assessment of its safety for potential biomedical applications.

A two-step preparation method was adapted to develop C-PC-loaded enriched transfersomal formulations, enabling its efficient incorporation and preservation of C-PC structural integrity despite environmental sensitivities. The stability of C-PC in the developed formulations was evaluated using spectrophotometric methods and antioxidant activity assays, confirming its structural stability and biological activity. Notably, glycerol-containing transfersomes demonstrated high encapsulation efficiency of C-PC and improved storage stability.

In addition, the developed transfersomal systems enhanced the deposition of C-PC in the outer layers of the skin, addressing the limitations associated with the topical delivery of hydrophilic macromolecules.

Importantly, this study is among the first to evaluate the protective effects of C-PC-loaded transfersomes in an *in vivo* model of early-stage skin carcinogenesis. The results demonstrate C-PC-loaded transfersomes attenuate early proinflammatory epidermal remodelling and modulate tumour-promoting processes, including inflammation, proliferation, and dysplastic changes.

Collectively, this study provides new insights into the stabilization and topical skin delivery of C-PC, highlighting the potential of C-PC-loaded transfersomal formulations to target early tumour-promoting processes.

PRACTICAL VALUE

The practical value of this dissertation lies in the development of sustainable strategies for the utilization of naturally occurring cyanobacterial biomass, addressing both environmental and biomedical challenges. The collection of excessive cyanobacterial biomass from water bodies helps mitigate ecological problems associated with harmful algal blooms while enabling the production of high-value bioactive compounds. In this context, the study demonstrates a circular, integrative approach in which solutions to environmental challenges are applied to the extraction of bioactive compounds and the development of products with potential health benefits.

The research confirms that C-PC samples can be successfully isolated from naturally collected cyanobacterial biomass and, through appropriate purification strategies, obtained in a form suitable for pharmaceutical applications. Particular emphasis was placed on a preliminary safety assessment based on the determination of selected heavy metals (Pb, Cd, As, and Hg) and cyanotoxins, which is essential when working with biomass collected from environmental water sources.

From a technological perspective, the study provides practical solutions for formulating C-PC samples for topical delivery systems. Hydrogels containing C-PC were developed with a focus on maintaining the stability of the active compound, and selected formulations demonstrated suitability for further investigation in wound healing applications.

Furthermore, advanced phospholipid-based nanocarriers (transfersomes) were developed to maintain the structural stability of C-PC and improve its skin delivery. These systems enhanced the deposition of C-PC in the outer skin layers, thereby addressing one of the major limitations associated with the skin delivery of hydrophilic macromolecules.

Importantly, *in vivo* findings demonstrated that C-PC-loaded transfersomal formulations preserved skin barrier integrity and attenuated DMBA/TPA-induced inflammatory, proliferative, and dysplastic skin changes observed during the early stages of skin carcinogenesis. These results highlight the potential of the developed systems as candidates for preventive dermatological applications.

Overall, this work demonstrates a sustainable, interdisciplinary approach that integrates environmental management, natural compound extraction, and pharmaceutical technology to create innovative solutions with both ecological and biomedical relevance.

THE LAYOUT OF THE DISSERTATION

This dissertation is based on five scientific articles and comprises a series of experimental studies, including the isolation and characterization of C-PC, the development of topical formulations, and the evaluation of its biological activity. The overall experimental workflow is presented in Fig. 1.

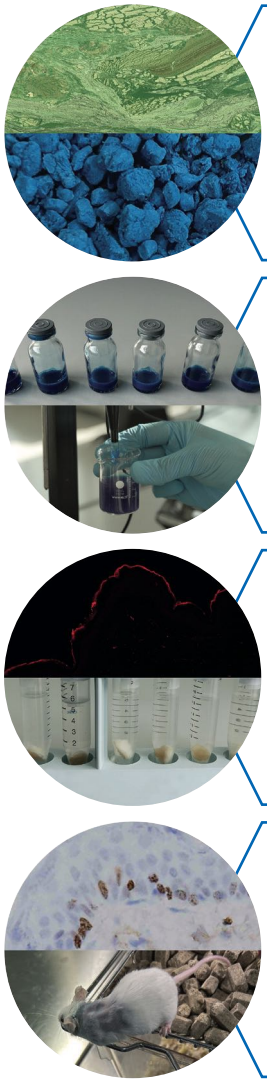

Isolation and characterization of C-PC
- Collection of cyanobacterial biomass from natural sources (*Papers 2–4*)
- Extraction and purification of C-PC (*Papers 2–4*)
- Determination of C-PC purity (*Papers 2–4*)
- Determination of heavy metal content in C-PC samples (*Papers 2*)

Development of technological formulations with C-PC
- Hydrogel systems: preparation, physicochemical and microbiological evaluation, *in vitro* release, and C-PC stability assessment (*Paper 3*)
- Transfersomal systems: preparation, physicochemical characterization, encapsulation efficiency, stability (*Paper 4*)

Evaluation of C-PC skin localization
- Qualitative *ex vivo* assessment of C-PC localization in the skin from solutions, hydrogels, and transfersomal formulations
- Human skin diffusion cell model
- Confocal laser scanning microscopy-based visualization of C-PC distribution within skin layers (*Papers 3* and *4*)

Evaluation of biological activity
- *In vitro* studies: antioxidant activity assessment, cell viability evaluation, and protective effects against oxidative stress (*Paper 4*)
- *In vivo* studies: evaluation of inflammatory, proliferative, and dysplastic skin changes during the early stages of DMBA/TPA-induced skin carcinogenesis; histological and immunohistochemical analyses (*Paper 5*)

Fig. 1. *Schematic overview of the dissertation workflow*

PhD CANDIDATE'S CONTRIBUTION

The doctoral candidate, Daiva Galinytė, performed the majority of the experimental work and made a substantial contribution to the research presented in Papers 1–5. She was primarily responsible for drafting the original versions of all manuscripts. Her individual contributions to each publication included the following activities:

Paper 1: Conceptualization of the review topic; systematic literature review and analysis; data curation and synthesis of published findings; preparation of the original manuscript draft; revision of the manuscript; and visualization of summarized data.

Paper 2: Participation in the conceptualization of the study; experimental work related to C-PC isolation and purification; determination of C-PC purity; preparation of samples for heavy metal analysis; data analysis and curation; preparation of the original manuscript draft; and visualization of the results.

Paper 3: Participation in the conceptualization and development of the experimental design; methodology development; preparation and optimization of C-PC hydrogel formulations; performance *in vitro* release experiments; participation in *ex vivo* skin permeation experiments; analysis and evaluation of confocal microscopy images; data analysis and curation; preparation of the original manuscript draft; and visualization of the results.

Paper 4: Participation in the conceptualization of the study and methodology development; preparation and physicochemical characterization of C-PC-loaded transfersomes, participation in *ex vivo* skin permeation experiments; analysis and evaluation of confocal microscopy images; analysis and interpretation of experimental data; preparation of the original manuscript draft; visualization of the results.

Paper 5: Participation in the study conceptualization and methodology development; conduct of in *in vivo* experiments; analysis and evaluation of immunohistochemical images; analysis and interpretation of experimental data; preparation of the original manuscript draft; visualization of the results.

CO-AUTHORS' CONTRIBUTION

Prof. Dr. Nijolė Savickienė supervised the doctoral research and coordinated the investigations presented in *Papers 1–5*, contributed to the conceptualization of all studies, methodological development and validation, provided scientific guidance throughout the research process, and reviewed and edited all manuscripts.

Prof. Dr. Jurga Bernatonienė contributed to the conceptualization and methodological development of the hydrogel studies presented in *Paper 3*, provided resources required for the experiments, and reviewed and edited *Papers 3* and *5*.

Dr. Jūratė Karosienė contributed to the implementation of the methodology for cyanobacterial biomass processing and C-PC extraction and purification. She introduced the doctoral candidate to the experimental procedures, coordinated the C-PC isolation process, provided the necessary resources for these experiments, and reviewed and edited *Papers 1–5*.

Dr. Judita Koreivienė provided the resources necessary for the experiments described in *Paper 4*.

Dmitrij Morudov contributed to the methodology related to C-PC isolation and purification and reviewed and edited *Paper 1*.

Prof. Dr. Rima Naginienė contributed to the methodology and resources related to heavy metal analysis and reviewed and edited *Paper 2*.

Dr. Dalia Baranauskienė conducted the investigation of heavy metals using inductively coupled plasma mass spectrometry (ICP-MS) described in *Paper 2*.

Dr. Jurgita Šulinskienė contributed to the methodological development and provided resources for the analytical experiment described in *Paper 2*.

Dr. Modestas Žilius contributed to the development and validation of the methodology used for *in vitro* release and *ex vivo* skin permeation experiments; supervised and performed the skin permeation experiments described in *Paper 3–4*.

Prof. Dr. Vitalis Briedis contributed to the development of the methodology and provided resources for the skin permeation studies described in *Papers 3–4*.

Prof. Dr. Dainius Haroldas Pauža contributed to the methodology related to confocal laser scanning microscopy used for skin permeation studies, providing resources for *Papers 3–4*.

Dr. Kristina Rysevaitė-Kyguolienė contributed to the methodological aspects of confocal microscopy analysis in the skin permeation studies described in *Papers 3–4*.

Dr. Matteo Aroffu contributed to the development of the methodology for transfersome preparation and characterization and, performed antioxidant activity and *in vitro* cytocompatibility experiment, and contributed to writing-reviewing and editing of *Paper 4*.

Prof. Dr. Maria Manconi contributed to the scientific discussion and reviewed and edited *Paper 4*.

Doc. Dr. Elvira Escribano Ferrer provided the methodology and performed cryogenic transmission electron microscopy (cryo-TEM) analysis of vesicle morphology described in *Paper 4*.

Prof. Dr. Maria Letizia Manca supervised the research internship at the University of Cagliari and coordinated the experimental work related to the preparation and characterization of transfersomal formulations; contributed to the development and optimization of the experimental methodology, provided resources for the experiments, and reviewed and edited *Paper 4*.

Prof. Dr. Nomeda Juodžiukynienė contributed to the conceptualization and methodological development of the *in vivo* study, performed histopathological evaluation, provided resources, and reviewed and edited *Papers 1* and *5*.

Dr. Gabrielė Balčiūnaitė-Murzienė contributed to the visualization of Paper 1 and reviewed and edited *Papers 1* and *2*.

Dr. Vilma Zigmantaitė contributed to the methodological aspects of the *in vivo* experiment, provided resources, and reviewed and edited *Paper 5*.

Prof. Dr. Ingrida Balnytė contributed to the methodology and investigation of immunohistochemistry experiments and reviewed and edited *Paper 5*.

Prof. Dr. Nataliia Hudz reviewed and edited *Paper 1*.

Prof. Dr. Arūnas Savickas contributed to the methodological development of the studies presented in *Papers 2–4*.

Dr. Ieva Kudlinskienė contributed to the methodology applied in *Paper 2*.

Dr. Rima Jūratė Gerbutavičienė reviewed and edited *Paper 1*.

LIST OF SCIENTIFIC PAPERS

Paper 1: **Dranseikienė, Daiva**; Balčiūnaitė-Murzienė, Gabrielė; Karosienė, Jūratė; Morudov, Dmitrij; Juodžiukynienė, Nomeda; Hudz, Nataliia; Gerbutavičienė, Rima Jūratė; Savickienė, Nijolė. Cyano-Phycocyanin: Mechanisms of Action on Human Skin and Future Perspectives in Medicine. // *Plants*. Basel: MDPI. ISSN 2223-7747, 2022, vol. 11, no 9, p. 1–18. doi:10.3390/plants11091249. [Impact factor: 4.5, quartile: Q1 (2022. InCites JCR SCIE)]

Paper 2: **Galinytė, Daiva**; Balčiūnaitė-Murzienė, Gabrielė; Karosienė, Jūratė; Morudov, Dmitrij; Naginienė, Rima; Baranauskienė, Dalė; Šulinskienė, Jurgita; Kudlinskienė, Ieva; Savickas, Arūnas; Savickienė, Nijolė. Determination of Heavy Metal Content: Arsenic, Cadmium, Mercury, and Lead in Cyano-Phycocyanin Isolated from the Cyanobacterial Biomass. // *Plants*. Basel: MDPI. ISSN 2223-7747, 2023, vol. 12, no 17, p. 1–16. doi:10.3390/plants12173150. [Impact factor: 4.0, quartile: Q1 (2023. InCites JCR SCIE)]

Paper 3: **Galinytė, Daiva**; Bernatonienė, Jurga; Žilius, Modestas; Rysevaitė-Kyguolienė, Kristina; Savickas, Arūnas; Karosienė, Jūratė; Briedis, Vitalis; Pauža, Dainius Haroldas; Savickienė, Nijolė. *In Vitro* Study of Cyano-Phycocyanin Release from Hydrogels and *Ex Vivo* Study of Skin Penetration. // *Pharmaceuticals*. Basel: MDPI. ISSN 1424-8247, 2024, vol. 17, no 9, p. 1–18. doi:10.3390/ph17091224. [Impact factor: 4.3, quartile: Q1 (2024. InCites JCR SCIE)]

Paper 4: **Galinytė, Daiva**; Aroffu, Matteo; Manconi, Maria; Žilius, Modestas; Rysevaitė-Kyguolienė, Kristina; Karosienė, Jūratė; Koreivienė, Judita; Briedis, Vitalis; Pauža, Dainius Haroldas; Savickas, Arūnas; Escribano Ferrer, Elvira; Manca, Maria Letizia; Savickienė, Nijolė. Cyano-phycocyanin Loaded Enriched Transfersomes for Enhanced Topical Skin Delivery and Antioxidant Protection. // International Journal of Pharmaceutics. Amsterdam: Elsevier. ISSN 0378-5173, 2025, vol. 683, article 126079, p. 1–16. doi: 10.1016/j.ijpharm.2025.126079. [Impact factor: 5.2, quartile: likely Q1]

Paper 5: **Galinytė, Daiva**; Juodžiukynienė, Nomeda; Balnytė, Ingrida; Zigmantaitė, Vilma; Karosienė, Jūratė; Bernatonienė, Jurga; Savickienė, Nijolė. Topical C-Phycocyanin-Loaded Transfersomes Attenuate Early Proinflammatory Epidermal Remodelling in a DMBA/TPA – Induced Mouse Model of Skin Dysplasia. // *Pharmaceutics.* Basel: MDPI. ISSN 1999-4923, 2026, vol. 18, no. 5, article 600. doi: 10.3390/pharmaceutics18050600. [Impact factor: 5.5, quartile: Q1]

CONFERENCE PRESENTATIONS

Conf. 1: **Dranseikienė, Daiva**; Balčiūnaite-Murzienė, Gabrielė; Karosienė, Jūratė; Morudov, Dmitrij; Juodžiukynienė, Nomeda; Hudz, Nataliia; Savickienė, Nijolė. Effects of Cyano-Phycocyanin on Skin and Future Perspectives in Medicine. International e-conference. The Joint International Scientific-Practical Conference "Contemporary Pharmacy: Issues, Challenges and Expectations 2022", May 6, 2022, Kaunas, Lithuania.

Conf. 2: **Galinytė, Daiva**; Balčiūnaitė-Murzienė, Gabrielė; Karosienė, Jūratė; Morudov, Dmitrij; Juodžiukynienė, Nomeda; Hudz, Nataliia, Raudonė, Lina; Savickienė, Nijolė. Antioxidant Activity of Cyano-Phycocyanin Isolated from Cyanobacterial Biomass Collected in Kaunas Lagoon. The 12th International Pharmacy Conference „Contemporary Pharmacy: Issues, Challenges and Expectations 2022". October 21, 2022, Kaunas, Lithuania.

Conf. 3: **Galinytė, Daiva**; Karosienė, Jūratė; Naginienė, Rima; Baranauskienė, Dalė; Šulinskienė, Jurgita; Hudz, Nataliia; Savickienė, Nijolė. Determination of Heavy Metals Concentrations in C-Phycocyanin. The Fourth Scientific and Practical Conference with International Participation „Planta+. Science, Practice and Education ", February 20, 2023, Kyiv, Ukraine.

Conf. 4: **Galinytė, Daiva**; Karosienė, Jūratė; Naginienė, Rima; Baranauskienė, Dalė; Šulinskienė, Jurgita; Hudz, Nataliia, Savickienė, Nijolė. The Content of Heavy Metals in C-Phycocyanin Isolated from the Biomass of Cyanobacteria with Dominant Genus *Aphanizomenon* and from the Biomass of Cyanobacteria with the Dominant Genus *Microcystis*. International conference „Health For All/ Rare diseases 2023", April 19, 2023, Kaunas, Lithuania.

Conf. 5: **Galinytė, Daiva**; Karosienė, Jūratė; Bernatonienė, Jurga; Hudz, Nataliia; Savickienė, Nijolė. The Stability of C-Phycocyanin in Various Gel Formulations. 1st International Conference „Plant Research: from Phytochemistry to Phytoactivity", April 21, 2023, Kaunas, Lithuania.

Conf. 6: **Galinytė, Daiva**; Bernatonienė, Jurga; Žilius, Modestas; Rysevaitė-Kyguolienė, Kristina; Karosienė, Jūratė; Savickienė, Nijolė. *In Vitro* Study of Cyano-Phycocyanin Release from Semi-solid Forms and *Ex Vivo* Study of Skin Penetration. International Conference „Contemporary Pharmacy: Issues, Challenges and Expectations 2024“, March 22, 2024, Kaunas, Lithuania.

Conf. 7: **Galinytė, Daiva**; Manca, Maria Letizia; Aroffu, Matteo; Karosienė, Jūratė; Savickienė, Nijolė. Evaluation of Physicochemical Properties, and Stability on Storage of Cyano-Phycocyanin Loaded in Transferosomes. International Conference „Contemporary Pharmacy: Issues, Challenges and Expectations 2025“, April 10, 2025, Kaunas, Lithuania.

Conf. 8: **Galinytė, Daiva**; Aroffu, Matteo; Žilius, Modestas; Rysevaitė-Kyguolienė, Kristina; Karosienė, Jūratė; Briedis, Vitalis; Pauža, Dainius Haroldas; Escribano Ferrer, Elvira; Manca, Maria Letizia; Savickienė, Nijolė. Cyano-phycocyanin loaded glycerotransfersomes: physicochemical evaluation and topical skin delivery. International Conference “Phytochemicals as Drugs, Foods and Biocommunicators“, October 22–24, 2025, Funchal, Madeira, Portugal.

Conf. 9: **Galinytė, Daiva**; Juodžiukynienė, Nomeda; Balnytė, Ingrida; Zigmantaitė, Vilma; Karosienė, Jūratė, Bernatonienė, Jurga; Savickienė, Nijolė. Impact of C-Phycocyanin-Loaded Transfersomes on Early Epidermal Proliferation in a Murine Skin Carcinogenesis Model. International Conference „Contemporary Pharmacy: Issues, Challenges and Expectations 2026“, March 27, 2026, Kaunas, Lithuania.

1. SUMMARY OF MATERIALS AND METHODS

1.1. Isolation and characterization of c-phycocyanin

1.1.1. Collection of cyanobacterial biomass

Cyanobacterial biomass was collected from the Kaunas Lagoon (Kaunas, Lithuania) and the Simnas fishpond (Simnas, Lithuania) during natural cyanobacterial blooms in August–October of 2019–2023.

In 2019–2022, biomass was collected using a plankton net, whereas in 2023 large-scale harvesting was performed using a cyanobacteria collection prototype developed for ecological biomass recovery during bloom events. The collected biomass was immediately frozen and stored at −20 °C until further processing.

Surface water samples were collected using a Ruttner water sampler for phytoplankton composition analysis. The dominant cyanobacterial species were identified microscopically.

Detailed procedures of biomass collection and taxonomic identification are described in Papers 2–4.

1.1.2. Determination of cyanotoxins

Cyanobacterial biomass was analysed for the presence of the most common cyanotoxins (microcystins, saxitoxins and anatoxins) using commercial enzyme-linked immunosorbent assay (ELISA) kits (Microcystin-N Plate Kit, Bracon Analytic Systems, Saco, ME, USA; Anatoxin-a ELISA Kit and Saxitoxin ELISA Kit, Eurofins Abraxis, Warminster, PA, USA), following the manufacturers' protocols.

1.1.3. C-phycocyanin extraction and purification

Extraction and purification of C-PC were performed according to the method described by Khazi et al. with minor modifications [42]. Cyanobacterial cells were disrupted using a freeze-thaw cycle (freezing at −20 °C and thawing at 20 ± 2 °C), followed by centrifugation (8,000 × g, 10 min). Protein precipitation was carried out overnight at 4 °C using a 50% saturated ammonium sulphate solution. The precipitated fraction was collected by centrifugation (10,000 × g, 10 min), resuspended in 10 mM sodium phosphate buffer (pH 7.0), and desalted using diafiltration with a 10 kDa membrane.

During purification optimization, both gel filtration chromatography (Sephadex G-25) and ion-exchange chromatography (Q-Sepharose XL) were evaluated. Ion-exchange chromatography was selected for further studies as

it yielded higher C-PC purity, which was required for formulation development and *in vivo* experiments.

Purified C-PC was freeze-dried and stored at −20 °C until further use.

Detailed extraction and purification procedures are described in Papers 2–4.

1.1.4. Determination of c-phycocyanin purity

The purity of C-PC was determined spectrophotometrically according to the method described by Bennett and Bogorad [43]. The purity index was calculated as the ratio of absorbance at 620 nm to 280 nm (A_{620}/A_{280}), which reflects the relative content of C-PC compared with total proteins.

The calculation formula is provided in Papers 2–4.

1.1.5. Determination of heavy metals in c-phycocyanin samples

The concentrations of selected heavy metals (Pb, Cd, As and Hg) were determined in four lyophilized C-PC samples obtained from different cyanobacterial sources. Three samples were isolated from cyanobacterial biomass collected in the Kaunas Lagoon (Kaunas, Lithuania) in 2019, 2020, and 2022. A commercially available C-PC sample isolated from cultivated *Limnospira platensis* (formerly *Arthrospira platensis* (Spirulina)) (Sigma-Aldrich) was used as a reference. Heavy metal concentrations were determined by inductively coupled plasma mass spectrometry (ICP-MS) after microwave-assisted acid digestion of the samples. The results were expressed as μg/g of C-PC on a dry weight.

Detailed analytical procedures are presented in Paper 2.

1.2. Formulation development

1.2.1. Hydrogel systems

1.2.1.1. Preparation of hydrogels and pH determination

Hydrogels containing 1% (w/w) C-PC were prepared using various gelling agents, including chitosan, sodium alginate, Soligel™, hydroxyethyl cellulose (HEC), sodium carboxymethyl cellulose (NaCMC), hydroxypropyl methylcellulose (HPMC), hydroxyethyl methylcellulose (HEMC), Carbopol® Ultrez 21, Pemulen™, and poloxamer 407.

Lyophilized C-PC powder was dissolved in purified water, after which the selected gelling agent was added under continuous stirring using a magnetic stirrer with a heated surface. The mixtures were stored at 4 °C until complete swelling occurred. In selected formulations, additional excipients

such as glycerol, propylene glycol (PG), and preservatives (SharoSENSE™ Plus 184, SharoSENSE™ 785, and Sharomix™ 721) were incorporated. Prepared hydrogels were stored at 4 °C prior to further investigations.

The pH of the prepared C-PC hydrogels was determined using a calibrated pH meter.

A detailed hydrogel preparation procedures are provided in Paper 3.

1.2.1.2. Determination of c-phycocyanin content in hydrogels

The content of C-PC in the hydrogel formulations was determined spectrophotometrically. A calibration curve was constructed using C-PC solutions in phosphate-buffered saline (PBS) within the concentration range of 0.1–0.6 mg/mL. Absorbance measurements were performed at 620 nm.

Hydrogel samples were dispersed in PBS and centrifuged to break the gel matrix and obtain a clear supernatant for analysis. The measured C-PC concentration was compared with the amount initially incorporated into the formulation.

Detailed procedures are described in Paper 3.

1.2.1.3. Microbiological analysis

Microbiological quality of C-PC hydrogels was evaluated at the National Public Health Care Laboratory (Kaunas, Lithuania). The presence of *Candida albicans*, *Escherichia coli*, *Pseudomonas aeruginosa*, *Staphylococcus aureus*, and the total count of aerobic mesophilic bacteria were determined according to international standards recommended by the Scientific Committee on Consumer Safety.

Detailed procedures are provided in Paper 3.

1.2.1.4. *In vitro* release study

In vitro release of C-PC from hydrogels was evaluated using modified Franz-type diffusion cells. Hydrogel samples were applied to the donor compartment, separated from the receptor phase by a polyvinylidene difluoride dialysis membrane. Phosphate-buffered saline was used as the receptor medium and maintained at 32 ± 0.1 °C under continuous stirring. Samples of the receptor medium were collected at predefined time intervals and analysed spectrophotometrically. C-PC flux was expressed as the amount of released compound per unit area of time.

Detailed experimental procedures and conditions are described in Paper 3.

1.2.2. Transfersomal systems

1.2.2.1. Preparation of c-phycocyanin loaded transfersomes

For transfersome preparation of C-PC was isolated from non-toxic cyanobacterial biomass dominated by *Aphanizomenon flos-aquae*.

C-PC-loaded transfersomes were prepared using a two-step method. In the first step, phospholipids and surfactants were hydrated with aqueous media containing glycerol, sodium hyaluronate, or their combination to obtain different enriched transfersome formulations. The dispersions were subjected to probe sonication to form vesicles. In the second step, C-PC was added to the preformed vesicles and further processed using ultrasonic treatment to facilitate encapsulation.

Detailed compositions and preparation procedures are described in Paper 4.

1.2.2.2. Transfersome characterization

The physicochemical properties of transfersomes were evaluated by measuring mean particle size (MD), polydispersity index (PI), and zeta potential (ZP) using dynamic light scattering. Measurements were performed at 25 °C using a Zetasizer Ultra.

Vesicle morphology and formation were further investigated using cryogenic transmission electron microscopy (cryo-TEM).

Detailed characterization procedures are described in Paper 4.

1.2.2.3. Encapsulation efficiency

Encapsulation efficiency (EE) of C-PC in transfersomes was determined using the dialysis method. After removal of non-encapsulated C-PC, vesicles were disrupted, and C-PC concentration was determined spectrophotometrically. EE was expressed as a percentage of C-PC retained within the vesicles.

Detailed procedures are described in Paper 4.

1.2.2.4. Stability studies

Physical stability of transfersomes was evaluated by monitoring changes in MD, PI, and ZP during storage for 8 months at 4 °C under light-protected conditions.

A detailed stability evaluation procedure is provided in Paper 4.

1.2.2.5. Determination of antioxidant activity

Antioxidant activity of C-PC and C-PC-loaded transfersomes was evaluated using the DPPH radical scavenging assay. The decrease in DPPH absorbance in the presence of the sample was measured spectrophotometrically. Results were expressed as antioxidant activity and as Trolox equivalent antioxidant capacity.

Detailed experimental procedures are described in Paper 4.

1.2.2.6. *In vitro* cytocompatibility and protective effect

Cytocompatibility and protective effects against oxidative stress were evaluated using human keratinocyte (HaCaT) cells. Cell viability was determined using the MTT assay after treatment with C-PC in solution or incorporated into transfersomes. The protective effect against oxidative damage was evaluated using hydrogen peroxide-induced oxidative stress.

Detailed experimental procedures are provided in Paper 4.

1.3. *Ex vivo* skin permeation study

Ex vivo skin permeation of C-PC formulations was evaluated using Bronaugh-type flow-through diffusion cells and human abdominal skin samples obtained after cosmetic surgery. The use of human skin for transdermal permeation studies was approved by the Kaunas Region Bioethical Committee (approval code BE-2-42, 22 Feb 2023). Skin samples were mounted in diffusion cells and exposed to the tested formulations. After the permeation experiment, the skin samples were processed for cryosectioning and analysed using confocal laser scanning microscopy to determine C-PC localization within skin layers.

Detailed experimental procedures are described in Paper 3 and 4.

1.4. *In vivo* evaluation of c-phycocyanin-loaded transfersomes in DMBA/ TPA induced mouse model of skin dysplasia

1.4.1. Experimental design

The *in vivo* study aimed to evaluate the effect of topical C-PC-loaded transfersomes on early tumour-promoting processes in the DMBA/TPA-induced mouse skin carcinogenesis model [44].

The experiment was approved by the State Food and Veterinary Service of the Republic of Lithuania (approval No. G2-236) and conducted at the Biological Research Centre of the Lithuanian University of Health Sciences.

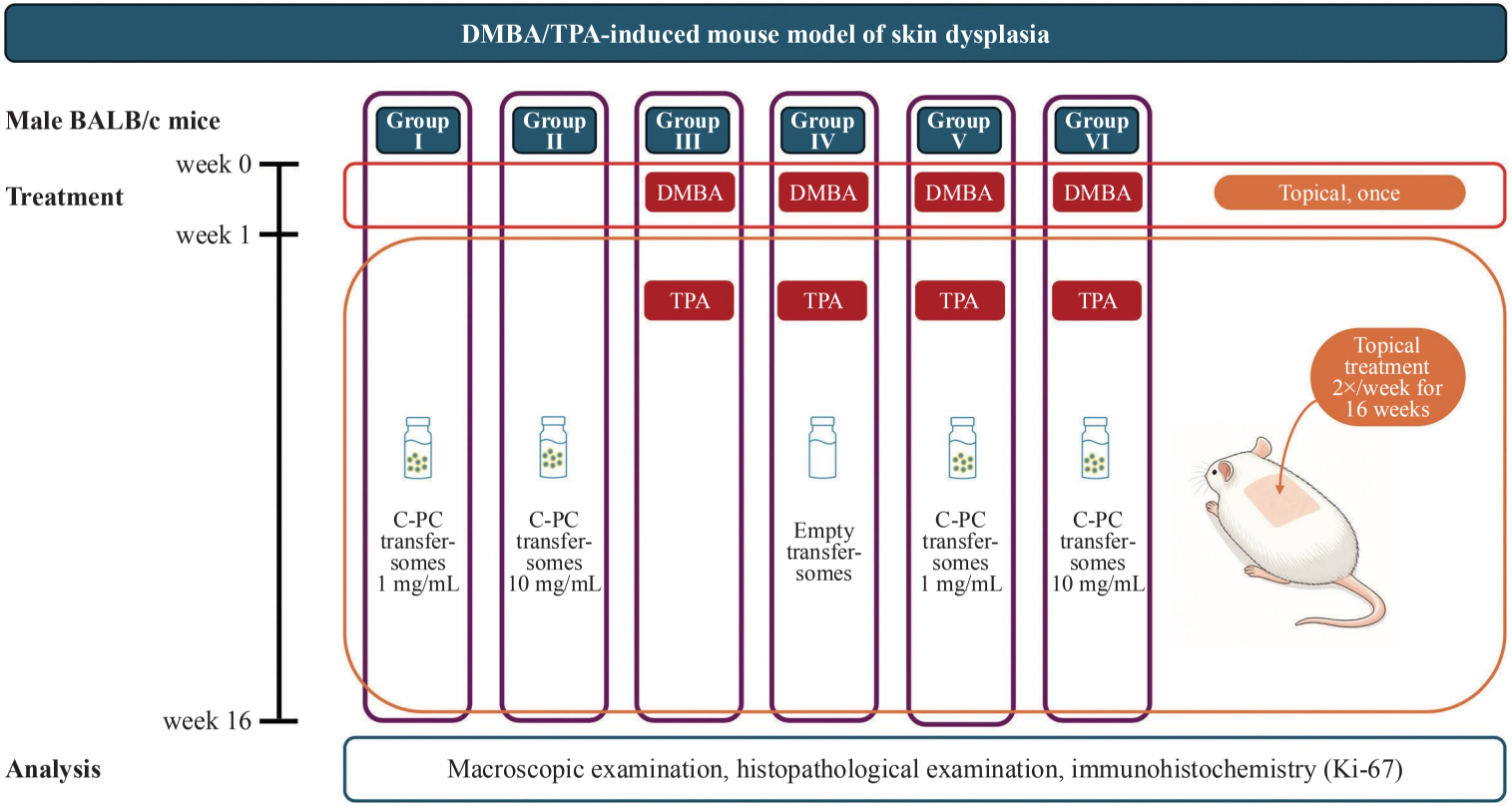

Fig. 2. *Graphical visualization of the in vivo study design*

Male BALB/c mice aged 8–12 weeks were randomly divided into six experimental groups. Treatments were applied topically to the dorsal skin area, and the experimental period lasted 16 weeks. Graphical visualization of the study design is presented in Fig. 2.

Detailed descriptions of the animal groups and experimental procedures are provided in Paper 5.

1.4.2. Histological sample preparation

Skin and internal organs were collected, fixed in neutral buffered formalin, embedded in paraffin, sectioned, and stained with hematoxylin and eosin for histopathological analysis.

Detailed procedures are described in Paper 5.

1.4.3. Histopathological examination

Histological sections were examined using light microscopy, and image analysis was performed to evaluate epidermal and dermal histomorphological parameters. The assessed epidermal parameters included epidermal thickness, rete ridge depth, hyperplasia, dysplastic alterations, mitotic activity, and spongiosis. Dermal alterations were evaluated by assessing inflammatory infiltrate, circulatory changes, and mast cell density.

Semi-quantitative alterations were graded using a four-point scale, whereas quantitative parameters were expressed as measurements (μm) or absolute counts per standardized area.

Histopathological examination of internal organs was also performed to evaluate the potential systemic toxicity of the tested formulations.

Detailed histopathological evaluation procedures are described in Paper 5.

1.4.4. Immunohistochemistry (Ki-67)

Immunohistochemical staining for the proliferation marker Ki-67 was performed on formalin-fixed, paraffin-embedded skin tissue sections. Antigen retrieval was carried out in citrate buffer (pH 6), followed by incubation with a monoclonal anti-Ki-67 antibody (clone SP6, Abcam). Immunoreactivity was detected using a polymer-based detection system and visualized with diaminobenzidine (DAB). The sections were counterstained with hematoxylin.

The proliferative activity of epidermal keratinocytes was assessed by quantifying Ki-67 expression in the basal and suprabasal layers of the epidermis. Representative microscopic fields were selected in areas showing hyperplastic or dysplastic epidermal alterations while avoiding ulcerated

regions. The number of Ki-67-positive nuclei and the total number of keratinocytes were determined, and the Ki-67 index was calculated as the percentage of positively stained cells relative to the total number of keratinocytes.

Detailed immunohistochemical staining and evaluation procedures are described in Paper 5.

1.5. Data analysis and statistics

Statistical analysis was performed using IBM SPSS Statistics software. All experiments were performed at least in triplicate.

Quantitative data were expressed as mean values with standard deviation or presented using other appropriate descriptive statistics. Data normality was assessed using the Shapiro-Wilk test, while homogeneity of variances was evaluated using Levene's test. Depending on data distribution, parametric or non-parametric statistical tests were applied. Differences between groups were evaluated using Student's t-test or one-way ANOVA followed by appropriate post hoc tests. Non- parametric data were analysed using the Kruskal-Wallis test with Bonferroni-adjusted comparisons. Correlations between selected variables were evaluated using Spearman's rank correlation coefficient. A p-value < 0.05 was considered statistically significant.

Detailed statistical methods are provided in the individual publications (Papers 2–5).

2. SUMMARY OF RESULTS

2.1. Characterization of cyanobacterial biomass and isolated c-phycocyanin

2.1.1. Cyanobacterial biomass composition and toxin screening

Microscopic evaluation revealed that the phytoplankton community composition varied between the sampling years. In 2019, *Aphanizomenon* spp., particularly *A. flos-aquae*, dominated the community, accounting for up to 99% of the total phytoplankton biomass. In contrast, *Microcystis* spp. predominated in 2020 and 2022, representing up to 98% of the total biomass. In 2023, microscopic analysis again confirmed the dominance of *A. flos-aquae*, which constituted more than 95% of the total phytoplankton biomass in the selected samples.

ELISA-based cyanotoxin screening of the biomass collected in 2023, dominated by *A. flos-aquae*, revealed no detectable toxins (microcystins, saxitoxins and anatoxins). While C-PC isolated from other biomass samples was used in some of the experiments, only the C-PC obtained from this non-toxic biomass was used for the preparation of transfersomes applied in the *in vivo* study.

The origin of the biomass used for C-PC isolation in the respective experiments is described in detail in Papers 2–5.

2.1.2. Purity of isolated c-phycocyanin

During the initial stages of the research (*Papers 2* and *3*), C-PC samples obtained from wild cyanobacterial biomass exhibited purity values ranging from 1.130 (0.020) to 2.207 (0.015). Higher purity values were obtained when ion-exchange chromatography was applied for purification, whereas lower purity levels were observed in samples purified using gel filtration chromatography.

In the later stages of the study involving transfersome formulation and *in vivo* study, C-PC with a higher purity level (3.227 (0.045)) was used. This level of purity was achieved after purification using ion-exchange chromatography. For these experiments, highly purified C-PC was selected to minimize the presence of other protein impurities and to potentially enhance its biological activity.

The exact purity of C-PC used in each experiment is specified in Papers 2–5.

2.1.3. Heavy metal content in c-phycocyanin samples

The concentrations of heavy metals in C-PC samples were determined using ICP-MS. Four lyophilized C-PC samples isolated from different cyanobacterial biomasses were analysed: three samples obtained from cyanobacteria collected in the Kaunas Lagoon during 2019–2022 and one reference sample isolated from cultivated *L. platensis*.

The results demonstrated that the concentrations of the investigated heavy metals (Pb, Cd, As, Hg) varied depending on the origin of the C-PC, specifically the cyanobacterial biomass from which it was isolated, as well as the dominant cyanobacterial genus. In C-PC isolated from biomass dominated by *A. flos-aquae* (2019), the concentrations of metals followed the order: Pb 0.378 (0.013) μg/g > As 0.150 (0.012) μg/g > Hg 0.050 (0.006) μg/g > Cd 0.020 (0.000) μg/g. Higher concentrations of most investigated heavy metals were detected in C-PC isolated from biomasses dominated by *Microcystis* spp. For example, in the sample collected in 2020, the highest concentration was observed for Pb 0.725 (0.006) μg/g, followed by Hg 0.443 (0.007) μg/g, Cd 0.233 (0.005) μg/g, and As 0.190 (0.008) μg/g. In C-PC isolated from biomass collected in 2022, the metal concentrations were ranked as follows: Pb 0.643 (0.015) μg/g > Cd 0.410 (0.014) μg/g > As 0.160 (0.008) μg/g > Hg 0.021 (0.003) μg/g. The reference C-PC sample isolated from cultivated *L. platensis* exhibited a different distribution of metals, with Hg 0.376 (0.016) μg/g and Cd 0.348 (0.005) μg/g being the predominant elements, while As showed the lowest concentration 0.045 (0.006) μg/g.

Overall, the ICP-MS analysis indicated that higher concentrations of heavy metals were detected in C-PC samples isolated from cyanobacterial biomass dominated by *Microcystis* spp., whereas lower levels were observed in C-PC obtained from biomass dominated by *A. flos-aquae* and in the reference sample from cultivated *L. platensis*. Although the influence of purification methods on heavy metal content was not the primary objective of this study, it was observed that C-PC purified using ion-exchange chromatography tended to exhibit lower concentrations of Pb, Cd, and As. However, this tendency should be interpreted with caution, as differences in heavy metal levels may also be influenced by other factors, including variations in the cyanobacterial species composition of the biomass samples. These findings were taken into account when selecting the C-PC source and purification strategy for subsequent formulation development and *in vivo* studies, prioritizing samples with lower heavy metal content and higher purity.

The detailed results of the heavy metal analysis and their interpretation are presented in Paper 2.

2.2. Evaluation of c-phycocyanin hydrogel formulations

To develop a topical hydrogel formulation suitable for C-PC delivery, a series of hydrogels were prepared and systematically evaluated. Particular attention was given to selecting gelling agents and preservative systems that would not negatively affect the structural stability of C-PC. The formulation development process included screening of gelling agents, optimization of preservative systems, microbiological evaluation, and investigation of *in vitro* release behaviour.

2.2.1. Screening of gelling agents for c-phycocyanin hydrogels

C-PC used in this study was isolated from cyanobacterial biomass collected from the Kaunas Lagoon (Kaunas, Lithuania) and exhibited a purity of 1.50 (0.006). The effect of different gelling agents on the structural stability of C-PC in hydrogel formulations was investigated using a series of 1% (w/w) C-PC hydrogels prepared with various natural and synthetic gelling agents.

The stability of C-PC within the prepared hydrogels was assessed spectrophotometrically by comparing the detected C-PC concentration with the initial amount incorporated during hydrogel preparation. After short term storage at 4 °C for 48 h, no statistically significant changes in C-PC concentration ($p > 0.05$) were observed in hydrogels formulated with sodium alginate, Soligel™, HEC, NaCMC, HPMC, or HEMC.

In contrast, a reduction in C-PC content was observed in hydrogels containing poloxamer 407 and chitosan, where the C-PC concentration decreased by 12.20% and 12.00%, respectively ($p < 0.05$). The most pronounced decrease in C-PC stability was detected in formulations prepared with Carbopol® Ultrez 21 and Pemulen™, where the C-PC concentration decreased by 71.80% and 50.30%, respectively ($p < 0.05$). This reduction was accompanied by a visible fading of the characteristic blue colour of the hydrogels.

Based on these results, six polysaccharide-based gelling agents – sodium alginate, Soligel™, HEC, NaCMC, HPMC, and HEMC – were selected for further investigation, as these formulations maintained C-PC stability without significant degradation.

Detailed results of the gelling agent screening are presented in Paper 3.

2.2.2. Screening of preservative systems for c-phycocyanin hydrogels

The effect of different preservative systems on C-PC structural stability in hydrogel formulations was investigated using hydrogels prepared with the previously selected polymeric matrices (sodium alginate, Soligel™, HEC, NaCMC, HPMC, and HEMC). Three environmentally friendly preservatives were evaluated: SharoSENSE™ Plus 184, SharoSENSE™ Plus 785, and Sharomix™ 721. C-PC stability in these formulations was assessed spectrophotometrically by comparing the measured C-PC concentration with the initially incorporated amount after storage at 4 °C for 48 h.

The results demonstrated that the choice of preservative significantly influenced C-PC stability in the hydrogels. Formulations containing SharoSENSE™ Plus 184 showed the greatest decrease in C-PC concentration, ranging from 6.60% to 64.40%, depending on the gelling agent used. This reduction was also accompanied by visible fading of the characteristic blue colour of the hydrogels.

Hydrogels preserved with Sharomix™ 721 exhibited smaller reductions in C-PC concentration, ranging from 9.30% to 16.60%. An even smaller decrease in C-PC concentration was observed in formulations containing SharoSENSE™ Plus 785, where the reduction ranged from 0.5% to 14.30%, depending on the polymeric matrix.

Statistical analysis revealed that hydrogels formulated with SharoSENSE™ Plus 184 and Sharomix™ 721 showed a significant reduction in C-PC concentration ($p < 0.05$). In contrast, no statistically significant decrease ($p > 0.05$) was observed when SharoSENSE™ Plus 785 was combined with sodium alginate, Soligel™, or HEC.

Based on these findings, SharoSENSE™ Plus 785 was selected as the most suitable preservative system for the development of C-PC hydrogels. Subsequently, hydrogels formulated with sodium alginate, Soligel™, and HEC in combination with SharoSENSE™ Plus 785 were selected for further evaluation.

Detailed experimental results are presented in Paper 3.

2.2.3. Microbiological evaluation of c-phycocyanin hydrogels

Following the selection of the most suitable preservative system, the microbiological quality of the developed C-PC hydrogels was evaluated. Three hydrogel formulations prepared with sodium alginate, Soligel™, and HEC in combination with the selected preservative SharoSENSE™ Plus 785 were analysed. Glycerol was included in all formulations as a humectant, and it did not negatively affect the stability of C-PC.

Microbiological testing demonstrated that the tested hydrogels met microbiological safety requirements. The investigated pathogenic microorganisms, including *Staphylococcus aureus*, *Pseudomonas aeruginosa*, *Candida albicans*, and *Escherichia coli*, were not detected in any of the tested formulations. Additionally, the total count of aerobic mesophilic microorganisms remained below 1.0×10^1 CFU/g in all samples.

These results indicate that the selected preservative system ensured adequate microbiological stability of the C-PC hydrogels.

Detailed microbiological results are presented in Paper 3.

2.2.4. *In vitro* release of c-phycocyanin from hydrogels

Based on the results of the gelling agent screening and microbiological evaluation, hydrogels prepared with sodium alginate, Soligel™, and HEC in combination with the preservative SharoSENSE™ Plus 785 were identified as suitable formulations for further studies. Among these, sodium alginate was selected as the gelling agent for the *in vitro* release study due to its compatibility with C-PC and its algal origin.

The influence of PG on the release behaviour of C-PC from the hydrogel matrix was investigated by comparing two: a hydrogel containing PG and a control formulation without PG.

The *in vitro* release study demonstrated that the presence of PG accelerated the release of C-PC from the hydrogel matrix. C-PC release from both formulations was detected after 30 min of the experiment. A release of 3.25% (258.30 (36.96) μg/cm²) was observed from the PG-containing hydrogel after 2 h, whereas a comparable level of release from the hydrogel without PG was reached only after 3h (3.59% (286.49 (72.59) μg/cm²)). These results indicate that the presence of PG promoted faster diffusion of C-PC from the hydrogel matrix. After 6 h, the hydrogel containing PG released approximately 10% of the incorporated C-PC (728.07 (19.35) μg/cm²), whereas the formulation without PG released around 7% (531.44 (26.81) μg/cm²). The difference between the two formulations was statistically significant ($p < 0.05$), indicating that PG promoted faster and greater release of C-PC from the hydrogel system.

Detailed results of the in vitro release study are presented in Paper 3.

2.3. Characterization of c-phycocyanin-loaded enriched transfersomes

2.3.1. Morphological and physicochemical characterization of transfersomes

C-PC-loaded enriched transfersomes were prepared as nanocarriers for the topical delivery of C-PC isolated from cyanobacterial biomass. The C-PC used in this study was obtained exclusively from non-toxic biomass confirmed by ELISA-based cyanotoxin screening and dominated by *A. flos-aquae*. The purified C-PC demonstrated high purity (3.227 (0.045)), confirming its suitability for further biological evaluation. Transfersomes were prepared using phospholipid S75 in combination with sodium deoxycholate as an edge activator to obtain flexible vesicular systems. To enhance the functional properties of the vesicles, glycerol, sodium hyaluronate, or their combination was incorporated into the formulations. In addition, selected systems were supplemented with cholesterol to evaluate its influence on vesicle characteristics. In total, six different C-PC-loaded enriched transfersome formulations were produced: Gly-T, Gly-Chol-T, Hyal-T, Hyal-Chol-T, Hyal-Gly-T, and Hyal-Gly-Chol-T.

The morphology of the prepared vesicles was evaluated using cryo-TEM. The obtained images confirmed the successful formation of nanosized vesicles with predominantly spherical morphology. Cryo-TEM analysis showed that vesicle lamellarity and size depended on formulation composition. Glycerol-based transfersomes were generally smaller and mainly characterized by unilamellar vesicles, whereas the incorporation of sodium hyaluronate resulted in the larger vesicles and the formation of more complex oligolamellar or multilamellar structures.

Consistent with the morphological features observed in cryo-TEM images, physicochemical characterization demonstrated that the prepared transfersomes were within the nanometre size range suitable for topical delivery. The mean vesicle diameter ranged from approximately 90 to 115 nm. Sodium hyaluronate-containing transfersomes exhibited slightly larger vesicle diameters compared with formulations without sodium hyaluronate. In addition, transfersomes supplemented with cholesterol tended to exhibit slightly smaller vesicle sizes than the corresponding formulations without cholesterol. All formulations showed relatively low polydispersity index values (< 0.2), indicating homogeneous particle size distribution. Measurements of zeta potential revealed strongly negative surface charges (approximately -33 to -44 mV), suggesting good colloidal stability of the nanosystems.

The encapsulation efficiency of C-PC varied between the investigated formulations. The highest encapsulation was observed in glycerol-based transfersomes (approximately 51%), whereas lower values (approximately 33–37%) were obtained in formulations containing sodium hyaluronate. The presence of cholesterol did not significantly influence the encapsulation efficiency.

Considering the obtained physicochemical parameters, glycerol-based transfersomes were identified as the most promising carriers for further studies due to their favourable particle size, homogeneity, surface charge, and encapsulation efficiency.

A more detailed description and illustrations of these results are provided in Paper 4.

2.3.2. Stability of c-phycocyanin-loaded transfersomes

The physical stability of the prepared transfersomes was evaluated during an eight-month storage period at 4 °C under refrigerated and light-protected conditions by monitoring changes in vesicle size, PI, and ZP. Throughout the storage period, no visible changes in the characteristic colour of the formulations were observed, indicating the preservation of C-PC within the vesicular systems. All formulations maintained negative zeta potential values during storage, suggesting good electrostatic stability of the vesicles. However, differences in long-term stability were observed depending on formulation composition. Transfersomes containing glycerol (Gly-T, Gly-Chol-T, Hyal-Gly-T, and Hyal-Gly-Chol-T) showed minimal changes in particle size over the entire storage period, indicating stable vesicular systems. In contrast, formulations containing sodium hyaluronate without glycerol (Hyal-T and Hyal-Chol-T) exhibited a noticeable increase in vesicle diameter beginning after approximately four to five months of storage. This increase was accompanied by a rise in polydispersity index values, indicating the formation of more heterogeneous vesicle populations and suggesting vesicle aggregation or fusion processes.

Overall, the results indicate that glycerol contributed to improved stability of the transfersome formulations, likely by reducing the tendency of hyaluronate-containing vesicles to aggregate during storage.

A detailed presentation of the stability results is provided in Paper 4.

2.3.3. Antioxidant activity of c-phycocyanin-loaded transfersomes

The antioxidant activity of C-PC in solution and encapsulated in enriched transfersomes was assessed using the DPPH radical scavenging assay. The results were expressed as antioxidant activity (AA) and Trolox equivalent antioxidant capacity (TEAC).

The C-PC solution demonstrated an antioxidant activity of approximately 36%, corresponding to about 23.3 μmol Trolox equivalents (TE)/g of dry C-PC. Slightly higher values were obtained for the C-PC-loaded transfersomes, with antioxidant activity ranging from approximately 38% to 42% and TEAC values between approximately 24 and 27 μmol TE/g. The small increase observed for the vesicular formulations may be associated with the intrinsic antioxidant properties of some transfersome components, particularly phosphatidylcholine and trace amounts of α-tocopherol present in the phospholipid S75. Importantly, the results indicate that incorporation of C-PC into enriched transfersomes did not reduce its antioxidant capacity.

These findings suggest that the preparation method preserved the functional properties of the pigment and confirm the suitability of the developed nanosystems for C-PC delivery.

A detailed description of the experimental results is presented in Paper 4.

2.3.4. *In vitro* cytocompatibility and protective effects in HaCaT cells

The cytocompatibility and protective effects of C-PC in solution and C-PC-loaded enriched transfersomes were evaluated using human keratinocyte cells (HaCaT), which were used as an *in vitro* model of the human epidermis. Based on the previously described physicochemical characterization and stability results, glycerol-containing transfersome formulations (Gly-T, Gly-Chol-T, Hyal-Gly-T and Hyal-Gly-Chol-T) were selected for this study due to their favourable stability and vesicle properties. Cell viability was assessed after exposure to different concentrations of C-PC (1–1000 μg/mL).

The highest tested concentration (1000 μg/mL) showed a pronounced cytotoxic effect, as cell viability decreased to below approximately 45% for all tested formulations. A slightly lower viability was observed for transfersome-based formulations compared with the C-PC solution, which may be related to the composition of the vesicular carriers at this elevated concentration. In contrast, substantially higher cell viability was observed at lower concentrations. At 100 μg/mL, cell viability remained around 80%, while concentrations of 10 μg/mL and 1 μg/mL maintained viability above 90% and 100%, respectively, with no notable differences between free and encapsulated C-PC.

Based on these results, the concentration of 10 μg/mL was selected for further evaluation of the protective effect against oxidative stress induced by hydrogen peroxide. Exposure of keratinocytes to hydrogen peroxide alone reduced cell viability to approximately 60%. However, treatment with C-PC, either in solution or encapsulated in enriched transfersomes, significantly improved cell survival, increasing viability to approximately 80%. No substantial differences were observed between the tested formulations.

Overall, these findings indicate that encapsulation of C-PC into enriched transfersomes does not negatively affect its biological activity and that the developed nanosystems preserve the antioxidant protective effect of C-PC against oxidative stress.

A detailed presentation of the results is provided in Paper 4.

2.3.5. *Ex vivo* skin permeation of c-phycocyanin

Ex vivo skin penetration studies were performed to evaluate the ability of C-PC to penetrate and accumulate in human skin when delivered from different formulations. The experiments compared conventional formulations, such as hydrogels, with vesicular nanocarriers to assess whether nanocarrier-based formulations could improve the cutaneous delivery of C-PC.

Initially, the penetration of C-PC released from hydrogel formulations was qualitatively evaluated using human skin samples mounted in diffusion cells, followed by visualization with confocal laser scanning microscopy. Two hydrogel formulations were evaluated: one containing PG and one without PG, in order to assess the influence of PG on the skin penetration of C-PC. The obtained results demonstrated that no detectable fluorescence signals were observed in skin samples when C-PC was applied in the hydrogel formulation without PG, indicating that C-PC was unable to penetrate the skin under these conditions. In contrast, detectable fluorescence signals were observed in the stratum corneum when the C-PC hydrogel containing PG was applied. This limited penetration is consistent with the physicochemical properties of C-PC, which is a high-molecular-weight and hydrophilic protein with restricted passive diffusion through the skin barrier. The presence of penetration-enhancing agents such as PG slightly increased the deposition of C-PC within the stratum corneum.

To improve the cutaneous delivery of C-PC, enriched transfersomes were developed as vesicular nanocarriers. In the *ex vivo* experiments, the skin penetration of C-PC- loaded transfersomes with and without cholesterol was compared with that of aqueous C-PC solutions and C-PC solutions containing PG as a penetration enhancer. Qualitative analysis of skin sections revealed that C-PC delivered from enriched transfersomes produced substantially

stronger fluorescence signals within the upper skin layers compared with the free C-PC solutions. A slightly more pronounced and thicker fluorescence band in the outer skin layer was observed for transfersomes without cholesterol compared with cholesterol-containing formulations. In contrast, C-PC applied in PBS solution without PG showed almost no detectable penetration, whereas the addition of PG resulted only in a slight increase in C-PC deposition within the stratum corneum.

Among the investigated nanocarrier systems, glycerol-enriched transfersomes demonstrated the most pronounced accumulation of C-PC in the stratum corneum during qualitative analysis. This finding suggests that the high deformability and flexibility of these vesicles contribute to enhanced C-PC deposition in the outer skin layers without the need for aggressive penetration-enhancing agents.

Overall, these results demonstrated that conventional formulations such as hydrogels or aqueous solutions allow only limited penetration of C-PC, whereas vesicular nanocarriers such as enriched transfersomes visibly enhance its accumulation in the skin. These findings highlight the potential of transfersomal systems for improving the topical delivery of hydrophilic macromolecules such as C-PC.

A detailed presentation of the results is provided in Papers 3 and 4.

2.4. *In vivo* effects of c-phycocyanin-loaded transfersomes in the DMBA/TPA skin carcinogenesis model

2.4.1. General observations on the effects of c-phycocyanin-loaded transfersomes on skin tumour development and animal well-being

In the *in vivo* study, a well-established two-stage DMBA/TPA mouse skin carcinogenesis model was applied. Non-carcinogen control groups (Groups I and II) received only topical C-PC-loaded transfersomes at concentrations of 1 mg/mL and 10 mg/mL, respectively, without exposure to the carcinogen. The applied formulations were well tolerated, no visible signs of skin irritation were observed in these animals throughout the experimental period.

During the first phase of the experiment (weeks 1–5), the carcinogen control group (Group III) exhibited significantly higher skin irritation scores compared with both the non-carcinogen groups (Groups I and II) and the carcinogen-treated groups receiving C-PC-loaded transfersomes (Groups V and VI) ($p < 0.05$).

After approximately five weeks of tumour promotion, animals exposed to the carcinogen developed pronounced skin irritation accompanied by

increased scratching behaviour. Mice in all carcinogen-treated groups displayed frequent scratching, and scratching-induced lesions gradually appeared. These lesions were typically located in the lower dorsal region, below the area where the topical formulations were applied, indicating that they were associated with scratching and grooming rather than direct irritation at the application site. The lesions manifested as superficial wounds caused by scratching and excessive licking.

Due to the severity of skin irritation, the experimental protocol was modified to ensure animal welfare. To reduce the irritating effect of the TPA-acetone vehicle while maintaining tumour – promoting activity, TPA was dissolved in a mixture of acetone and polyethylene glycol (PEG). This modified formulation was applied between weeks 6 and 12 of the experiment. The use of the acetone-PEG mixture reduced the intensity of skin irritation and decreased the occurrence of scratching-induced lesions, allowing the continuation of the study under improved welfare conditions. During the second phase of the experiment, following the modification of the TPA vehicle to a PEG/acetone mixture, differences between the experimental groups remained evident but were less pronounced. The carcinogen control group continued to differ significantly from the non-carcinogen groups ($p < 0.05$), whereas no statistically significant differences were observed among the carcinogen-treated groups.

During the final phase of the experiment (weeks 13–16), TPA dissolved in acetone was reintroduced to intensify tumour promotion and further stimulate the carcinogenesis process. Following this reintroduction, skin irritation severity increased again, and the carcinogen control group (Group III) once more exhibited higher irritation scores compared with the group treated with carcinogen together with C-PC-loaded transfersomes (Group V).

Throughout the experimental period, animals were monitored for changes in body weight. Body weight increased progressively during the study, reflecting normal physiological growth of the animals. At the beginning of the experiment, body weight ranged approximately from 18 to 22 g, while at the end of the 16-week experimental period, it reached approximately 26–32 g. These values remained within physiological limits for BALB/c mice of this age, and no signs of systemic toxicity or treatment-related mortality were observed.

By the end of the experimental period, the most pronounced macroscopic skin alterations were observed in the carcinogen control group. These animals exhibited evident skin dryness, erythema, and inflammatory changes of the dorsal skin. In addition, small papule-like lesions were observed in the majority of animals in this group, suggesting early hyperproliferative epidermal alterations associated with tumour-promoting processes. In contrast, animals

treated with transfersome-based formulations together with the carcinogen generally displayed milder macroscopic skin alterations, including reduced skin irritation, erythema, and scaling. Only two animals in the group treated with empty transfersomes together with the carcinogen (Group IV) developed small papule-like lesions, whereas no papule-like lesions formation was observed in the groups treated with C-PC-loaded transfersomes together with the carcinogen (Groups V and VI). Overall, animals receiving transfersomes together with the carcinogen showed improved skin condition compared with the carcinogen-only group.

Detailed macroscopic evaluation of skin alterations and body weight monitoring results are presented in Paper 5.

2.4.2. Histopathological evaluation of skin tissue

Histopathological examination of dorsal skin samples revealed clear structural differences between the experimental groups. Particular attention was given to epidermal alterations associated with early tumour-promoting processes, including epidermal thickness, rete ridge depth, hyperplasia, dysplasia, mitotic activity, and inflammatory changes.

In the groups not exposed to the carcinogen (Groups I and II), epidermal architecture remained comparable to normal skin morphology. The epidermis was thin, ranging from approximately 10 to 20 μm, and consisting of only a few keratinocyte layers, with regularly arranged nuclei. Rete ridges were short and uniform, with a depth of approximately 0–10 μm. No signs of epidermal hyperplasia, dysplasia, oedema, or inflammatory infiltrates were detected. These findings were consistent with the macroscopic observations and indicate that topical application of C-PC-loaded transfersomes on intact skin did not induce structural or proliferative alterations of the epidermis.

In contrast, animals exposed to the carcinogen exhibited pronounced histopathological alterations characteristic of inflammation-driven epidermal remodelling. A marked increase in epidermal thickness and elongation of rete ridges was observed in all carcinogen-treated groups, reflecting hyperplastic and proliferative changes of the epidermis. The most pronounced alterations were detected in the carcinogen-only group (Group III), where substantial epidermal thickening (110.78 (7.63) μm) and deep epidermal invaginations into the dermis, with the rete ridge depths reaching approximately 80–150 μm, were frequently observed. A significantly lower degree of epidermal thickening was observed in the groups treated with transfersome-based formulations together with the carcinogen. In the group treated with empty transfersomes (Group IV), epidermal thickness reached 61.35 (5.93) μm, whereas treatment with C-PC-loaded transfersomes at a concentration of

1 mg/mL (Group V) resulted in an epidermal thickness of 76.65 (6.46) µm ($p < 0.05$ compared with Group III). Rete ridge elongation in these groups was also less pronounced than in the carcinogen-only group.

Epidermal dysplasia also differed considerably among the experimental groups. Epidermal dysplasia was graded as mild, moderate, or severe according to the extent of architectural and cytological alterations observed in the epidermis. In the carcinogen-only group (Group III), severe dysplasia was observed in 80% of animals, whereas the remaining 20% exhibited moderate dysplasia. In contrast, animals receiving transfersome-based formulations together with the carcinogen showed a shift toward milder dysplastic changes. In particular, treatment with C-PC-loaded transfersomes (Group V) was associated with a higher proportion of animals exhibiting mild dysplasia (40%) and a lower proportion exhibiting severe dysplasia (30%) compared with the carcinogen-only group (Group III).

A similar pattern was observed for epidermal hyperplasia. Histopathological evaluation revealed that 50% of animals in the carcinogen-only group (Group III) exhibited moderate epidermal hyperplasia, whereas the remaining 50% exhibited severe hyperplasia. Animals treated with empty transfersomes (Group IV) or C-PC-loaded transfersomes (Group V) showed predominantly mild to moderate hyperplasia. Mild hyperplasia was observed in 50% of animals in Group IV and 30% in Group V, whereas moderate hyperplasia was observed in 50% and 60%, respectively. Although hyperplasia was still present in carcinogen-exposed groups receiving transfersomes, its severity was reduced compared with that in the carcinogen-only group.

Quantitative assessment of mitotic activity demonstrated minimal proliferative activity in the non-carcinogen groups (Groups I and II). In contrast, carcinogen exposure markedly increased the number of mitotic figures within the epidermis (12 (1.23) mitoses per 2.37 mm^2). Treatment with C-PC-loaded transfersomes significantly reduced mitotic activity to 6.9 (0.38) mitoses per 2.37 mm^2 in Group V and 8 (0.91) in Group VI ($p < 0.05$ compared with the carcinogen-only group), indicating partial suppression of carcinogen-induced epidermal proliferation.

Epidermal oedema (spongiosis) was detected exclusively in carcinogen-exposed groups and was most pronounced in the carcinogen-only group. In animals receiving transfersome-based formulations together with the carcinogen, the degree of oedema varied but was generally less severe.

In addition to epidermal alterations, pronounced dermal inflammatory changes were observed. The carcinogen-only group (Group III) exhibited predominantly severe dermal inflammation, with 70% of animals presenting severe inflammatory changes, accompanied by hyperaemia, oedema, and increased mast cell density (38.6 (2.48) mast cells per 2.37 mm^2), indicating

marked activation of the inflammatory microenvironment. In contrast, animals treated with C-PC-loaded transfersomes, particularly those in Group V, demonstrated a shift toward milder inflammatory changes, with 60% of animals exhibiting mild inflammation, and significantly reduced mast cell density (23.6 (2.09) mast cells per 2.37 mm^2) compared with the carcinogen control group (Group III; $p < 0.05$).

Correlation analysis revealed a positive association between the severity of dermal inflammation and mast cell density (Spearman's $\rho = 0.438$, $p < 0.001$), suggesting that mast cell accumulation may contribute to the inflammatory microenvironment associated with carcinogen-induced skin alterations.

Overall, histopathological findings indicate that topical treatment with transfersome-based formulations attenuated several key features of early carcinogenesis-related epidermal remodelling, including epidermal thickening, dysplasia severity, proliferative activity, and dermal inflammation.

Detailed histopathological results are presented in Paper 5.

2.4.3. Immunohistochemical assessment of epidermal proliferation and its association with histopathological parameters

Immunohistochemical analysis of the proliferation marker Ki-67 was performed to evaluate epidermal proliferative activity among the experimental groups. Ki-67 expression was assessed separately in the basal and suprabasal layers of the epidermis, and the total epidermal Ki-67 index was also calculated.

In the non-carcinogen control groups (Groups I and II), the epidermis remained thin, with basal keratinocytes constituted a substantial proportion of the total epidermal cell population. Although a moderate proportion of Ki-67-positive cells was observed in the basal layer, suprabasal Ki-67 expression remained low (approximately 2–4%). Together with the absence of histopathological abnormalities, this proliferative pattern was considered to reflect physiological epidermal turnover rather than pathological proliferation.

In contrast, exposure to the carcinogen markedly increased epidermal proliferative activity. The carcinogen-only group (Group III) exhibited significantly elevated Ki-67 expression in both basal (65.4 (3.67)%) and suprabasal (26.78 (3.47)%) epidermal layers compared with the non-carcinogen control groups (Groups I and II; $p < 0.05$).

Topical treatment with transfersome-based formulations resulted in a partial reduction of epidermal proliferative activity, particularly in the suprabasal layer. Application of C-PC-loaded transfersomes containing 10 mg/mL C-PC significantly reduced epidermal proliferative activity, with the basal

Ki-67 index decreasing by approximately 28% and the suprabasal Ki-67 index by approximately 61% compared with the carcinogen-only group ($p < 0.05$). The more pronounced reduction in suprabasal proliferation suggests attenuation of tumour-promoting epidermal remodelling.

Analysis of the total epidermal Ki-67 index demonstrated a similar tendency. The group treated with carcinogen together with the higher concentration of C-PC-loaded transfersomes showed a statistically significant 29% reduction in the total Ki-67 index compared with the carcinogen-only group ($p < 0.05$). However, the total index appeared to be less sensitive in detecting intergroup differences than separate analyses of basal and suprabasal proliferation.

Correlation analysis further demonstrated significant associations between proliferative activity and histopathological alterations of the epidermis. A positive correlation was observed between suprabasal Ki-67 expression and epidermal thickness (Spearman's $\rho = 0.64$, $p < 0.05$), as well as between suprabasal Ki-67 expression and rete ridge depth (Spearman's $\rho = 0.71$, $p < 0.05$). In addition, increased epidermal proliferative activity was associated with higher dysplasia grades (Spearman's $\rho = 0.66$, $p < 0.05$).

Overall, these findings indicate that carcinogen exposure induces marked epidermal hyperproliferation, while topical treatment with C-PC-loaded transfersomes at 10 mg/mL attenuates this proliferative response. The reduction of Ki-67 expression together with improvements in histopathological parameters suggests that C-PC-loaded transfersomes may modulate early tumour-promoting processes in the epidermis.

Detailed immunohistochemical results are presented in Paper 5.

2.4.4. Histopathological assessment of internal organs

Histopathological examination of internal organs (liver, spleen, lungs, heart, kidneys, brain, testes, and mesenteric lymph nodes) revealed no treatment-related pathological alterations in any experimental group. All examined tissues preserved normal histological architecture, with no evidence of degenerative, inflammatory, or neoplastic changes. These findings suggest that topical application of C-PC-loaded transfersomes was not associated with histopathological alterations in the examined internal organs.

3. DISCUSSION

The present study investigated the development of topical C-PC delivery systems and their biological activity. The findings provide new insights into the potential applications of C-PC, including the safety of C-PC derived from naturally occurring cyanobacterial biomass, the development of suitable topical delivery systems, and the biological effects associated with its potential to modulate an inflammation-driven skin carcinogenesis.

The discussion of the results begins with the evaluation of cyanobacterial biomass as a potential source of C-PC and the safety aspects associated with its use. Phycocyanin can be obtained from multiple biological sources, including eukaryotic organisms such as red algae and glaucophytes, as well as prokaryotic cyanobacteria [9, 30]. In this study, C-PC was isolated from cyanobacterial biomass collected during natural cyanobacterial blooms in August–October 2019–2023 from two freshwater bodies: the Kaunas Lagoon (Kaunas, Lithuania) and the Simnas fishpond (Simnas, Lithuania). Cyanobacteria represent a morphologically diverse group of oxygenic, photoautotrophic Gram-negative prokaryotes that occur in unicellular, colonial, and filamentous forms [45]. It is worth noting that cyanobacteria are among the most ancient photosynthetic microorganisms on Earth and have persisted for billions of years due to their remarkable adaptive capacity. During their long evolutionary history, they have developed numerous survival strategies. One such strategy is the production of bioactive secondary metabolites, including cyanotoxins, which may provide advantages for cyanobacteria but can also pose risks to aquatic ecosystems, animals, and human health [46]. Cyanotoxins can be broadly classified according to their primary targets and mechanisms of action into hepatotoxins (microcystins (MCs), nodularins (NODs), cylindrospermopsin (CYN)), neurotoxins (anatoxin-a (ATX-a), saxitoxins (STXs)), and dermatotoxins (aplysiatoxins (APTXs), lyngbyatoxins (LTXs), and lipopolysaccharides (LPS)) [47]. In freshwater ecosystems, the primary genera producing toxins include *Microcystis*, *Dolichospermum* (formerly *Anabaena*), *Aphanizomenon*, *Planktothrix,* and *Chrysosporum* [48]. Depending on the geographic location and environmental conditions, different cyanobacterial species produce specific cyanotoxins. For example, *Microcystis* spp. are commonly reported as producers of MCs, whereas *Aphanizomenon* spp. have been associated with the production of Antx-a, CYN, STXs, and MCs [49]. However, studies conducted in the Curonian Lagoon (Baltic Sea region, Lithuania) have shown that *Aphanizomenon* strains isolated from this environment did not produce detectable levels of major cyanobacterial toxins, including MCs, CYN, STXs, or Antx-a [50]. Given the potential

health risks associated with cyanotoxin contamination, evaluating biomass safety is an essential step before its use in experimental studies. Conventional approaches for detecting cyanotoxins in cyanobacterial samples commonly rely on analytical techniques such as enzyme-linked immunosorbent assay (ELISA) and liquid chromatography-mass spectrometry (LC-MS), which enable the identification and quantification of various cyanotoxins [51]. In the present study, the collected cyanobacterial biomass was screened for the most common cyanotoxins (microcystins, saxitoxins and anatoxins) using an ELISA-based assay. Analysis of the biomass collected in 2023, dominated by *A. flos-aquae*, revealed no detectable cyanotoxins. Only this non-toxic biomass was used for C-PC isolation and for preparing transfersomal formulations for the *in vivo* study, thereby confirming the safety of the experimental approach and eliminating potential interference of cyanotoxins in observed biological effects.

In response to environmental challenges posed by excessive cyanobacterial blooms, efforts have been undertaken to collect this biomass from the Kaunas Lagoon and other freshwater bodies and to explore ways to further utilize it. Cyanobacterial biomass can be utilized to produce high-value bioactive compounds and bioenergy products, thereby contributing to circular economy strategies [45]. Among cyanobacteria, species of the genus *Limnospira*, particularly *Limnospira platensis* (formerly *Arthrospira platensis)*, are the most extensively studied and represent the primary commercial source of C-PC due to their high pigment content and well-established cultivation technologies [12, 45, 52]. However, other cyanobacteria, including A. *flos-aquae*, have also been identified as promising sources of C-PC and other bioactive compounds [9, 45, 53]. Analyses of *Aphanizomenon* strains isolated from the Curonian Lagoon (Baltic Sea region, Lithuania) revealed the presence of several bioactive compounds, including chlorophyll-a, chlorophyllide-a, aphanizophyll, myxoxanthophyll, canthaxanthin, echinenone, zeaxanthin, α-carotene, β-carotene, lycopene, and the phycobiliprotein C-PC [50]. In contrast, cyanobacteria of the genus *Microcystis* form colonies embedded in a mucilaginous matrix composed of complex polysaccharides containing monosaccharides such as xylose, mannose, glucose, fucose, galactose, and rhamnose [2]. Although *Microcystis* species are best known for forming harmful blooms and producing cyanotoxins, they also synthesize a wide range of biologically active compounds. These include bioactive peptides such as microginins, which exhibit inhibitory activity against metalloproteases, including angiotensin-converting enzyme (ACE), as well as other compounds with potential antiviral activity, such as microvirin [1].

The composition of cyanobacterial biomass collected from the Kaunas Lagoon varied, depending on the year, sampling time, and location. Biomass

collected in 2020 and 2022 was dominated by *Microcystis* spp., accounting for up to 98% of the total biomass, whereas samples collected in 2019 and 2023 were predominantly composed of *A. flos-aquae*, representing 95–99% of the phytoplankton biomass.

The recovery of C-PC from cyanobacterial biomass remains a technological challenge due to the structural complexity of algal cells and the protein's sensitivity. As a water-soluble intracellular protein, C-PC requires cell disruption prior to extraction, followed by purification steps to separate it from other cellular components. The efficiency of this process depends on multiple factors, including pH, temperature, and other extraction conditions, all of which may significantly affect protein yield, purity, and stability. Despite extensive research, there is currently no standardized method for C-PC recovery, and the selected approach plays a critical role in determining the final product's quality [30, 54]. In this study, C-PC extraction and purification from wild cyanobacterial biomass were performed according to the method described by Khazi et al. (1980), with several modifications adapted by the NRC [42].

The purity of C-PC is a critical parameter determining its biological performance and applicability. It is commonly evaluated using the absorbance ratio A_{620}/A_{280}, which reflects the relative content of C-PC compared to total proteins. Several classification systems have been proposed, generally distinguishing food-grade, reagent-grade, and analytical-grade C-PC based on this ratio. For example, C-PC is often considered food-grade at $A_{620}/A_{280} \leq 0.7$, reagent-grade at 0.7–3.9, and analytical-grade at ≥ 4.0 [16, 29]. Other authors suggest slightly different thresholds depending on the intended application, such as cosmetic or pharmaceutical use [30, 52]. However, these classifications are not fully standardized, and considerable variability exists in the reported purity ranges across studies. In many cases, the purity of C-PC used in biological experiments varies widely or isn't reported, making it difficult to directly compare results or establish dose-effect relationships. This lack of standardization represents a significant limitation in the interpretation of C-PC studies. In the present study, C-PC purity varied depending on the applied purification strategy. During the initial stages of this study (*Papers 2* and *3*), the C-PC obtained exhibited purity values ranging from 1.130 to 2.207, indicating reagent-grade material. Higher purity values were achieved using ion-exchange chromatography, whereas lower purity was observed following gel filtration. In contrast, in the later stages of the study, a substantially higher-purity C-PC sample (purity 3.227) was used for transfersome formulation and *in vivo* evaluation. The selection of higher-purity C-PC was intended to reduce the presence of co-extracted proteins and other impurities that may interfere with biological activity and affect the

interpretation of experimental outcomes. Therefore, the variability in C-PC purity across studies should be carefully considered when interpreting biological effects, particularly in relation to dose-dependent responses.

In addition to cyanotoxin analysis and purity evaluation, this study also gave particular attention to the determination of heavy metal content in C-PC samples obtained from different cyanobacterial biomasses. Heavy metals were assessed in C-PC isolated from naturally occurring cyanobacterial biomass and compared with those detected in C-PC obtained from cultivated *L. platensis*. The assessment of heavy metals is particularly important, as cyanobacteria are known to have a strong capacity to bind and accumulate metal ions from their environment. This ability is associated with both environmental exposure and intrinsic cellular characteristics. Heavy metals such as Pb, Cd, As, and Hg are of particular concern due to their persistence, bioaccumulation potential, and strong toxic effects on the human body, even at low concentrations, where they may induce oxidative stress and disrupt cellular processes [55]. Bioactive compounds extracted from such biomass, including C-PC, may therefore contain trace levels of heavy metals depending on the environmental conditions in which the organisms were grown. Cyanobacterial cells can take up metal ions through both passive and active mechanisms. Passive adsorption occurs rapidly via electrostatic interactions between positively charged metal ions and negatively charged functional groups present on the cell surface, including carboxyl, hydroxyl, amino, and phosphate groups associated with cell wall components such as polysaccharides, proteins, and lipopolysaccharides. In contrast, active uptake involves the transport of metal ions across the cell membrane via specific transport systems and is dependent on cellular metabolism [56–60]. The capacity for metal accumulation may vary between cyanobacterial genera due to differences in cell morphology and surface structure. For instance, *Microcystis* spp., which form colonies surrounded by a mucilaginous extracellular matrix, may exhibit a higher metal-binding capacity than filamentous species such as *A. flos-aquae* [57, 61]. This may contribute to the increased accumulation of metals observed in biomass dominated by *Microcystis* spp. In the present study, a quantitative comparison demonstrated that Pb concentration in *Microcystis*-derived C-PC was approximately 1.7–1.9-times higher than in *A. flos-aquae.* Even more pronounced differences were observed for Cd and Hg, particularly in the 2020 sample, where Cd and Hg levels were more than tenfold and eightfold higher, respectively. In contrast, differences in As concentration were less pronounced, with only a 1.07–1.27-fold increase in *Microcystis*-derived samples. These findings are in agreement with previous studies demonstrating that *Microcystis aeruginosa* exhibits a particularly high affinity for metals such as Hg, Cd, and Pb [62]. In addition, variations

observed between *Microcystis* samples collected in different years (S2, 2020 vs S3, 2022) suggest that environmental factors, such as water composition and pollution levels, may significantly influence heavy metal accumulation in cyanobacterial biomass. The biomass analysed in this study was collected from the Kaunas Lagoon, a highly altered water body affected by anthropogenic pressures, including agriculture, wastewater discharge, and historical pollution [63]. Long-term monitoring data indicate that while heavy metal concentrations in surface water remain relatively stable, their accumulation in bottom sediments has increased over time. This trend is reflected in the present results, particularly for Cd, which showed higher concentrations in C-PC samples collected later. In contrast, arsenic concentrations showed only minor variation between samples, which is consistent with relatively stable As levels in the aquatic environment [64].

Importantly, cyanobacteria's ability to accumulate heavy metals is directly relevant to the safety and quality of bioactive compounds extracted from their biomass. C-PC itself contains functional groups capable of interacting with metal ions, and such interactions may induce conformational changes in the protein structure, affect its stability, and alter its biological activity [58, 65–67]. The differences in heavy metal content may also be partly influenced by the applied purification strategies. In this study, gel filtration chromatography was used for C-PC isolated from *Microcystis*-dominated biomass, whereas ion-exchange chromatography was applied for samples derived from *A. flos-aquae*. As these methods rely on different separation principles, they may differ in their ability to remove co-extracted contaminants. In particular, ion-exchange chromatography, based on charge interactions, may allow more efficient removal of certain impurities, including metal ions, compared to size-based separation methods [68–71].

In addition to wild cyanobacterial biomass, C-PC isolated from cultivated *L. platenis* (S4) was also evaluated, providing a comparison between natural and commercially sourced material. The metal profile of S4 differed from that of wild biomass, with relatively higher concentrations of Hg and Cd, particularly in comparison with C-PC derived from *A. flos-aquae*, but lower levels of Pb and As compared to samples obtained from natural sources. These findings indicate that cultivation under controlled conditions does not necessarily eliminate heavy metal contamination, as metal uptake may still occur depending on culture medium composition and processing conditions. At the same time, the lower Pb levels in S4 suggest that certain metals may be more strongly associated with environmental exposure in natural aquatic systems.

It should be noted that the primary aim of this study was to evaluate heavy metal concentrations across different C-PC samples, rather than to

establish direct correlations between metal content and influencing factors such as cyanobacterial species, environmental conditions, or purification methods. Therefore, the observed differences should be interpreted with caution, and further targeted studies are required to elucidate the underlying mechanisms. Nevertheless, the results provided important insights that informed decision-making for subsequent experimental stages. In particular, C-PC derived from *A. flos-aquae* biomass and purified using ion-exchange chromatography was selected for the preparation of final formulations and *in vivo* studies, as this combination demonstrated a more favourable safety profile with lower levels of heavy metal contamination.

In this context, careful monitoring of heavy metal contamination is essential when C-PC is intended for biotechnological, pharmaceutical, or cosmetic applications. In the European Union, the presence of heavy metals such as lead, cadmium, arsenic, and mercury in both cosmetic products and medical devices is tightly regulated. These elements are not permitted as intentional ingredients and only tolerated as technically unavoidable trace impurities that do not pose a risk to human health. While Regulation (EC) No 1223/2009 and the EU Medical Device Regulation (EU) 2017/745 provide the overarching legal framework for controlling such hazardous substances, the practical assessment and monitoring of trace heavy metals increasingly rely on harmonised analytical standards such as ISO 21392:2021, which specifies validated ICP-MS methods for their determination in finished products [72–74].

While the controlling of heavy metal contamination is essential from a safety and regulatory perspective, it is equally important to consider how the intrinsic structural characteristics of C-PC influence its functional performance and stability. C-PC is a water-soluble phycobiliprotein composed of protein subunits and chromophores known as phycocyanobilins [9]. The protein structure of C-PC consists of α and β subunits, each having a molecular weight of approximately 17–19 kDa [32, 75]. The α-subunit contains one phycocyanobilin chromophore covalently attached via thioether linkage to cysteine residue Cys84, whereas the β-subunit carries two chromophores bound to Met86 and Cys153 [76]. Phycocyanobilin is an open-chain tetrapyrrole chromophore responsible for the characteristic blue coloration of C-PC and its light-absorbing properties, with an absorption maximum at approximately 615–620 nm [32, 75, 77, 78]. The α and β subunits associate to form an (αβ) monomer. Structural analysis indicates that this monomer is stabilized by multiple hydrogen bonds and salt bridges. Three monomers are then assembled into an $(\alpha\beta)_3$ trimer, which serves as the basic structural unit of C-PC. Within the trimeric structure, each α-subunit forms approximately five hydrogen bonds and two salt bridges with the β-subunit

of a neighbouring monomer. Two trimers further associate in a face-to-face arrangement to form a hexameric $(\alpha\beta)_6$ quaternary structure [78]. This hexameric assembly is stabilized by numerous noncovalent interactions between the trimeric discs [79]. Recent structural studies have also revealed a non-conventional octameric $(\alpha\beta)_8$ assembly of C-PC, suggesting that the protein's structural organization may be more diverse than previously assumed [78]. In solution, the hexameric $(\alpha\beta)_6$ form of C-PC remains stable mainly in concentrated phosphate buffer at neutral or slightly acidic pH. Under conditions of lower phosphate buffer or protein concentration, the hexameric structure may dissociate into trimeric $(\alpha\beta)_3$ or monomeric $(\alpha\beta)$ forms [78]. The stability of the C-PC molecule is maintained by thioether bonds linking the chromophores to cysteine residues within the protein structure. In addition, amino acids such as serine, histidine, and aspartic acid help maintain the structural integrity of the molecule. Moreover, C-PC negatively charged regions as well as functional groups, such as carboxyl, amino, and thiol groups, that can interact with metal ions. In particular, cysteine residues, especially the β-84 position, have been identified as potential binding sites for heavy metals [65, 66]. A large proportion of hydrophobic amino acids, including glycine, alanine, valine, leucine, isoleucine, proline, phenylalanine, methionine, and tryptophan, are distributed on the surface of the C-PC hexamer. These residues may facilitate interactions with reactive oxygen species, thereby contributing to the molecule's radical scavenging activity [80]. The open-chain tetrapyrrole chromophore, by a unique system of conjugated double bonds, also contributes to the antioxidant activity of C-PC through radical-scavenging mechanisms [30]. Recent studies suggest that the structural resemblance of phycocyanobilin (PCB) to bilirubin may further contribute to the biological activity of C-PC. This similarity has been proposed to enhance heme oxygenase-1 expression, an important regulator of intracellular antioxidant defence pathways, thereby helping to reduce inflammation and oxidative stress associated with radiation-induced damage. In addition, due to its unique molecular structure, C-PC has been reported to inhibit triphosphopyridine nucleotide oxidase, which may contribute to protection against excessive oxidative processes [10].

The structural characteristics of C-PC, including its multimeric organization and reactive functional groups, are closely related not only to its biological activity but also to its physicochemical stability. C-PC is particularly sensitive to external factors such as pH, temperature, and light, which may induce conformational changes, dissociation of its subunits, and loss of functional properties. Therefore, particular attention must be paid to C-PC stability when developing technological formulations containing this bioactive compound.

Light exposure is one of the key factors affecting C-PC stability. As a photosensitive pigment, C-PC should be stored in light-protected conditions, as its degradation rate depends on both light intensity and wavelength. Exposure to light from fluorescent lamps or to ultraviolet light has been shown to accelerate degradation processes and reduce its antioxidant activity [81].

Temperature is another critical factor influencing C-PC stability. In general, C-PC derived from mesophilic cyanobacteria remains stable up to approximately 40 °C, whereas exposure to higher temperatures, particularly around 60 °C, leads to rapid degradation. However, the thermal stability of C-PC is strongly dependent on its biological origin. C-PC obtained from extremophilic cyanobacteria typically exhibits enhanced resistance to extreme temperature and pH conditions, thereby increasing its suitability for industrial applications. For instance, C-PC from thermophilic cyanobacteria such as *Thermosynechococcus elongatus* and *Thermosynechococcus vulcanus* demonstrates improved thermal stability, while C-PC isolated from cold-adapted cyanobacteria such as *Pseudanabaena* spp. remains stable at low temperatures [79]. These differences can be attributed to variations in the protein structure of C-PC derived from different microorganisms, which directly influence its thermal stability and degradation behaviour [82].

The pH of the surrounding environment also plays a crucial role in maintaining C-PC stability. C-PC is generally stable within a relatively narrow pH range (approximately pH 5.0–7.5) [12, 81]. Similar to temperature effects, pH stability may vary depending on the cyanobacterial source. For instance, C-PC isolated from thermotolerant *Oscillatoria* spp. has been shown to remain relatively stable over a broader pH range (pH 4–10), with significant degradation occurring only under highly acidic conditions (pH 2) [79].

These factors can induce structural changes in C-PC that promote aggregation and degradation, leading to loss of its characteristic blue colour and a reduced antioxidant activity [76, 81]. However, the combined effects of multiple environmental factors on C-PC stability, as well as the mechanisms underlying these interactions, remain poorly understood.

A. flos-aquae and *Microcystis aeruginosa*, like most freshwater cyanobacteria, are a mesophilic organism, with optimal growth at moderate temperatures. Consequently, C-PC derived from these species is expected to exhibit stability characteristics typical of mesophilic cyanobacteria, including limited thermal stability at elevated temperatures. In addition to environmental factors, other components of technological formulations may also influence C-PC stability. Interactions with excipients, including gelling agents, preservatives, and other formulation constituents, may either stabilize or destabilize

the protein depending on their physicochemical properties [16]. Therefore, selecting suitable formulation components are particularly important when developing C-PC-based systems. In this context, special attention in the present study was devoted to the development of hydrogel formulations. Hydrogels are considered suitable carriers for hydrophilic compounds such as C-PC due to their high-water content and structural compatibility [83, 84]. However, the selecting of an appropriate gelling agent is critical, as polymer-protein interactions may significantly influence C-PC stability.

Our study demonstrated that different gelling agents exert distinct effects on the stability of C-PC. Notably, C-PC remained relatively stable in hydrogels formulated with polysaccharide-based biopolymers, including sodium alginate, Soligel™, HEC, NaCMC, HPMC, and HEMC. These findings are consistent with previous studies indicating that polysaccharides can enhance C-PC stability. One mechanism underlying this effect is glycation, during which covalent interactions may form between reducing sugars and protein amino groups, thereby improving physicochemical properties of the resulting conjugates. In addition, polysaccharides bearing negatively charged functional groups, such as carboxyl or sulphate moieties, can interact electrostatically with positively charged amino acid residues on the surface of C-PC. Such interactions may contribute to improved structural stability and preservation of protein functionality [81]. In contrast, a decrease of approximately 12% in C-PC concentration was observed in chitosan-based hydrogels, which may be attributed to the combined effect of a mildly elevated temperature during preparation (not exceeding 40 °C) and a slightly acidic environment (pH 5.0). Although these conditions individually are not considered critical, their combined influence may have contributed to the partial destabilization of C-PC. The most pronounced decrease in C-PC concentration was observed in hydrogels formulated with Carbopol® Ultrez 21 and Pemulen™, where C-PC content decreased more than 50%. Importantly, these changes were accompanied by a visible fading of the characteristic blue coloration, indicating degradation of the chromophore structure. In Carbopol® Ultrez 21 formulations, sodium hydroxide was used for neutralization, resulting in a final pH of 4.5, whereas Pemulen™ formulations were neutralized with triethanolamine, yielding a pH of 6.8. Such pH conditions, together with potential polymer-protein interactions, may have contributed to the observed instability of C-PC.

The influence of preservative systems on C-PC stability was also evaluated, as preservatives may interact with protein-based active compounds, thereby affecting their structural integrity. The results demonstrated that different preservative systems exerted varying effects on C-PC stability, with SharoSENSE™ Plus 785 showing the least impact on C-PC degradation

among the tested systems. Based on these findings, hydrogels formulated with sodium alginate, Soligel™, and HEC, in combination with SharoSENSE™ Plus 785, were selected as the most suitable systems for further investigation, as they ensured both the structural stability of C-PC and microbiological safety. Among these, sodium alginate-based hydrogels were chosen for subsequent *in vitro* release studies due to their favourable stability profile and biocompatibility. Further investigations focused on evaluating the influence of PG on C-PC release from the hydrogel matrix.

The *in vitro* release study revealed a nearly linear release profile of C-PC from both hydrogel formulations, with and without PG (R^2 = 0.9995 and 0.9977, respectively), indicating a diffusion-controlled release mechanism while maintaining the integrity of the hydrogel matrix during the release period. The presence of PG significantly enhanced the release rate of C-PC, as evidenced by higher slope values and greater cumulative amounts released over time. This effect can be attributed to multiple mechanisms: when PG acts as a cosolvent, increasing the solubility within the hydrogel matrix, elevating the thermodynamic activity of the C-PC, and promoting its diffusion into the surrounding medium [85]. In addition, PG may interfere with intermolecular interactions within the hydrogel network. In alginate-based systems, the polymer matrix can effectively retain active compounds such as C-PC, but the presence of PG may weaken these interactions, for example, by disrupting hydrogen bonding or competing for binding sites. This reduces diffusion resistance and promotes the release of C-PC from the hydrogel [86]. In addition, PG may induce structural modifications within the hydrogel matrix, such as increased porosity or plasticization, thereby facilitating diffusion of C-PC molecules [86]. Similar effects of PG on drug release from polymeric systems have been reported in previous studies. For example, PG has been shown to enhance the release of loxoprofen from polymer matrices and licochalcone A from Carbomer 940 hydrogels, which is generally attributed to its ability to weaken drug-polymer interactions, for instance by competing for binding sites or disrupting intermolecular forces within the matrix [87, 88]. Notably, only approximately 10% of the C-PC was released within 6 h, indicating that the majority of the protein remained entrapped within the hydrogel matrix. This suggests strong interactions between C-PC and the polymer network. This behaviour may also be related to the intrinsic properties of sodium alginate as a controlled-release polymer [89]. Previous studies have shown that the release of C-PC from alginate-based systems is influenced by the ratio between the active compound and the polymer matrix, with lower C-PC-to-alginate ratios resulting in reduced release efficiency [90]. In the present study, the relatively low C-PC concentration (1%) may have further contributed to limited release, suggesting that increasing the

proportion of C-PC relative to the polymer could enhance its release from the hydrogel.

Importantly, the enhanced *in vitro* release of C-PC from PG-containing hydrogel translated into improved *ex vivo* skin permeation. While no penetration of C-PC was observed from hydrogels without PG, the presence of PG enabled the localization of C-PC within the stratum corneum. This effect is likely associated with PG's dual role, which not only increases the availability of C-PC at the skin surface by enhancing its release but also modifies the skin barrier. PG is known to interact with the lipid matrix of the stratum corneum, increasing lipid fluidity and permeability, thereby facilitating the diffusion of hydrophilic molecules into the outer skin layers [91-93]. Nevertheless, the extent of C-PC penetration remained limited, with the protein primarily localized within the stratum corneum. This indicates that, despite the enhancing effect of PG, delivering large hydrophilic biomolecules into deeper skin layers remains a significant challenge. Moreover, although chemical penetration enhancers such as PG can improve skin permeation by disrupting the lipid organization of the stratum corneum, this effect is not without limitations [33]. Alteration in the skin barrier may lead to irritation or potential long-term damage, which is undesirable, particularly in the context of preventive formulations for skin cancer intended for prolonged use, including by individuals with sensitive skin.

From a therapeutic perspective, deep skin penetration of C-PC may not always be necessary. Hydrogels containing C-PC may be particularly suitable for applications such as wound healing, where the active compound can act locally without extensive penetration through the stratum corneum. C-PC has been widely reported to promote wound healing through multiple complementary biological mechanisms. At the cellular level, C-PC stimulates fibroblast proliferation and migration, partly by inducing the G1 phase of the cell cycle and increasing the expression of cyclin-dependent kinases (cdK1 and cdK2) and activating signalling pathways such as phosphoinositide-3 kinase (PI-3K) pathway, which are essential for tissue regeneration [94, 95]. In addition, C-PC enhances key processes involved in the wound-healing cascade, including collagen deposition, granulation tissue formation, re-epithelialization, and angiogenesis, ultimately accelerating wound closure in *vivo* [10, 15, 16]. These regenerative effects are closely linked to the strong antioxidant and anti-inflammatory properties of C-PC, which help to reduce oxidative stress and downregulate pro-inflammatory cytokines such as TNF-α and IL-6, while promoting a favourable healing environment [15, 96]. Furthermore, C-PC contributes to wound healing by modulating the immune response, particularly by promoting the transition of macrophages from a pro-inflammatory (M1) to an anti-inflammatory (M2) phenotype, which supports

tissue regeneration [10]. Importantly, recent studies demonstrate that C-PC can be incorporated into advanced biomaterial systems, including nanoparticle-based and hydrogel formulations, thereby further enhancing its therapeutic potential. For example, C-PC-functionalized nanoparticles, such as copper sulphide-based systems, have been successfully incorporated into hydrogel matrices, resulting in improved antibacterial activity and enhanced wound-healing performance [10, 18]. In addition, C-PC has been incorporated into multifunctional hydrogel systems together with other bioactive compounds, such as gallic acid or probiotics, leading to enhanced antioxidant, anti-inflammatory, and antibacterial properties, as well as improved wound-healing outcomes [16, 97].

Taken together, these findings support the use of C-PC-containing hydrogels as promising topical systems for wound healing applications, where the active compound can exert its therapeutic effects locally without the need for extensive penetration through intact skin barriers. Based on these results, the developed C-PC hydrogel formulations could be further evaluated in wound-healing models to better assess their therapeutic efficacy under physiologically relevant conditions.

However, for other dermatological applications requiring deeper skin penetration without irritation, the limited ability of C-PC to permeate through the stratum corneum remains a significant challenge. This limitation underscores the need for advanced delivery strategies that enhance both the stability and skin penetration of C-PC. In this context, nanotechnology-based systems, such as transfersomes, represent a promising approach, as they are designed to improve the delivery of bioactive compounds across the skin barrier while protecting their structural integrity. Compared with other topical nanocarriers, such as conventional liposomes, transfersomes exhibit significantly higher skin penetration due to their ultra-deformable structure. In contrast to ethosomes, which contain ethanol, transfersomes may pose a lower risk of skin irritation [31]. In this study, C-PC-loaded transfersomes were prepared using a two-step approach that preserved the structural stability of C-PC while avoiding the use of organic solvents and stressful processing conditions. Preliminary experiments demonstrated that direct incorporation of C-PC into the primary dispersion, followed by sonication with a high-intensity ultrasonic disintegrator, resulted in approximately 80% degradation of C-PC, highlighting its sensitivity to mechanical and thermal stress. Therefore, an alternative loading strategy was employed, based on a two-step (remote loading) approach, in which empty transfersomes were first prepared, followed by the incorporation of C-PC into the pre-formed vesicles using ultrasonic bath sonication [98, 99]. This method, which relies on diffusion of the active compound into the vesicular system, enabled the preservation of

C-PC stability. No statistically significant decrease in C-PC concentration was observed in the final formulations, confirming that this approach maintains both the quantity and structural integrity of C-PC. The preservation of C-PC stability within the transfersome formulations was further supported by antioxidant activity assays. No significant differences were observed between free C-PC and C-PC encapsulated in transfersomes, indicating that the formulation process did not impair its functional properties. Since the biological activity of C-PC is closely associated with its structural integrity, the maintained antioxidant activity suggests that no major conformational changes occurred during preparation. C-PC was incorporated into transfersomes enriched with glycerol, sodium hyaluronate, or their combination to further improve the functional and technological properties of the delivery system. Glycerol was included due to its humectant and penetration-enhancing properties, as well as its ability to improve vesicle stability and flexibility, which are important for efficient skin delivery [100–102]. In addition, glycerol may increase the formulation's viscosity, thereby facilitating topical application [103, 104]. Sodium hyaluronate was selected for its well-established hydrating and skin-repairing properties, which are particularly beneficial in dermatological applications [104]. Previous studies have also demonstrated that transfersomes enriched with glycerol, hyaluronic acid, or their combination can enhance protein accumulation in both the epidermis and dermis, suggesting improved delivery performance [39]. In addition, cholesterol was incorporated into selected formulations (Gly-Chol-T, Hyal-Chol-T, and Hyal-Gly-Chol-T) to evaluate its effects on the physicochemical and technological properties of the developed transfersomes, as it is known to modulate membrane rigidity and stability [33, 103, 105, 106].

The physicochemical characterization of all developed transfersomal formulations demonstrated that the obtained nanosystems possessed properties suitable for topical delivery. Specifically, all formulations exhibited nanoscale mean diameters (< 115 nm), narrow size distributions (PI < 0.2), and sufficiently negative zeta potentials (< -30 mV). The vesicles were spherical, unilamellar, or oligolamellar depending on the formulation. It has been reported that nanosized (≤ 300 nm), homogeneous phospholipid vesicles can promote the delivery of active compounds into deeper skin layers, with their effectiveness being enhanced by vesicle flexibility [107]. Despite these comparable basic characteristics, notable differences emerged when evaluating encapsulation efficiency and long-term stability. Gly-T and Gly-Chol-T showed significantly higher encapsulation efficiency (~52%) compared to hyaluronate-containing systems (~33–37%), suggesting that simpler compositions may favour more efficient incorporation of hydrophilic macromolecules such as C-PC. It should be noted that, given the hydrophilic nature

of C-PC, the obtained encapsulation efficiency is appropriate and consistent with previously reported values. Hydrophilic compounds are generally associated with lower encapsulation efficiencies (typically 10–50%), as they tend to remain in the aqueous phase rather than being incorporated into the lipid bilayer of vesicular systems [108]. Stability studies further highlighted the critical role of formulation composition. The developed C-PC-loaded transfersomes were stored under conditions previously identified as optimal for preserving C-PC stability, namely at 4 °C and protected from light exposure. Under these conditions, glycerol-containing systems maintained their physicochemical properties over the 8-month storage period, whereas hyaluronate-only formulations (Hyal-T and Hyal-Chol-T) exhibited clear signs of instability, including an increase in particle size from approximately 108 and 101 nm at t_0 to 324 and 188 nm after 8 months, respectively) and increased polydispersity (from values < 0.2 to values ≥ 0.3). The inclusion of cholesterol may have contributed to improved stability, as it slightly reduced vesicle size, likely due to its role in stabilizing and tightening the phospholipid bilayer structure [109]. In addition, cholesterol-containing formulations generally exhibited more negative zeta potential values, which may further enhance colloidal stability [110]. Overall, glycerol appeared to play a key role in maintaining formulation stability by mitigating hyaluronate-mediated vesicle aggregation or fusion, even in systems containing both components (i.e., Hyal-Gly-T and Hyal-Gly-Chol-T). This stabilizing effect is likely associated with glycerol's stabilization of phospholipid bilayers, thereby preserving vesicle structure during storage [100–102].

A clear cytotoxic effect on HaCaT cells was observed at a C-PC concentration of 1000 µg/mL, whereas lower concentrations of 10 and 1 µg/mL maintained cell viability above 90% and 100%, respectively, with no significant differences between free and encapsulated C-PC. Importantly, all tested formulations preserved the cytoprotective activity of C-PC at 10 µg/mL under oxidative stress conditions, restoring cell viability from approximately 60% to 80% following H_2O_2 exposure. These findings are consistent with previous reports demonstrating that C-PC enhances cell viability under oxidative stress or UV-induced stress conditions [17, 36].

Based on the combined evaluation of encapsulation efficiency, stability, and biological performance, Gly-T and Gly-Chol-T were identified as the most promising formulations. These systems were therefore selected for further *ex vivo* skin penetration studies, in which their permeation was compared with that of C-PC in PBS solution, both with and without PG, to evaluate whether PG promotes C-PC permeation more effectively than the transfersomal systems themselves.

Due to its high molecular weight and hydrophilic nature, C-PC from solution exhibited limited penetration into the skin, with fluorescence detected only in a few regions of the stratum corneum. In contrast, PG, known for its ability to interact with the lipid matrix of the stratum corneum, increase lipid fluidity, and enhance skin permeability, led to increased C-PC accumulation in the superficial skin layer, as evidenced by a narrow fluorescent band. Notably, a more intense, thicker fluorescent signal was observed with C-PC-loaded transfersomes, particularly with Gly-T, indicating enhanced accumulation of C-PC in the stratum corneum. This enhanced accumulation can be attributed to the presence of edge activator – sodium deoxycholate, which increases membrane elasticity and confers high deformability to the transfersomes. This allows the vesicles to adapt to the narrow intercellular pathways of the stratum corneum. In addition, an osmotic gradient across the skin surface may further facilitate their movement through the skin barrier [31]. The slightly higher accumulation observed for Gly-T compared to cholesterol-containing formulations may be related to differences in vesicle flexibility, as cholesterol is known to stabilize and rigidify the phospholipid bilayer structure, potentially reducing deformability and limiting skin penetration [109]. Similarly, variability in skin delivery has been reported in the literature depending on the carrier system. For instance, C-PC incorporated into PEG-hyalurosomes demonstrated measurable accumulation in both the epidermal and dermal layers of neonatal pig skin after 8 h of application [35]. Liposomal formulations evaluated on human skin showed no evidence of transdermal permeation, with the compound largely confined to the superficial layers and only a small fraction (approximately 3%) of the applied dose retained [37]. It should be noted, however, that direct comparison between these studies is limited by the use of different skin models, including human, porcine, and other biological membranes, which may differ substantially in their barrier properties and permeability characteristics.

Although transfersomal systems enhanced the accumulation of C-PC in the stratum corneum, deeper skin penetration was not observed under the applied experimental conditions, as determined by qualitative analysis. However, the increased accumulation of C-PC in the stratum corneum may indicate the formation of a surface reservoir, from which the active compound could be gradually released into deeper skin layers over time. This enhanced accumulation may be advantageous for cosmetic and preventive dermatological applications, particularly in contexts where antioxidant protection is needed, such as exposure to UV radiation and environmental pollutants.

The Gly-T formulation was further evaluated in an *in vivo* model to determine whether C-PC-loaded transfersomes could serve as a preventive strategy during the early stages of skin carcinogenesis initiation. To achieve

this objective, the widely established DMBA/TPA mouse model was employed. In this model, a single topical application of DMBA is followed by repeated TPA treatments. DMBA acts as a mutagenic initiator, inducing irreversible genetic alterations by forming of covalent DNA adducts, that may subsequently lead in irreversible mutations, although no apparent histological changes are observed at this stage [111, 112]. Subsequent repeated applications of TPA function as a pro-inflammatory tumour promoter, stimulating clonal expansion of initiated cells and driving the progression of carcinogenesis [113].

Skin carcinogenesis in this model follows a multistep process characterized by epidermal hyperproliferation, development of benign papilloma, and potential progression to squamous cell carcinoma, depending on the duration of exposure, carcinogen dose, and experimental conditions [114]. Carcinogenesis itself is a complex, multistage process involving initiation, promotion, progression, and, ultimately, malignant transformation [113].

In the present study, pronounced skin irritation in the carcinogen-treated group was observed after 4–5 weeks, characterized by marked erythema, dryness, scaling, and the appearance of superficial lesions. Due to animal welfare requirements, the TPA vehicle was modified from acetone to an acetone/PEG mixture, resulting in a temporary reduction of skin irritation and partial skin recovery. Nevertheless, in one animal from Group III, a skin nodule of up to 6 mm developed during this period. Upon reintroduction of TPA in acetone from week 13, a clear increase in skin irritation and inflammatory responses was again observed.

Although tumour formation in this model typically occurs within approximately 7 to 20 weeks of continuous promotion [114], the full development of invasive squamous cell carcinoma was not achieved within the 16-week experimental period. However, the carcinogen-treated group exhibited clear macroscopic signs of early pathological changes, including pronounced dryness, scaling, erythema, inflammatory alterations, and small papule-like lesions on the dorsal skin. These observations were confirmed by histopathological analysis, which revealed significant epidermal thickening, hyperplasia, dysplasia, and increased inflammatory activity in both the epidermis and dermis compared with non-carcinogen-treated groups. In addition, carcinogen exposure markedly increased epidermal mitotic activity, reaching 12 (1.23) mitoses per 2.37 mm^2, whereas the control groups without carcinogen exposure exhibited only 2–3 mitoses per 2.37 mm^2. A significant increase in mast cell density was also observed in the carcinogen-treated group (38.6 (2.48) mast cells per 2.37 mm^2) compared with non-carcinogen-treated groups (approximately 20–26 mast cells per 2.37 mm^2), indicating activation of the dermal inflammatory microenvironment. Immunohistochemical analy-

sis further demonstrated significantly elevated Ki-67 expression in both basal (65.4 (3.67)%) and suprabasal (26.78 (3.47)%) epidermal layers compared with the non-carcinogen group. Ki-67 is a nuclear protein widely used as a marker of cellular proliferation. It is expressed during all active phases of the cell cycle (G1, S, G2, and M), but is absent in quiescent cells (G0), making it a reliable indicator of proliferative activity in both normal and pathological tissues. Importantly, increased Ki-67 expression may also be observed in preneoplastic or non-tumorous tissues exposed to carcinogenic stimuli, reflecting early proliferative changes that precede tumour formation [113, 115].

These findings are consistent with the concept that chronic inflammation plays a central role in early tumour promotion by creating a microenvironment favourable for carcinogenesis [24]. Inflammatory mediators and signalling pathways contribute to sustained epidermal hyperproliferation, impaired differentiation, and progressive architectural disorganization of the skin. At the molecular level, these processes are closely linked to dysregulation of cell cycle control, particularly at the G1/S transition. Activation of cell cycle regulators such as cyclin-dependent kinase 4 (CDK4), together with modulation of NF-κB signalling, plays a critical role in promoting epidermal tumorigenesis [21].

Taken together, although invasive carcinoma was not achieved within the experimental timeframe, the observed structural and inflammatory alterations represent biologically relevant early stages of carcinogenesis. These stages are particularly important for evaluating preventive strategies, as modulation of the inflammatory microenvironment and epidermal proliferation at this stage may significantly influence subsequent tumour development.

In the carcinogen-treated groups receiving transfersome-based formulations with or without C-PC, the skin appeared visibly less irritated than in carcinogen-only group (Group III). These animals exhibited only mild dryness, and a few showed superficial skin erosions, while only two animals in the group treated with empty transfersomes developed small papule-like lesions. Histopathological analysis further confirmed these observations, demonstrating significantly reduced epidermal thickness, decreased rete ridge depth, lower grades of hyperplasia and dysplasia, and a less pronounced inflammatory response compared with the carcinogen-only group. Notably, these improvements were also clearly observed in the group treated with empty transfersomes.

The observed protective effect of empty transfersomes may be explained by the critical role of the skin barrier during the tumour promotion stage of carcinogenesis. The stratum corneum functions as the primary barrier regulating transepidermal water loss and limiting the penetration of external agents. The skin barrier is a complex, integrated system composed of

physical, chemical, microbiological, and immunological components, that contribute to maintaining tissue homeostasis and preventing inflammation [116]. Glycerol plays a key role in maintaining epidermal hydration and barrier integrity, as it is abundantly present in the stratum corneum and is involved in water retention and lipid organization. In addition, glycerol transport via aquaporin-3 in keratinocytes helps maintain appropriate hydration levels, whereas disruption of this system has been associated with various skin disorders, including psoriasis and nonmelanoma skin cancer [117]. Furthermore, glycerol may indirectly support skin homeostasis through interactions with the cutaneous microbiome. Commensal microorganisms can metabolize glycerol into bioactive compounds, such as lactic acid, which inhibit the growth of pathogenic bacteria and promote the expression of genes associated with barrier function [118]. Beyond its role as a humectant, glycerol has also been shown to exert anti-inflammatory effects, including reduction of erythema, epidermal thickness, and inflammatory responses in experimental skin models [119]. In this context, glycerol-containing transfersomal formulations may modulate cutaneous responses by supporting barrier stabilization and improving skin hydration, thereby contributing to the maintenance of epidermal homeostasis and attenuation of inflammatory processes.

In addition to carrier-related effects, C-PC may also contribute to maintaining skin barrier integrity. Key structural proteins such as involucrin, loricrin, and filaggrin play essential roles in the formation of the cornified envelope and in maintaining the stratum corneum's moisture. Disruption of their expression is associated with impaired barrier function and increased susceptibility to environmental damage. Experimental evidence suggests that C-PC can counteract such alterations by enhancing the expression of these proteins [17].

Structural epidermal and dermal alterations, such as epidermal thickening, rete ridge elongation, hyperplasia, dysplasia, and inflammation, likely reflect the cumulative effects of carcinogen exposure over the entire experimental period. The experimental design, which included modifications of the TPA vehicle to comply with animal welfare requirements, introduced phases of varying irritation intensity. This may have resulted in differential contributions of early and late carcinogenic stimuli to the observed endpoints. In contrast, proliferative and inflammatory markers, including Ki-67 expression, mitotic activity, and mast cell density, are more sensitive to recent TPA-induced stimulation, particularly during the final experimental phase. In the present study, treatment with C-PC-loaded transfersomes significantly reduced mitotic activity and mast cell density at both tested concentrations. Moreover, the higher C-PC concentration resulted in a statistically significant

reduction in total, basal, and suprabasal Ki-67 expression compared with the carcinogen-only group. A significant positive correlation was also observed between dermal inflammation severity and mast cell density, while suprabasal Ki-67 expression showed a strong association with epidermal thickness, rete ridge depth, and dysplasia grade. These findings indicate that C-PC-loaded transfersomes can modulate both proliferative and inflammatory processes during the early promotion stage of carcinogenesis. It may also be hypothesized that increased disruption of the skin barrier could facilitate deeper penetration of C-PC, potentially leading to a more pronounced biological effect. Previous studies suggest that C-PC exerts antitumor activity through multiple mechanisms, including cell cycle arrest in specific phases, induction of apoptosis, and regulation of oxidative stress and inflammatory pathways [120]. Among these, its antioxidant properties appear to play a particularly important role. C-PC has been shown to significantly reduce intracellular reactive oxygen species (ROS) levels in human keratinocytes and fibroblasts exposed to oxidative stress, while simultaneously enhancing the activity of antioxidant enzymes, such as superoxide dismutase (SOD) and catalase (CAT), and nonenzymatic antioxidants, such as glutathione (GSG), reducing lipid peroxidation, and increasing total antioxidant capacity [15, 16, 29]. Reduction of oxidative stress is closely linked to attenuation of inflammatory responses. In the present study, a complete reduction of moderate and severe inflammation was observed in the low-dose C-PC transfersome group, whereas the higher concentration demonstrated only partial attenuation, particularly in severe inflammation. This was accompanied by a decrease in mast cell accumulation in the dermis, further supporting a modulatory effect on the inflammatory microenvironment. These findings are consistent with previous reports demonstrating that C-PC can regulate inflammatory signalling pathways, including inhibition of COX-2 and reduction of pro-inflammatory cytokines: IL-1α, IL-1β, IL-4, IL-6, tumour necrosis factor TNF-α, while promoting anti-inflammatory mediators, such as IL-10 [15, 78]. Targeting early pathogenic mechanisms, such as oxidative stress, inflammation, and abnormal cellular proliferation, has been consistently recognized as a key strategy for preventing skin tumour development. This concept is well supported by previous studies demonstrating that modulation of these pathways can effectively attenuate carcinogenesis. For example, pterostilbene has been shown to significantly reduce tumour incidence, tumour multiplicity, and epidermal hyperplasia in the DMBA/TPA-induced multistage skin carcinogenesis model, accompanied by decreased Ki-67 expression, indicating suppression of keratinocyte proliferation [113]. Similarly, natural compounds such as *Ganoderma lucidum* extracts have been reported to attenuate UV-induced skin carcinogenesis by reducing chronic inflamma-

tion and restoring normal epidermal architecture [115]. In addition, pharmacological agents such as the non-β-blocking enantiomer of carvedilol have demonstrated the ability to inhibit UV-induced oxidative stress, inflammatory signalling, and epidermal hyperproliferation in the mouse skin, further supporting the importance of targeting these early pathogenic processes [121]. Meanwhile, C-PC has been shown to reduce the expression of pro-inflammatory cytokines, decrease epidermal thickness, and suppress proliferative processes in psoriasis models [122, 123].

In terms of safety, the results demonstrated that the topical application of C-PC-loaded transfersomes to healthy skin was well tolerated. No signs of skin irritation were observed, even at the relatively high concentration of 10 mg/mL. Histopathological evaluation of non-carcinogen-treated groups confirmed these findings, as the epidermis retained its normal architecture, characterized by a thin, well-organized structure with only a few keratinocyte layers, uniform nuclei, and short, regular rete ridges. No evidence of hyperplasia, dysplasia, oedema, or inflammatory infiltration was detected, indicating that C-PC-loaded transfersomes did not induce structural or proliferative alterations in intact skin. Furthermore, histological examination of internal organs revealed no histopathological alterations, indicating the absence of histopathological evidence of systemic toxicity following topical application of C-PC-loaded transfersomes. The safety profile observed in the present study is consistent with previous reports demonstrating the low toxicity of C-PC across various *in vivo* models. Both topical and injectable formulations of C-PC have been reported to be well tolerated, with no evidence of organ damage or adverse histological changes, even at relatively high doses [10, 22, 124].

This study demonstrated the successful isolation of C-PC from cyanobacterial biomass collected from natural water sources, highlighting not only its biomedical potential but also the possibility of using naturally occurring biomass as a sustainable resource. Particular attention was given to the purity, safety, and stability of the isolated C-PC to ensure its suitability for biomedical applications. The development of C-PC-loaded transfersomal formulations improved the topical delivery of C-PC. The results showed that transfersomes increased the deposition of C-PC in the stratum corneum and had beneficial effects during the early promotion stage of skin carcinogenesis, including reduced inflammatory and proliferative markers and less pronounced histopathological changes associated with early tumour development.

However, several limitations of the present study should be acknowledged. First, the safety assessment of the cyanobacterial biomass and isolated C-PC was limited. Cyanotoxins were analysed in the collected biomass,

and C-PC samples used for the preparation of transfersomal formulations in the *in vivo* study was isolated from non-toxic biomass. In addition, the concentrations of selected heavy metals (Pb, Cd, As, and Hg) were determined in C-PC samples. However, a more comprehensive safety assessment including a wider range of potential contaminants is needed to fully evaluate the suitability of the raw material for pharmaceutical applications. Second, the structural stability of C-PC was evaluated during the preparation of hydrogels and transfersomes. In addition, the physical stability of C-PC-loaded transfersomal formulations was assessed by monitoring changes in MD, PI and ZP during 8 months of storage at 4 °C under light-protected conditions. However, the structural stability of C-PC after long-term storage and microbiological quality of the formulations were not evaluated. Therefore, further studies are needed to assess the long-term stability and microbiological safety of the developed formulations. Third, the *ex vivo* skin permeation studies provided qualitative information on the localization of C-PC in the skin. However, quantitative determination of C-PC accumulation and penetration into individual skin layers was not performed. Therefore, future studies should include quantitative analytical methods to better evaluate the skin delivery of C-PC. Furthermore, the experimental model focused on the early-stages of DMBA/TPA-induced skin carcinogenesis, and the progression to invasive squamous cell carcinoma was not achieved during the study period. Therefore, the effects of C-PC-loaded transfersomes on the later stages of carcinogenesis remain unclear. Future studies should evaluate their impact on the progression of precancerous lesions and squamous cell carcinoma, as well as their efficacy in other models, such as UV-induced skin damage. In addition, only male animals were included in the experimental design. As sex-related differences in skin physiology, hormonal regulation, and inflammatory responses may influence carcinogenesis and treatment outcomes, future studies involving both sexes would provide a better understanding of the observed effects. Finally, the developed formulations were not directly compared with an established topical therapeutic agent used in clinical practice. Such comparative studies would be valuable for assessing the efficacy and clinical potential of C-PC-loaded transfersomal formulations.

4. SUMMARY OF THE CONCLUSIONS

1. C-PC samples were isolated from naturally collected cyanobacterial biomass, and its quality parameters were found to depend on biomass composition and the purification methods used. Higher C-PC purity was achieved using ion-exchange chromatography. It was also determined that the content of heavy metals in C-PC samples was influenced by the dominant cyanobacterial genus in the biomass, environmental conditions, and the purification method. Considering safety aspects, C-PC samples isolated from *A. flos-aquae* biomass and purified by ion-exchange chromatography, with higher purity and lower heavy-metal contamination, were selected for further studies.
2. Topical technological formulations containing C-PC were successfully developed, and their physicochemical properties, as well as C-PC structural stability, were found to depend on formulation composition. Hydrogels based on polysaccharide gelling agents (sodium alginate, Soligel™, HEC, NaCMC, HPMC, and HEMC) ensured better C-PC stability, whereas synthetic polymers (Carbopol® Ultrez 21, Pemulen™) and certain conditions (pH, temperature) negatively affected its structural stability. The choice of preservatives also had a significant impact, with SharoSENSE™ Plus 785 ensuring optimal C-PC stability and microbiological safety. *In vitro* studies demonstrated that PG significantly increased the release rate of C-PC from the hydrogel. However, a substantial portion of C-PC remained entrapped within the hydrogel, indicating strong interactions between the protein and the polymer network and suggesting controlled-release properties. The developed controlled-release hydrogels containing C-PC may be further investigated in wound-healing models. To improve C-PC stability and skin delivery, nanotechnology-based transfersomal formulations were also developed. The application of a two-step preparation method preserved the structural integrity and biological activity of C-PC, as confirmed by spectrophotometric analysis, antioxidant activity, and cytocompatibility studies. All developed transfersomal formulations exhibited physicochemical properties suitable for topical application, while glycerol-containing formulations (Gly-T and Gly-Chol-T) showed higher encapsulation efficiency and better long-term stability.

3. *Ex vivo* studies demonstrated that C-PC skin delivery from technological formulations depends on the delivery system and formulation composition. C-PC exhibited limited penetration from conventional formulations (hydrogels and solutions) due to its high molecular weight and hydrophilic nature, and in the absence of penetration enhancers, was practically undetectable in the skin. PG slightly increased C-PC accumulation in the stratum corneum, although its effect remained limited. Transfersomal nanocarrier systems improved C-PC delivery into the skin by increasing its deposition in the stratum corneum and demonstrated superiority over other tested systems. Although deeper skin penetration was not observed, increased deposition in the stratum corneum may act as a reservoir allowing gradual diffusion of C-PC into deeper skin layers. However, this assumption requires quantitative confirmation in future studies.
4. *In vivo* studies demonstrated that C-PC-loaded transfersomal formulations attenuated DMBA/TPA-induced inflammatory, proliferative, and dysplastic skin changes. C-PC-loaded transfersomes reduced macroscopic skin alterations, including erythema, dryness, scaling, and papule formation. Histopathological analysis showed that C-PC formulations attenuated epidermal thickening, rete ridge elongation, hyperplasia, and dysplasia, and reduced mitotic activity compared with the carcinogen-only group. A decrease in mast cell density and inflammatory response was also observed. Immunohistochemical analysis confirmed an antiproliferative effect, as C-PC transfersomes significantly reduced Ki-67 expression, particularly in the suprabasal epidermal layer. C-PC transfersomes were well tolerated and did not induce structural or proliferative changes in healthy skin.

SUMMARY IN LITHUANIAN

Įvadas

Melsvabakterės (melsvadumbliai) yra vienos seniausių Žemėje gyvuojančių organizmų rūšių – jos atsirado prieš daugiau kaip 3,5 mlrd. metų ir atliko svarbų vaidmenį formuojantis deguonimi prisotintai Žemės atmosferai [1, 2]. Melsvabakterių gebėjimas daugintis ir išlikti nuolat kintančiomis aplinkos sąlygomis atspindi jų pažangius adaptacinius mechanizmus, susijusius su šių organizmų sintetinamais biologiškai aktyviais junginiais, pasižyminčiais citotoksinėmis, priešgrybelinėmis, priešbakterinėmis ir priešvirusinėmis savybėmis, kurios užtikrina apsaugą, konkurencinį pranašumą ir išlikimą [1]. Melsvabakterės yra natūrali vandens ekosistemų dalis, tačiau klimato kaita, didėjanti CO_2 koncentracija ir eutrofikacija lemia dažnesnius, intensyvesnius ir ilgesnius jų žydėjimo epizodus, sukeliančius ekologines problemas bei riziką visuomenės sveikatai [3–6]. Intensyvus melsvabakterių žydėjimas sutrikdo ekosistemų pusiausvyrą, nes didina organizmų konkurenciją dėl pagrindinių išteklių, pvz., šviesos, deguonies ir maistinių medžiagų [6]. Be to, melsvabakterės gali gaminti bioaktyvius, potencialiai toksiškus junginius, keliančius pavojų žmogaus sveikatai [7]. Didėjantis šios problemos mastas skatina ieškoti veiksmingų sprendimo būdų [3]. Viena iš skubių priemonių yra melsvabakterių perteklinės biomasės mechaninis surinkimas [5]. Vadovaujantis tvarumo ir žiedinės ekonomikos principais, surinktą melsvabakterių biomasę galima panaudoti kaip vertingą žaliavą bioaktyviems junginiams išgauti [8].

C-fikocianinas (C-PC) yra vienas iš melsvabakterėse esančių bioaktyvių junginių. Tai vandenyje tirpus pigmentas, priklausantis fikobiliproteinų grupei ir atliekantis svarbų vaidmenį fotosintezėje – sugeria šviesos energiją ir perduoda ją chlorofilo turintiems fotosintezės kompleksams [9]. Be šios funkcijos, C-PC pasižymi įvairiapusiu biologiniu aktyvumu, susijusiu su jo antioksidacinėmis ir priešuždegiminėmis savybėmis [10, 11]. C-PC antioksidacinis poveikis pasižymi gebėjimu neutralizuoti reaktyviąsias deguonies formas ir reguliuoti oksidacinio streso signalinius kelius, mažinant ląstelių pažeidimus [12, 13]. C-PC taip pat stiprina endogeninę antioksidacinę apsaugą, didindamas superoksido dismutazės, katalazės ir glutationo peroksidazės aktyvumą bei mažindamas lipidų peroksidaciją [14]. Priešuždegiminis poveikis siejamas su ciklooksigenazės-2 (COX-2) slopinimu ir prouždegiminių citokinų (IL-1, IL-6, TNF-α) raiškos mažinimu [9, 15, 16]. Be to, C-PC pasižymi apsauginiu poveikiu nuo ultravioletinių (UV) spindulių sukeltos odos pažaidos – mažina reaktyviųjų deguonies formų kiekį, slopina matrikso

metaloproteinazių aktyvumą ir padeda išsaugoti kolageno struktūrą, todėl yra perspektyvi medžiaga, galinti pristabdyti fotosenėjimo procesus [14, 17]. Taip pat nustatyta, kad C-PC skatina audinių regeneraciją ir žaizdų gijimą [10, 16, 18]. Molekuliniu lygmeniu C-PC veikia ląstelių apoptozės ir senėjimo procesus per PI3K/AKT/mTOR signalinius kelius bei reguliuoja melanogenezę per p38/MAPK ir ERK kelius [19, 20]. C-PC pasižymi priešnavikiniu aktyvumu melanomos atveju – slopina ląstelių proliferaciją ir migraciją, moduliuoja MAPK signalinius kelius bei ląstelės ciklo reguliatorius, gali slopinti angiogenezę ir naviko progresavimą, selektyviai veikdamas navikines ląsteles [21]. Be to, jis gali moduliuoti naviko mikroaplinką, stiprindamas imuninį atsaką ir didindamas CD4+ bei CD8+ T limfocitų ir B ląstelių infiltraciją [22]. Apibendrinant, C-PC yra daugiafunkcinis junginys, veikiantis pagrindinius su odos senėjimu ir kancerogeneze susijusius procesus: oksidacinį stresą, uždegimą, ekstraląstelinio matrikso degradaciją, ląstelių senėjimą ir melanogenezę. Tačiau C-PC profilaktinio taikymo galimybės vietinio poveikio sistemose, skirtose ankstyvosioms odos plokščialąstelinės karcinomos (cSCC) stadijoms, tebėra nepakankamai ištirtos, ypač *in vivo* sąlygomis.

Odos vėžio paplitimas pasaulyje nuolat didėja ir sudaro apie trečdalį visų onkologinių susirgimų [23]. Ši tendencija siejama su visuomenės senėjimu ir pažangesniais diagnostikos metodais [24]. Odos plokščialąstelinė karcinoma yra viena dažniausių piktybinių odos neoplazijų, kurios vystosi dažniausiai palaipsniui – nuo aktininės keratozės (AK) ir intraepiderminės displazijos iki invazinės karcinomos. Šį procesą lydi epidermio struktūros pokyčiai, padidėjusi keratinocitų proliferacija ir sutrikusi diferenciacija [24]. Odos plokščialąstelinės karcinomos vystymąsi sąlygoja daugybė rizikos veiksnių, pvz., UV spinduliuotė, vyresnis amžius, šviesios odos tipas, imunosupresija, rūkymas ir paveldimumas [25]. Odos senėjimas skirstomas į vidinį (chronologinį) ir išorinį (fotosenėjimą), kurį daugiausia lemia UV spinduliuotė [26]. UV spinduliai skatina reaktyviųjų deguonies formų susidarymą, sukelia oksidacinį stresą ir pažeidžia odos antioksidacinę sistemą [17]. Odos senėjimui būdingas regeneracijos sumažėjimas, struktūriniai pokyčiai, sutrikusi barjerinė funkcija, lėtesnis žaizdų gijimas bei homeostazės disbalansas. Ląstelių senėjimas (senescencija) – vienas pagrindinių odos senėjimo veiksnių, pasižyminčių galutinai nuslopintu ląstelių ciklu bei su senescencija susijusio sekrecinio fenotipo formavimusi, kuriam būdinga prouždegiminių citokinų, matriksą ardančių fermentų ir augimo veiksnių sekrecija [27]. Tokie pokyčiai, kartu su lėtiniu uždegimu, sudaro mikroaplinką, palankią navikų vystymuisi [26]. Molekuliniu lygmeniu ankstyvą cSCC vystymąsi lemia TP53 (TP53 – naviką slopinantis genas, koduojantis p53 baltymą – vieną svarbiausių ląstelės ciklo ir DNR pažaidos kontrolės reguliatorių, dažnai vadinamą „genomo sergėto-

ju“) funkcijos praradimas, ląstelės ciklo reguliacijos sutrikimai ir prouždegiminių signalinių kelių aktyvacija [24].

Atsižvelgiant į šiuos mechanizmus, ypač svarbios yra prevencinės priemonės, nukreiptos į ankstyvuosius patogenezės etapus – oksidacinį stresą, uždegimą ir ekstraląstelinio matrikso remodeliavimą. Šiuo požiūriu C-PC yra perspektyvus junginys, galintis prisidėti prie ankstyvųjų odos plokščialąstelinės karcinomos stadijų prevencijos [28].

Kuriant vietinio poveikio technologines formuluotes su C-PC, būtina užtikrinti tinkamą šio junginio grynumą, stabilumą ir skvarbą į odą. C-PC grynumas vertinamas pagal spektrofotometriškai nustatytą absorbcijos santykį (A_{620}/A_{280}) ir yra tiesiogiai susijęs su jo biologiniu veiksmingumu ir taikymo galimybėmis [29]. Kai C-PC išskiriamas iš natūralios melsvabakterių biomasės, svarbu įvertinti galimą jos užterštumą cianotoksinais ir sunkiaisiais metalais, nes tai gali kelti saugumo problemų ir riboti C-PC panaudojimo galimybes.

C-PC stabilumo užtikrinimas taip pat yra vienas pagrindinių iššūkių, kuriant technologines formuluotes su šia biologiškai aktyvia medžiaga. Iš mezofilinių melsvabakterių rūšių išskirtas C-PC paprastai yra termiškai nestabilus ir gali denatūruotis aukštesnėje nei 40 °C temperatūroje. Be to, jo stabilumas stipriai priklauso nuo pH – optimalus stabilumas stebimas esant pH, artimam neutraliam, o rūgštinėje ar šarminėje terpėje jis reikšmingai sumažėja [12]. C-PC taip pat yra jautrus aplinkos veiksniams, pvz., šviesai ir slėgiui, jo stabilumą gali paveikti sąveika su kitais technologinės formuluotės komponentais [16, 30]. Visi šie veiksniai gali turėti įtakos C-PC struktūriniam vientisumui ir biologiniam aktyvumui, todėl į juos būtina atsižvelgti kuriant technologines formuluotes.

Kitas svarbus vietinio poveikio technologinių formuluočių kūrimo aspektas yra veikliosios medžiagos skvarba į odą. Raginis sluoksnis (stratum corneum), išorinis odos sluoksnis, susidarantis iš 10–15 sluoksnių negyvų, keratinu turtingų ląstelių (keratinocitų), yra pagrindinis barjeras vietiškai ir transdermiškai vartojamoms medžiagoms prasiskverbti [31]. Pasyvi skvarba per raginį sluoksnį priklauso nuo junginių fizikocheminių savybių, pvz., mažos molekulinės masės, vidutinio lipofiliškumo ir subalansuoto tirpumo tiek vandeninėje, tiek lipidinėje terpėje [26]. Tuo tarpu C-PC yra hidrofilinė makromolekulė, kurios subvienetų α- ir β-polipeptidinių grandinių molekulinė masė yra atitinkamai apie 10–19 kDa ir 14–21 kDa, o kiekvienas subvienetas yra kovalentiškai susijungęs su fikocianobilino chromoforais, suteikiančiais būdingą spalvą ir šviesos sugerties savybes [11, 32]. Šie subvienetai gali jungtis į aukštesnės struktūros kompleksus – trimerus $(\alpha\beta)_3$ (~120 kDa) ir heksamerus $(\alpha\beta)_6$ (~240 kDa), o tai dar labiau riboja jų gebėjimą prasiskverbti per odos barjerą [11]. Taigi, ribota C-PC skvarba į odą išlieka viena

pagrindinių problemų ir svarbia kryptimi kuriant veiksmingas vietinio poveikio technologines formuluotes.

Siekiant įveikti raginio sluoksnio barjerines savybes ir pagerinti veikliųjų medžiagų skvarbą į odą, sukurta įvairių strategijų. Galima išskirti cheminius veiksnius ir fizinius metodus. Cheminiai skvarbą gerinantys junginiai, pvz., glikoliai, etanolis, terpenai ir azono dariniai, sutrikdo raginio sluoksnio lipidų struktūrą, todėl pagerina veikliųjų medžiagų difuziją, tačiau gali dirginti odą ir sukelti ilgalaikius pažeidimus [16, 33]. Dažnai naudojamas propilenglikolis (PG), tačiau duomenų apie jo veiksmingumą, gerinant C-PC skvarbą, vis dar trūksta. Siekiant pagerinti transderminį veikliųjų medžiagų tiekimą taip pat tiriami fiziniai metodai, pvz., jonoforezė, sonoforezė, elektroporacija, mikroadatos ir terminė ar mechaninė abliacija. Nors šie metodai yra veiksmingi, jie dažnai siejami su diskomfortu, didelėmis sąnaudomis ir prastesniu pacientų gydymo režimo laikymusi, todėl jų praktinis taikymas yra ribotas [31, 33]. Tuo tarpu, tiekimo sistemos, sukurtos nanotechnologijų pagrindu, tampa perspektyvia kryptimi vaistinių medžiagų tiekimui į odą pagerinti. Nanonešikliai pagerina veikliųjų medžiagų prasiskverbimą, apsaugo jas nuo degradacijos ir iš dalies įveikia raginio sluoksnio barjerinę funkciją [31, 34]. Ankstesni tyrimai parodė, kad nanodispersinės sistemos gali pagerinti baltyminės kilmės junginių, pvz., C-PC, patekimą į odą, padidindamos jų skvarbą per raginį sluoksnį [14]. Tiriamos įvairios fosfolipidinės vezikulinės sistemos, pvz., liposomos, etosomos ir skvarbą gerinančius komponentus turinčios vezikulės, skirtos bioaktyvių junginių, taip pat ir C-PC, tiekimui į odą [35–37]. Transfersomos – ypač perspektyvi nanodispersinė sistema. Tai yra fosfolipidinės vezikulės, turinčios membranos lankstumą didinančių komponentų, leidžiančių joms prasiskverbti per tarpląstelinius raginio sluoksnio lipidų kelius [38]. Tyrimai parodė, kad transfersomos pagerina baltyminės kilmės junginių patekimą į gilesnius odos sluoksnius ir jų biologinį aktyvumą [39, 40]. Be to, šios sistemos didina veikliųjų medžiagų stabilumą, gerina tirpumą ir palengvina hidrofilinių biomolekulių, pvz., baltymų ir peptidų, tiekimą į odą [33, 41]. Atsižvelgiant į tai, šio tyrimo tikslas buvo sukurti ir įvertinti technologines formuluotes su C-PC, siekiant pagerinti C-PC stabilumą ir skvarbą į odą, taip pat ištirti jų galimą apsauginį poveikį ankstyvosioms odos kancerogenezės stadijoms.

Šios disertacijos tikslas – išskirti C-PC iš natūraliai surinktos melsvabakterių biomasės, įvertinti jo kiekybinius ir kokybinius rodiklius, sukurti stabilias ir efektyvia odos skvarba pasižyminčias vietinio poveikio C-PC technologines formuluotes, bei ištirti jų poveikį uždegiminiams, proliferaciniams ir displaziniams pokyčiams odoje ankstyvosiose odos kancerogenezės stadijose.

Darbo uždaviniai:

1. Išskirti C-PC iš natūraliai surinktos melsvabakterių biomasės ir nustatyti C-PC mėginių grynumą bei atlikti sunkiųjų metalų kiekybinę analizę.
2. Sukurti vietinio poveikio technologines formuluotes su C-PC mėginiais ir įvertinti jų fizikines- chemines savybes bei C-PC stabilumą šiose sistemose.
3. Įvertinti C-PC skvarbą į odą iš sukurtų formuluočių *ex vivo* sąlygomis.
4. Įvertinti technologinių formuluočių su C-PC poveikį uždegiminiams, proliferaciniams ir displaziniams pokyčiams odoje ankstyvosiose odos kancerogenezės stadijose, naudojant DMBA/TPA sukeltą pelių kancerogenezės modelį.

Mokslinis naujumas ir praktinė reikšmė

Atliktų tyrimų rezultatais siekiama prisidėti prie tvarumo idėjų sklaidos ir žiedinės ekonomikos principų puoselėjimo. Perteklinės melsvabakterių biomasės surinkimas iš vandens telkinių padeda spręsti ekologines problemas, susijusias su vandens „žydėjimu“, ir sudaro galimybes panaudoti šią biomasę aukštos pridėtinės vertės biologiškai aktyviems junginiams, pavyzdžiui, C-PC, išgauti.

Tyrimas patvirtina, kad taikant tinkamus ekstrahavimo ir gryninimo metodus, C-PC gali būti sėkmingai išskiriamas iš gamtoje surinktos melsvabakterių biomasės. Šiame darbe ypatingas dėmesys skirtas medžiagos saugumui vertinti – ištirtas sunkiųjų metalų (švino, kadmio, arseno ir gyvsidabrio) kiekis C-PC mėginiuose. Sunkiųjų metalų nustatymas yra svarbus eksperimentinėje medžiagoje, kuri išskirta iš natūralios kilmės melsvabakterių biomasės, kaupiančios metalų jonus iš aplinkos.

Technologiniu požiūriu tyrimas pateikia praktinius sprendimus C-PC formuluotėms kurti. Eksperimentų metu sukurti hidrogeliai su C-PC, ypatingą dėmesį skiriant veikliosios medžiagos stabilumui išsaugoti. Sukurtos formuluotės gali būti toliau tiriamos žaizdų gijimo modeliuose.

Pirmą kartą buvo sukurtos transfersomos su C-PC, kurių gamybai pritaikytas dviejų pakopų metodas leido efektyviai įterpti C-PC į transfersomų struktūrą, išsaugant šios medžiagos stabilumą ir apsaugant nuo temperatūros, pH svyravimų bei organinių tirpiklių poveikio. C-PC struktūrinis stabilumas ir biologinis aktyvumas buvo patvirtinti spektrofotometriniais ir antioksidacinio aktyvumo tyrimais. Glicerolio turinčios C-PC transfersomos pasižymė-

jo dideliu C-PC įterpimo efektyvumu ir išliko stabilios 8 mėnesius laikant 4 °C temperatūroje, apsaugotos nuo šviesos poveikio.

Ex vivo skvarbos į odą tyrimas parodė, kad C-PC įterpimas į transfersomas pagerino jo kaupimąsi išoriniuose odos sluoksniuose. Šis tyrimas yra vienas pirmųjų, kuriame įvertintas C-PC turinčių transfersomų apsauginis poveikis *in vivo* ankstyvosios odos plokščialąstelinės karcinomos vystymosi modelyje. Gauti rezultatai parodė, kad C-PC transfersomos slopina uždegiminius procesus ir mažina epidermio proliferacinius bei displazinius pakitimus, kurie siejami su ankstyvaisiais naviko vystymosi etapais.

Šis darbas atskleidžia tvarų tarpdisciplininį požiūrį, apjungiantį aplinkosauginius aspektus, natūralių junginių išgavimą ir farmacinių technologijų plėtrą, siekiant kurti inovatyvius sprendimus, turinčius tiek ekologinę, tiek biomedicininę reikšmę.

Tyrimo objektas ir metodai

Tyrimo objektas – C-PC, išskirtas iš natūraliai surinktos melsvabakterių biomasės, bei jo pagrindu sukurtos vietinio poveikio technologinės formuluotės (hidrogeliai ir transfersomos).

Melsvabakterių biomasė buvo renkama 2019–2023 m. rugpjūčio–spalio mėn. iš Kauno marių ir Simno žuvininkystės tvenkinio (Lietuva) melsvabakterių žydėjimų metu. Biomasė surinkta naudojant planktono tinklą ir inovatyvų melsvabakterių surinkimo prototipą. Surinkta biomasė laikyta −20 °C temperatūroje. Dominuojančios rūšys nustatytos mikroskopiškai. Cianotoksinų (mikrocistinų, saksitoksinų ir anatoksinų) kiekis nustatytas ELISA metodu.

C-PC buvo išskirtas taikant šaldymo ir atitirpinimo metodą melsvabakterių ląstelėms suardyti, centrifugavimą ir baltymų nusodinimą amonio sulfatu, vėliau C-PC išgrynintas gelinės filtracijos arba jonų mainų chromatografijos metodu. Grynumas nustatytas spektrofotometriškai (A_{620}/A_{280} santykis). Sunkiųjų metalų (Pb, Cd, As, Hg) kiekis nustatytas induktyviai susietos plazmos masių spektrometrijos (ICP-MS) metodu.

C-PC turinčios formuluotės buvo kuriamos hidrogelinių ir transfersominių sistemų pagrindu. Hidrogeliai paruošti naudojant įvairias gelifikuojančias medžiagas. Jų pH nustatytas potenciometriškai, C-PC kiekis – spektrofotometriškai, mikrobiologinė kokybė įvertinta taikant standartizuotus mikrobiologinius metodus, o veikliosios medžiagos išsiskyrimas tirtas difuzijos metodu. Transfersomos buvo gaminamos dviejų pakopų metodu. Jos ruoštos iš fosfolipidų ir natrio deoksicholato, panaudojant skirtingas drėkinančias terpes (glicerolį, hialuronatą ar jų derinį) ir taikant tiesioginį sonikavimą ultra-

garso zondu. Į suformuotas transfersomas C-PC buvo įterpiamas taikant papildomą sonikavimą ultragarsu. Dalelių dydis, polidispersiškumo indeksas ir zeta potencialas nustatyti dinaminės šviesos sklaidos metodu, morfologija vertinta kriogeninės transmisinės elektroninės mikroskopijos būdu. C-PC įterpimo efektyvumas nustatytas dializės metodu, o stabilumas vertintas pagal dalelių dydžio, polidispersiškumo indekso ir zeta potencialo pokyčius, laikant 8 mėnesius 4 °C temperatūroje, apsaugant nuo šviesos poveikio. Antioksidacinis aktyvumas nustatytas DPPH metodu, ląstelių suderinamumas ir apsauginis poveikis nuo oksidacinio streso – naudojant žmogaus keratinocitų (HaCaT) ląstelių liniją ir MTT testą (ląstelių gyvybingumo įvertinimui) *in vitro*.

C-PC skvarba į odą tirta *ex vivo* naudojant Bronaugh tipo difuzines kameras ir žmogaus odos mėginius, o C-PC lokalizacija odoje nustatyta konfokaline lazerine mikroskopija.

In vivo tyrimai atlikti naudojant DMBA/TPA sukeltą pelių odos kancerogenezės modelį. Histologiniai ir imunohistocheminiai tyrimai (Ki-67) taikyti epidermio proliferaciniams ir uždegiminiams pokyčiams įvertinti. Tyrimų rezultatai apdoroti matematiniais statistiniais metodais, naudojant „IBM SPSS Statistics“ programinę įrangą. Duomenų analizėje taikyti parametriniai ir neparametriniai testai, reikšmingumo lygmuo nustatytas $p < 0,05$. *Išsamūs metodų aprašymai ir naudotos medžiagos pateikti publikacijose (1–5 straipsniuose).*

Diskusija ir rezultatų apžvalga

Šio tyrimo metu sukurtos vietinio poveikio technologinės formuluotės su C-PC mėginiais, išskirtais iš gamtoje surinktos melsvabakterių biomasės. Ypatingas dėmesys buvo skiriamas C-PC mėginių grynumui, saugumui, stabilumui ir skvarbai į odą užtikrinti. Gauti rezultatai pateikia naujų įžvalgų apie C-PC taikymo galimybes ankstyvųjų odos plokštelinės karcinomos stadijų profilaktikoje.

Fikocianinas yra aptinkamas tiek eukariotiniuose organizmuose, pavyzdžiui, raudonuosiuose dumbliuose ir glaukofituose, tiek ir prokariotiniuose organizmuose – melsvabakterėse [9, 30]. Tyrimo metu C-PC mėginiai išskirti iš melsvabakterių biomasės, surinktos natūralių žydėjimų metu 2019–2023 m. rugpjūčio–spalio mėn. dviejuose gėlo vandens telkiniuose: Kauno mariose (Kaunas, Lietuva) ir Simno žuvininkystės tvenkinyje (Simnas, Lietuva). Melsvabakterių biomasės sudėtis kito priklausomai nuo metų, mėginių ėmimo laiko ir vietos. 2020 ir 2022 m. surinktoje biomasėje dominavo *Micro-*

cystis spp. (iki 98 proc. visos biomasės), o 2019 ir 2023 m. mėginiuose vyravo *A. flos-aquae* (95–99 proc. fitoplanktono biomasės).

Melsvabakterės, priklausomai nuo rūšies, geografinės vietos ir aplinkos sąlygų, gali gaminti cianotoksinus, kurie pagal pagrindinius taikinius ir veikimo mechanizmus skirstomi į hepatotoksinus (mikrocistinai (MCs), noduliarinai (NODs), cilindrospermopsinas (CYN)), neurotoksinus (anatoksinas-a (ATX-a), saksitoksinai (STXs)) ir dermatotoksinus (aplysiatoksinai (APTXs), lyngbyatoksinai (LTXs) ir lipopolisacharidai (LPS)) [47]. *Microcystis* spp. dažniausiai gamina MCs, o *Aphanizomenon* spp. – Antx-a, CYN, STXs ir MCs [49]. Cianotoksinai gali kelti riziką gyvūnų ir žmogaus sveikatai [46], todėl būtina įvertinti gamtoje surinktos melsvabakterių biomasės užterštumą šiomis medžiagomis, norint ją naudoti eksperimentiniuose tyrimuose. Cianotoksinų kiekiui nustatyti buvo atliktas ELISA testas. 2023 m. surinktoje biomasėje, kurioje dominavo *A. flos-aquae*, cianotoksinų nerasta, todėl ši biomasė buvo naudota C-PC mėginiams išskirti, transfersomoms gaminti ir tolesniems *in vivo* tyrimams, užtikrinant eksperimentinio modelio saugumą ir eliminuojant galimą cianotoksinų poveikį stebimiems biologiniams efektams.

C-PC grynumas yra vienas esminių rodiklių, tiesiogiai susijusių su jo biologiniu aktyvumu ir pritaikomumu. Jis dažniausiai vertinamas pagal absorbcijos santykį (A_{620}/A_{280}), atspindintį C-PC kiekį bendro baltymų kiekio atžvilgiu. Mokslinėje literatūroje C-PC grynumas mažesnis už 0,7 priskiriamas maisto, 0,7–3,9 – reagentų, o 4,0 ar didesnis – analizės kokybei [16, 29]. Vis dėlto ši klasifikacija nėra standartizuota, o literatūroje pateikiami grynumo klasifikavimo intervalai gali skirtis. Šiame tyrime naudoti skirtingo grynumo C-PC pavyzdžiai. Pradiniuose tyrimo etapuose C-PC grynumas svyravo nuo 1,130 (±0,020) iki 2,207 (±0,015) ir atitiko reagentinio laipsnio kokybę. Didesnio grynumo C-PC mėginius pavyko išskirti taikant jonų mainų chromatografiją. Vėlesniuose etapuose transfersomų gamybai ir *in vivo* tyrimui naudotas taip pat reagentų kokybės C-PC, kurio grynumas – 3,227(0,045). Didesnis C-PC grynumas užtikrina mažesnį priemaišų, galinčių turėti įtakos biologiniam aktyvumui ir eksperimentinių tyrimų rezultatams, kiekį. Melsvabakterėms būdingas metalų jonų kaupimas iš aplinkos [55], todėl šiame tyrime ypatingas dėmesys buvo skirtas sunkiųjų metalų (Pb, Cd, As ir Hg) kiekiui nustatyti C-PC mėginiuose. Ištirti keturi C-PC mėginiai, išskirti iš skirtingų melsvabakterių biomasės: trys mėginiai gauti iš melsvabakterių, surinktų Kauno mariose 2019–2022 m., ir vienas palyginamasis mėginys, kuriame C-PC buvo išskirtas iš kultivuotos *L. platensis*. Sunkiųjų metalų koncentracijos C-PC mėginiuose priklausė nuo melsvabakterių biomasės kilmės ir dominuojančios genties. C-PC, išskirto iš biomasės, kurioje dominavo *A. flos-aquae* (2019 m.), mėginiuose nustatytos metalų

koncentracijos nuo didžiausios iki mažiausios išsidėstė šia tvarka: Pb 0,378 (0,013) µg/g > As 0,150 (0,012) µg/g > Hg 0,050 (0,006) µg/g > Cd 0,020 (0,000) µg/g. Didesnis sunkiųjų metalų kiekis nustatytas C-PC mėginiuose, išskirtuose iš biomasės, kurioje dominavo *Microcystis* spp. Pavyzdžiui, 2020 m. mėginyje didžiausia koncentracija nustatyta Pb – 0,725 (0,006) µg/g, Hg – 0,443 (0,007) µg/g, Cd – 0,233 (0,005) µg/g ir As – 0,190 (0,008) µg/g. C-PC, išskirto iš 2022 m. surinktos biomasės, mėginiuose nustatytų metalų koncentracijos pasiskirstė taip: Pb 0,643 (0,015) µg/g > Cd 0,410 (0,014) µg/g > As 0,160 (0,008) µg/g > Hg 0,021 (0,003) µg/g. C-PC mėginyje, išskirtame iš kultivuotos *L. platensis*, didžiausios koncentracijos buvo Hg – 0,376 (0,016) µg/g ir Cd – 0,348 (0,005) µg/g, o mažiausia koncentracija As – 0,045 (0,006) µg/g. Sunkiųjų metalų kokybinė – kiekybinė analizė parodė, kad C-PC mėginiuose, išskirtuose iš *Microcystis* spp. buvo didesnės sunkiųjų metalų koncentracijos negu mėginiuose iš *A. flos-aquae* ir kultivuotos *L. platensis*. Kitų tyrėjų tyrimai taip pat atskleidžia, kad gebėjimas surišti sunkiuosius metalus priklauso nuo melsvabakterių genties. Pavyzdžiui, *Microcystis* spp., sudarančios kolonijas, apsuptas ekstraląsteline gleivių matrica, pasižymėjo didesniu gebėjimu surišti metalų jonus nei siūlinės dumblių rūšys, pvz., *A. flos-aquae* [57, 61]. *Microcystis aeruginosa* pasižymi dideliu afinitetu sunkiųjų metalų jonams, pvz., Hg^{2+}, Cd^{2+} ir Pb^{2+} [62]. Skirtingais metais surinktuose *Microcystis* mėginiuose (S2, 2020 m. ir S3, 2022 m.) nustatytos skirtingos sunkiųjų metalų koncentracijos rodo, kad aplinkos veiksniai – vandens kokybė ir taršos lygis, taip pat gali turėti įtakos šių metalų kaupimuisi melsvabakterių biomasėje [63]. Ilgalaikiai Kauno marių stebėsenos duomenys patvirtina, kad sunkiųjų metalų koncentracijos paviršiniame vandenyje reikšmingai nekinta, tačiau jų kaupimasis dugno nuosėdose laikui bėgant didėja [64]. Ši tendencija atsispindi ir šio tyrimo gautuose rezultatuose, pvz., mėginiuose, surinktuose vėlesniais metais, Cd koncentracija buvo didesnė. C-PC turi funkcinių grupių, galinčių sąveikauti su metalų jonais. Tokios sąveikos gali sukelti baltymo struktūrinius pokyčius, paveikti jo stabilumą ir biologinį aktyvumą [58, 65–67]. C-PC gryninimo metodai taip pat gali turėti įtakos sunkiųjų metalų kiekiui C-PC mėginiuose. Šio tyrimo metu buvo naudoti skirtingi C-PC gryninimo metodai: gelio filtracijos chromatografija ir jonų mainų chromatografija. Jonų mainų chromatografija, susijusi su krūvio sąveikomis, gali būti efektyvesnė surišant sunkiųjų metalų priemaišas nei atskyrimo metodai, kuriuose dalelės skirstomos pagal dydį [68–71]. Palyginamajame C-PC mėginyje iš kultivuojamos *L. platensis* nustatytos santykinai didesnės Hg ir Cd koncentracijos, ypač palyginus su mėginiu iš *A. flos-aquae*, tačiau mažesnės Pb ir As koncentracijos, palyginus su C-PC mėginiais iš gamtoje surinktos biomasės. Šie rezultatai rodo, kad net ir kontroliuojamos auginimo sąlygos nebūtinai visiškai pašalina sunkiųjų

metalų taršą, kuriai įtaką gali daryti auginimo terpės sudėtis bei technologiniai procesai. Tačiau mažesnės Pb koncentracijos šiame mėginyje leidžia daryti prielaidą, kad kai kurie metalai yra labiau susiję su aplinkos poveikiu natūraliose vandens ekosistemose.

Šio tyrimo tikslas buvo nustatyti sunkiųjų metalų koncentracijas skirtinguose C-PC mėginiuose ir įvertinti C-PC mėginių saugumą tolimesniems tyrimo etapams, tačiau nebuvo siekta nustatyti tiesioginių sąsajų tarp metalų kiekio ir jį lemiančių veiksnių, pvz., melsvabakterių rūšies, aplinkos sąlygų ar gryninimo metodų. Šiems mechanizmams išaiškinti reikalingi išsamūs papildomi tyrimai. Vis dėlto gauti rezultatai suteikė svarbių įžvalgų, kurios buvo panaudotos priimant sprendimus vėlesniuose tyrimų etapuose. Galutinių technologinių formuluočių gamybai ir *in vivo* tyrimui buvo pasirinkti C-PC mėginiai, išskirti iš *A. flos-aquae* biomasės, ir gryninti taikyta jonų mainų chromatografija. Šiuose C-PC mėginiuose nustatytas mažesnis sunkiųjų metalų kiekis.

Sunkiųjų metalų įvertinimas C-PC mėginiuose yra būtinas, taikant C-PC mėginius biotechnologijos, farmacijos ar kosmetikos srityse. Europos Sąjungoje sunkieji metalai – švinas, kadmis, arsenas ir gyvsidabris, yra griežtai reglamentuojami kosmetikos produktuose ir medicinos priemonėse. Šie sunkieji metalai negali būti gaminių sudedamosiomis dalimis ir leidžiami tik kaip technologiškai neišvengiamos likutinės priemaišos, nekeliančios rizikos žmogaus sveikatai. Nors Reglamentas (EB) Nr. 1223/2009 ir ES medicinos priemonių reglamentas (ES) 2017/745 nustato bendrą teisinę šių pavojingų medžiagų kontrolės sistemą, praktinis jų vertinimas ir stebėsena vis dažniau grindžiami harmonizuotais analitiniais standartais, pvz., ISO 21392:2021 standartu, kuriame nurodyti validuoti ICP-MS metodai, skirti sunkiųjų metalų kiekiui galutiniuose produktuose nustatyti [72–74]. Kitas reikšmingas etapas C-PC technologinių formuluočių kūrime – šios medžiagos struktūrinio stabilumo išsaugojimas. C-PC yra vandenyje tirpus fikobiliproteinas, sudarytas iš baltyminių subvienetų ir chromoforų, vadinamų fikocianobilinais [9], kurie atsakingi už C-PC būdingą mėlyną spalvą ir absorbcijos maksimumą, esant 615–620 nm šviesos bangos ilgiui [32, 75, 77, 78]. C-PC multimerinė struktūra, kartu su chromoforais ir aktyviomis funkcinėmis grupėmis sąlygoja jo biologinį aktyvumą ir jautrumą išorės veiksniams – pH, temperatūrai ir šviesai, kurie gali sukelti konformacinius pokyčius, subvienetų disociaciją ir funkcinių savybių praradimą. C-PC yra šviesai jautrus pigmentas, todėl turi būti laikomas tamsoje – jo suirimo greitis priklauso tiek nuo šviesos intensyvumo, tiek nuo bangos ilgio. Nustatyta, kad liuminescencinis apšvietimas arba ultravioletinės spinduliuotės poveikis spartina irimo procesus bei mažina antioksidacinį aktyvumą [81]. Iš mezofilinių melsvabakterių išskirti C-PC mėginiai išlieka stabilūs iki 40 °C temperatūroje, pH 5,0–7,5 [12, 79, 81].

Didesni pH svyravimai ir aukštesnė temperatūra gali sukelti struktūrinius C-PC pokyčius [76, 81]. Nėra pakankamai ištirta kelių aplinkos veiksnių kompleksinė įtaka C-PC stabilumui. Be minėtų aplinkos veiksnių, C-PC struktūrinį stabilumą gali veikti ir technologinių formuluočių komponentai, pvz., gelifikuojančios medžiagos, konservantai, kurie stabilizuoja arba sąlygoja baltymo suirimą, priklausomai nuo jų fizikocheminių savybių [16]. Todėl tinkamų komponentų parinkimas yra itin svarbus kuriant technologines formuluotes su C-PC mėginiais. Šis tyrimas parodė, kad skirtingos gelifikuojančios medžiagos daro nevienodą įtaką C-PC struktūriniam stabilumui. Nustatyta, kad C-PC išliko santykinai stabilus hidrogeliuose, suformuluotuose panaudojant polisacharidinius biopolimerus, pvz., natrio alginatą, *Soligel*™, hidroksietilceliuliozę (HEC), natrio karboksimetilceliuliozę (NaCMC), hidroksipropilmetilceliuliozę (HPMC) ir hidroksietilmetilceliuliozę (HEMC). Tai patvirtina kitų tyrėjų rezultatus, įrodančius, kad polisacharidai gali padidinti C-PC stabilumą. Vienas iš šio poveikio mechanizmų yra glikacija, kurios metu gali susidaryti kovalentinės sąveikos tarp redukuojančių cukrų ir baltymo amino grupių, pagerinančios susidariusių konjugatų fizikines – chemines savybes. Be to, polisacharidai, turintys neigiamai įkrautas funkcines grupes (pvz., karboksilo ar sulfato), gali elektrostatiniu būdu sąveikauti su teigiamai įkrautomis aminorūgščių liekanomis C-PC paviršiuje, taip padidindami C-PC struktūrinį stabilumą ir išsaugodami baltymo funkcionalumą [81]. Chitozano pagrindu suformuotuose hidrogeliuose buvo stebimas apie 12 proc. C-PC koncentracijos sumažėjimas, kuris gali būti siejamas su kombinuotu C-PC struktūrinį stabilumą įtakojančių veiksnių poveikiu, pvz., kaitinimas (iki 40 °C temperatūros) gamybos proceso metu ir rūgščios terpės (pH 5,0) poveikis. Nors atskirai šie veiksniai nėra kritiniai C-PC struktūriniam stabilumui, tačiau jų sąveika galėjo sąlygoti dalinį C-PC suirimą. Reikšmingas C-PC koncentracijos sumažėjimas nustatytas hidrogeliuose, suformuluotuose naudojant *Carbopol® Ultrez 21* ir *Pemulen*™ – C-PC koncentracija sumažėjo daugiau nei 50 proc. Šiuos pokyčius patvirtino ir vizualiai stebimas būdingos mėlynos spalvos išblukimas, pažymintis chromoforo struktūros pažeidimus. *Carbopol® Ultrez 21* formuluotėse neutralizacijai buvo naudojamas natrio hidroksidas (galutinis pH 4,5), o *Pemulen*™ – trietanolaminas (galutinis pH 6,8). Tokios pH sąlygos kartu su galimomis polimero ir baltymo sąveikomis galėjo prisidėti prie stebėto C-PC struktūrinio stabilumo praradimo. Remiantis šiais rezultatais, buvo atrinktos šešios hidrogelių formuluotės, pagamintos šių gelifikuojančių medžiagų pagrindu: natrio alginato, *Soligel*™, HEC, NaCMC, HPMC ir HEMC, kuriose toliau buvo tirtas skirtingų konservantų sistemų (*SharoSENSE*™ *Plus 184*, *SharoSENSE*™ *Plus 785* ir *Sharomix*™ *721*) poveikis C-PC struktūriniam stabilumui. Konservantai taip pat turėjo įtakos C-PC struktūriniam stabilu-

mui. Formuluotėse su *SharoSENSE™ Plus 184*, priklausomai nuo naudotos gelifikuojančios medžiagos, nustatytas didžiausias C-PC koncentracijos sumažėjimas (nuo 6,60 proc. iki 64,40 proc.), tuo tarpu naudojant *SharoSENSE™ Plus 785* kartu su natrio alginatu, *Soligel™* ar HEC statistiškai reikšmingo C-PC koncentracijos sumažėjimo nenustatyta ($p > 0,05$). Remiantis šiais rezultatais, tolimesniems tyrimams buvo pasirinkti natrio alginato, *Soligel™* ir HEC pagrindu sukurti hidrogeliai kartu su *SharoSENSE™ Plus 785*. Mikrobiologiniai tyrimai parodė, kad tirtos hidrogelio formuluotės atitiko mikrobiologinio saugumo reikalavimus. Tiriami patogeniniai mikroorganizmai – *Staphylococcus aureus*, *Pseudomonas aeruginosa*, *Candida albicans* ir *Escherichia coli*, nebuvo aptikti nė vienoje iš tirtų formuluočių, o bendras aerobinių mezofilinių mikroorganizmų skaičius visuose mėginiuose išliko mažesnis nei $1,0 \times 10^1$ KSV/g. Taigi, parinkta konservantų sistema užtikrino C-PC hidrogelių mikrobiologinį stabilumą.

Natrio alginato pagrindu pagaminti hidrogeliai buvo pasirinkti *in vitro* C-PC atpalaidavimo iš hidrogelio tyrimui, kurio metu taip pat buvo įvertinta ir PG įtaka C-PC atpalaidavimui. *In vitro* C-PC atpalaidavimo tyrimas parodė beveik linijinį C-PC išsiskyrimo profilį iš abiejų hidrogelių formuluočių – su PG ir be PG (atitinkamai $R^2 = 0,9995$ ir 0,9977). Tai rodo pastovų difuzijos būdu kontroliuojamą išsiskyrimo mechanizmą ir hidrogelio struktūros išlaikymą C-PC išsiskyrimo laikotarpiu. Po 6 val. iš PG turinčio hidrogelio išsiskyrė apie 10 proc. įterpto C-PC (728,07 (19,35) $\mu g/cm^2$), o iš formuluotės be PG – apie 7 proc. (531,44 (26,81) $\mu g/cm^2$). PG statistiškai reikšmingai padidino C-PC išsiskyrimo greitį. Tai parodė didesnis kreivės nuolydis ir didesnis išsiskyrusio junginio kiekis laikui bėgant. Šis PG poveikis gali būti paaiškinamas keliais mechanizmais. PG veikia kaip papildomas tirpiklis, didinantis C-PC tirpumą hidrogelio matricoje ir jo termodinaminį aktyvumą, skatinantis difuziją į aplinkinę terpę [85]. Alginato pagrindu sudarytose sistemose polimerinė matrica gali efektyviai sulaikyti veikliąsias medžiagas, pvz., C-PC, tuo tarpu PG gali silpninti tarpmolekulines sąveikas hidrogelio struktūroje, pavyzdžiui, suardydamas vandenilinius ryšius arba konkuruodamas dėl prisijungimo vietų. Dėl to sumažėja difuzijos pasipriešinimas ir skatinamas C-PC išsiskyrimas iš hidrogelio [86]. Panašus PG poveikis vaistinių medžiagų išsiskyrimui iš polimerinių sistemų aprašytas ir ankstesniuose tyrimuose, pavyzdžiui, PG padidino loksoprofeno išsiskyrimą iš polimerinių matricų ir likochalkono A iš *Carbomer 940* hidrogelių [87, 88]. Tačiau per 6 valandas išsiskyrė tik santykinai nedidelė C-PC dalis (apie 10 proc.). Tikėtina, kad didelė baltymo dalis išliko sulaikyta hidrogelio matricoje. Natrio alginatas pasižymi kontroliuojamo atpalaidavimo savybėmis [89]. Ankstesni tyrimai parodė, kad C-PC išsiskyrimas iš alginato sistemų priklauso nuo veikliosios medžiagos ir polimero santykio – mažesnis C-PC kiekis lemia

mažesnį išsiskyrimo efektyvumą [90]. Šiame tyrime C-PC koncentracija hidrogelyje buvo 1 proc., taigi, padidinus C-PC koncentraciją galimai padidėtų ir C-PC kiekio atpalaidavimo procentinė dalis. PG ne tik padidino C-PC atpalaidavimą iš hidrogelio *in vitro* sąlygomis, bet ir skatino skvarbą į odą *ex vivo* modelyje. C-PC fluorescencija odoje nebuvo stebima hidrogelio be PG atveju, o PG dėka buvo stebima C-PC fluorescencija raginiame odos sluoksnyje. PG sąveikauja su raginio sluoksnio lipidų matrica, didindamas lipidų takumą ir pralaidumą, taip palengvindamas hidrofilinių molekulių difuziją į odą [91–93]. Vis dėlto C-PC skvarba išliko ribota. Net ir panaudojant skvarbą skatinančias medžiagas, pvz., PG, didelių hidrofilinių biomolekulių skvarba į gilesnius odos sluoksnius išlieka ribota. Be to, skvarbą skatinančios medžiagos gali sukelti odos dirginimą arba ilgalaikį pažeidimą. Toks poveikis yra nepageidautinas, kuriant profilaktines priemones ankstyvosioms odos plokščialąstelinės karcinomos stadijoms, arba skirtas jautriai odai bei ilgalaikiam naudojimui. Terapiniu požiūriu C-PC skvarba per raginį odos sluoksnį ne visada yra būtina. Hidrogeliai su C-PC gali būti veiksmingi odos žaizdoms gydyti, kai veiklioji medžiaga veikia vietiškai, todėl nereikalinga intensyvi skvarba į gilesnius odos sluoksnius. Žaizdų modeliuose C-PC stimuliuoja fibroblastų proliferaciją ir migraciją, iš dalies indukuodamas ląstelių ciklo G1 fazę, didindamas nuo ciklinų priklausomų kinazių (cdK1 ir cdK2) raišką bei aktyvindamas signalines kaskadas, pvz., fosfatidilinozitolio-3-kinazės (PI-3K) kelią, kurios yra būtinos audinių regeneracijai [94, 95]. C-PC skatina granuliacinio audinio formavimąsi, reepitelizaciją ir angiogenezę, tokiu būdu pagreitina žaizdos gijimą *in vivo* sąlygomis [10, 15, 16]. C-PC tai pat mažina oksidacinį stresą ir slopina prouždegiminių citokinų, pvz., TNF-α ir IL-6, raišką, sukurdamas palankią terpę žaizdoms gyti [15, 96]. Dėl šių savybių C-PC gali būti integruojamas į pažangias daugiafunkcines hidrogelines formuluotes, pagerinančias žaizdų gijimo procesą [16, 97]. Remiantis gautais duomenimis, sukurtos C-PC hidrogelinės formuluotės galėtų būti toliau tiriamos žaizdų gijimo modeliuose, siekiant išsamiau įvertinti jų efektyvumą.

Tuo tarpu su nanotechnologijomis susijusios sistemos, pvz., transfersomos, gali pagerinti bioaktyvių junginių pernašą į odą, išsaugodamos odos barjerinio sluoksnio struktūrinį vientisumą. Dėl dalelių formos lankstumo transfersomos, palyginus su kitomis nanonešiklių sistemomis, pvz., liposomomis, pasižymi geresne skvarba į odą. Priešingai nei etanolio turinčios etosomos, transfersomos rečiau sukelia odos dirginimą [31].

Šiame tyrime, C-PC transfersomos buvo pagamintos taikant dviejų pakopų metodą, kuris padėjo išsaugoti C-PC struktūrinį stabilumą. Pirminiai bandymai parodė, kad tiesioginis sonikavimas ultragarso zondu neigiamai veikė C-PC struktūrinį stabilumą ir sumažino C-PC koncentraciją galutinėje

formuluotėje apie 80 proc. Atsižvelgiant į C-PC jautrumą mechaniniam ir terminiam poveikiui, buvo pasirinkta alternatyvi C-PC įterpimo į transfersomas strategija. Pirmiausia, buvo pagamintos tuščios transfersomos, o vėliau C-PC įterptas į jas taikant papildomą sonikavimą ultragarso vonelėje [98, 99]. C-PC struktūrinį stabilumą transfersomų formuluotėse taip pat patvirtino antioksidacinio aktyvumo tyrimas, kurio metu nebuvo nustatyti statistiškai reikšmingi aktyvumo skirtumai tarp laisvo C-PC ir C-PC įterpto į transfersomas. Kadangi C-PC biologinis aktyvumas yra glaudžiai susijęs su jo struktūra, šio tyrimo rezultatai leidžia daryti prielaidą, kad neįvyko reikšmingų konformacinių pokyčių C-PC struktūroje transfersomų gamybos metu. C-PC buvo įterptas į transfersomas, praturtintas gliceroliu, natrio hialuronatu arba jų deriniu. Be to, dalis formuluočių buvo papildytos cholesteroliu, siekiant įvertinti jo poveikį fizikocheminėms ir technologinėms nanosistemų savybėms, kadangi žinoma, jog cholesterolis moduliuoja membranos standumą ir stabilumą [33, 103, 105, 106]. Iš viso buvo pagamintos šešios skirtingos C-PC transfersomų formuluotės: Gly-T, Gly-Chol-T, Hyal-T, Hyal-Chol-T, Hyal-Gly-T ir Hyal-Gly-Chol-T. Visos formuluotės pasižymėjo nanosistemų charakteristikomis, tinkamomis vietiniam biologiškai aktyvių medžiagų tiekimui į odą. Vidutinis vezikulių skersmuo svyravo nuo ~90 iki 115 nm. Natrio hialuronatą turinčios transfersomos pasižymėjo šiek tiek didesniu vezikulių dydžiu, palyginant su formuluotėmis be šio komponento. Be to, cholesteroliu praturtintos transfersomos paprastai buvo šiek tiek mažesnės nei atitinkamos formuluotės be cholesterolio. Visos formuluotės pasižymėjo mažu polidispersiškumo indeksu (< 0,2), rodančiu homogenišką dalelių dydžio pasiskirstymą. Zeta potencialo matavimai parodė stipriai neigiamą paviršiaus krūvį (apie −33 iki −44 mV), pažymintį tinkamą nanosistemų koloidinį stabilumą. Vezikulės buvo sferinės, vienasluoksnės arba kelių sluoksnių, priklausomai nuo formuluotės. Palyginus C-PC įterpimo efektyvumą ir ilgalaikį stabilumą, tarp formuluočių nustatyti reikšmingi skirtumai. Gly-T ir Gly-Chol-T formuluotės pasižymėjo didesniu C-PC įterpimo efektyvumu (~52 proc.) nei hialuronato turinčios sistemos (~33–37 proc.). Tokie rezultatai rodo, kad formuluotės, kurių sudėtyje yra mažiau papildomų komponentų, gali būti palankesnė efektyvesniam hidrofilinių makromolekulių, pvz., C-PC, įterpimui. Cholesterolis neturėjo reikšmingos įtakos C-PC įterpimo efektyvumui. Atsižvelgiant į hidrofilinę C-PC prigimtį, pasiektas įterpimo efektyvumas gali būti laikomas pakankamu ir atitinkančiu literatūros duomenis, nes hidrofiliniai junginiai paprastai pasižymi mažesniu įterpimo efektyvumu (dažniausiai ~10–50 proc.) [108]. Paruoštų transfersomų fizinis stabilumas buvo vertinamas atsižvelgiant į vezikulių dydžio, polidispersiškumo indekso ir zeta potencialo pokyčius per aštuonių mėnesių laikotarpį, laikant mėginius 4 °C temperatūroje, saugant juos nuo šviesos

poveikio. Per visą laikymo laikotarpį nepastebėta jokių matomų formuluočių spalvos pokyčių. Visoms formuluotėms išliko būdingos neigiamos zeta potencialo reikšmės, patvirtinančios gerą vezikulių elektrostatinį stabilumą. Transfersomos, turinčios glicerolio (Gly-T, Gly-Chol-T, Hyal-Gly-T ir Hyal-Gly-Chol-T), per visą laikymo laikotarpį pasižymėjo minimaliais dalelių dydžio pokyčiais, įrodančiais vezikulinių sistemų stabilumą. Tačiau formuluotėse, kuriose buvo natrio hialuronato, bet nebuvo glicerolio (Hyal-T ir Hyal-Chol-T), po 4–5 mėnesių buvo pastebėtas žymus vezikulių skersmens padidėjimas. Šis pokytis susijęs su polidispersiškumo indekso padidėjimu, būdingu vezikulių agregacijos ar susiliejimo procesams. Rezultatai rodo, kad glicerolis galėjo turėti įtakos transfersomų stabilumui. Šis poveikis tikėtina susijęs su glicerolio gebėjimu stabilizuoti fosfolipidinius dvisluoksnius ir išsaugoti vezikulių struktūrą laikymo metu [100–102]. Cholesterolio turinčiose formuluotės dalelių dydis buvo mažesnis, tikėtina, dėl tankesnės ir stabilesnės membranos struktūros [109]. Taip pat cholesterolį turinčios formuluotės pasižymėjo didesniu neigiamu zeta potencialu. Taigi, cholesterolio įdėjimas į formuluotes taip pat galėjo padidinti koloidinį stabilumą ilgalaikio laikymo sąlygomis.

In vitro tyrime buvo nustatytas citotoksinis poveikis žmogaus keratinocitų ląstelėms (*HaCaT)* esant 1000 μg/ml C-PC koncentracijai. Mažesnės koncentracijos – 10 ir 1 μg/ml – palaikė ląstelių gyvybingumą atitinkamai daugiau nei 90 proc. ir 100 proc., statistiškai reikšmingi skirtumai tarp laisvo ir į transfersomas įterpto C-PC nebuvo nustatyti. Tai dar kartą įrodo, kad transfersomų gamybos metodas išsaugojo C-PC struktūrinį stabilumą ir funkcines savybes. C-PC formuluotės pasižymėjo citoprotekciniu poveikiu esant 10 μg/ml koncentracijai H_2O_2 sukelto oksidacinio streso sąlygomis – ląstelių gyvybingumas padidėjo nuo 60 proc. iki 80 proc. Šie rezultatai atitinka ankstesnius tyrimus, įrodančius, kad C-PC didina ląstelių gyvybingumą oksidacinio streso ar UV sukeltos pažaidos sąlygomis [17, 36]. Remiantis C-PC įterpimo efektyvumo, ilgalaikio stabilumo ir biologinio aktyvumo vertinimo rezultatais, Gly-T ir Gly-Chol-T formuluotės buvo pasirinktos tolimesniems tyrimams.

Ex vivo skvarbos į odą tyrimuose, C-PC skvarba į odą iš šių dviejų formuluočių (Gly-T ir Gly-Chol-T) buvo palyginama su C-PC skvarba į odą iš PBS tirpalo, tiek su PG, tiek be šios medžiagos, siekiant įvertinti, ar PG efektyviau skatina C-PC skvarbą į odą nei pačios transfersominės sistemos. Dėl didelės molekulinės masės ir hidrofilinės prigimties C-PC skvarba iš tirpalo buvo ribota – fluorescencija aptikta tik pavienėse raginio sluoksnio srityse. Tuo tarpu PG paskatino didesnę C-PC skvarbą į išorinius odos sluoksnius – buvo matoma siaura fluorescencinė zona visame odos paviršiuje. Ryškesnis ir storesnis fluorescencinis signalas, pažymintis didesnę C-PC skvarbą, stebėtas

naudojant C-PC transfersomas, ypač Gly-T. Transfersomų sudėtyje esantis natrio deoksicholatas didina membranos elastingumą ir suteikia transfersomoms lankstumą, leidžiantį joms prisitaikyti prie siaurų tarpląstelinių raginio sluoksnio kanalų. Be to, osmosinis gradientas odos paviršiuje gali papildomai skatinti jų judėjimą į gilesnius odos sluoksnius. [31]. Šiek tiek mažesnė C-PC skvarba į odą iš Gly-Chol-T palyginus su Gly-T gali būti susijusi su vezikulių lankstumo skirtumais, kadangi cholesterolis stabilizuoja ir standina fosfolipidinį dvisluoksnį, taip potencialiai mažindamas lankstumą ir ribodamas skvarbą į odą [109]. Nors transfersominės pernašos sistemos padidino C-PC kaupimąsi raginio sluoksnio srityje, kokybinės analizės metu nebuvo nustatyta skvarba į gilesnius odos sluoksnius. Ankstesni *ex vivo* tyrimai taip pat parodė, kad C-PC iš liposomų skverbiasi tik į paviršinius odos sluoksnius, o odoje nustatyta tik nedidelė paviršiui užtepto C-PC kiekio dalis (apie 3 proc.) [37]. Tuo tarpu, C-PC, įterptas į PEG-hialurosomas, buvo nustatytas naujagimių paršelių epidermyje ir dermoje po 8 val. panaudojimo [35]. Vis dėlto šių tyrimų tiesioginis palyginimas yra ribotas dėl skirtingų odos modelių, kurie gali skirtis savo barjerinėmis savybėmis ir pralaidumu. Tačiau didesnis C-PC kaupimasis išoriniuose odos sluoksniuose gali lemti veikliosios medžiagos laipsnišką skverbimąsi giliau į odą. Toks efektas naudingas vietinio poveikio sistemoms, taikomoms odos pažaidų profilaktikai, ypač tais atvejais, kai reikalinga antioksidacinė apsauga, pavyzdžiui, esant UV spinduliuotės arba aplinkos taršos poveikiui.

Transfersomų su C-PC poveikis uždegiminiams, proliferaciniams ir displaziniams pokyčiams odoje ankstyvosiose odos kancerogenezės stadijose buvo toliau tiriamas *in vivo*, naudojant DMBA/TPA sukeltą pelių kancerogenezės modelį.

C-PC transfersomos buvo gerai toleruojamos ir nesukėlė struktūrinių ar proliferacinių pokyčių sveikoje odoje (I ir II grupės). Epidermis išliko plonas (apie 10–20 μm), sudarytas iš kelių keratinocitų sluoksnių su taisyklingai išsidėsčiusiais branduoliais. Rete keteros buvo trumpos ir vienodos, jų gylis siekė apie 0–10 μm. Nebuvo nustatyta epidermio hiperplazijos, displazijos, edemos ar uždegimo požymių.

Ryškiausi makroskopiniai odos pakitimai buvo stebėti kancerogeno kontrolinėje grupėje (III grupė). Gyvūnų oda nugaros srityje buvo sausa, stipriai pleiskanojanti, su ryškiais eritemos ir uždegimo požymiais. Be to, daugumai šios grupės gyvūnų išsivystė nedidelės papulės tipo struktūros, pažyminčios ankstyvus hiperproliferacinius epidermio pokyčius, susijusius su navikų vystymosi skatinimu. Priešingai, gyvūnams, kuriems taikytos transfersomų pagrindu sukurtos formuluotės kartu su kancerogenu, dažniausiai nustatyti lengvesni makroskopiniai pakitimai: lengvas odos sausumas, pleiskanojimas, vietomis lengvas odos paraudimas. Tik dviem gyvūnams,

kuriems taikytos transfersomų pagrindu sukurtos formuluotės be C-PC kartu su kancerogenu (IV grupė), susiformavo mažos papulės tipo struktūros, tuo tarpu grupėse, kurioms naudotos C-PC transfersomos kartu su kancerogenu (V ir VI grupės), tokie dariniai neišsivystė.

Histopatologinis odos mėginių tyrimas atskleidė aiškius struktūrinius skirtumus tarp eksperimentinių grupių. Kancerogenu teptoje odoje buvo nustatyti histopatologiniai pakitimai, būdingi uždegimo sukeltiems epidermio pokyčiams. Visose gyvūnų grupėse, kuriose eksperimento metu naudotas kancerogenas, nustatytas epidermio sustorėjimas ir rete keterų pailgėjimas, atspindintis hiperplazinius ir proliferacinius pokyčius. Ryškiausi pakitimai stebėti kancerogeno kontrolinėje grupėje (III grupė): žymus epidermio sustorėjimas (110,78 (7,63) μm) ir gilios epidermio invaginacijos į dermą, rete keterų gylis siekė apie 80–150 μm. Statistiškai reikšmingai mažesnis epidermio sustorėjimas, palyginus su kancerogeno kontroline grupe, buvo nustatytas grupėse, kurioms taikytos transfersomų formuluotės kartu su kancerogenu ($p < 0,05$). Grupėje, kurioje naudota transfersomų pagrindu sukurta formuluotė be C-PC (IV grupė), epidermio storis siekė 61,35 (5,93) μm, o grupėje (V grupėje) panaudojant C-PC transfersomas (1 mg/ml) – 76,65 (6,46) μm. Rete keterų pailgėjimas šiose grupėse taip pat buvo mažiau ryškus nei grupėje, kurioje taikytas tik kancerogenas. Epidermio displazija taip pat skyrėsi tarp grupių. Ji buvo vertinama kaip lengva, vidutinė arba sunki pagal epidermyje nustatytų architektūrinių ir citologinių pakitimų raišką. Kancerogeno kontrolinėje grupėje (III grupė) 80 proc. gyvūnų nustatyta sunki epidermio displazija, o likusiems 20 proc. – vidutinė displazija. Tuo tarpu V grupėje, kurioje buvo taikomos C-PC transfersomas, 40 proc. gyvūnų nustatyta lengva displazija, o sunki displazija nustatyta tik 30 proc. gyvūnų. Panaši tendencija stebėta ir vertinant epidermio hiperplaziją. Kancerogeno kontrolinėje grupėje 50 proc. gyvūnų nustatyta vidutinė, o likusiems 50 proc. – sunki epidermio hiperplazija. Tuo tarpu grupėse, kuriose naudotos transfersomos be C-PC (IV grupė) arba C-PC turinčios transfersomos (V grupė), dominavo lengvi ir vidutiniai hiperplaziniai pokyčiai. Lengva hiperplazija nustatyta 50 proc. IV grupės ir 30 proc. V grupės gyvūnų, o vidutinė – atitinkamai 50 proc. ir 60 proc. gyvūnų. Kiekybinis mitotinio aktyvumo vertinimas parodė minimalų proliferacinį aktyvumą grupėse, kuriose eksperimento metu nenaudotas kancerogenas (I ir II grupės), o kancerogeno poveikis statistiškai reikšmingai padidino mitozių skaičių epidermyje (12 (1,23) mitozės/2,37 mm^2; $p < 0,05$). Tuo tarpu C-PC transfersomų taikymas lėmė statistiškai reikšmingą mitotinio aktyvumo sumažėjimą – V grupėje nustatyta 6,9 (0,38), o VI grupėje – 8 (0,91) mitozės/2,37 mm^2 ($p < 0,05$, palyginus su kancerogeno kontroline grupe). Šie rezultatai rodo, kad C-PC transfersomos slopino kancerogeno sukeltą epidermio proliferaciją. Be

epidermio pokyčių, nustatyti ir ryškūs uždegiminiai pakitimai dermoje. Kancerogeno kontrolinėje grupėje (III grupė) 70 proc. gyvūnų nustatytas sunkus dermos uždegimas, lydimas hiperemijos, edemos ir padidėjusio putliųjų ląstelių tankio (38,6 (2,48) ląstelės/2,37 mm^2), rodančio uždegiminę mikroaplinką odoje. Taikant gyvūnams C-PC transfersomas, ypač V grupėje, dažniau nustatyti lengvi uždegiminiai pokyčiai – jie nustatyti 60 proc. gyvūnų. Be to, V grupėje nustatytas statistiškai reikšmingai mežesnis putliųjų ląstelių tankis (23,6 (2,09) ląstelės/2,37 mm^2), palyginus su kancerogeno kontroline grupe ($p < 0,05$). Koreliacinė analizė parodė teigiamą ryšį tarp dermos uždegimo laipsnio ir putliųjų ląstelių tankio (Spearmano $\rho = 0,438$, $p < 0,001$), pažymintį, kad putliųjų ląstelių kaupimasis gali prisidėti prie uždegiminės mikroaplinkos formavimosi, susijusios su kancerogeno sukeltais odos pakitimais. Taigi histopatologiniai duomenys rodo, kad transfersomų pagrindu sukurtų formuluočių vietinis naudojimas sumažino epidermio proliferacinius ir displazinius pokyčius bei uždegiminį procesą tiek epidermyje, tiek dermoje.

Imunohistocheminė proliferacijos žymens Ki-67 analizė taip pat parodė, kad vietinis transfersomų pagrindu sukurtų formuluočių naudojimas turėjo įtakos epidermio proliferacinio aktyvumo sumažėjimui, ypač suprabaziniame sluoksnyje. C-PC transfersomos (10 mg/ml konc., VI grupė), statistiškai reikšmingai sumažino epidermio proliferaciją: bazinio sluoksnio Ki-67 indeksas sumažėjo apie 28 proc., o suprabazinio sluoksnio – apie 61 proc., palyginus su kancerogeno kontroline grupe ($p < 0,05$). Bendro epidermio Ki-67 indekso analizė parodė panašią tendenciją. Grupėje, kurioje taikyta kancerogeno kartu su didesnės koncentracijos C-PC transfersomomis eksperimento schema, bendras Ki-67 indeksas sumažėjo statistiškai reikšmingai – apie 29 proc., palyginus su gautais rezultatais grupėje, kurioje naudotas tik kancerogenas ($p < 0,05$), tačiau bendras Ki-67 indeksas buvo mažiau jautrus nustatant skirtumus tarp grupių. Koreliacinė analizė taip pat patvirtino sąsajas tarp proliferacinio aktyvumo ir histopatologinių epidermio pakitimų, pvz., epidermio sustorėjimo, rete keterų gylio bei displazinių pokyčių. Taigi, kancerogenas sukėlė reikšmingą epidermio hiperproliferaciją, o vietinis C-PC transfersomų taikymas slopino šį proliferacinį atsaką. Ki-67 raiškos sumažėjimas kartu su histopatologinių rodiklių pokyčiais leidžia daryti prielaidą, kad C-PC turinčios transfersomos gali moduliuoti ankstyvuosius navikų vystymosi procesus epidermyje.

Histopatologinis vidaus organų (kepenų, blužnies, plaučių, širdies, inkstų, smegenų, sėklidžių ir mezenterinių limfmazgių) tyrimas neparodė jokių su gydymu susijusių patologinių pakitimų nei vienoje eksperimentinėje grupėje. Visi tirti audiniai buvo įprastos histologinės struktūros, nenustatyta degeneracinių, uždegiminių ar neoplastinių pokyčių. Šie rezultatai rodo, kad

vietinis C-PC transfersomų naudojimas nesukėlė histopatologiškai nustatomų organų pažeidimų.

Tyrimo metu C-PC buvo išskirtas iš gamtoje surinktos perteklinės melsvabakterių biomasės. Ypatingas dėmesys skirtas C-PC grynumui, saugumui ir stabilumui užtikrinti. Surinkta melsvabakterių biomasė buvo ištirta dėl užterštumo cianotoksinais, o *in vivo* tyrime naudotoms transfersominėms formuluotėms skirti C-PC mėginiai buvo išskirti iš netoksiškos biomasės. C-PC mėginiuose taip pat buvo nustatytos pasirinktų sunkiųjų metalų (PB, Cd, As ir Hg) koncentracijos, tačiau būtinas išsamesnis farmacinių produktų gamybai skirtos žaliavos saugumo vertinimas, apimantis platesnį galimos taršos spektrą. C-PC struktūrinis stabilumas buvo vertinamas technologinių formuluočių (hidrogelių ir transfersomų) gamybos metu. Taip pat buvo vertinamas C-PC turinčių transfersominių formuluočių fizikinis stabilumas per 8 mėnesių laikymo laikotarpį tamsioje aplinkoje, esant 4 °C temperatūrai, tačiau po ilgalaikio laikymo C-PC struktūrinis stabilumas nebuvo vertintas. Taip pat nebuvo atliktas šių transfersominių formuluočių mikrobiologinio užterštumo vertinimas, todėl būtų tikslinga atlikti minėtus papildomus tyrimus. *Ex vivo* kokybiniai skvarbos į odą tyrimai parodė, kad C-PC transfersomos sąlygojo C-PC kaupimąsi raginiame odos sluoksnyje, tačiau nebuvo vertintas kiekybinis C-PC pasiskirstymas skirtinguose odos sluoksniuose. Tęsiant pradėtus tyrimus, tikslinga būtų toliau taikyti kiekybinius analizės metodus C-PC kiekiui odoje nustatyti. *In vivo* tyrimas parodė, kad C-PC turinčios transfersominės formuluotės sumažino uždegiminius, proliferacinius ir displazinius pokyčius odoje, būdingus ankstyvosioms DMBA/TPA sukeltoms odos karcerogenezės stadijoms. Odos plokščialąstelinės karcinomos išsivystymas nebuvo pasiektas per nustatytą tyrimo laikotarpį. Kituose tyrimuose būtų svarbu įvertinti C-PC transfersomų poveikį vėlesnėse kancerogenezės stadijose, pvz., aktininės keratozės ir plokščialąstelinės karcinomos progresavimą. Be to, šių formuluočių profilaktinio poveikio tyrimai alternatyviuose modeliuose, pvz., UV spinduliuotės sukeltos odos pažaidos, suteiktų papildomų įžvalgų apie jų taikymo galimybes dermatologijoje. *In vivo* tyrime buvo naudojami tik pelių patinėliai. Siekiant išsamiau įvertinti C-PC transfersomų poveikį, kituose tyrimuose vertėtų įtraukti abiejų lyčių gyvūnus, kadangi nuo lyties priklausomi odos fiziologijos, hormoninės reguliacijos ir uždegiminio atsako skirtumai gali daryti įtaką kancerogenezės procesui bei atsakui į vietinio poveikio priemonių taikymą. Sukurtų transfersominių formuluočių poveikis nebuvo palygintas su klinikinėje praktikoje naudojamais vietinio poveikio terapiniais preparatais. Tokie lyginamieji tyrimai būtų naudingi siekiant išsamiau įvertinti C-PC turinčių transfersominių formuluočių veiksmingumą ir jų potencialias pritaikymo dermatologijoje galimybes.

Išvados

1. C-PC mėginiai buvo išskirti iš natūraliai surinktos melsvabakterių biomasės, o C-PC kokybiniai rodikliai priklausė nuo biomasės sudėties ir taikytų gryninimo metodų. Didesnis C-PC grynumas buvo pasiektas, taikant jonų mainų chromatografiją. Taip pat nustatyta, kad sunkiųjų metalų kiekiui C-PC mėginiuose turėjo įtakos biomasėje dominuojanti melsvabakterių gentis, aplinkos sąlygos, ir gryninimo metodas. Atsižvelgiant į saugumo aspektus, tolimesniems tyrimams buvo pasirinktas iš *A. flos-aquae* biomasės išskirtas ir jonų mainų chromatografija išgrynintas C-PC, pasižymėjęs didesnio grynumo ir mažesnio užterštumo sunkiaisiais metalais profiliu.

2. Sukurtos vietinio poveikio technologinės formuluotės su C-PC, o jų fizikocheminės savybės ir C-PC struktūrinis stabilumas šiose sistemose priklausė nuo formuluočių sudėties. Nustatyta, kad polisacharidinių gelifikuojančių medžiagų pagrindu pagaminti hidrogeliai (natrio alginatas, *Soligel*™, HEC, NaCMC, HPMC ir HEMC) užtikrino geresnį C-PC stabilumą, o sintetiniai polimerai (*Carbopol*® *Ultrez 21*, *Pemulen*™) ir tam tikros sąlygos (pH, temperatūra) neigiamai veikė C-PC struktūrinį stabilumą. *SharoSENSE*™ *Plus 785* užtikrino geriausią C-PC struktūrinį stabilumą ir reikiamą mikrobiologinį saugumą. *In vitro* tyrimai parodė, kad PG statistiškai reikšmingai padidino C-PC atpalaidavimo greitį iš hidrogelio matricos. Siekiant pagerinti C-PC struktūrinį stabilumą ir skvarbą į odą, buvo sukurtos nanotechnologijomis pagrįstos transfersominės formuluotės. Taikant dviejų pakopų gamybos metodą pavyko išsaugoti C-PC struktūrinį vientisumą ir biologinį aktyvumą, tai pagrindžiant spektrofotometriniu metodu, antioksidacinio aktyvumo ir citokompatibilumo tyrimais. Visos sukurtos transfersomų formuluotės pasižymėjo vietiniam naudojimui tinkamomis fizikocheminėmis savybėmis, o glicerolio turinčios formuluotės (Gly-T ir Gly-Chol-T) išsiskyrė didesniu įterpimo efektyvumu ir geresniu ilgalaikiu stabilumu.

3. *Ex vivo* tyrimai parodė, kad C-PC skvarba į odą iš technologinių formuluočių priklauso nuo naudojamos pernašos sistemos ir formuluotės sudėties. Nustatyta, kad iš tradicinių formuluočių (hidrogelio ir tirpalo) C-PC skvarba į odą buvo ribota dėl didelės C-PC molekulinės masės ir hidrofilinės prigimties – be skvarbą didinančių medžiagų C-PC praktiškai nebuvo aptinkamas odoje. PG padidino C-PC kaupimąsi raginio sluoksnio srityje, tačiau jo poveikis išliko ribotas. Transfersominės nanonešiklių sistemos pagerino C-PC patekimą į odą, padidindamos jo kaupimąsi raginiame sluoksnyje, ir demonstravo pranašumą prieš kitas tirtas

sistemas. Nors C-PC skvarba į gilesnius odos sluoksnius nebuvo nustatyta, padidėjęs jo kaupimasis raginiame sluoksnyje gali sudaryti prielaidas laipsniškam C-PC patekimui į gilesnius odos sluoksnius, tačiau šiai prielaidai patvirtinti reikalingi papildomi kiekybiniai tyrimai.

4. *In vivo* tyrimas parodė, kad C-PC turinčios transfersominės formuluotės sumažino DMBA/TPA sukeltus uždegiminius, proliferacinius ir displazinius pokyčius odoje. C-PC transfersomos sumažino makroskopinius odos pažeidimus – eritemą, sausumą, pleiskanojimą ir papulių formavimąsi. Histopatologiniai tyrimai parodė, kad C-PC turinčios formuluotės slopino epidermio sustorėjimą, hiperplaziją ir displaziją, taip pat mažino mitotinį aktyvumą, palyginti su kancerogeno kontroline grupe. Nustatytas putliųjų ląstelių kiekio ir uždegiminio atsako sumažėjimas. Imunohistocheminė analizė patvirtino antiproliferacinį poveikį – C-PC transfersomos reikšmingai sumažino Ki-67 ekspresiją, ypač suprabaziniame epidermio sluoksnyje. C-PC transfersomos buvo gerai toleruojamos ir nesukėlė struktūrinių ar proliferacinių pokyčių sveikoje odoje.

REFERENCES

1. da Silva Pinto Neto J, Serra GM, Xavier LP, Santos AV. Chemodiversity and biotechnological potential of microginins. *Int J Mol Sci* **2025**;26(13):6117. doi:10.3390/ijms26136117.
2. Thuan NH, An TT, Shrestha A, Canh NX, Sohng JK, Dhakal D. Recent advances in exploration and biotechnological production of bioactive compounds in three cyanobacterial genera: Nostoc, Lyngbya, and Microcystis. *Front Chem* **2019**;7:604. doi:10.3389/fchem.2019.00604.
3. Hu H, Zhang Z, Chen B, Zhang Q, Xu N, Paerl HW, et al. Potential health risk assessment of cyanobacteria across global lakes. *Appl Environ Microbiol* **2024**;90(11):e01936-24. doi:10.1128/aem.01936-24.
4. Mishra S, Stumpf RP, Schaeffer BA, Werdell PJ. Recent changes in cyanobacteria algal bloom magnitude in large lakes across the contiguous United States. *Sci Total Environ* **2023**;897:165253. doi:10.1016/j.scitotenv.2023.165253.
5. Chen L, Giesy JP, Adamovsky O, Svirčev Z, Meriluoto J, Codd GA, et al. Challenges of using blooms of Microcystis spp. in animal feeds: a comprehensive review of nutritional, toxicological and microbial health evaluation. *Sci Total Environ* **2021**;764:142319. doi:10.1016/j.scitotenv.2020.142319.
6. Aranda YN, Bhatt P, Ates N, Engel BA, Simsek H. Cyanophage-cyanobacterial interactions for sustainable aquatic environment. *Environ Res* **2023**;229:115728. doi:10.1016/j.envres.2023.115728.
7. Guo Y, Dong X, Li H, Tong Y, Liu Z, Jin J. Cyanophage engineering for algal blooms control. *Viruses* **2024**;16(11):1745. doi:10.3390/v16111745.
8. Sarma S, Sharma S, Rudakiya D, Upadhyay J, Rathod V, Patel A, et al. Valorization of microalgae biomass into bioproducts promoting circular bioeconomy: a holistic approach of bioremediation and biorefinery. *3 Biotech* **2021**;11(8):378. doi:10.1007/s13205-021-02911-8.
9. Andonova V, Nikolova K, Iliev I, Georgieva S, Petkova N, Feizi-Dehnayebi M, et al. Spectral characteristics, in silico perspectives, density functional theory (DFT), and therapeutic potential of green-extracted phycocyanin from Spirulina. *Int J Mol Sci* **2024**;25(17):9170. doi:10.3390/ijms25179170.
10. Dong J, Lang Y, He J, Cui J, Liu X, Yuan H, et al. Phycocyanin-based multifunctional microspheres for treatment of infected radiation-induced skin injury. *Biomaterials* **2025**;317:123061. doi:10.1016/j.biomaterials.2024.123061.
11. Shafiei M, Shafiei M, Mohseni Sani N, Guo W, Guo S, Vali H, et al. A new and promising C-phycocyanin-producing cyanobacterial strain, Cyanobium sp. MMK01: practical strategy towards developing a methodology to achieve C-phycocyanin with ultra-high purity. *Front Microbiol* **2024**;15:1394617. doi:10.3389/fmicb.2024.1394617.
12. Duman Y, Tufan G. Chromatographic purification of C-phycocyanin from Spirulina platensis: assessing antioxidant activity and stability. *J Sci Food Agric* **2024**;104(12):7326–34. doi:10.1002/jsfa.13553.
13. Zhang S, Huang C, Sun Z, Jiao P, Ding B, Ding L, et al. C-phycocyanin and quaternized chitosan-based antibiotic-free hydrogels with antioxidant and antibacterial activity for wound healing. *Int J Biol Macromol* **2025**;302:140647. doi:10.1016/j.ijbiomac.2025.140647.

14. Zhou Y, Bai R, Huang Y, Li W, Chen J, Cheng Z, et al. The anti-photoaging effect of C-phycocyanin on ultraviolet B-irradiated BALB/c-nu mouse skin. *Front Bioeng Biotechnol* **2023**;11:1229387. doi:10.3389/fbioe.2023.1229387.
15. Qu J, Geng X, Qin S, Li J, Li W. The utilization of TGase-crosslinked phycocyanin-collagen hydrogels for the purpose of facilitating skin wound healing. *Int J Biol Macromol* **2025**;320:145932. doi:10.1016/j.ijbiomac.2025.145932.
16. Negm El-Dein A, Soliman TN, Ezzat A, et al. Innovative hydrogel formulation combining phycocyanin and probiotic for enhancing skin regeneration and accelerated wound healing: a preclinical investigation in Wistar rats. *Probiotics Antimicrob Proteins* **2026**;18(2):2037–55. doi:10.1007/s12602-025-10635-x.
17. Jang YA, Kim BA. Protective effect of Spirulina-derived C-phycocyanin against ultraviolet B-induced damage in HaCaT cells. *Medicina* **2021**;57(3):273. doi:10.3390/medicina57030273.
18. Xu Z, Jin Y, Zhang C, HePeng Y, Yang S, Chen X, et al. A methacrylated pullulan hydrogel incorporating phycocyanin-functionalized copper sulfide nanoparticles for photothermal antibacterial therapy and improved wound healing. *Int J Biol Macromol* **2025**;315(Pt 1):144446. doi:10.1016/j.ijbiomac.2025.144446.
19. Liu G, Li X, Yang F, Qi J, Shang L, Zhang H, et al. C-phycocyanin ameliorates the senescence of mesenchymal stem cells through ZDHHC5-mediated autophagy via PI3K/AKT/mTOR pathway. *Aging Dis* **2023**;14(4):1425–40. doi:10.14336/AD.2023.0121.
20. Kose A, Oncel SS. Design of melanogenesis regulatory peptides derived from phycocyanin of the microalgae Spirulina platensis. *Peptides* **2022**;152:170783. doi:10.1016/j.peptides.2022.170783.
21. Salgado MTSF, Fernandes-Silva E, Matsumoto AM, et al. C-phycocyanin decreases proliferation and migration of melanoma cells: in silico and in vitro evidences. *Bioorg Chem* **2022**;122:105757. doi:10.1016/j.bioorg.2022.105757.
22. Salgado MTSF, Silva MCS, Fratelli C, Braga ARC, Lopes TBG, Ferreira E, et al. Bioactive C-phycocyanin exerts immunomodulatory and antitumor activity in mice with induced melanoma. *Toxicol Appl Pharmacol* **2024**;484:116874. doi:10.1016/j.taap.2024.116874.
23. Roky AH, Islam MM, Ahasan AMF, Mostaq MS, Mahmud MZ, Amin MN, et al. Overview of skin cancer types and prevalence rates across continents. *Cancer Pathog Ther* **2024**;3(2):89–100. doi:10.1016/j.cpt.2024.08.002.
24. Fania L, Didona D, Di Pietro FR, Verkhovskaia S, Morese R, Paolino G, et al. Cutaneous squamous cell carcinoma: from pathophysiology to novel therapeutic approaches. *Biomedicines* **2021**;9:171. doi:10.3390/biomedicines9020171.
25. Li Z, Lu F, Zhou F, Song D, Chang L, Liu W, et al. From actinic keratosis to cutaneous squamous cell carcinoma: the key pathogenesis and treatments. *Front Immunol* **2025**;16:1518633. doi:10.3389/fimmu.2025.1518633.
26. Quan T. Molecular insights of human skin epidermal and dermal aging. *J Dermatol Sci* **2023**;112(2):48–53. doi:10.1016/j.jdermsci.2023.08.006.
27. Ho CY, Dreesen O. Faces of cellular senescence in skin aging. *Mech Ageing Dev* **2021**;198:111525. doi:10.1016/j.mad.2021.111525.
28. Perez M, Abisaad JA, Rojas KD, Marchetti MA, Jaimes N. Skin cancer: primary, secondary, and tertiary prevention. *Part I. J Am Acad Dermatol* **2022**;87(2):255–68. doi:10.1016/j.jaad.2021.12.066.

29. Puglisi R, Biazzi E, Gesmundo D, Vanni R, Tava A, Cenadelli S. The antioxidant activity of a commercial and a fractionated phycocyanin on human skin cells in vitro. *Molecules* **2022**;27:5276. doi:10.3390/molecules27165276.
30. Mao M, Han G, Zhao Y, Xu X, Zhao Y. A review of phycocyanin: production, extraction, stability and food applications. *Int J Biol Macromol* **2024**;280(Pt 3):135860. doi:10.1016/j.ijbiomac.2024.135860.
31. Akram MW, Jamshaid H, Rehman FU, Zaeem M, Khan JZ, Zeb A. Transfersomes: a Revolutionary Nanosystem for Efficient Transdermal Drug Delivery. *AAPS PharmSciTech* **2021**;23(1):7. doi:10.1208/s12249-021-02166-9.
32. Adjali A, Clarot I, Chen Z, Marchioni E, Boudier A. Physicochemical Degradation of Phycocyanin and Means to Improve Its Stability: A Short Review. *J Pharm Anal* **2022**; 12:406–14. doi:10.1016/j.jpha.2021.12.005.
33. Akl MA, Eldeen MA, Kassem AM. Beyond Skin Deep: Phospholipid-Based Nanovesicles as Game-Changers in Transdermal Drug Delivery. *AAPS PharmSciTech* **2024**; 25(6):184. doi:10.1208/s12249-024-02896-6.
34. Zewail M, Gaafar PME, Abou Youssef NAH, Ali ME, Ragab MF, Kamal MF, Noureldin MH, Abbas H. Novel *Spirulina platensis* Bilosomes for Combating UVB-Induced Skin Damage. *Pharmaceuticals* **2023**;16(1):36. doi:10.3390/ph16010036.
35. Castangia I, Manca ML, Catalan-Latorre A, Maccioni AM, Fadda AM, Manconi M. Phycocyanin-Encapsulating Hyalurosomes as Carrier for Skin Delivery and Protection from Oxidative Stress Damage. *J Mater Sci Mater Med* **2016**;27:75. doi: 10.1007/s10856-016-5687-4.
36. Castangia I, Manca ML, Caddeo C, Bacchetta G, Pons R, Demurtas D, Diez-Sales O, Fadda AM, Manconi M. Santosomes as Natural and Efficient Carriers for the Improvement of Phycocyanin Reepithelising Ability *In Vitro* and *In Vivo*. *Eur J Pharm Biopharm* **2016**;103:149–58. doi:10.1016/j.ejpb.2016.03.033.
37. Manconi M, Pendas J, Ledon N, Moreira T, Sinico C, Saso L, Fadda AM. Phycocyanin Liposomes for Topical Anti-Inflammatory Activity: *In Vitro* and *In Vivo* Studies. *J Pharm Pharmacol* **2009**;61:423–30. doi:10.1211/jpp/61.04.0002.
38. Allaw M, Pleguezuelos-Villa M, Manca ML, Caddeo C, Aroffu M, Nacher A, Díez-Sales O, Ruiz Saurí A, Escribano Ferrer E, Fadda AM, Manconi M. Innovative Strategies to Treat Skin Wounds with Mangiferin: Fabrication of Transfersomes Modified with Glycols and Mucin. *Nanomedicine* **2020**;15(17):1671–85. doi:10.2217/nnm-2020-0116.
39. Aroffu M, Abi Rached R, Castangia I, Italiani P, D'Apice L, Fernández-Busquets X, Nacher A, Manconi M, Pedraz JL, Manca M. A Preliminary Investigation on Hydrogel Disks Imbibed with Enriched Transfersomes as a Promising Tool to Promote the Cutaneous Deposition of Vaccine Antigens. *J Drug Deliv Sci Technol* **2024**;102:106399. doi:10.1016/j.jddst.2024.106399.
40. Doustvaghe YK, Haeri A, Sisakht MM, Amirkhani MA, Vatanpour H. Recombinant Human Epidermal Growth Factor-Loaded Liposomes and Transferosomes for Dermal Delivery: Development, Characterization, and Cytotoxicity Evaluation. *Drug Dev Res* **2024**;85(5):e22234. doi:10.1002/ddr.22234.
41. Matharoo N, Mohd H, Michniak-Kohn B. Transferosomes as a Transdermal Drug Delivery System: Dermal Kinetics and Recent Developments. *Wiley Interdiscip Rev Nanomed Nanobiotechnol* **2024**;16(1):e1918. doi:10.1002/wnan.1918.

42. Khazi MI, Demirel Z, Liaqat F, Dalay MC. Analytical Grade Purification of Phycocyanin from Cyanobacteria. In: Biofuels from Algae, Spilling, K., Ed.; Methods in Molecular Biology, vol. 1980. Humana: New York, NY, USA. **2018**. pp. 173–9. doi:10.1007/7651_2018_202.
43. Bennett A, Bogorad L. Complementary Chromatic Adaptation in a Filamentous Blue-Green Alga. *J Cell Biol* **1973**;58:419–35. doi:10.1083/jcb.58.2.419.
44. Li H, Brakebusch C. Analyzing Skin Tumor Development in Mice by the DMBA/TPA Model. *Methods Cell Biol* **2021**;163:113–21. doi:10.1016/bs.mcb.2020.08.004.
45. Águila-Carricondo P, García-García R, de la Roche JP, Galán PL, Bautista LF, Espada JJ, Vicente G. *Aphanizomenon flos-aquae*: A Biorefinery for Health and Energy – Unleashing Phycocyanin's Power and Biogas Potential. *Mar Drugs* **2025**;23(6):225. doi:10.3390/md23060225.
46. Karosienė J, Savadova-Ratkus K, Toruńska-Sitarz A, Koreivienė J, Kasperovičienė J, Vitonytė I, Błaszczyk A, Mazur-Marzec H. First Report of Saxitoxins and Anatoxin – a Production by Cyanobacteria from Lithuanian Lakes. *Eur J Phycol* **2020**;55(3):327–38. doi:10.1080/09670262.2020.1734667.
47. Drobac Backović D, Tokodi N. Cyanotoxins in Food: Exposure Assessment and Health Impact. *Food Res Int* **2024**;184:114271. doi:10.1016/j.foodres.2024.114271.
48. Fournier C, Quesada A, Cirés S, Saberioon M. Discriminating Bloom-Forming Cyanobacteria Using Lab-Based Hyperspectral Imagery and Machine Learning: Validation with Toxic Species under Environmental Ranges. *Sci Total Environ* **2024**;932:172741. doi:10.1016/j.scitotenv.2024.172741.
49. Bernard C, Ballot A, Thomazeau S, Maloufi S, Furey A, Mankiewicz-Boczek J, Pawlik-Skowrońska B, Capelli C, Salmaso N. Cyanobacteria Associated with the Production of Cyanotoxins. In: Handbook of Cyanobacterial Monitoring and Cyanotoxin Analysis. Meriluoto J, Spoof L, Codd GA, Eds. Wiley: Chichester. **2017**. pp. 501–25.
50. Overlingė D, Toruńska-Sitarz A, Cegłowska M, Szubert K, Mazur-Marzec H. Phylogenetic and Molecular Characteristics of Two *Aphanizomenon* Strains from the Curonian Lagoon, Southeastern Baltic Sea and Their Biological Activities. *Sci Rep* **2024**;14(1):24686. doi:10.1038/s41598-024-76064-y.
51. Pham ML, Maghsoomi S, Brandl M. An Electrochemical Aptasensor for the Detection of Freshwater Cyanobacteria. *Biosensors* **2024**;14(1):28. doi:10.3390/bios14010028.
52. Pispas K, Manthos G, Sventzouri E, Geroulia M, Mastropetros SG, Ali SS, Kornaros M. Optimizing Phycocyanin Extraction from Cyanobacterial Biomass: A Comparative Study of Freeze-Thaw Cycling with Various Solvents. *Mar Drugs* **2024**;22(6):246. doi:10.3390/md22060246.
53. Dahmen I, Chtourou H, Hadrich F, Baccar N, Sayadi S, Ayadi H, Chamkha M. *Phormidium versicolor* PC Skin Cream Evaluation for Its Stability and Biological Activities. *Appl Microbiol Biotechnol* **2024**;108:541. doi:10.1007/s00253-024-13359-0.
54. Usai L, Torre S, Aktay N, Dunford NT, Citi V, Flori L, Nieri P, Lutzu GA. Recent Advancements in Production and Extraction Methods of Phycobiliprotein C-Phycocyanin by *Arthrospira (Spirulina) platensis*: A Mini Review. *Curr Microbiol* **2024**; 81(12):428. doi:10.1007/s00284-024-03964-7.
55. Lourembam J, Haobam B, Singh KB, Verma S, Rajan JP. The Molecular Insights of Cyanobacterial Bioremediations of Heavy Metals: The Current and the Future Challenges. *Front Microbiol* 2024;15:1450992. doi:10.3389/fmicb.2024.1450992.
56. Mehta SK, Gaur JP. Use of Algae for Removing Heavy Metal Ions from Wastewater: Progress and Prospects. *Crit Rev Biotechnol* **2005**;25:113–52. doi: 10.1080/0738855 0500248571.

57. Jia Y, Chen W, Zuo Y, Lin L, Song L. Heavy Metal Migration and Risk Transference Associated with Cyanobacterial Blooms in Eutrophic Freshwater. *Sci Total Environ* **2018**; 613–614:1324–30. doi:10.1016/j.scitotenv.2017.09.180.
58. Rahman Z, Singh VP. The Relative Impact of Toxic Heavy Metals (THMs) (Arsenic, Cadmium, Chromium(VI), Mercury, and Lead) on the Total Environment: An Overview. *Environ Monit Assess* **2019**;191:419. doi:10.1007/s10661-019-7528-7.
59. Rosen BP. Biochemistry of Arsenic Detoxification. *FEBS Lett* **2002**;529:86–92. doi:10.1016/s0014-5793(02)03186-1.
60. Mathema VB, Thakuri BC, Sillanpää M. Bacterial *mer* Operon-Mediated Detoxification of Mercurial Compounds: A Short Review. *Arch Microbiol* **2011**;193:837–44. doi:10.1007/s00203-011-0751-4.
61. Cirés S, Ballot A. A review of the phylogeny, ecology, and toxin production of bloom-forming Aphanizomenon spp. and related species within the Nostocales (Cyanobacteria). *Harmful Algae* **2016**;54:21–43. doi:10.1016/j.hal.2015.09.007.
62. Chen JZ, Tao XC, Xu J, Zhang T, Liu ZL. Biosorption of lead, cadmium, and mercury by immobilized Microcystis aeruginosa in a column. *Process Biochem* **2005**;40:3675–9. doi:10.1016/j.procbio.2005.03.066.
63. Kauno Marios Regional Park. Hidrologija [Internet]. Available from: https://kaunomarios.lt/gamta,p2#Hidrologija [cited 2026 Mar 21].
64. Environmental Protection Agency. Upių, ežerų ir tvenkinių cheminė būklė [Internet]. Available from: https://aaa.lrv.lt/lt/veiklos-sritys/vanduo/upes-ezerai-ir-tvenkiniai/upiu-ezeru-ir-tvenkiniu-bukle/upiu-ezeru-ir-tvenkiniu-chemine-bukle [cited 2026 Mar 21].
65. Bellamy-Carter J, Sound JK, Leney AC. Probing heavy metal binding to phycobiliproteins. *FEBS J* **2022**;289:4646–56. doi:10.1111/febs.16396.
66. Gelagutashvili E. Interaction of heavy metal ions with C-phycocyanin: binding isotherms and cooperative effects [Internet]. *arXiv* **2007**. Available from: https://arxiv.org/abs/0707.3019
67. Chi Z, Hong B, Tan S, Wu Y, Li H, Lu CH, et al. Impact assessment of heavy metal cations to the characteristics of photosynthetic phycocyanin. *J Hazard Mater* **2020**; 391:122225. doi:10.1016/j.jhazmat.2020.122225.
68. Ashaolu TJ, Samborska K, Lee CC, Tomas M, Capanoglu E, Tarhan O, et al. Phycocyanin, a super functional ingredient from algae: properties, purification, characterization, and applications. *Int J Biol Macromol* **2021**;193:2320–31. doi:10.1016/j.ijbiomac.2021.11.064.
69. Patel A, Mishra S, Pawar R, Ghosh PK. Purification and characterization of C-phycocyanin from cyanobacterial species of marine and freshwater habitat. *Protein Expr Purif* **2005**;40:248–55. doi:10.1016/j.pep.2004.10.028.
70. Jungbauer A, Hahn R. Ion-exchange chromatography. In: Methods in enzymology. Amsterdam: Elsevier; **2009**. Vol. 463. pp. 349–71. doi:10.1016/S0076-6879(09)63022-6.
71. Moraes CC, Kalil SJ. Strategy for a protein purification design using C-phycocyanin extract. *Bioresour Technol* **2009**;100:5312–7. doi:10.1016/S0076-6879(09)63022-6.
72. European Parliament and Council. Regulation (EC) No 1223/2009 of the European Parliament and of the Council of 30 November 2009 on cosmetic products. *Off J Eur Union* **2009**;L342:59–209.
73. European Parliament and Council. Regulation (EU) 2017/745 of the European Parliament and of the Council of 5 April 2017 on medical devices. *Off J Eur Union* **2017**; L117:1–175.

74. ISO 21392:2021. Cosmetics – analytical methods – determination of trace elements in cosmetic products using ICP-MS. Geneva: International Organization for Standardization; **2021**.
75. Aoki J, Sasaki D, Asayama M. Development of a method for phycocyanin recovery from filamentous cyanobacteria and evaluation of its stability and antioxidant capacity. *BMC Biotechnol* **2021**;21:40. doi:10.1186/s12896-021-00692-9.
76. Li Y, Wang Z, Liu H, Chen T, Du Y, Hu J, et al. Controlled ionic-induced self-assembly of phycocyanin: structure, binding mechanism, and molecular dynamics simulation. *Food Chem* **2025**;477:143603. doi:10.1016/j.foodchem.2025.143603.
77. Fernández SI, Hernández ME, Gómez LA. Arthrospira platensis and its potential for skin regeneration in animal models as support for initiating clinical trials in humans: a systematic review. *Biomedicines* **2025**;13(9):2239. doi:10.3390/biomedicines13092239.
78. Minato T, Teramoto T, Adachi N, Hung NK, Yamada K, Kawasaki M, et al. Non-conventional octameric structure of C-phycocyanin. *Commun Biol* **2021**;4(1):1238. doi:10.1038/s42003-021-02767-x.
79. Patel SN, Sonani RR, Gupta GD, Singh NK, Upadhyaya C, Sonavane B, et al. Structure and stability of phycocyanin from thermotolerant Oscillatoria. *FEBS Lett* **2025**; 599(10):1420–32. doi:10.1002/1873-3468.70048.
80. Patel SN, Sonani RR, Chaubey MG, Gupta GD, Singh NK, Kumar V, et al. Crystal structure of Synechococcus phycocyanin: implications of light-harvesting and antioxidant properties. *3 Biotech* **2023**;13(7):247. doi:10.1007/s13205-023-03665-1.
81. Yuan B, Li Z, Shan H, Dashnyam B, Xu X, McClements DJ, et al. A review of recent strategies to improve the physical stability of phycocyanin. *Curr Res Food Sci* **2022**; 5:2329–37. doi:10.1016/j.crfs.2022.11.019.
82. Chittapun S, Suwanmanee K, Kongsinkaew C, Pornpukdeewattana S, Chisti Y, Charoenrat T. Thermal degradation kinetics and purification of C-phycocyanin from thermophilic and mesophilic cyanobacteria. *J Biotechnol* **2025**;398:76–86. doi:10.1016/j.jbiotec.2024.11.018.
83. Wang T, Yi W, Zhang Y, Wu H, Fan H, Zhao J, et al. Sodium alginate hydrogel containing platelet-rich plasma for wound healing. *Colloids Surf B Biointerfaces* **2023**; 222:113096. doi:10.1016/j.colsurfb.2022.113096.
84. Peng W, Li D, Dai K, Wang Y, Song P, Li H, et al. Recent progress of collagen, chitosan, alginate and other hydrogels in skin repair and wound dressing applications. *Int J Biol Macromol* **2022**;208:400–8. doi:10.1016/j.ijbiomac.2022.03.002.
85. Carrer V, Alonso C, Pont M, Zanuy M, Cordoba M, Espinosa S, et al. Effect of propylene glycol on the skin penetration of drugs. *Arch Dermatol Res* **2020**;312:337–52. doi:10.1007/s00403-019-02017-5.
86. Tran HN, Kim IG, Kim JH, Bhattacharyya A, Chung EJ, Noh I. Incorporation of cell-adhesive proteins in 3D-printed lipoic acid-maleic acid-poly(propylene glycol)-based tough gel ink for cell-supportive microenvironment. *Macromol Biosci* **2023**;23: 2300316. doi:10.1002/mabi.202300316.
87. Yang D, Liu C, Quan P, Fang L. A systematic approach to determination of permeation enhancer action efficacy and sites: molecular mechanism investigated by quantitative structure-activity relationship. *J Control Release* **2020**;322:1–12. doi:10.1016/j.jconrel.2020.03.014.
88. Wang Z, Xue Y, Zhu Z, Hu Y, Zeng Q, Wu Y, et al. Quantitative structure-activity relationship of enhancers of licochalcone A and glabridin release and permeation enhancement from carbomer hydrogel. *Pharmaceutics* **2022**;14:262. doi:10.3390/pharmaceutics14020262.

89. Zhang M, Zhang Q, Chen X, Jiang T, Song P, Wang B, et al. Mussel-inspired nanocomposite hydrogel based on alginate and antimicrobial peptide for infected wound repair. *Int J Biol Macromol* **2022**;219:1087–99. doi:10.1016/j.ijbiomac.2022.08.165.
90. Adli SA, Ali F, Azmi AS, Anuar H, Nasir NAM, Hasham R, et al. Development of biodegradable cosmetic patch using a polylactic acid/phycocyanin-alginate composite. *Polymers* **2020**;12:1669. doi:10.3390/polym12081669.
91. Lane ME. Skin penetration enhancers. *Int J Pharm* **2013**;447:12–21. doi:10.1016/j.ijpharm.2013.02.040.
92. Mistry J, Notman R. Mechanisms of the drug penetration enhancer propylene glycol interacting with skin lipid membranes. *J Phys Chem* **2024**;128(16):3885–97. doi:10.1021/acs.jpcb.3c06784.
93. Yu HL, Goh CF. Glycols: the ubiquitous solvent for dermal formulations. *Eur J Pharm Biopharm* **2024**;196:114182. doi:10.1016/j.ejpb.2024.114182.
94. Madhyastha HK, Radha KS, Sugiki M, Omura S, Maruyama M. C-phycocyanin transcriptionally regulates uPA mRNA through cAMP-mediated PKA pathway in human fibroblast WI-38 cells. *Biochim Biophys Acta Gen Subj* **2006**;1760:1624–30. doi:10.1016/j.bbagen.2006.08.012.
95. Madhyastha HK, Radha KS, Nakajima Y. uPA-dependent and independent mechanisms of wound healing by C-phycocyanin. *J Cell Mol Med* **2008**;12:2691–703. doi:10.1111/j.1582-4934.2008.00272.x.
96. Zhang R, Wang L, Meng L, Shang W, Ren Y, Qi Q, et al. A slime-inspired phycocyanin/κ-carrageenan-based hydrogel bandage with ultra-stretchability, self-healing, antioxidative, and antibacterial activity for wound healing. *Int J Biol Macromol* **2025**;289:138786. doi:10.1016/j.ijbiomac.2024.138786.
97. Gong W, Huang HB, Wang XC, He WY, Hu JN. Coassembly of fiber hydrogel with antibacterial activity for wound healing. *ACS Biomater Sci Eng* **2023**;9(1):375–87. doi:10.1021/acsbiomaterials.2c00716.
98. Pisani S, Di Martino D, Cerri S, Genta I, Dorati R, Bertino G, et al. Investigation and comparison of active and passive encapsulation methods for loading proteins into liposomes. *Int J Mol Sci* **2023**;24:13542. doi:10.3390/ijms241713542.
99. Antimisiaris SG, editor. Liposomes in drug delivery: what, where, how and when to deliver. Cambridge (MA): Academic Press; **2021**. pp. 101–20.
100. Sapkota R, Munt DJ, Kincaid AE, Dash AK. Liposomes and transfersomes in the delivery of papain for the treatment of keloids and hypertrophic scars. *PLoS One* **2023**;18(12):e0290224. doi:10.1371/journal.pone.0290224.
101. Manca ML, Cencetti C, Matricardi P, Castangia I, Zaru M, Díez-Sales O, et al. Glycerosomes: use of hydrogenated soy phosphatidylcholine mixture and its effect on vesicle features and diclofenac skin penetration. *Int J Pharm* **2016**;511:198–204. doi:10.1016/j.ijpharm.2016.07.009.
102. Alam MS, Sultana N, Rashid MA, Alhamhoom Y, Ali A, Waheed A, et al. Quality by design-optimized glycerosomes-enabled nanosunscreen gel of rutin hydrate. *Gels* **2023**;9:752. doi:10.3390/gels9090752.
103. Manca ML, Manconi M, Zaru M, Valenti D, Peris JE, Matricardi P, et al. Glycerosomes: investigation of role of 1,2-dimyristoyl-sn-glycero-3-phosphatidylcholine (DMPC) on the assembling and skin delivery performances. *Int J Pharm* **2017**;532:401–7. doi:10.1016/j.ijpharm.2017.09.026.
104. Zhu J, Tang X, Jia Y, Ho CT, Huang Q. Applications and delivery mechanisms of hyaluronic acid used for topical/transdermal delivery – a review. *Int J Pharm* **2020**;578:119127. doi:10.1016/j.ijpharm.2020.119127.

105. Kumbhar PS, Kamble V, Vishwas S, Kumbhar P, Kolekar K, Gupta G, et al. Unravelling the success of transfersomes against skin cancer: journey so far and road ahead. *Drug Deliv Transl Res* **2024**;14:2325–44. doi:10.1007/s13346-024-01607-9.
106. Shah S, Dhawan V, Holm R, Nagarsenker MS, Perrie Y. Liposomes: advancements and innovation in the manufacturing process. *Adv Drug Deliv Rev* **2020**;154–155:102–22. doi:10.1016/j.addr.2020.07.002.
107. Danaei M, Dehghankhold M, Ataei S, Hasanzadeh Davarani F, Javanmard R, Dokhani A, et al. Impact of particle size and polydispersity index on the clinical applications of lipidic nanocarrier systems. *Pharmaceutics* **2018**;10:57. doi:10.3390/pharmaceutics 10020057.
108. Guillot AJ, Martinez-Navarrete M, Garrigues TM, Melero A. Skin drug delivery using lipid vesicles: a starting guideline for their development. *J Control Release* **2023**;355: 624–54. doi:10.1016/j.jconrel.2023.02.006.
109. Chakraborty S, Doktorova M, Molugu TR, Heberle FA, Scott HL, Dzikovski B, et al. How cholesterol stiffens unsaturated lipid membranes. *Proc Natl Acad Sci U S A* **2020**; 117(36):21896–905. doi:10.1073/pnas.2004807117.
110. Honary S, Zahir F. Effect of zeta potential on the properties of nano-drug delivery systems – a review (Part 2). *Trop J Pharm Res* **2013**;12:265–73. doi:10.4314/tjpr.v12i2.20.
111. Abel EL, Angel JM, Kiguchi K, DiGiovanni J. Multi-stage chemical carcinogenesis in mouse skin: fundamentals and applications. *Nat Protoc* **2009**;4:1350–62. doi:10.1038/ nprot.2009.120.
112. DiGiovanni J. Modification of multistage skin carcinogenesis in mice. *Prog Exp Tumor Res* **1991**;33:192–229. doi:10.1159/000419252.
113. Surien O, Masre SF, Basri DF, Ghazali AR. Chemopreventive effects of oral pterostilbene in multistage carcinogenesis of skin squamous cell carcinoma mouse model induced by DMBA/TPA. *Biomedicines* **2022**;10(11):2743. doi:10.3390/biomedicines 10112743.
114. Choi J, West CE, Roh YS, Sutaria N, Kwatra SG, Kwatra MM. Mouse models for actinic keratoses. *J Pharmacol Toxicol Methods* **2021**;110:107071. doi:10.1016/j.vascn. 2021.107071.
115. Shahid A, Huang M, Liu M, Shamim MA, Parsa C, Orlando R, et al. The medicinal mushroom Ganoderma lucidum attenuates UV-induced skin carcinogenesis and immunosuppression. *PLoS One* **2022**;17(3):e0265615. doi:10.1371/journal.pone.0265615.
116. Rajkumar J, Chandan N, Lio P, Shi V. The skin barrier and moisturization: function, disruption, and mechanisms of repair. *Skin Pharmacol Physiol* **2023**;36(4):174–85. doi:10.1159/000534136.
117. Madiraju SR, Possik E, Al-Mulla F, Nolan CJ, Prentki M. Glycerol and glycerol-3-phosphate: multifaceted metabolites in metabolism, cancer, and other diseases. *Endocr Rev* **2026**;47:93–120. doi:10.1210/endrev/bnaf033.
118. Salgaonkar N, Kadamkode V, Kumaran S, Mallemala P, Christy E, Appavoo S, et al. Glycerol fermentation by skin bacteria generates lactic acid and upregulates genes associated with skin barrier function. *Exp Dermatol* **2022**;31:1364–72. doi:10.1111/exd.14604.
119. Choudhary V, Kaddour-Djebbar I, Custer VE, Uaratanawong R, Chen X, Cohen E, et al. Glycerol improves skin lesion development in the imiquimod mouse model of psoriasis: experimental confirmation of anecdotal reports from patients with psoriasis. *Int J Mol Sci* **2021**;22:8749. doi:10.3390/ijms22168749.
120. Fernandes e Silva E, Da Silva Figueira F, Lettnin AP, Carrett-Dias M, Filgueira DMB, Kalil S, et al. C-phycocyanin: cellular targets, mechanisms of action and multidrug resistance in cancer. *Pharmacol Rep* **2018**;70:75-80. doi:10.1016/j.pharep.2017.07.018.

121. Liang S, Shamim MA, Shahid A, Chen M, Cleveland KH, Parsa C, et al. Prevention of skin carcinogenesis by the non-β-blocking R-carvedilol enantiomer. *Cancer Prev Res* **2021**;14(5):527–40. doi:10.1158/1940-6207.CAPR-20-0609.
122. Jun SY, Jang JY, Yoon SJ, Park J, Cho YJ, Shin HS, et al. C-phycocyanin derived from Spirulina maxima attenuates the symptoms of psoriasis in mouse models. *Res Sq* **2020**;1-15. doi:10.21203/rs.3.rs-31467/v1.
123. Jang JY, Lee BM, Jun SY, Yang YJ, Shin HS. Attenuation of psoriasis symptoms following treatment with C-phycocyanin from Spirulina maxima in a mouse model. *Biotechnol Bioprocess Eng* **2022**;27:407–14. doi:10.1007/s12257-022-0022-z.
124. Braune S, Krüger-Genge A, Kammerer S, Jung F, Küpper JH. Phycocyanin from Arthrospira platensis as potential anti-cancer drug: review of in vitro and in vivo studies. *Life* **2021**;11:91. doi:10.3390/life11020091.

CURRICULUM VITAE

Name, Surname:	**Daiva Galinytė**
Address:	Lithuanian University of Health Sciences, Medical Academy, Faculty of Pharmacy, Department of Pharmacognosy, Sukilėlių av. 14, Kaunas, Lithuania
Mobile phone:	+370 614 28604
E-mail:	daiva.galinyte@stud.lsmu.lt

Work experience

01/02/2023– current	Advanced practice pharmacist, UAB Eurovaistinė
01/10/2020– 01/01/2023	Pharmacy manager, UAB Eurovaistinė
01/11/2019– 01/06/2020	Pharmacovigilance coordinator, UAB Ideal Trade
01/07/2017– 01/11/2019	Pharmacovigilance coordinator, UAB Actiofarma
01/06/2013– 01/07/2017	Senior specialist, Drug safety and information department, State medicines control agency
01/07/2008– 01/09/2017	Pharmacy manager, UAB Eurovaistinė
01/06/2008– 01/07/2008	Pharmacist, UAB Eurovaistinė

Education

15/09/2021– 15/09/2025	PhD studies, Pharmacy, Lithuanian University of Health Sciences
01/09/2003– 30/06/2008	Master of Pharmacy, Lithuanian University of Health Sciences

Awards and grants

05/09/2023	BSBV 1 Incubation Program Grant

International experience

28/042025– 02/05/2025	Artificial Intelligence (AI) in the Healthcare. Clinical Pharmacy and Optimization of Pharmacotherapy: New Advances in Research and Clinical Practice, Charles University, Czech Republic
16/04/2024– 16/06/2024	Traineeship, University of Cagliari, Department of Life and Environmental Sciences, Cagliari, Italy.

COPIES OF PUBLICATIONS

Paper 1

Title: Cyano-Phycocyanin: Mechanisms of Action on Human Skin and Future Perspectives in Medicine

Authors: Dranseikienė, Daiva; Balčiūnaitė-Murzienė, Gabrielė; Karosienė, Jūratė; Morudov, Dmitrij; Juodžiukynienė, Nomeda; Hudz, Nataliia; Gerbutavičienė, Rima Jūratė; Savickienė, Nijolė

Plants, 11, 9 (2022)

plants

MDPI

Review

Cyano-Phycocyanin: Mechanisms of Action on Human Skin and Future Perspectives in Medicine

Daiva Dranseikienė [1,*], Gabrielė Balčiūnaitė-Murzienė [2], Jūratė Karosienė [3], Dmitrij Morudov [3], Nomeda Juodžiukynienė [4], Nataliia Hudz [5,6], Rima Jūratė Gerbutavičienė [7] and Nijolė Savickienė [1]

[1] Department of Pharmacognosy, Faculty of Pharmacy, Academy of Medicine, Lithuanian University of Health Sciences, Sukileliu av. 13, 50162 Kaunas, Lithuania; nijole.savickiene@lsmuni.lt
[2] Faculty of Pharmacy, Institute of Pharmaceutical Technologies, Academy of Medicine, Lithuanian University of Health Sciences, Sukileliu av. 13, 50162 Kaunas, Lithuania; gabriele.balciunaite@lsmuni.lt
[3] Laboratory of Algology and Microbial Ecology, Nature Research Centre, Akademijos St. 2, 08412 Vilnius, Lithuania; jurate.karosiene@gamtc.lt (J.K.); dmitrij.morudov@gamtc.lt (D.M.)
[4] Department of Veterinary Pathobiology, Faculty of Veterinary, Academy of Veterinary, Lithuanian University of Health Sciences, Tilzes St. 18, 47181 Kaunas, Lithuania; nomeda.juodziukyniene@lsmuni.lt
[5] Department of Drug Technology and Biopharmaceutics, Danylo Halytsky Lviv National Medical University, Pekarska St, 69, 79000 Lviv, Ukraine; natali_gudz@ukr.net
[6] Department of Pharmacy and Ecological Chemistry, University of Opole, Kopernika pl. 11a, 45-040 Opole, Poland
[7] Department of Drug Technology and Social Pharmacy, Faculty of Pharmacy, Academy of Medicine, Lithuanian University of Health Sciences, Sukileliu av. 13, 50162 Kaunas, Lithuania; rima.gerbutaviciene@lsmuni.lt
* Correspondence: daiva.galinyte@stud.lsmu.lt

Citation: Dranseikienė, D.; Balčiūnaitė-Murzienė, G.; Karosienė, J.; Morudov, D.; Juodžiukynienė, N.; Hudz, N.; Gerbutavičienė, R.J.; Savickienė, N. Cyano-Phycocyanin: Mechanisms of Action on Human Skin and Future Perspectives in Medicine. *Plants* **2022**, *11*, 1249. https://doi.org/10.3390/plants11091249

Academic Editor: Laura Cornara

Received: 28 February 2022
Accepted: 30 April 2022
Published: 5 May 2022

Abstract: Cyano-phycocyanin is one of the active pigments of the blue-green algae and is usually isolated from the filamentous cyanobacteria *Arthrospira platensis Gomont* (Spirulina). Due to its multiple physiological functions and non-toxicity, cyano-phycocyanin may be a potential substance for the topical treatment of various skin diseases. Considering that the conventional medicine faces drug resistance, insufficient efficacy and side effects, the plant origin compounds can act as an alternative option. Thus, the aim of this paper was to review the wound healing, antimicrobial, antioxidative, anti-inflammatory, antimelanogenic and anticancer properties and mechanisms of cyano-phycocyanin topical activities on human skin. Moreover, possible applications and biotechnological requirements for pharmaceutical forms of cyano-phycocyanin for the treatment of various skin diseases are discussed in this review.

Keywords: cyano-phycocyanin; cyanobacteria; skin diseases; wound healing; antimicrobial effect; antioxidative activity; anti-inflammatory effect; antimelanogenic effect; anticancer effect

1. Introduction

Over the past decade, researchers have focused their attention on microalgae and cyanobacteria [1]. Cyanobacteria, also known as blue-green algae, are the most primitive photosynthetic organisms on Earth which accumulate many active components with a broad range of important biological and pharmacological properties. Phycocyanins are light-absorbing biliproteins and biologically active compound that exist in all cyanobacterial species [2,3].

Phycocyanins are divided into three major types based on their spectral characteristics: cyano-phycocyanin (C-PC), derived from blue-green algae, R-phycocyanin (R-PC), derived from red algae, allophycocyanin, derived from both blue-green algae and red algae [4,5]. Wang L. and others (2014) also distinguished R-phycocyanin II (R-PC II) which is derived from marine cyanobacterium *Synechococcus* species [5].

Phycocyanins are oligomeric proteins composed of α and β subunits [4,5]. Each (αβ) monomer of C-PCs has three chromophores of phycocyanobilin. α Subunit carries one phycocyanobilin and the β subunit does two phycocyanobilins [5]. The molecular weights of α and β subunits are approximately 18 and 20 kDa, respectively. For R-PCs, an α subunit contains one phycocyanobilin but the β subunit carries one phycocyanobilin and one phycoerythrobilin [5]. Therefore, in the visual range of the light C-PCs, a one-peak absorption spectrum at approximately 610–620 nm is commonly shown, while R-PCs have two peaks in the absorption spectrum at wavelengths of 550 nm and 615–620 nm. The peak at approximately 550 nm comes from phycoerythrobilins and conspicuously expressed absorption maximum at approximately 615–620 nm is related to phycocyanobilins. Allophycocyanin has an absorption maximum at 650 nm [5–8]. R-PC from the marine red macroalga *Polysiphonia urceolata* (*Lightfoot ex Dillwyn*) *Greville* is composed of one α and two β subunits. Their molecular mass was 17.5 kDa, 21.3 kDa and 22.6 kDa, respectively. The α subunit had a strong absorption band from the chromophore of phycocyanobilin at a wavelength of the absorption maximum of approximately 597 nm and two β subunits which showed a strong absorption band from phycoerythrobilin at a wavelength of the absorption maximum of approximately 553 nm and an absorption shoulder from phycocyanobilin at a wavelength of approximately 600 nm [5].

C-PC is a hydrophilic and blue-colored biliprotein which is highly stable in the pH range of 5–8 [8]. Its isoelectric point ranges from 4.1 to 6.4. C-PC should be purified at a temperature of 4 ± 1 °C, as it is highly sensitive to heating [9].

A filamentous cyanobacteria *Arthrospira platensis Gomont* is the primary source of commercial C-PC [10]. In general, microalgae can grow in a broad range of habitats, pH levels and temperatures, and they have minimal growth requirements [11]. Kuddus M. and others distinguished four different options for C-PC production: photoautotrophic, mixotrophic, heterotrophic and recombinant production. They highlight that the cultivation under controlled conditions and low-cost downstream processing could be an economical advantage to meet the existing demand of C-PC [4]. The multistage process is required for C-PC isolation from algae and purification. First, variety of physical (sonication, cavitation, osmotic, repeated freezing and thawing) and chemical (usage of acids, alkali, detergents, enzymes) methods or their combinations are used for cell disruption. After cell breakage, the product is isolated from the supernatant by centrifugation. Purification is performed by extraction with ammonium sulfate, while separation is generally achieved by the column chromatographic methods using adsorbents, anion exchangers or gel filtration chromatography. Freeze drying is considered to be the most suitable method for pigment drying [12]. The purity of C-PC is usually established by dividing C-PC absorbance at a wavelength of its absorption maximum at 620 nm to a specific absorbance at a wavelength of 280 nm, which is related to the total protein, especially aromatic amino acids (A620/A280). The purity of 0.7 is assumed to be food grade, 3.9—as reactive grade and greater than 4.0—as analytical grade [4,9,13]. C-PC sparked attention due to its exceptional capability to show radical scavenging activity, slow down inflammatory processes, and reduce oxidative stress. Furthermore, it has been proven to have an anti-mutative, antimicrobial, antitumor, and wound healing properties [2–4,9].

The aim of this paper was to review recent studies on the mechanisms of C-PC topical activities on human skin. Physiological properties of C-PC for the topical applications are given in Figure 1. Moreover, we discussed possible applications and biotechnological requirements for pharmaceutical forms of C-PC for the treatment of various skin diseases.

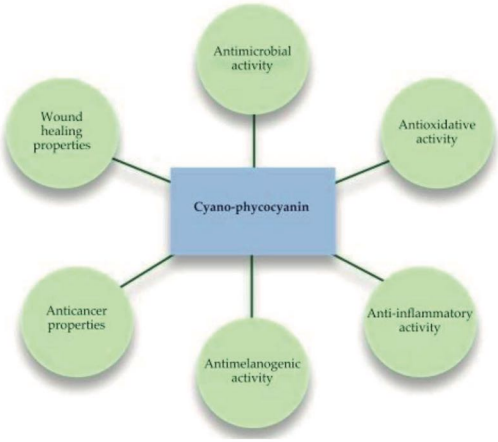

Figure 1. Physiological properties of C-PC for the topical application.

2. Biological Activity of C-PC

2.1. Wound Healing Effect

Skin acts as a barrier between the internal body and the external surrounding environment; therefore, wounds in the skin cause the loss of the integral anatomic continuity. Environmental conditions, physical accidents and general skin conditions, including but not limited to dryness and dermatitis, may contribute to skin wounds [1,14]. Cellular, molecular, biochemical, and physiological processes are a part of the skin recovery after the injury. The healing starts immediately following the arbitrary injury with the formation of a blood clot and the onset of inflammation. The proliferation and migration of dermal and epidermal cells, and a matrix synthesis occurs within 4 days, filling the wound area, and hence rebuilding the skin barrier. Finally, the tissue remodeling and maturing cycle enables a full recovery of the damaged skin tissue [15]. Some health conditions including but not limited to chronic diseases or bacterial infections could potentially undermine the recovery process [1]. Keeping this in mind, it is critical to identify bioeffective and natural ways of wound healing.

Madhyastha H.R. and others (2008) were the first to identify the effects of C-PC on wound healing. The effects of C-PC on fibroblast proliferation and urokinase-type plasminogen activator (uPA) migration were both investigated. It was demonstrated by in vitro studies that C-PC treatment (75 μg/mL) expedited the cell growth by inducing the G1 phase, thus resulting in an early event of cell cycle. It supports cell proliferation with no significant changes in the G2 or S phase. In addition, C-PC also increases the expression of cyclin-dependent kinases (cdK1 and cdK2), which play a significant role in the regulation of the cell cycle progression, ultimately leading to cell proliferation. This study determined that uPA is not considered as a significant molecule in controlling the proliferation and cell cycle in fibroblasts, but that it is involved in the cell migration process. The researchers also found that C-PC regulates uPA gene via cyclic adenosine monophosphate (cAMP) mediated mechanism that depends on protein kinase A (PKA) pathway [16].

The fibroblast cell motility in uPA condition induced by C-PC was greatly increased, however, it was ineffective in inducing cell motility in the absence of uPA. C-PC-induced fibroblast migration was greatly affected by uPA where migratory signals were facilitated by the Rho-family GTPases including Cdc 42 and Rac 1 via phosphoinositide-3 kinase (PI-3K) pathway. Cell migration and survival are greatly dependent on PI-3K which plays a key role in signal transduction leading to cellular processes [16,17]. The C-PC dose up

to 100 μg/mL did not affect the viability of human fibroblast cells TIG 3-20, and the data confirmed that C-PC was not cytotoxic at doses sufficient to stimulate cell proliferation and migration. The wound healing effect of C-PC was also established by in vivo studies with mice [17]. The control and C-PC treatment groups did not show any significant differences in the initial phase of treatment, but it was observed that C-PC treatment achieved an 80% closure of the wound in contrast to 50% closure in the control models by the end of the first week [17]. Therefore, considering increasing fibroblast proliferation and cellular migration towards the wound under the influence of C-PC, we can regard it as the active component of medicinal products for the treatment of external and internal wounds, for example, ulcers.

Gur C.S. and others (2013) conducted in vitro and in vivo studies and confirmed the C-PC effect on wound healing. The effects of both Spirulina extract and C-PC isolated from crude Spirulina extract with a purity of 4.0 and higher were compared using cultured human keratinocyte and rat models. Proliferation, healing, and migration were increased in a dose-dependent manner. C-PC showed the best growth stimulation effect at 33.5 μg/mL dose. Additionally, in vivo study revealed that 1.25% of C-PC had a great impact on efficiency on the 7th day [18].

Therefore, the studies demonstrated that C-PC significantly contributes to wound healing and tissue regeneration by inducing fibroblast proliferation and enhancing cellular migration.

2.2. Antimicrobial Effect

The maintenance of the skin microbiome is important for the successful treatment of wounds and restoring the normal function of the skin. Bacteria, fungi, viruses, and mites are the major components of skin microbiota [19]. Healthy skin hosts a diversified community of microorganisms that inhabit specific areas of the body. For example, *Propionibacterium* species mainly are in the sebaceous glands. *Corynebacterium* and *Staphylococcus* species prevail in moist microenvironments [20]. The fungi of the genus *Malassezia* are at the core body and arm areas, while such a diverse combination of *Malassezia* spp., *Aspergillus* spp., *Cryptococcus* spp., *Rhodotorula* spp., *Epicoccum* spp., *Cryptococcus* spp., *Epicoccum* spp. and others colonized foot sizes [21]. In addition, acidic skin pH is determined by natural moisturizing factors and metabolites from skin commensal microbiota [19]. The skin microbiome acts as the physical barrier for the prevention of the invasive pathogens [21].

Various skin diseases including but not limited to those caused by bacteria, viruses or fungi may develop due to the skin microbiome and the immune system dysfunction. The imbalance between commensal and pathogenic microorganisms in the skin may even cause systemic diseases [21]. In such cases, it is important to select an appropriate antimicrobial therapy. The use of synthetic antimicrobials frequently faces the major problem of resistance. As a result, increased focus is on the antimicrobial agents of natural origin.

2.2.1. Antibacterial Effect

C-PC (16 μg/mL) from *Oscillatoria minima Gicklhorn* demonstrated the inhibitory effect against such bacteria as *Pseudomonas fragi*, *Escherichia coli*, *Pseudomonas vulgaris*, *Bacillus subtilis*, *Klebsiella oxytoca*, and *Streptococcus pyogenes*, while *Enterobacter aerogenes* and *Staphylococcus aureus* were not inhibited by C-PC [9].

Osman A. and others (2015) performed an in vitro study which revealed C-PC antibacterial activity against Gram-positive *Bacillus cereus*, *Staphylococcus aureus* and Gram-negative *Escherichia coli* and *Klebsiella pneumonia* bacteria strains. The inhibitory effect of C-PC (10–100 μg/mL) was compared with sterilized distilled water as the negative control and benzyl penicillin, clindamycin, ofloxacin and doxycycline as the positive controls. A concentration-dependent C-PC antibacterial activity was observed against before the mentioned bacterial strains. The activity against Gram-positive bacteria was slightly higher compared to that against Gram-negative ones. The anabaena C-PC (C-PC extracted from *Anabaena oryzae Fritsch*) concentrations corresponding to 50% inhibition of the tested bacteria (IC50): *Bacillus cereus*, *Staphylococcus aureus*, *Escherichia coli* and

Klebsiella pneumonia were 30.56–31.25 μg/mL, while IC50 of the Spirulina C-PC (C-PC extracted from *Spirulina platensis*) for these bacteria were 33.32–40.96 μg/mL compared with benzylpenicillin: 35.93–221.2 μg/mL. These results suggest that Anabaena C-PC activity on Gram-positive bacteria is similar to benzylpenicillin, while relatively superior to Spirulina C-PC. The study also revealed that Anabaena C-PC induced morphological changes such as irregular wrinkled outer surface, fragmentation, adhesion, and aggregation in bacteria cell walls and membranes, but it had no specific activity on the biosynthesis of bacterial proteins [3]. Numerous studies showed that more than 90% of atopic dermatitis patients had *Staphylococcus aureus* colonization. *S. aureus* contributes to atopic dermatitis in a couple of ways. *S. aureus* can activate protease receptors in the disruption of the epidermal barrier by releasing endotoxins and enterotoxins. It is followed by mast cell stimulation, inflammation and keratinocyte dysregulation. Moreover, *S. aureus* upregulates the production of type 2 cytokines, such as thymic stromal lymphopoietin (TSLP), interleukin (IL)-4 and IL-13. High concentrations of IL-4 and IL-13 reduce keratinocyte-generated antimicrobial peptides. which are necessary to manage pathogenic organisms [20]. Therefore, the C-PC antibacterial action against *S. aureus* could be applied in the treatment of atopic dermatitis.

The study by Nihal B. et al. (2018) investigated the antimicrobial activity of C-PC extracted from Spirulina against the two major Gram-positive bacteria species linked to acne vulgaris: *Propionibacterium acne* (*P. acne*) and *Staphylococcus epidermidis* (*S. epidermidis*). *P. acne* is an anaerobic, rod-shaped bacteria present in the base of the hair follicle that breaks downs sebum and feeds on it [22]. The increase in these bacteria can lead to inflammatory processes in the skin. *P. acne* hyperproliferation in the sebaceous lipid environment generates reactive oxygen species (ROS) and proinflammatory compounds. The cytokine cascade injects the follicular wall structural changes of sebaceous glands and, therefore, causes variations in the sebum composition [1].

S. epidermidis is a part of normal skin microbiota and less founded in the mucosal flora. *S. epidermidis* might be found inside the acne vulgaris-affected pores. In the current study, two different formulations with C-PC were prepared, using water soluble and oleaginous bases; both were tested against the aforementioned bacteria. The formulation comprising a water-soluble base (PEG400, PEG4000, stearyl alcohol, glycerin, water) was superior to that one with the oleaginous base (paraffin hard, wool fat, cetostearyl alcohol, white soft paraffin, liquid paraffin). The study highlighted that, on the one hand, the water soluble base formulation had MIC values of 1.5 mg/mL and 1.8 mg/mL with a zone inhibition of 26.1 mm and 24.6 mm against *P. acne* and *S. epidermidis*, respectively. On the other hand, the oleaginous base formulation showed the MIC values as 1.6 mg/mL and 2.1 mg/mL, respectively, and the diameter of the bacteria growth inhibition as 23.4 mm and 21.3 mm, respectively [22]. These results might be caused by better C-PC solubility in water and, respectively, by better releasing C-PC from the dosage form. This also suggests that C-PC can be used as the natural component in hydrophilic ointments and creams for the treatment of acne.

Consequently, C-PC induces morphological changes in bacterial cell walls and membranes and is more effective against Gram-positive bacteria. It is worth noting that the purity of C-PC has a significant effect on antimicrobial activity.

2.2.2. Antifungal Effect

An antifungal activity of the different concentrations and purity of C-PC from *Spirulina platensis* was compared by Muragan T. and others (2011). The purity of the crude extract was 1.17 and the concentration of C-PC was 0.8 mg/mL, while partially purified C-PC purity and concentration were 2.68 and 0.9 mg/mL, respectively. After purification by the micro-scale flash column chromatography, purified C-PC purity was 3.74 and concentration was 1.85 mg/mL. Two concentrations of 40 μg/mL and 80 μg/mL of the crude C-PC were tested for five fungal pathogens: *Candida albicans*, *Aspergillus niger*, *Aspergillus flavus*, *Penicillium species* and *Rhizopus* species. Neither of the concentrations inhibited the growth of the tested fungi. Meanwhile, the partially purified and column purified C-PC

inhibited the growth at the minimum concentration 45 µg/mL. It was demonstrated that the purification improves fungi growth inhibition [23].

2.3. Anti-Oxidative Effect

Solar radiation reaching Earth is one of the factors that can affect and alter the skin barrier [24]. Ultraviolet (UV) radiation has both positive and negative impacts on the skin or body itself. Phototherapy has a strong effect on the endocrine system, rheumatoid arthritis, multiple sclerosis, inflammatory bowel diseases, body metabolism and psychological conditions. Moreover, phototherapy might also be used to treat various skin diseases [25]. It is important to note that prolonged direct sunlight and UV rays' exposure, especially UVB radiation with the wavelength of 280–320 nm, can cause significant changes in the skin by promoting the production of ROS, including single oxygen, superoxide anion, hydrogen peroxide, hydroxyl, alkoxyl, and hydroperoxyl radicals. Under normal physiological conditions, ROS are generated during cellular respiration. The skin has an antioxidant defense system, which consist of antioxidant molecules such as vitamin C, E, glutathione, lipoic acid, uric acid, carotenes, coenzyme Q, etc. and enzymes. Enzymes with antioxidant activities include superoxide dismutase, catalase, peroxiredoxins, sulfiredoxins, thioredoxin and glutathione systems. One of their numerous functions is to prevent oxidative damages and cell death [26–28]. However, the abnormal ROS level increase caused by continuous UV exposure damages the body's antioxidant defense system, induces oxidative stress, and results in an injury of DNA, lipids, proteins and other cellular components [27–29]. These effects can influence different cellular processes in skin related to carcinogenesis and cancer progression, for example, cutaneous melanoma, or at least skin aging [26].

Numerous publications show that UV light is a significant factor both in malignant melanoma (MM) and non-melanoma skin cancer (NMSC) development. In vitro studies demonstrated that oxidative stress is elevated in melanoma cells [24,26]. Although classical theories agree that ROS provokes the initiation and progression of cancer, the role of ROS is ambiguous. Abundant evidence shows that ROS can act as tumor-promoting and tumor-suppressing agents [26]. Oxidative stress induced by disseminated melanoma cells in the circulating system potentially impedes the metastatic process. In addition, the antioxidant application greatly depends on the dose, dose-dependent redox balance and rebalance processes. Some antioxidants contribute to carcinogenesis prevention or, conversely, promote carcinogenesis. For example, some polyphenols such as rosmarinic acid or salicylic acid may have anticancer properties or cancerogenic effects depending on their concentration [26].

The antioxidant activity of C-PC is mostly measured by utilizing 2,2-diphenyl-1-picrylhydrazyl (DPPH) radical scavenging assay and 2,2′-azino-bis(3-ethyl benzothiazoline-6-sulfonic acid) diammonium salt (ABTS) radical scavenging assay. DPPH radical scavenging assay is related to the reduction in DPPH radical (deep violet colored) to yellow colored diphenyl picrylhydrazine in the existence of a hydrogen donor. Meanwhile, ABTS+ radical decolorization assay operates on the principle of producing $ABTS^{+}$ by the oxidation of ABTS with potassium persulfate and reducing the occurrences of hydrogen-donating antioxidants [9]. Venugopal V.C. and coauthors (2020) evaluated the antioxidant activity of C-PC isolated from *Oscillatoria minima* and compared it with the butylated hydroxyanisole (BHA) antioxidant properties. The 1 mg/mL C-PC concentration showed 44% of DPPH radical scavenging activity, while BHA- showed approximately 90%. The same concentration of purified C-PC showed 95% of ABTS+ radical scavenging activity, while BHA was only approximately 70%. It might be presumed that the purified C-PC can decrease the formation of polar radicals and therefore, protect against different oxidative damages caused by ROS [9]. Another study performed by Gantar M. and coauthors (2012) evaluated the antioxidant activity of the purified C-PC isolated from the *Limnothrix* sp. strain 37-2-1 by DPPH method. The dry biomass of this strain contains 18% of C-PC, while, based on the literature data, the dry biomass of Spirulina constitutes 10–15% of C-PC. The researchers used the simple method for obtaining C-PC without the use of ion exchange chromatography.

The procedure included the pigment precipitation from the cell lysate with an appropriate concentration of ammonium sulfate, purification with activated carbon and chitosan, and the sample concentration using tangential flow filtration. This method gave C-PC with a purity ratio of 4.3, which met the requirement for purity of analytical grade. The results revealed 100% antioxidant activity at the concentration of 0.15 mg/mL. These results also showed that the purity of C-PC increased the antioxidant properties. Moreover, the study demonstrated that cyanobacteria other than Spirulina can be a potentially superior source of C-PC [30].

Jang Y.A. and others (2021) tested the inhibition of ROS production by C-PC in UVB-induced human dermal keratinocyte cell line (HaCat cells). The UVB-induced ROS production was reduced by 51.2 and 55.1%, in cells treated with 40 and 80 μg/mL C-PC, respectively. Moreover, the same study revealed that C-PC (20, 40, 80 μg/mL) significantly reduced the matrix metalloproteinase-1 (MMP-1) and matrix metalloproteinase-2 (MMP-2) levels, which were elevated following the UVB radiation and associated with collagen degradation and photoaging. The increased expression of proteins involucrin, filaggrin and loricrin, which play an essential role in the formation of the skin barrier and hydration, was also observed after C-PC treatment [27]. These studies can be used for the development of creams for the treatment of the skin damages caused by sun light.

The in vitro study with human dermal fibroblasts and human epidermal keratinocytes showed that C-PC (1.0–20.0 μg/mL) can provoke the expression of heme oxygenase-1 (HO-1) at the mRNA and protein levels in a dose-dependent manner. HO-1 is an important molecule with inflammatory properties which is the host defense against oxidative stress. This activity of C-PC is mediated by the activation of nuclear factor erythroid-derived 2 (NF-E2) like 2 (Nrf-2) via phosphorylation of protein kinase C (PKC) α/β II. In addition, the expression of anti-apoptotic factor B-cell lymphoma 2 (Bcl-2) was significantly increased in UVB-irradiated cells after C-PC treatment, while the expression of the proapoptotic factors such as p53, Bax and caspase-3 was decreased. Moreover, the significant decrease in the DNA fragmentation in the UVB-irradiated cells was also observed in C-PC-treated cells [31].

These studies suggest that C-PC could be a potential antioxidant to slow down skin aging, including the formation of wrinkles, and even a promising tool in the treatment of skin cancer.

2.4. Anti-Inflammatory Effect

Oxidative stress is mostly connected to the expression of cyclooxygenase-2 (COX-2), inflammation and lipid peroxidation in the cell membrane [26]. COX-2 catalyzes the conversation of arachidonic acid to prostaglandins and other eicosanoids. The overexpression of COX-2 is related to high levels of prostaglandin E2 (PGE2), which stimulates the proliferation of cells and mediates immunosuppression. Moreover, PGE2 plays a role in the inhibition of apoptosis by the upregulation of Bcl-2 gene; alternatively, arachidonic acid stimulates apoptosis. High levels of PGE2 are remarked in several malignancies including those of the bladder, pancreas, colon, cervix, breast, prostate, lung and skin. Meanwhile, C-PC inhibited COX-2 in a rat histiocytic tumor line AK-5 cells. Moreover, the same study revealed C-PC abilities to generate ROS in the tumor cells, activate caspase-3 and downregulate the expression of antiapoptotic substance Bcl-2, thereby making cancer cells vulnerable to apoptotic death. It is important to emphasize the fact that C-PC continued to induce apoptosis even after 24 h [32]. The main effects of COX-2 in cases of melanoma were also related to the augmentation of PGE2 production [33]. Some evidence has suggested that the overexpression of COX-2 is associated with tumor protein p53 mutation. Enache A.O. and coauthors (2018) observed the positive linear relation between p53 and COX-2 in a large proportion of basal cell carcinoma (BCC) cases [34]. Another study by Karahan N. and colleagues (2011) also confirmed that COX-2 expression is increased in BCC and suggested that COX-2 inhibition may be effective in BCC treatment, particularly for tumors with a higher level of COX-2 or a more aggressive phenotype [35]. Therefore, the use of

several non-steroidal anti-inflammatory active substances with antiproliferative activity and selective COX-2 inhibitors such as celecoxib and C-PC could be a logical approach to prevent or treat cancer based on various studies [33].

The studies also showed that C-PC had stronger selective COX-2 inhibitory properties than celecoxib or rofecoxib. C-PC showed a positive effect in reducing levels of PGE2, and therefore, stimulated the proliferation of T and B immune cells and the immune response [36]. Other studies also confirmed that COX-2 plays a crucial role in the regulation of cell growth. The inhibition of COX-2 expression more significantly affected the growth suppression than inhibition of COX-2 catalytic activity. Consequently, these findings indicated the existence of two different COX-2 signaling pathways in cell growth regulation [37].

Gupta and others (2012) revealed that 50, 200 or 400 μg C-PC topical treatment effectively reduced 12-*O*-tetradecanoyl-phorbol-13-acetate (TPA) altered COX-2 and IL-6 expression in a dose-dependent manner. COX-2 is involved in the regulation of the IL-6 gene expression. The elevated levels of IL-6 increase the phosphorylation of the signal transducer and activator of transcription-3 (STAT3) protein. In addition, Il-6 plays a role in a tumor development and in several cellular processes [38].

Therefore, C-PC could be the natural anti-inflammatory agent with a stronger selective COX-2 inhibitory properties compared to celecoxib and rofecoxib. The inhibition of COX-2 and IL-6 expression, as well as the observed downregulation of Bcl-2 expression suggests that C-PC should be considered an acceptable anti-inflammatory and anticancer compound.

2.5. Antimelanogenic Effect

Skin pigmentation is an important defense mechanism against oxidative stress or UV radiation and is associated with the skin ageing. Abnormal hyperpigmentation in human skin may cause aesthetic problems and lead to serious skin diseases. The biosynthesis of melanin occurs in the specialized cytoplasmic organelles of melanocytes called melanosomes [39]. Melanogenesis is a multistage process that incorporates a number of enzymatic and chemical reactions occurring in the melanosomes [40]. Melanosomes contain the key enzymes which regulate the production of pigments such as tyrosinase (TYR), tyrosinase-related protein-1 (TYRP-1) and tyrosinase related protein-2 (TYRP-2). The upregulation of the expression of these key genes could promote melanogenesis in melanocytes and might be caused by the activation of the microphthalmia-associated transcription factor (MIFT) [41]. Three principal signal pathways for the regulation of melanogenesis can be distinguished: melanocortin-1 receptor (MC1-R) signaling pathway, the Wnt/β -catenin signaling pathway, the tyrosine kinase receptor KIT/stem cell factor (SCF) pathway. All these pathways activate the master regulator-MITF [40]. The cAMP/PKA signaling pathway is considered as the most significant signaling pathway of melanogenesis. The function of the melanocytes is modulated by the receptor melanocortin-1 (MC1-R). The binding of α-melanocyte-stimulating hormone (α-MSH) to MC1-R on the membrane of melanocytes activates adenylate cyclase and increases intracellular cAMP. In addition, this activates the PKA-cAMP response element-binding protein (CREB) pathway and then increases MITF and promotes melanogenesis. MC1-R plays a principal role in the regulatory process of skin pigmentation. Moreover, it is a melanoma susceptibility gene [41].

The studies revealed that many pharmacologically active substances can inhibit or stimulate melanin biosynthesis [39]. Wu L. and others (2011) studied the C-PC effect on α-MSH-stimulated melanogenesis and revealed that C-PC inhibited the tyrosinase activity and melanin formation depending on the dose (0.05 to 0.1 mg/mL). In addition, C-PC (0.1 mg/mL) significantly increased the accumulation of cAMP from 4.8 to 7.9 pmol/mL during the first 10 min. The researchers concluded that C-PC exerts cAMP-associated signaling to regulate melanogenesis via manipulating α-MSH-induced melanogenesis. The decrease in tyrosinase gene expression and melanin synthesis suggests the linkage between cAMP and mitogen-activated protein kinase (MAPK)/extracellular signal-regulated kinases (ERK) pathway. The C-PC-induced response of MAPK-ERK pathway-associated factors,

ERK1/2 and MEK, were evaluated and it was determined that C-PC treatment significantly increased the phosphorylated ERK1/ERK 2 (p-ERK1/2) level and the phosphorylation of MEK after 540 min. Moreover, the expression of the MITF protein was also significantly inhibited at 540 min following C-PC treatment. It is known that ERK is associated with the degradation of MIFT. Moreover, C-PC inhibited the phosphorylation of p38 leading to the decline in phosphorylated-CREB. The hindrances of CREB phosphorylation as the transcription factor of MIFT leads to a subsequent reduction in MIFT transcription. Therefore, Wu's and others' (2011) study demonstrated that C-PC promoted the degradation of MITF protein through the upregulation of the MAPK/ERK signaling pathway, and the suppressed activation of CREB via the down-regulation of the p38 MAPK pathway [42].

The findings lead to consider C-PC as a potential melanogenesis inhibitor that can reduce skin pigmentation and aging processes caused by UV radiation.

2.6. Anticancer Effect

Cancer is characterized by the uncontrolled growth and spread of abnormal cells. The main forms of skin cancer include basal cell carcinoma (BCC), cutaneous squamous cell carcinoma (cSCC) and melanoma. Melanoma is the most aggressive form of skin carcinomas, representing the principal cause of death associated with skin tumors [29]. Nowadays, the increasing number of melanoma skin cancer and MM cases is observed and mainly associated with an exposure to direct sunlight [24].

C-PC has more than one specific target in a cancer treatment and its antitumor effects might be demonstrated by the following mechanisms:

- Cell cycle suppression in the specific phases;
- The modification of the cellular redox state;
- The initiation of apoptosis and necrosis [32,43].

The apoptotic effect of phycocyanin was noticed in many in vitro and in vivo studies. Chromatin margination and condensation into dense granules or blocks, increasing percentage of cells in sub-G0/G1 phase, microvilli loss, membrane blebbing and cell shrinkage are the most commonly observed apoptotic features [44]. Studies have also confirmed that C-PC-induced apoptosis is mediated by the release of cytochrome C from mitochondria in the mouse macrophage cell line RAW 264.7. The treatment with 20 μM C-PC provoked the typical nuclear condensation and 16.6% of cells in the sub-G0/G1 phase. DNA fragmentation was observed in a dose-dependent manner. Moreover, the effect of C-PC on RAW 264.7 cells appeared to be associated with the reduction in PGE2 levels as the outcome of COX-2 inhibition [45]. C-PC antiproliferative action was justified by the accumulation of sub-G1 cell populations, DNA fragmentation and nuclear condensation in human melanoma A375 cells [46]. The study by Hao and others (2018) also showed a significant inhibition of the melanoma A375 cells growth after C-PC (6 μM) treatment, while the proliferation of HaCat cells was not influenced. C-PC antineoplastic effect on melanoma cells is associated with the downregulation of growth factor receptor-bound protein 2 (GRB2)-ERK1/2 pathway [47].

C-PC can promote the expression of Fas, a cell surface receptor, that directly triggers cell death by apoptosis [48], and intercellular cell-adhesion molecule-1 (ICAM-1) protein, while suppressing the Bcl-2 protein expression. Thus, the study revealed that C-PC could stimulate the activation of the pro-apoptotic gene and down regulate the expression of an anti-apoptotic gene. Furthermore, the study with HeLa cells noted the activation of caspases 2, 3, 4, 6, 8, 9 and 10 after C-PC treatment and suggested that C-PC-induced apoptosis was caspase-dependent [44]. The downregulation of Bcl-2 after C-PC treatment was also confirmed by another in vitro study with AK-5 tumor cells. This effect of C-PC may be significant because most the tumors are resistant to apoptosis because of the expression of Bcl-2. Thus, the downregulation of Bcl-2 may make the tumor cell more sensitive to other antineoplastic drugs. [32].

Recent in vivo investigation with mice tested the efficacy of C-PC in the representative genes of tumor development in mice skin. The tumorigenesis was induced by 12-0-tetradecanyol-phorbol-13-acetate (TPA) as a tumor-promoting agent. TPA induced the

rate-limiting polyamine-biosynthetic enzyme ornithine decarboxylase (ODC). The elevated levels of ODC can play a role in epidermal tumorigenesis and are involved in cell cycle progression [38]. ODC can be induced by UVB and hormones and is greatly increased in SCC and BCC cases compared to levels in the normal skin tissue [49]. Topical applications with C-PC (50, 200 and 400 µg) showed an inhibitory effect (17, 38 and 50%, respectively) of TPA-mediated upregulation of ODC at the protein level and inhibitory effect of ODC (28.73, 42.89 and 43.06%, respectively) at the mRNA level [38].

Transglutaminase 2 (TG2) was another examined enzyme. This nuclear enzyme is dependent on Ca^{2+}. TG2 catalyzes the transfer of primary amines into protein substrates. This enzyme induces apoptosis and cell differentiation. It can also inhibit the process of metastasis. The topical treatment with the same C-PC doses increased TG-2 protein level by 35.52, 141.2 and 219% and TG-2 mRNA 16.05, 50.67 and 59.60%, respectively [38]. It is quite well established that the overexpression of TG2 promotes the spontaneous apoptosis of cells or makes cells highly sensitive to apoptosis-inducing agents. However, there have also been studies indicating that an increased expression of TG2 may prolong cell survival by preventing apoptosis as TG2 causes the constitutive activation of NF-KB in cancer cells and TG2 could be an attractive alternate target for inhibiting constitutive NF-KB activation and rendering cancer cells sensitive to anticancer drugs [50]. Therefore, studies regarding the connection of TG2 and apoptosis are controversial. Some authors highlighted that TG2 dual function, antiapoptotic or a proapoptotic ones, depends on the cell type and its location within the cell. The high concentrations (>1 mM) of Ca^{2+} induces the activation of TG2, which promotes the inter- and intramolecular cross-linking of proteins and causes cell death, while low levels (<1 mM) of Ca^{2+} and high concentrations (>9 µM) of guanosine triphosphate (the conditions that generally predominate inside cells) promotes the signaling of cell-survival mediated by TG2 [51]. The isopeptide bond reactions catalyzed by transglutaminases have great physiologic significance in the human body. Isopeptide bonds are frequently found in hair and skin. They accumulate during wound healing, apoptosis, and blood clotting. Several pathologic conditions, such as neurodegeneration, progressive tissue fibrosis, autoimmune diseases, infectious diseases, and ailments related to the integrity of the stratum corneum of the epidermis can be provoked by the dysregulation of transglutaminase functions [52]. TG2 expression proved to be positive in regulating the number of cancer cell types, especially in tumors with high resistance to chemotherapeutic drugs or metastasis [51]. The biologically active substances, that can affect tumor-encoded genes whose expression contributes to the development of drug resistance and metastasis may be significant in the cancer treatment. Chhabra A. and others (2009) also accentuated that the therapeutic efficacy of anticancer drugs can be increased by the downregulation or inhibition of TG2 by weak interfering RNA or by small molecule inhibitors [51].

Gupta N.K. and others studied the C-PC effect on the TPA-altered expression of phosphorylated signal transducer and activator of transcription-3 (pSTAT3) and confirmed the antitumor properties of C-PC. TPA application increased the level of pSTAT3 compared to the control group, while in the presence of C-PC, this TPA-caused upregulation of pSTAT3 protein was inhibited depending on the dose. It was established that IL-6 promotes the activation of STAT3, and accordingly, tumor development [38].

In summary, it can be stated that C-PC has clear potential in cancer treatment due to its antioxidative properties, the ability to inhibit COX-2 expression, reduce PGE2 level and induce apoptosis in tumor cells. Considering that C-PC can activate the pro-apoptotic gene and downregulate the expression of the anti-apoptotic gene, C-PC could be combined with other anticancer drugs, reducing the effective dose of anticancer drugs, minimizing side effects and tumor resistance to chemotherapeutic treatment.

2.7. Summary of C-PC Topical Activities

The discussed investigations of C-PC topical activities are given in Table 1.

Table 1. Investigations of C-PC topical activities.

No	Study Profile	Origin of C-PC	Dose/Concentration of C-PC	Activity	Reference
1	WI-38 fibroblast cells	*Spirulina fusiformis Voronichin*	25, 50, 100 µg/mL	uPA gene regulation through cAMP-mediated PKA pathway	Madhyastha et al. (2006) [16]
2	Human fibroblast cells TIG 3-20	*Spirulina fusiformis*	10–200 µg/mL	wound healing promotion by upregulating uPA, GTPases Cdc 42 and Rac 1 stimulation through PI-3K pathway fibroblast proliferation induction via the cyclin-dependent kinases cdK1 and cdK2 cellular migration towards the wound enhancement in a uPA-dependent manner	Madhyastha et al. (2007) [17]
3	Male mice	*Spirulina fusiformis*	75 µg/mL	wound area reduction	Madhyastha et al. (2007) [17]
4	Human keratinocytes	*Spirulina platensis*	0.0335, 0.335, 3.35, 33.5 µg/mL	proliferation, healing, and migration promotion	Gur et al. (2012) [18]
5	Male rats	*Spirulina platensis*	1.25, 2.5%	wound healing process improvement	Gur et al. (2012) [18]
6	*Pseudomonas fragi* *Escherichia coli* *Pseudomonas vulgaris* *Bacillus subtilis* *Klebsiella oxytoca* *Streptococcus pyogenes* *Enterobacter aerogenes* *Staphylococcus aureus*	*Oscillatoria minima*	16 µg/mL	antibacterial activity against *Pseudomonas fragi*, *Escherichia coli*, *Pseudomonas vulgaris*, *Bacillus subtilis*, *Klebsiella oxytoca*, *Streptococcus pyogenes*	Venugopal et al. (2020) [9]
7	*Bacillus cereus* *Staphylococcus aureus* *Escherichia coli* *Klebsiella pneumonia*	*Anabaena oryzae*	10, 25, 50, 75, 100 µg/mL	antibacterial activity morphological changes in the cell walls and membranes	Osman et al. (2015) [3]
8	*Propionibacterium acne* *Staphylococcus epidermidis*	*Spirulina platensis*	10% C-PC extract of the formulation of oleaginous base compared with the same concentration of water-soluble base	antibacterial activity	Nihal et al. (2018) [22]
9	*Candida albicans* *Aspergillus niger* *Aspergillus flavus* *Penicillium species* *Rhizopus species*	*Spirulina platensis*	40–80 µg/mL	antifungal activity	Murugan et al. (2011) [23]
10	-	*Oscillatoria minima*	1 mg/mL	anti-oxidative activity (DPPH, ABTS methods)	Venugopal et al. (2020) [9]
11	-	*Lamotrix sp. 37-2-1* *Spirulina platensis*	0.05–0.3 mg/mL	anti-oxidative activity (DPPH)	Gantar et al. (2012) [30]
12	Human dermal keratinocyte (HaCat) cells	*Spirulina platensis*	5, 10, 20, 40, 80 µg/mL	ROS production inhibition protection against UVB-induced damage MMP-1 and MMP-9 expression inhibition involucrin, filaggrin and loricrin expression promotion	Jang et al. (2021) [27]
13	Human dermal fibroblasts Human epidermal keratinocytes	-	1–20 µg/mL	protection against UVB-induced apoptosis HO-1 expression induction Nrf-2 via phosphorylation of PKC α/β II activation	Kim et al. (2018) [31]
14	Rat histiocytic tumor cells AK-5	*Spirulina platensis*	30 µM	DNA fragmentation and apoptosis in tumor cells induction Bcl-2 down regulation	Pardhasaradhi et al. (2021) [32]

Table 1. *Cont.*

No	Study Profile	Origin of C-PC	Dose/Concentration of C-PC	Activity	Reference
15	Female mice	*Spirulina platensis*	50, 200, 400 μg/mL	COX-2 and IL-6 expression reduction ODC, pSTAT3 downregulation TG2 upregulation	Gupta N.K. and Gupta K.P. (2021) [38]
16	Murine melanoma cells	*Spirulina platensis*	0.05, 0.1, 0.2 μg/mL	tyrosinase activity, melanin production, p38 phosphorylation, MIFT inhibition cAMP accumulation p-ERK1/2 level, phosphorylation of MEK induction	Wu et al. (2011) [42]
17	RAW 264.7 mouse macrophage cell line	*Spirulina platensis*	20 μM	apoptosis induction nuclear condensation DNA fragmentation accumulation of sub-G1 cell populations COX-2 inhibition	Reddy et al. (2003) [45]
18	A375 melanoma cells	-	6 μM	melanoma cells inhibition GRB2-ERK1/2 pathway downregulation	Hao et al. (2018) [47]
19	HeLa cells	*Spirulina platensis*	Different concentrations	apoptosis induction cells in sub-G0/G1 phase augmentation increased expression of Fas and ICAM-1 caspases 2, 3, 4, 8, 9, 10 activations Bcl-2 downregulation	Li et al. (2010) [44]

3. Advanced Technology for Functionalization of C-PC

As a barrier between the internal body and the external environment, the skin may be affected by many conditions such as viral, bacterial, fungal and parasitic infections or UV radiation, that can result in various disorders such as trauma, inflammation, rashes, pigmentation disorders, tumors and even cancer [53]. Nowadays, a wide range of therapeutic methods are used for skin disorders; nevertheless, some of them are limited by adverse reactions, skin barrier or resistance [54].

For example, the excessive use of cleansing cosmetics can disturb the hydrophilic barrier and natural microbiota, cause skin irritations and lead to the atopic skin conditions [54]. This situation is often observed in the inappropriate treatment of acne or self-medication. Acne is a long-term skin condition that occurs when hair sacs become clogged with dead skin cells. It is categorized into non-inflammatory (characterized by spots, blackheads, whiteheads) and inflammatory (characterized by red and swollen pimples) types [22]. Acne can also be treated with prescription creams and gels that inhibit pore swelling and reduce external inflammation. In addition, isotretinoin may be prescribed in some cases. However, treatment with isotretinoin is strictly contraindicated in pregnant and lactating women because of its teratogenic effect. For these reasons, there is a growing interest in the natural effective remedies that can have complex impact on acne skin.

Antioxidant, antimicrobial and anti-inflammatory effects of C-PC suggest its use in acne treatment. Nival B. and others (2018) tested two different formulations with C-PC as topical anti-acne preparations. The oleaginous base consisted of hard paraffin, wool fat, cetosstearyl alcohol, soft paraffin, liquid paraffin and C-PC extract. Meanwhile, water-soluble base was composed of PEG400, PEG4000, stearyl alcohol, glycerin, water and C-PC extract. The consistency of the water-soluble base was superior to that of an oleaginous base because of better spreadability characteristics. Moreover, in vitro drug form diffusion of water-soluble base formulation was found to be at 92% after 5 h compared to oleaginous base formulation only at 88%. Water-soluble base formulation also demonstrated higher antibacterial activity against *P. acne* and *S. epidermidis* [22]. These results can be also explained by good C-PC solubility in water. Moreover, mineral oils such as paraffins and silicone oils can also promote fat accumulation in the skin, therefore, water-based formulations may be more appropriate for acne treatment.

The skin is highly effective selective penetration barrier. The multilayered membrane allows the substances to penetrate via passive diffusion to some extent. However, only relatively low molecular weight (<500 Da) substances with an adequate lipophilicity can penetrate via passive diffusion into the deeper skin layers or through the skin. Meanwhile, peptides and proteins are poorly absorbed because their molecules are generally large and hydrophilic [55].

Successful topical treatment depends on the active substances. Moreover, the inactive ingredients through which the drug is delivered to the skin and the type of application modality play a crucial role. In clinical practice, there are many limitations associated with semi-solid formulations, such as ointments, creams, oils or gels. Localized side effects and insufficient skin penetration often become a major challenge in development of new forms for topical use. For these reasons, nanotechnology can be an efficient system for cutaneous delivery in the treatment of skin diseases and in cosmetics [53].

The use of natural compounds and their transport in pharmaceutical forms are capable of controlling the release and absorption can be used as an effective treatment way for various skin diseases. For example, lipid-based nano-systems have a structural similarity to lipids in the skin. This similarity promotes the interaction between the lipid matrix of the nano-system and the epidermis intracellular lipids. It improves the skin hydration and penetration of the encapsulated molecules [53].

It was observed that liposomes can become a great carrier for the topical delivery of large molecular weight proteins such as C-PC. The use of traditional phospholipid vesicles improved the in vivo anti-inflammatory activity depending on the dose. Moreover, the use of liposomes allows to halve the C-PC dose in order to produce the same anti-inflammatory effect as free protein [55]. However, the penetration enhancer-containing vesicles (PEVs), especially propylene glycol, improved the dermal and transdermal delivery of the high molecular weight protein C-PC compared to the conventional liposomes and ethosomes [56]. Castangia I. and others (2016) study revealed that phycocyanin encapsulated into hyalurosomes, especially PEG-hyalurosomes, can penetrate the deeper skin layers and show better antioxidative properties on stressed human keratinocytes [57]. New biocarriers, named santosomes, were also suggested by Castangia I. and others (2016). Nanovesicles are formed of hydrogenated phosphatidylcholine, cholesterol and the essential oil of *Santolina insularis (Gennari ex Fiori) Arrigoni*. Propylene glycol was added as a hydrophilic penetration enhancer, and C-PC was incorporated into the modified nanovesicles. *S. insularis* belongs to *Asteraceae* family and is an endemic plant of Sardinia. The plant accumulates mono- and sesquiterpenes, which are good penetration enhancers able to improve the absorption of different substances through the skin. After toxicity assessment, the optimal dilution was selected: 100 μg/mL of phosphatidylcholine, 50 μg/mL of C-PC and 25 μg/mL of essential oil. C-PC was capable of entering human keratinocytes when delivered by santosomes even after 1 h of treatment and stayed consistently high for 24 h, while free C-PC was unable to enter the cells. In addition, the delivery by santosomes prolonged the antioxidative and anti-inflammatory effect of C-PC and its ability to restore, repair and protect the skin [58]. Skin restoration and wound healing are complex physiological processes consisting of multiple stages and reconstruction. Wound healing, especially burns, diabetic ulcers and bedsores, are a big challenge for a healthcare system. Dev A. and others (2020) suggested an injectable hydrogel from natural polysaccharide κ-carrageenan (κ-CRG) and C-PC. Antimicrobial, antioxidant, anti-inflammatory and wound healing effects of C-PC were accommodated for this injectable and regenerative wound dressing matrix. κ-CRG-C-Pc hydrogel improved fibroblast migration, blood clotting and wound closure capabilities. Furthermore, κ-CRG hydrogel was degraded within twenty-four hours after application, while κ-CRG-C-Pc hydrogel remains in the wound for six days. The best results of wound healing were observed after eight days of treatment with κ-CRG-C-Pc hydrogel. In addition, the κ-CRG-C-Pc hydrogel treatment group showed maximum collagen synthesis and superior hemostatic capabilities that could help in wound closure and tissue restructuring in the wound site [59]. Madhyastha and others' (2020) in vitro study

with the skin fibroblast cells revealed that C-PC conjugated with the silver nanoparticles (AgcPCNPs) increased the fibroblast migration towards the wound area. This nanoparticles form combined the wound healing properties of C-PC and the broad-spectrum antibacterial activity of the silver ions [60].

Polylactic acid (PLA) patches with C-PC were utilized for the treatment of less complicated wounds. PLA was chosen as a nontoxic biodegradable polymer which possesses similar properties to conventional plastic patches, while C-PC was used as an active ingredient with antioxidant and anti-inflammatory properties. Alginate was embedded in the PLA matrix with C-PC to create prolonged release patches (effective for approximately 20 h). The patches had the best properties (elasticity, release of C-PC) while the percentage ratio of C-PC and alginate components in the patch was 40/60 [61].

The engineered biosilica could be beneficial as a mesoporous biomaterial for anticancer drug delivery. Diatoms are unicellular eukaryotes, performing photosynthesis. Their cell walls are formed of amorphous SiO_2 and called frustules. These silica frustules are characterized by specific pores as small as 20 nm and can be applied as nanocarriers. C-PC combination with mesoporus biosica improved C-PC stability and biocompatibility and was effective in photodynamic tumor cells therapy. Even the highest concentrations of free C-PC or functionalized biosilica caused below 10% of RAW264.7 cell death without illumination. Thus, the results demonstrated the safety of free C-PC and C-PC modified biosilica. Samples with 150 μg/mL C-PC and light irradiation had less than 25% of cell death, while under the same illumination, functionalized biosilica (5–150 μg/mL) showed 66–81% of RAW264.7 cell death, respectively. This study introduces a new field of C-PC biomedical applications [62]. Jiang L. and others (2019) also suggested a novel cervical tumor targeted nano-drug. Carboxymethylchitosan (CMC) served as a nanomaterial for the nano-formulation construction. CMC is well soluble in water, biodegradable, biocompatible and a non-toxic substance. Thus, the combination of C-PC and CMC improved the C-PC stability, ensured the slow release of C-PC and increased the C-PC efficacy in cancer treatment. Moreover, CD59 specific ligand peptide (CD59sp) was used to act as a targeted molecule which selectively combines CD59. It is known that CD59 is elevated in many solid tumors and lowly expressed in normal cells. CD59 takes part in suppressing the formation of a complement attack complex (MAC). As a result of this, suppressing tumor cells avoid the response of the immune system. Thus, C-PC/CMC-CD59sp nanoparticles (C-PC/CMC-CD59spNPs) significantly provoke G0/G1 cell cycle arrest in cervical cancer HeLa and SiHa cells compared to C-PC and C-PC/CMC nanoparticles. The cell proliferation was inhibited in a dose-dependent manner. Nanoparticles with C-PC induced early apoptosis in both HeLa and SiHa cells, increased the expression of cleaved caspase-3 protein, and decreased the expression of bcl-2 protein; however, C-PC/CMC-CD59spNPs inhibited MMP-2 protein expression and the growth of cervical cancer tumor more significantly [63].

Due to its complex effects, C-PC is increasingly being considered as a potential biological active substance in skin diseases, even including cancer. As other proteins, C-PC requires more attention during manufacture/formulation and the administration processes because of its unique structure and unstable physical-chemical properties [19]. According to most authors, pH and temperature are the key factors affecting the stability of C-PC [11]. It can be noted that the optimum pH range for C-PC preparations is 5.5–6.0 [64]. At values close to temperatures of 25–45 °C, the C-PC solution degrades very slowly. The degradation of C-PC is initiated at temperature above 45 °C, and the denaturation of protein is accelerated at temperatures above 70 °C [65]. It is observed that the stability of C-PC decreases with time and temperature; however, the reactive grade C-PC showed significantly lower thermal stability than food-grade C-PC [65].

Moreover, C-PC is sensitive to light, therefore, the best storage conditions should be in the dark [65].

As C-PC is very sensitive to environmental stress, various additives are used to enhance the stability of C-PC. The chemical structure and the concentration of the preservatives must be safe for humans. Moreover, they must not denature protein or adversely

affect its properties. Mono- and disaccharides (glucose, fructose, saccharose, trehalose, lactose, maltose and sorbitol), and organic acids (citric acid, ascorbic acid, and benzoic acid) or inorganic salts (sodium chloride, calcium chloride) may be used as preservatives [65]. Many studies focus on the additives that can increase the thermostability of C-PC [11]. The addition of glucose could enhance the activation energy up to 4 times due to the polymerization of protein C-PC by sugar, and prevent the damage of the C-PC structure by heating [66]. Moreover, 2.5% sodium chloride is also considered as an efficient preservative for C-PC stability [64]. The mentioned instability of C-PC limits its use in medical applications and the development of new products. Therefore, the processes with no heating, no ultrasound, and no organic solvents should be prioritized. Moreover, another way preventing the proteins degradation may be the usage of encapsulated forms (nanofibers, microparticles, or nanoparticles) [65]. The employment of aqueous two-phase systems using polymer/salt (4% PEG and 18% salt, w/w) and polymer/polymer (6% PEG and 10% dextran, w/w) as a carrier material for C-PC double encapsulation increased the stability and the purity of C-PC. Moreover, this double encapsulation extended the shelf life of C-PC for the 6 months without markedly changing the powder characteristics [67]. Guo J.W. and others (2021) also confirmed the effectiveness of chemical penetration enhancers, transferosomes, nanoparticles delivery system, or cell-penetrating peptide-modified nanocarriers in transdermal delivery of proteins. In addition, the same researchers warned that larger molecular weight peptides or proteins may cause the inflammation. Therefore, the appropriate dose of protein/peptides should be very responsibly chosen in the topical delivery system [19].

Thus, C-PC is hydrophilic protein highly sensitive to environmental conditions, especially pH and temperature. Maintaining pH between 5.5 and 6.0 and the temperature under 45 °C is required for its stability. Preservatives such as glucose, fructose and sodium chloride help prevent the degradation of protein. The use of modern nanotechnologies may be the key in topical applications of C-PC for the treatment of various skin diseases.

4. Conclusions

Studies have revealed that C-PC significantly contributes to wound healing and tissue regeneration by inducing fibroblast proliferation and enhancing cellular migration. In addition, C-PC induces morphological changes in bacterial cell walls and membranes and is more effective against Gram-positive bacteria. Due to the inhibition of ROS production and antimelanogenic properties, C-PC can be considered a potential compound to slow down the aging process of skin. It is worth noting that the purity of C-PC has a significant effect on antimicrobial and antioxidative activity. C-PC is a natural anti-inflammatory agent with a stronger selective COX-2 inhibitory properties compared to celecoxib and rofecoxib. Based on the reviewed studies, it can be stated that C-PC has clear potential in cancer treatment due to its antioxidative effects, its ability to inhibit COX-2 expression, reduce PGE2 level and induce apoptosis in tumor cells. Considering that C-PC could increase the activation of pro-apoptotic genes and downregulate the expression of anti-apoptotic genes, C-PC could be further investigated for the treatment of skin cancer as monotherapy or in combination with other anticancer agents to reduce tumor resistance to chemotherapy treatment and its side effects. The adoption of modern nanotechnologies and stabilizers usage could ensure C-PC stability, the penetration of key skin layers and applications of C-PC to the topical treatment of various skin diseases.

Author Contributions: D.D. analyzed the data, wrote and edited the manuscript; N.S. and G.B.-M. supervised; J.K., D.M., R.J.G., N.H. and N.J. reviewed and edited the manuscript. All authors have read and agreed to the published version of the manuscript.

Funding: This research was funded by the Lithuanian Agency for Science, Innovation and Technology (MITA) agreement No 01.2.2-MITA-K-702-10-0008, grant number E!13474 ECO-AQUA-RECYCLE.

Institutional Review Board Statement: Not applicable.

Informed Consent Statement: Not applicable.

Data Availability Statement: The data are contained within the article.

Conflicts of Interest: The authors declare that there is no conflict of interest regarding the publication of the present article.

References

1. Ragusa, I.; Nardone, G.N.; Zanatta, S.; Bertin, W.; Amadio, E. Spirulina for skin care: A bright blue future. *Cosmetics* **2021**, *8*, 7. [CrossRef]
2. Safaei, M.; Maleki, H.; Soleimanpour, H.; Norouzy, A.; Zahiri, H.S.; Vali, H.; Noghabi, K.A. Development of a novel method for the purification of C-phycocyanin pigment from a local cyanobacterial strain *Limnothrix* sp. NS01 and evaluation of its anticancer properties. *Sci. Rep.* **2019**, *9*, 9474. [CrossRef] [PubMed]
3. Osman, A.; Salama, A.; Ghany, A.A.; Sitohy, M. Antibacterial activity and mechanism of action of phycocyanin extracted from an Egyptian strain of *Anabaena oryzae* SOS13. *Zagazig J. Agric. Biochem. Appl.* **2015**, *42*, 30–321.
4. Kuddus, M.; Singh, P.; Thomas, G.; Al-Hazimi, A. Recent development in production and biotechnological applications of C-phycocyanin. *BioMed Res. Int.* **2013**, *2013*, 742859. [CrossRef] [PubMed]
5. Wang, L.; Qu, Y.; Fu, X.; Zhao, M.; Wang, S. Isolation, Purification and Properties of an R-Phycocyanin from the Phycobilisomes of a Marine Red Macroalga *Polysiphonia urceolata*. *PLoS ONE* **2014**, *9*, e87833. Available online: https://journals.plos.org/plosone/article/file?id=10.1371/journal.pone.0087833&type=printable (accessed on 28 December 2021). [CrossRef] [PubMed]
6. Wang, Y.; Gong, X.; Wang, S.; Chen, L. Separation of Native Allophycocyanin and R-Phycocyanin from Marine Red Macroalga *Polysiphonia urceolata* by the Polyacrylamide Gel Electrophoresis Performed in Novel Buffer Systems. *PLoS ONE* **2014**, *9*, e106369. Available online: https://journals.plos.org/plosone/article/file?id=10.1371/journal.pone.0106369&type=printable (accessed on 2 January 2022). [CrossRef]
7. Glazer, A.N. Phycobilisome: A macromolecular complex optimized for light energy transfer. *Biochim. Biophys. Acta (BBA) Rev. Bioenerg.* **1984**, *768*, 29–51. [CrossRef]
8. Park, W.S.; Kim, H.J.; Li, M.; Lim, D.H.; Kim, J.; Kwak, S.S.; Kang, C.M.; Ferruzzi, M.G.; Ahn, M.J. Two classes of pigments, carotenoids and C-Phycocyanin, in Spirulina powder and their antioxidant activities. *Molecules* **2018**, *23*, 2065. [CrossRef]
9. Venugopal, V.C.; Thakur, A.; Chennabasappa, L.K.; Mishra, G.; Singh, K.; Rathee, P.; Ranjan, A. Phycocyanin extracted from *Oscillatoria minima* shows antimicrobial, algicidal, and antiradical activities: In silico and in vitro analysis. *Antiinfl. Anti-Allergy Agents Med. Chem.* **2020**, *19*, 240–253. [CrossRef]
10. Aoki, J.; Sasaki, D.; Asayama, M. Development of a method for phycocyanin recovery from filamentous cyanobacteria and evaluation of its stability and antioxidant capacity. *BMC Biotechnol.* **2021**, *21*, 40. [CrossRef]
11. Hsieh-Lo, M.; Castillo, G.; Ochoa-Becerra, M.A.; Mojica, L. Phycocyanin and phycoerythrin: Strategies to improve production yield and chemical stability. *Algal Res.* **2019**, *42*, 101600. [CrossRef]
12. Kuddus, M.; Singh, P.; Thomas, G.; Ali, A. *Biotechnology of Bioactive Compounds: Sources and Applications*, 1st ed.; John Wiley & Sons: Hoboken, NJ, USA, 2015; pp. 287–288.
13. Patil, G.; Chethana, S.; Sridevi, A.S.; Raghavarao, K.S.M.S. Method to obtain C-phycocyanin of high purity. *J. Chromatogr.* **2006**, *1127*, 76–81. [CrossRef] [PubMed]
14. Liu, P.; Choi, J.W.; Lee, M.K.; Choi, Y.H.; Nam, T.J. Wound healing potential of Spirulina protein on CCD-986sk cells. *Mar. Drugs* **2019**, *17*, 130. [CrossRef] [PubMed]
15. Syarina, P.N.A.; Karthivashan, G.; Abas, F.; Arulselvan, P.; Fakurazi, S. Wound healing potential of *Spirulina platensis* extracts on human dermal fibroblast cells. *EXCLI J.* **2015**, *14*, 385–393. [PubMed]
16. Madhyastha, H.K.; Radha, K.S.; Sugiki, M.; Omura, S.; Maruyama, M. C-phycocyanin transcriptionally regulates uPA mRNR through cAMP mediated PKA pathway in human fibroblast WI-38 cells. *Biochim. Biophys. Acta (BBA) Gen. Subj.* **2006**, *1760*, 1624–1630. [CrossRef]
17. Madhyastha, H.K.; Radha, K.S.; Nakajima, Y. uPA dependent and independent mechanisms of wound healing by C-phycocyanin. *J. Cell. Mol. Med.* **2008**, *12*, 2691–2703. [CrossRef]
18. Gur, C.S.; Erdogan, D.K.; Onbasılar, I.; Atilla, P.; Cakar, N.; Gurhan, I.D. In Vitro and in Vivo investigations of the wound healing effect of crude Spirulina extract and C-Phycocyanin. *J. Med. Plants Res.* **2013**, *7*, 425–433.
19. Guo, J.W.; Jee, S.H. Strategies to develop a suitable formulation for inflammatory skin disease treatment. *Int. J. Mol. Sci.* **2021**, *22*, 6078. [CrossRef]
20. Aguilera, A.C.; Dagher, I.A.; Kloepfer, K.M. Role of the Microbiome in Allergic Disease Development. *Curr. Allergy Asthma Rep.* **2020**, *20*, 44. [CrossRef]
21. Byrd, A.L.; Belkaid, Y.; Segre, J.A. The human skin microbiome. *Nat. Rev. Microbiol.* **2018**, *16*, 143–155. [CrossRef]
22. Nihal, B.; Gupta, N.V.; Gowda, D.V.; Mariapan, M. Formulation and development of topical anti acne formulation of Spirulina extract. *Int. J. Appl. Pharm.* **2018**, *10*, 229. [CrossRef]
23. Murugan, T.; Radhamadhavan. Screening for antifungal and antiviral activity of C-phycocyanin from Spirulina platensis. *J. Pharm. Res.* **2011**, *4*, 4161–4163.

24. Zebracka, A.; Matysiak, M.; Jastrzebska, M.D.; Skrzypczak, L.K. Molecular and environmental aspects of skin cancers. *J. Pre-Clin. Res.* **2015**, *9*, 158–162. [CrossRef]
25. Kim, K.M.; Im, A.R.; Park, S.K.; Shin, H.S.; Chae, S.W. Protective effects of timosaponin AIII against UVB-radiation induced inflammation and DNA injury in human epidermal keratinocytes. *Biol. Pharm. Bull.* **2019**, *42*, 1524–1531. [CrossRef]
26. Obrador, E.; Smith, F.L.; Dellinger, R.W.; Salvador, R.; Meyskens, F.L.; Estrela, J.M. Oxidative stress and antioxidants in the pathophysiology of malignant melanoma. *Biol. Chem.* **2019**, *400*, 589–612. [CrossRef]
27. Jang, Y.A.; Kim, B.A. Protective effects of Spirulina- derived C-Phycocyanin against ultraviolet B-induced damage in HaCaT cells. *Medicina* **2021**, *57*, 273. [CrossRef]
28. Jung, S.M.; Min, S.K.; Lee, H.C.; Kwon, Y.S.; Jung, M.H.; Shin, H.S. Spirulina PCL nanofiber wound dressing to improve cutaneous wound healing by enhancing antioxidative mechanism. *J. Nanomater.* **2016**, *1*, 6135727. [CrossRef]
29. Allegra, A.; Pioggia, G.; Tonacci, A.; Musolino, C.; Gangemi, S. Oxidative stress and photodynamic therapy of skin cancers: Mechanisms, challenges and promising developments. *Antioxidants* **2020**, *9*, 448. [CrossRef]
30. Gantar, M.; Simovic, D.; Djilas, S.; Gonzalez, W.W.; Miksovska, J. Isolation, characterization and antioxidative activity of C-phycocyanin from *Limnothrix* sp. strain 37-2-1. *J. Biotechnol.* **2012**, *159*, 21–26. [CrossRef]
31. Kim, K.M.; Lee, J.Y.; Im, A.; Chae, S. Phycocyanin protects against UVB-Induced Apoptosis Through the PKC α/β II-Nrf-2/HO-1 Dependent Pathway in Human Primary Skin Cells. *Molecules* **2018**, *23*, 478. [CrossRef]
32. Pardhasaradhi, B.V.V.; Ali, A.M.; Kumari, A.L.; Reddanna, P.; Khar, A. Phycocyanin-mediated apoptosis in AK-5 tumor cells involves down-regulation of Bcl-2 and generation of ROS. *Mol. Cancer Ther.* **2003**, *2*, 1165–1170. [PubMed]
33. Tudor, D.V.; Baldea, I.; Lupu, M.; Kacso, T.; Kutasi, E.; Hopartean, A.; Stretea, R.; Filip, A.G. COX-2 as a potential biomarker and therapeutic target in melanoma. *Cancer Biol. Med.* **2020**, *17*, 20–31. [CrossRef] [PubMed]
34. Enache, A.O.; Stepan, A.E.; Margaritescu, C.; Patrascu, V.; Ciurea, R.N.; Simionescu, C.E.; Camen, A. Immunoexpression of p53 and COX-2 in basal cell carcinoma. *Rom. J. Morphol. Embryol.* **2018**, *59*, 1115–1120. [PubMed]
35. Karahan, N.; Baspinar, S.; Bozkurt, K.K.; Caloglu, E.; Ciris, I.M.; Kapucuoglu, N. Increased expression of COX-2 in recurrent basal cell carcinoma of the skin: A pilot study. *Indian J. Pathol. Microbiol.* **2011**, *54*, 526–531.
36. Liu, Q.; Huang, Y.; Zhang, R.; Cai, T.; Cai, Y. Medical application of Spirulina platensis derived C-phycocyanin. *Evid. Based Complementary Altern. Med.* **2016**, *2016*, 7803846.
37. Higashi, Y.; Kanekura, T.; Kanzaki, T. Enhanced expression of cyclooxygenase (COX)-2 on human skin epidermal cancer cells: Evidence for growth suppression by inhibiting COX-2 expression. *Int. Union Against Cancer* **2000**, *86*, 667–671. [CrossRef]
38. Gupta, N.K.; Gupta, K.P. Effects of C-Phycocyanin on the representative genes of tumor development in mouse skin exposed to 12-O-tetradecanoyl-phorbol-13-acetate. *Environ. Toxicol. Pharmacol.* **2012**, *34*, 941–948. [CrossRef]
39. Rzepka, Z.; Buszman, E.; Beberok, A.; Wrzesniok, D. From tyrosine to melanin: Signaling pathways and factors regulating melanogenesis. *Postepy Hig. I Med. Dosw.* **2016**, *70*, 695–708. [CrossRef]
40. Qian, W.; Liu, W.; Zhu, D.; Cao, Y.; Tang, A.; Gong, G.; Su, H. Natural skin-whitening compounds for the treatment of melanogenesis. *Exp. Ther. Med.* **2020**, *20*, 173–185. [CrossRef]
41. Fu, C.; Chen, J.; Lu, J.; Yi, L.; Tong, X.; Kang, L.; Pei, S.; Ouyang, Y.; Jiang, L.; Ding, Y.; et al. Roles of inflammation factors in melanogenesis. *Mol. Med. Rep.* **2020**, *21*, 1421–1430. [CrossRef]
42. Wu, L.C.; Lin, Y.Y.; Yang, S.Y.; Weng, Y.T.; Tsai, Y.T. Antimelanogenic effect of c-phycocyanin through modulation of tyrosinase expression by upregulation of ERK and downregulation of p38 MAPK signaling pathways. *J. Biomed. Sci.* **2011**, *18*, 74. [CrossRef] [PubMed]
43. Silva, E.F.; Figueira, F.S.; Lettnin, A.P.; Carrett-Dias, M.; Filgueira, D.M.V.B.; Kalil, S.; Trindade, G.S.; Votto, A.P.S. C-Phycocyanin: Cellular targets, mechanisms of action and multi drug resistance in cancer. *Pharmacol. Rep.* **2017**, *70*, 75–80. [CrossRef] [PubMed]
44. Li, B.; Gao, M.H.; Zhang, X.C.; Chu, X.M. Molecular immune mechanism of C-phycocyanin from Spirulina platensis induces apoptosis in HeLa cells in vitro. *Biotechnol. Appl. Biochem.* **2006**, *43*, 155–164. [PubMed]
45. Reddy, M.C.; Subhashini, J.; Mahipal, S.V.K.; Bhat, V.B.; Reddy, P.S.; Kiranmai, G.; Madvastha, K.M.; Reddanna, P. C-Phycocyanin, a selective cyclooxygenase-2 inhibitor, induces apoptosis in lipopolysaccharide- stimulated RAW 264.7 macrophages. *Biochem. Biophys. Res. Commun.* **2003**, *304*, 385–392. [CrossRef]
46. Chen, T.; Wong, Y.S. In vitro antioxidant and antiproliferative activities of selenium-containing phycocyanin from selenium enriched Spirulina platensis. *J. Agric. Food Chem.* **2008**, *56*, 4352–4358. [CrossRef]
47. Hao, S.; Li, S.; Wang, J.; Zhao, L.; Zhang, C.; Huang, W.; Wang, C. Phycocyanin reduces proliferation of melanoma cells through downregulating GRB2/ERK signaling. *J. Agric. Food Chem.* **2018**, *66*, 10921–10929. [CrossRef]
48. Hongo, T.; Morimoto, Y.; Iwagaki, H.; Kobashi, K.; Yoshii, M.; Urushihara, N.; Hizuta, A.; Tanaka, N. Functional expression of Fas and Fas ligand on human colonic intraepithelial T lymphocytes. *J. Int. Med. Res.* **2000**, *28*, 132–142. [CrossRef]
49. Elmets, C.A.; Athar, M. Targeting ornithine decarboxylase for the prevention of nonmelanoma skin cancer in humans. *Cancer Prev. Res.* **2010**, *3*, 8–11. [CrossRef]
50. Mann, A.P.; Verma, A.; Sethi, G.; Manavathi, B.; Wang, H.; Fok, J.Y.; Kunnumakkara, A.B.; Kumar, R.; Aggarwal, B.B.; Mehta, K. Overexpression of tissue transglutaminase leads to constitutive activation of nuclear factor-kB in cancer cells: Delineation of a novel pathway. *Cancer Res.* **2006**, *66*, 8788–8795. [CrossRef]
51. Chhabra, A.; Verma, A.; Mehta, K. Tissue transglutaminase promotes or suppresses tumors depending on cell context. *Anticancer Res.* **2009**, *29*, 1909–1919.

52. Mehta, K.; Eckert, R. *Transglutaminases: Family of Enzymes with Diverse Functions. Progress in Experimental Tumor Research*, 1st ed.; Karger Publishers: Basel, Switzerland, 2005; Volume 38.
53. Esposito, E.; Nastruzzi, C.; Sguizzato, M.; Cortesi, R. Nanomedicines to treat skin pathologies with natural molecules. *Curr. Pharm. Des.* **2019**, *25*, 2323–2337. [CrossRef] [PubMed]
54. Majtan, J.; Bucekova, M.; Jesenak, M. Natural products and skin diseases. *Molecules* **2021**, *26*, 4489. [CrossRef] [PubMed]
55. Manconia, M.; Pendas, J.; Ledon, N.; Moreira, T.; Sinico, C.; Saso, L.; Fadda, A.M. Phycocyanin liposomes for topical anti-inflammatory activity: In-vitro in-vivo studies. *J. Pharm. Pharmacol.* **2009**, *61*, 423–430. [CrossRef] [PubMed]
56. Caddeo, C.; Chessa, M.; Vassallo, A.; Pons, R.; Diez-Sales, O.; Fadda, A.M.; Manconi, M. Extraction, purification and Nanoformulation of Natural Phycocyanin (from Klamath algae) for Dermal and Deeper Soft Tissue Delivery. *J. Biomed. Nanotechnol.* **2013**, *9*, 1929–1938. [CrossRef]
57. Castangia, I.; Manca, M.L.; Catalan- Latorre, A.; Maccioni, A.M.; Fadda, A.M.; Manconi, M. Phycocyanin- encapsulating hyalurosomes as carrier for skin delivery and protection from oxidative stress damage. *J. Mater. Sci. Mater. Med.* **2016**, *27*, 75. [CrossRef]
58. Castangia, I.; Manca, M.L.; Caddeo, C.; Bacchetta, G.; Pons, R.; Demurtas, D.; Diez-Sales, O.; Fadda, A.M.; Manconi, M. Santosomes as natural and efficient carriers for the improvement of phycocyanin reepithelising ability in vitro and in vivo. *Eur. J. Pharm. Biopharm.* **2016**, *103*, 149–158. [CrossRef]
59. Dev, A.; Mohanbhai, S.J.; Kushwaha, A.C.; Sood, A.; Sardiowala, M.N.; Choudhury, S.R.; Karmakar, S. Corrigendum to 'κ-carrageenan-c-phycocyanin based smart injectable hydrogels for accelerated wound recovery and real-time monitoring. *Acta Biomater.* **2022**, *138*, 576. [CrossRef]
60. Madhyastha, H.; Madhyastha, R.; Thakur, A.; Kentaro, S.; Dev, A.; Singh, S.; Chandrashekharappa, R.B.; Kumar, H.; Acevedo, O.; Nakajima, Y.; et al. C-Phycocyanin primed silver nano conjugates: Studies on red blood cell stress resilience mechanism. *Colloids Surf. B Biointerfaces* **2020**, *194*, 111211. [CrossRef]
61. Adli, S.A.; Ali, F.; Azmi, A.S.; Anuar, H.; Nasir, N.A.M.; Hasham, R.; Idris, M.K.H. Development of biodegradable cosmetic patch using a polylactic acid/phycocyanin- alginate composite. *Polymers* **2020**, *12*, 1669. [CrossRef]
62. Pu, Y.; Wei, M.; Witkowski, A.; Krzywda, M.; Wang, Y.; Li, W. A hybrid biomaterial of biosilica and C-phycocyanin for enhanced photodynamic effect towards tumor cells. *Biochem. Biophys. Res. Commun.* **2020**, *553*, 573–579. [CrossRef]
63. Jiang, L.; Wang, Y.; Zhu, F.; Liu, G.; Liu, H.; Ji, H.; Zheng, S.; Li, B. Molecular mechanism of anti-cancer activity of the nano-drug C-PC/CMC-CD59sp NPs in cervical cancer. *J. Cancer* **2019**, *10*, 92–104. [CrossRef] [PubMed]
64. Chaiklahan, R.; Chirasuwan, N.; Bunnag, B. Stability of phycocyanin extracted from Spirulina sp.: Influence of temperature, pH and preservatives. *Process Biochem.* **2012**, *47*, 659–664. [CrossRef]
65. Adjali, A.; Clarot, I.; Chen, Z.; Marchioni, E.; Boudier, A. Physicochemical degradation of phycocyanin and means to improve its stability: A short review. *J. Pharm. Anal.* **2021**. [CrossRef]
66. Hadiyanto, H.; Christwardana, M.; Sutanto, H.; Suzery, M.; Amelia, D.; Aritonang, R.F. Kinetic study on the effects of sugar addition on the thermal degradation of phycocyanin from *Spirulina* sp. *Food Biosci.* **2018**, *22*, 85–90. [CrossRef]
67. Chandralekha, A.; Prashanth, H.S.; Tavanandi, H.; Raghavarao, K.S.M.S. A novel method for double encapsulation of C-phycocyanin using aqueous two-phase systems for extension of shelf life. *J. Food Sci. Technol.* **2021**, *58*, 1750–1763. [CrossRef] [PubMed]

Paper 2

Title: Determination of Heavy Metal Content: Arsenic, Cadmium, Mercury, and Lead in Cyano-Phycocyanin Isolated from the Cyanobacterial Biomass

Authors: Galinytė, Daiva; Balčiūnaitė-Murzienė, Gabrielė; Karosienė, Jūratė; Morudov, Dmitrij; Naginienė, Rima; Baranauskienė, Dalė; Šulinskienė, Jurgita; Kudlinskienė, Ieva; Savickas, Arūnas; Savickienė, Nijolė

Plants, 12, 17 (2023)

plants

MDPI

Article

Determination of Heavy Metal Content: Arsenic, Cadmium, Mercury, and Lead in Cyano-Phycocyanin Isolated from the Cyanobacterial Biomass

Daiva Galinytė [1,*], Gabrielė Balčiūnaitė-Murzienė [2], Jūratė Karosienė [3], Dmitrij Morudov [3], Rima Naginienė [4], Dalė Baranauskienė [4], Jurgita Šulinskienė [4], Ieva Kudlinskienė [5], Arūnas Savickas [6] and Nijolė Savickienė [1]

[1] Department of Pharmacology, Faculty of Pharmacy, Academy of Medicine, Lithuanian University of Health Sciences, Sukileliu Av. 13, 50162 Kaunas, Lithuania; nijole.savickiene@lsmuni.lt
[2] Faculty of Pharmacy, Institute of Pharmaceutical Technologies, Academy of Medicine, Lithuanian University of Health Sciences, Sukileliu Av. 13, 50162 Kaunas, Lithuania; gabriele.balciunaite@lsmuni.lt
[3] Laboratory of Algology and Microbial Ecology, Nature Research Centre, Akademijos St. 2, 08412 Vilnius, Lithuania; jurate.karosiene@gamtc.lt (J.K.); dmitrij.morudov@gamtc.lt (D.M.)
[4] Laboratory of Toxicology, Neurosciences Institute, Academy of Medicine, Lithuanian University of Health Sciences, Eivenių Str. 4, 50161 Kaunas, Lithuania; rima.naginiene@lsmuni.lt (R.N.); dale.baranauskiene2@lsmu.lt (D.B.); jurgita.sulinskiene@lsmu.lt (J.Š.)
[5] JSC "Naujasis Nevėžis", Jiesios St. 2, 53288 Ilgakiemis, Lithuania; ieva.kudlinskiene@nevezis.lt
[6] Department of Drug Technology and Social Pharmacy, Academy of Medicine, Lithuanian University of Health Sciences, Sukileliu Av. 13, 50162 Kaunas, Lithuania; arunas.savickas@lsmu.lt
* Correspondence: daiva.galinyte@stud.lsmu.lt

check for updates

Citation: Galinytė, D.; Balčiūnaitė-Murzienė, G.; Karosienė, J.; Morudov, D.; Naginienė, R.; Baranauskienė, D.; Šulinskienė, J.; Kudlinskienė, I.; Savickas, A.; Savickienė, N. Determination of Heavy Metal Content: Arsenic, Cadmium, Mercury, and Lead in Cyano-Phycocyanin Isolated from the Cyanobacterial Biomass. *Plants* **2023**, *12*, 3150. https://doi.org/10.3390/plants12173150

Academic Editor: Stefano Accoroni

Received: 31 May 2023
Revised: 22 August 2023
Accepted: 25 August 2023
Published: 1 September 2023

Abstract: Cyano-phycocyanin (C-PC) is a light-absorbing biliprotein found in cyanobacteria, commonly known as blue-green algae. Due to its antioxidative, anti-inflammatory, and anticancer properties, this protein is a promising substance in medicine and pharmaceuticals. However, cyanobacteria tend to bind heavy metals from the environment, making it necessary to ensure the safety of C-PC for the development of pharmaceutical products, with C-PC isolated from naturally collected cyanobacterial biomass. This study aimed to determine the content of the most toxic heavy metals, arsenic (As), cadmium (Cd), mercury (Hg), and lead (Pb) in C-PC isolated from different cyanobacterial biomasses collected in the Kaunas Lagoon during 2019–2022, and compare them with the content of heavy metals in C-PC isolated from cultivated *Spirulina platensis* (*S. platensis*). Cyanobacteria of *Aphanizomenon flos-aquae* (*A. flos-aquae*) dominated the biomass collected in 2019, while the genus *Microcystis* dominated the biomasses collected in the years 2020 and 2022. Heavy metals were determined using inductively coupled plasma mass spectrometry (ICP-MS). ICP-MS analysis revealed higher levels of the most investigated heavy metals (Pb, Cd, and As) in C-PC isolated from the biomass with the dominant *Microcystis* spp. compared to C-PC isolated from the biomass with the predominant *A. flos-aquae*. Meanwhile, C-PC isolated from cultivated *S. platensis* exhibited lower concentrations of As and Pb than C-PC isolated from naturally collected cyanobacterial biomass.

Keywords: cyano-phycocyanin; *Microcystis*; *Aphanizomenon*; *Spirulina platensis*; heavy metals

1. Introduction

In recent decades, there has been an observed increase in the mass of cyanobacteria and the intensity of blooms in water bodies, influenced by eutrophication processes, the rising CO_2 content in the atmosphere and surface waters, and global climate warming. The excessive presence of cyanobacteria in water bodies poses problems for the entire water ecosystem. One potential solution is the collection of cyanobacteria from water bodies and utilizing the collected biomass across various fields [1]. The aim of our research was to isolate C-PC from cyanobacterial biomass collected in nature and employ it in the production of pharmaceutical or cosmetic products. Ensuring the safety of the active ingredient is

crucial during the development of such products. The concern is that cyanobacteria, like many other algae, possess a remarkable ability to sorb metal ions. Studies have shown that specific concentrations of heavy metals affect algal growth, bioactivity, and the process of photosynthesis. Indeed, the entire aquatic ecosystem is at risk when algae are exposed to high concentrations of heavy metals [2]. Cyanobacteria is even used as a bioindicator of water pollution due to its ability to accumulate contaminants. It has been observed that metals can bind to C-PC as well [3]. Generally, heavy metals are elements with a high atomic weight (between 63.5 g/mol and 200.6 g/mol) and a density exceeding 5.0 g/cm^3. Therefore, out of 90 naturally occurring elements, 53 can be classified as heavy metals [4,5]. Metals are non-degradable, can accumulate in water and sediments, and persist in the environment for long periods of time, posing a threat to all living organisms when their concentrations exceed certain thresholds [6,7]. Certain heavy metals, such as As, Cd, Pb, and Hg, are particularly problematic due to their high levels of toxicity [4,8,9]. Heavy metals often contaminate surface water through the discharge of industrial or domestic wastewater disposed into sewers or water bodies [6]. Furthermore, pollutants can also be transported to water bodies from the soil through intensive agricultural practices or deposited from the atmosphere [2]. The high solubility of heavy metals in water makes them accessible to aquatic organisms, causing toxicity [10]. Therefore, there is a valid concern about the binding of heavy metals to C-PC. The level of C-PC contamination with metal ions depends on various factors, including the geographical location of the water body, the concentrations of heavy metals, the algae content in the water body, the water temperature, the pH, and the methods used for isolation and purification [6,10–12]. Consequently, the need for necessary monitoring and evaluation of heavy metals in C-PC using the latest research methods is crucial to ensure the safety aspects related to the content of heavy metals in raw materials of natural origin and to maintain their quality.

This study aimed to determine the concentrations of the most toxic heavy metals, namely lead (Pb), cadmium (Cd), arsenic (As), and mercury (Hg), in C-PC isolated from different biomasses of cyanobacteria collected in water bodies. The dominant genus and species of cyanobacteria depend on the geographical location, environmental and growth conditions [1]. For example, in the Kaunas Lagoon, where the biomass was collected for this study, cyanobacteria of *A. flos-aquae* dominated the biomass collected in 2019, while the genus *Microcystis* dominated the biomasses collected in the years 2020 and 2022. The content of heavy metals in C-PC isolated from the biomass of cyanobacteria collected in nature was compared with the concentrations of heavy metals in C-PC isolated from cultivated *S. platensis*. Purified C-PC is usually obtained from *S. platensis* by combining ammonium sulfate precipitation and different chromatographic methods [13]. Since cultivated *S. platensis* is protected as much as possible from the effects of heavy metals, C-PC of this origin was chosen as a comparison substance.

2. Results

To the best of our knowledge, this study represents the first investigation into the concentrations of heavy metals in C-PC isolated from cyanobacterial biomass collected in the Kaunas Lagoon, Lithuania. The results of the heavy metals analysis using ICP-MS on dry weight (dw) C-PC samples are presented in Figure 1. In the case of C-PC isolated from cyanobacterial biomass with dominant *A. flos-aquae* in 2019 (S1), the order of metal concentrations varied as follows: Pb 0.378 (0.013) μg/g > As 0.150 (0.012) μg/g > Hg 0.050 (0.006) μg/g > Cd 0.020 (0.000) μg/g (Figure 1a). The purity coefficient of C-PC (A620/A280) from sample S1 was 2.207 (0.015). For C-PC isolated from cyanobacterial biomass dominated by the genus *Microcystis* in 2020 (S2), the heavy metal concentrations ranged as follows: Pb 0.725 (0.006) μg/g, Hg 0.443 (0.007) μg/g, Cd 0.233 (0.005) μg/g, and As 0.190 (0.008) μg/g (Figure 1b). The determined purity coefficient of C-PC from sample S2 was 1.811 (0.028). In comparison with sample S2, the concentrations of heavy metals in C-PC from cyanobacterial biomass also dominated by the genus *Microcystis* but collected in 2022 (S3) varied in the following range: Pb 0.643 (0.015) μg/g > Cd 0.410 (0.014) μg/g

> As 0.160 (0.008) µg/g > Hg 0.021 (0.003) µg/g (Figure 1c). The purity coefficient of C-PC from sample S3 was slightly lower than that of sample S2, reaching 1.463 (0.021). The concentrations of heavy metals in C-PC from cultivated *S. platensis* (S4) was also determined as follows: Hg 0.376 (0.016) µg/g > Cd 0.348 (0.005) µg/g > Pb 0.200 (0.008) µg/g > As 0.045 (0.006) µg/g (Figure 1d), and the purity coefficient of C-PC from sample S4 was identified as 1.130 (0.020). The purity coefficients of the C-PC samples are presented in Figure 2. The highest purity ratio was found in sample S1 and the lowest in sample S4, but both had lower amounts of the most tested heavy metals than samples S2 and S3.

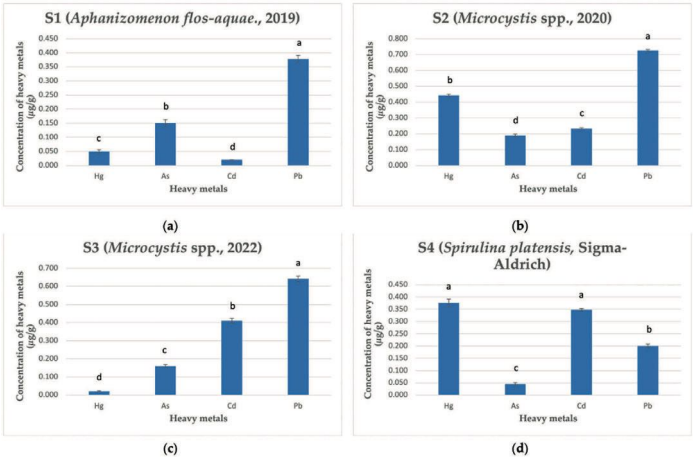

Figure 1. Content of heavy metals in C-PC samples (µg/g dw). (**a**) Heavy metal concentrations in sample S1. (**b**) Heavy metal concentrations in sample S2. (**c**) Heavy metal concentrations in sample S3. (**d**) Heavy metal concentrations in sample S4. Different letters above the bars indicate significant differences among the different metal concentrations ($p < 0.05$) identified using Dunnett's T3 test. Means and standard deviations are presented. The experiment was repeated 4 times.

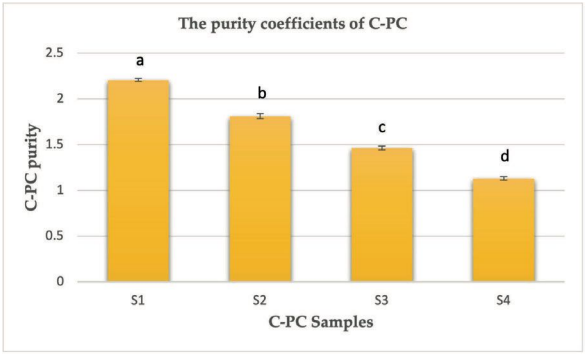

Figure 2. The purity coefficients of C-PC samples S1, S2, S3, and S4. Different letters above the bars indicate significant differences ($p < 0.05$) identified using Bonferroni's test. Means and standard deviations are presented. The experiment was repeated 3 times.

As shown in Figure 1, C-PC extracted from cyanobacterial biomass collected in nature exhibited the highest levels of lead, particularly in samples S2 and S3 (*Microcystis*, 2020 and 2022), compared to the other tested elements. On the other hand, mercury and cadmium were the most predominant metals detected in the C-PC isolated from *S. platensis*.

2.1. Lead (Pb)

Figure 3a depicts the significant variation in lead levels among the different C-PC samples. The concentrations of lead ranged from 0.200 µg/g to 0.725 µg/g (dry weight), with the highest value observed in samples S2 and S3 (0.725 µg/g and 0.643 µg/g dw, respectively). These results indicate that C-PC isolated from the cyanobacterial biomass dominated by the genus *Microcystis* had the highest lead content. Sample S1 (*A. flos-aquae*, 2019) exhibited a concentration of lead that was more than 1.7 times lower, measuring 0.378 µg/g dw. The lowest concentration of lead (0.200 µg/g dw) was found in sample S4 (*S. platensis*). A significant difference in the lead content was observed among all four sample groups ($p < 0.05$). The order of the concentrations of Pb, as detected from the samples, was S2 > S3 > S1 > S4.

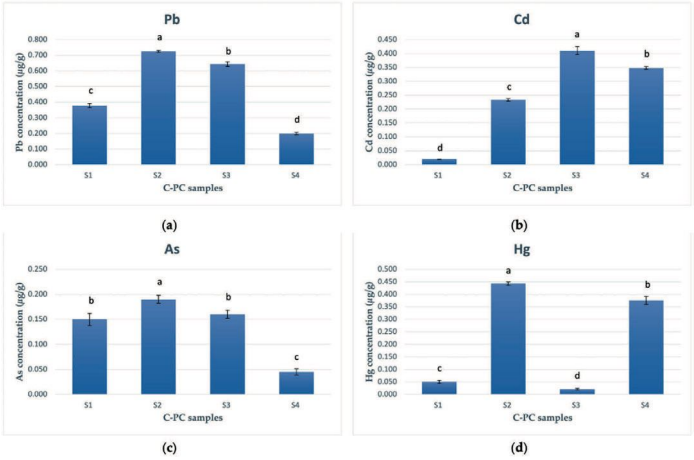

Figure 3. Graphical representation of heavy metal concentrations (µg/g dw) in C-PC samples. (**a**) Pb concentration. (**b**) Cd concentration. (**c**) As concentration. (**d**) Hg concentration. Different letters above the bars indicate significant differences among the different metals ($p < 0.05$) identified using Bonferroni's test. Means and standard deviations are presented. The experiment was repeated 4 times.

2.2. Cadmium (Cd)

The concentrations of Cd in the four C-PC samples ranged from 0.020 µg/g to 0.410 µg/g dw The highest Cd value (0.410 µg/g dw) was detected in sample S3 (*Microcystis*, 2022), followed by sample S4 (*S. platensis*)—0.348 µg/g dw and sample S2 (*Microcystis*, 2020)—0.233 µg/g dw. The lowest content of Cd (0.020 µg/g dw) was found in sample S1 (*A. flos-aquae*, 2019). Significant differences in Cd content were identified among all four sample groups ($p < 0.05$). The order of the concentrations of Cd was S3 > S4 > S2 > S1 (Figure 3b).

2.3. Arsenic (As)

No significant difference in As content was observed between samples S1 (0.150 µg/g dw) and S3 (0.160 µg/g dw), where C-PC was isolated from the biomass of *A. flos-aquae* and

Microcystis spp. (2022), respectively. However, a statistically higher concentration of As was detected in C-PC from *Microcystis* biomass collected in 2020 (0.190 μg/g dw). The lowest value of As (0.045 μg/g dw) was determined in sample S4 (*S. platensis*). The order of the concentrations of arsenic observed among the samples was S2 > S3 > S1 > S4 (Figure 3c).

2.4. Mercury (Hg)

The highest concentration of Hg was determined in sample S2 (0.443 μg/g dw) followed by sample S4 (0.376 μg/g dw). A more than seven-fold lower concentration of Hg was found in sample S1 (0.050 μg/g dw), and the lowest Hg content was detected in sample S3 (0.021 μg/g dw). The results regarding the concentrations of mercury in the tested samples are controversial, since the highest and lowest Hg content was observed in the C-PC isolated from *Microcystis* biomass. Nevertheless, a significant difference in Hg content was observed among all four groups ($p < 0.05$). The order of the concentrations of Hg, from highest to lowest, as determined from the C-PC samples, was S2 > S4 > S1 > S3 (Figure 3d).

The results of ICP-MS analysis revealed higher concentrations of the tested metals in C-PC isolated from the cyanobacterial biomass collected from nature, particularly when the genus *Microcystis* dominated (in the years 2020 and 2022). On the other hand, samples S1 (*A. flos-aquae*, 2019) and S4 (*S. platensis*) exhibited lower concentrations of the tested metals. Cultivated *S. platensis* is more protected from heavy metal exposure from the environment. Meanwhile, the metals from natural and anthropogenic sources are released into aquatic systems [6]. The dominant genus of cyanobacteria, and the overall metal content in the aquatic system, can influence the binding of metals via C-PC. In addition, the purification processes of C-PC are also important. Gel filtration chromatography was utilized for purifying C-PC from *Microcystis* spp. (samples S2 and S3), resulting in purity coefficients of 1.811 (0.028) and 1.463 (0.021), respectively. Ion exchange chromatography was employed to isolate C-PC from *A. flos-aquae* (sample S1), with the resulting purity coefficient of 2.207 (0.015).

3. Discussion

3.1. Heavy Metal Content in the Water Body

The accumulation of metals in cyanobacteria is influenced by the metal concentrations in the water body. In this study, the cyanobacterial biomass was collected from the Kaunas Lagoon (Lithuania), the largest artificial water body in Lithuania. The Kaunas Lagoon was created in 1959 after the construction of the Kruonis hydro accumulative power plant and the damming of the Nemunas river—the longest river in Lithuania. As a result, the Kaunas Lagoon belongs to the Nemunas basin and is classified as a highly altered water body. In addition, it is considered at risk due to sewage, agriculture, and historical pollution [14]. Heavy metal monitoring in surface water has been conducted in Lithuania since 1993. According to the State Environmental Monitoring Program for 2018–2023, approved by the Government of the Republic of Lithuania on 3 October 2018, by resolution no. 996 "On the approval of the State Environmental Monitoring Program for 2018–2023", the monitoring of metals in water, bottom sediments, and biota in the Kaunas Lagoon is carried out every three years. Bottom sediments are tested for metals that tend to accumulate in sediments, while the biota is tested for those metals that have established environmental quality standards, such as mercury (Hg). Therefore, we only have the results of the heavy metals in the Kaunas Lagoon from the year 2021 (reflecting the period from 2019 to 2022). To assess the pollution of the Kaunas Lagoon with heavy metals, we analyzed ten years of monitoring results. We considered the content of heavy metals (Pb, Cd, As, and Hg) in the surface water and bottom sediments of the Kaunas Lagoon from 2013 to 2022 based on the monitoring procedures of lakes and ponds in the country (Figure 4). The monitoring results revealed that the concentration of Cd in the surface water of the Kaunas Lagoon remained unchanged over the ten-year period (0.05 μg/L). Nonetheless, the concentration of cadmium increased in the bottom sediments. In the

C-PC samples, a statistically significant increase in the concentration of Cd was observed from 0.020 μg/g (sample S1, 2019) to 0.410 μg/g (sample S3, 2022). The concentration of lead in the bottom sediments also increased from 14 mg/kg in 2015 to 28 mg/kg in 2021. In the C-PC samples, there was an almost two-fold increase in the concentration of Pb in 2020 (sample S2) compared to 2019 (sample S1) ($p < 0.05$). In 2022 (sample S3), the concentration of Pb in C-PC was 11% lower than in 2020 (sample S2), but still 70% higher than in 2019 (sample S1). The significantly lower concentrations of Cd and Pb in sample S1 (*Aphanizomenon*, 2019) could be attributed to the differences in the C-PC purification methods or the dominant algal genus. The concentration of As in the surface water remained relatively constant over the entire ten-year period, with no statistically significant differences observed between the C-PC samples from 2019 and 2022 ($p > 0.05$). The mercury concentration in the surface water and sediments remained relatively stable over the ten years. In 2021, the concentrations of hazardous substances in the water of the Kaunas Lagoon did not exceed the environmental quality standards based on both the maximum allowed concentrations and the annual average standards. However, in the biota of the Kaunas lagoon, the concentration of mercury (119 μg/kg) exceeded the maximum allowed concentration six times (20 μg/kg) [15].

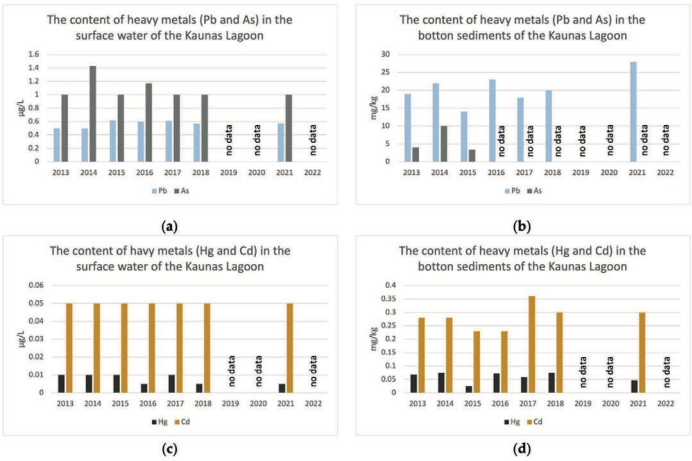

Figure 4. Heavy metal content (μg/L) in the surface water and bottom sediments of the Kaunas Lagoon. (**a**) Pb and As content in the surface water of the Kaunas Lagoon. (**b**) Pb and As content in the bottom sediments of the Kaunas Lagoon. (**c**) Hg and Cd content in the surface water of the Kaunas Lagoon. (**d**) Hg and Cd content in the bottom sediments of the Kaunas Lagoon [15].

After evaluating the condition of the water bodies in Lithuania in 2022, it was determined that 57% of rivers and 62% of lakes within the Nemunas basin area did not meet the criteria for good condition. The majority of water bodies failing to meet these requirements are located in the regions with intensive agriculture and farming. Agricultural activities, sewage discharge, hydromorphological effects, natural processes, and changing climatic conditions are the primary sources of water pollution in Lithuania. These factors contribute to the classification of the Kaunas Lagoon as a risk water body. Nonetheless, it is encouraging that more and more attention is being paid to the state of the water bodies in Lithuania; the reliability of these assessments has increased, and the states of the water bodies are not deteriorating. However, it has been acknowledged that it will take a considerable amount of time for water condition indicators to recover, even with the implementation of

the necessary improvement measures. One such measure to achieve a good water body condition involves the removal of excess aquatic vegetation [16].

Overall, heavy metal contamination in the surface water is a global issue, and is particularly prevalent in Africa and Asia, where the highest concentrations of heavy metals are found. Lower concentrations are observed in European surface water [3].

The water temperature and pH levels can also influence the binding of heavy metals. The average annual water temperature in the Kaunas Lagoon decreased from 14.89 °C in 2019 to 14.01 °C in 2022, while the pH in 2019–2021 remained at 8.5, and slightly decreased in 2022 to 8.4 (Figure 5) [15]. However, detailed studies are required to assess whether these slight changes in the temperature and pH in the water of the Kaunas Lagoon could have influenced the accumulation of heavy metals in the cyanobacterial biomass.

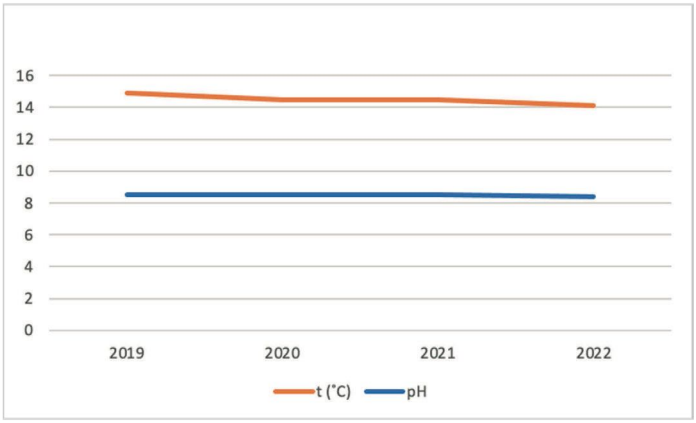

Figure 5. Changes in the average annual water temperature and pH of the Kaunas Lagoon in 2019–2022.

Clearly, our water bodies are susceptible to heavy metal pollution. Cyanobacteria, including phycocyanin, have a tendency to bind heavy metals from the surrounding environment.

3.2. Aspects of Heavy Metal Binding by Cyanobacteria and C-PC

Cyanobacteria have a remarkable ability to bind metals from the surrounding environment. It is known that dead algal cells can absorb more metals than living ones. The term "bio-sorption" is typically used to describe the sorption of metals by dead biomass, while "accumulation" refers to the living cells. Two distinct processes affect the accumulation of heavy metals in cyanobacteria: passive initial uptake and active uptake. The passive initial uptake process does not depend on cell metabolism and lasts a few seconds or minutes. During this time, metal ions are adsorbed onto the cell surface. In water, metals are predominantly found in their cationic form. The cell wall of cyanobacteria contains various functional groups, such as hydroxyl ($–OH^-$), carboxyl ($–COOH^-$), sulfhydryl ($–SH^-$), amino ($–NH_2^-$), and phosphoryl (PO_3^{-3}), which are associated with cell wall components, among which include the following: teichuronic acid, teichoic acids, peptidoglycans, polysaccharides, and proteins. These functional groups provide a negative charge to the cell surface, allowing metal ions to be adsorbed on the cell surface due to electrostatic interactions. The dissociation constant, pKa, is specific to each functional group and determines the dissociation into the corresponding anions and protons at a particular pH. This supports the fact that changes in the pH of the water body affect the binding of heavy metals. The second process is much slower and depends on metabolism; metal

ions pass through the cell membrane into the cytoplasm [6,11]. The cell membrane acts as a barrier and prevents unwanted substances from entering the cell. However, different transport proteins, responsible for nutrient absorption, assist heavy metals in crossing the membrane [4]. For instance, As^{5+} is taken up via phosphate transporters, while As^{2+} uses glycerol transport proteins [17]. Pb^{2+} and Cd^{2+} enter the cell through divalent metal transport channels and carrier proteins, including divalent cation transporter 1 (DCT1) [4]. Both organic and inorganic forms of mercury compounds can be transported via the specific transport proteins MerC and MerT [18].

The capacity for metal sorption may vary among the genera of cyanobacteria due to the differences in their cell component distributions and the types of functional groups present. *Microcystis aeruginosa* and *Microcystis flos-aquae* form multicellular aggregates surrounded by a colonial capsule or an exopolymeric matrix. A strong interaction between the mucus layer from *Microcystis* spp. and cations has been shown. The several functional groups, especially the carboxyl groups, arranged in the cell walls of *Microcystis* spp. provide biosorption sites for metal binding and lead to a high capacity for binding heavy metals [11]. While the genus *Aphanizomenon* is planktonic cyanobacteria with straight trichomes, it can exist as single filaments or form aggregated trichomes in parallel fascicles, reaching a size of up to 2 cm [19]. It has been demonstrated that *Microcystis aeruginosa* exhibits a high affinity for binding Hg^{2+}, Cd^{2+}, and Pb^{2+} [20]. A more elevated cell surface influences the more remarkable ability of *Microcystis aeruginosa* to absorb Hg^{2+} than *A. flos-aquae* [21]. Our study also supports the high affinity of *Microcystis* for Hg, Cd, and Pb ions.

S. platensis is a filamentous, non-differentiated, spiral-shaped, multicellular cyanobacteria [22]. Gelagutashvili E et al. reported that *S. platensis* has a higher sorption capacity for cadmium [23]. However, metals, such as lead, mercury, cadmium, and arsenic, can also be found in *Spirulina* products [22]. In our study, C-PC isolated from *S. platensis* predominantly contained Hg and Cg among the metals examined.

C-phycocyanin is a light-harvesting phycobiliprotein that plays an important role in phycobilisomes, which are attached to the outer membrane of the chloroplast thylakoid [24,25]. Phycobiliproteins are oligomers, with the hexamer being the basic building block [26]. Each monomer of C-PC consists of α- and β-polypeptide chains with three covalently binding open-chain tetrapyrrole chromophores, known as phycocyanobilins. This binding occurs through a thioether bond between a cysteine residue and the A ring of tetrapyrrole. The α-subunit of C-PC contains a phycocyanobilin covalently attached to α-84 cysteine, while the β-subunit contains two phycocyanobilins that are linked to the β-84 and β-155 cysteine residues of the apoprotein, respectively [26]. The mechanisms underlying heavy metal binding to C-phycocyanin may vary with the different metal cations, but they are not fully understood [12]. Gelagutashvili E. and others distinguished two feasible ways of heavy metal ion binding to C-PC: site-specific and non-specific (diffuse) binding. Hexamers of C-PC have a globular structure, and the negative electrostatic field is dominant. Therefore, cations of heavy metals can be electrostatically attached to the strong anionic area at the center of the hexamer. This interaction is non-specific, while the binding of the metal ions form site-specific bonds to the thiol groups of the protein. Gelagutashvili E. and others' research suggested that cysteine at the β-84 position is one of the specific binding sites for metal ions in C-PC [23]. Heavy metals can affect the conformational changes in C-PC and inhibit the photosynthesis processes of cyanobacteria [3,4]. Higher concentrations of toxic metals lead to more changes in the structure of the C-PC macromolecule [3]. Pb^{2+} and Cd^{2+} form aggregations with C-PC molecules and modify their secondary structure (α helix). Research has shown that the effect of Pb^{2+} on the Tyr residues of PC was more significant than the Trp residues, while the effect of Cd^{2+} was more significant on the Trp residue of PC. The changes in the protein skeleton are possibly related to the loss of C-PC function [27,28].

The binding affinities of the heavy metal ions depend on the specific metal. The binding constants are arranged in descending order, as follows: Hg > Ag > Pb > Cr > Cu [23]. In addition, the binding affinities of the heavy metals depend on the metal concentrations, and that is why the research results may vary. The binding of the heavy metals induces

conformational changes in the C-PC molecules and fluorescence quenching. For instance, Chi Z. and others referred to the fluorescence quenching effect on the C-PC with the order of $Hg^{2+} > Cu^{2+} \approx Ag^{+} > Pb^{2+} > Cr^{3+} > Zn^{2+}$ at a concentration of 50 µM, while the lower concentrations changed the order to $Hg^{2+} > Cu^{2+} > Ag^{+} > Zn^{2+} > Cd^{2+} > Pb^{2+}$. Understanding the influence of heavy metal ions on C-PC at low concentrations is essential for assessing the toxicity of accumulated heavy metal ions in aquatic systems. Studies conducted at lower concentrations may be more important for evaluating the mechanisms of heavy metal binding to C-PC and their impact of toxicity on aquatic systems since they better reflect natural conditions. However, it should be noted that the highest concentrations of heavy metals result in more changes in the structure of the C-PC macromolecule [3].

The findings of our study revealed that lower concentrations of heavy metals were found in C-PC isolated from the cyanobacterial biomass with the dominant *A. flos-aquae* compared to the C-PC samples isolated from the biomass with the dominant *Microcystis* spp. The mucus layer and the larger cell surface area of *Microcystis* spp. may have influenced these results.

3.3. The Influence of the Purification Method on the Heavy Metal Content in C-PC

C-PC isolation from cyanobacterial biomass encompasses different steps, such as cell disruption, primary extraction, and purification [29]. Our study conducted gel filtration chromatography on a Sephadex G-25 column to purify C-PC from biomass with dominant *Microcystis* spp. Meanwhile, ion exchange chromatography on a Q-Sepharose XL column was used to purify C-PC from biomass with predominant *A. flos-aquae*. Both methods are well-documented and commonly employed for C-PC purification. Purification methods must protect the product from degradation (as C-PC is known to be sensitive to pH and temperature changes), help obtain the highest possible purity level, and maintain cost-effectiveness [29]. The combination of these two methods is also often used for C-PC purification [30]. The attraction of oppositely charged molecules supports the ion exchange chromatography of proteins. The protein's surface can be charged depending on the isoelectric point and the pH of the environment. The ion exchanger usually has a base matrix with porous beads that provide a sufficient adsorption surface. Positively or negatively charged ligands are immobilized on this matrix. Cation and anion exchangers are distinguished, which are negatively and positively charged, respectively. The protein is negatively charged above its isoelectric point and binds to an anion exchanger. On the contrary, the protein is positively charged below its isoelectric point and binds to cation exchangers [31]. The significant advantage of ion exchange chromatography is that it ensures mild separation conditions that enable the proteins from conformational changes [32]. C-PC should be purified depending on the field of use [33]. The purity of C-PC is typically estimated according to the absorbance ratio of A620/A280, wherein a purity of 0.7 is considered a food grade, 3.9 as a reactive grade, and values greater than 4.0 as an analytical grade [34].

The purity grades of the C-PC samples S1, S2, S3, and S4 were 2.207 (0.015), 1.811 (0.028), 1.463 (0.021), and 1.130 (0.020), respectively (Figure 2). However, the purity coefficients of C-PC do not reflect heavy metal contamination (Figure 1) in our study.

An anionic Q-Sepharose XL matrix used for ion exchange chromatography could influence the lower concentrations of heavy metals in C-PC isolated from cyanobacterial biomass with the dominant *A. flos-aquae*. However, further detailed studies are required to confirm this hypothesis. In addition, it is important to note that our study did not aim to find correlations between these purification methods. Metal content was determined to evaluate the safety of the isolated phycocyanin for further research.

3.4. Regulation of Heavy Metal Content in Products

Since heavy metals are naturally present in the environment, they can also be present as traces in food products, medical devices, or pharmaceuticals. Heavy metals can enter the final product with active substances or excipients through contaminated wa-

ter, manufacturing equipment, or container systems. Phycocyanin is used as a natural blue dye in food (chewing gum, dairy products, drinks, desserts, etc.) and cosmetics (e.g., lipsticks) [33,35]. C-PC also demonstrates numerous medical applications due to its antioxidant, anti-inflammatory, and antitumor properties [36,37]. Therefore, the possible contamination of C-PC with heavy metals should be carefully monitored to ensure the quality and safety of the final product.

3.4.1. Food Products

Heavy metal content in food must be maintained as low as can be reasonably achieved following good working practices [38]. The maximum levels for specific contaminants in foodstuff, including lead, cadmium, and mercury, are set under the Commission Regulation (EU) 2023/915 for the protection of public health. The maximum levels of lead and mercury in food supplements is set at 3 mg/kg and 0.10 mg/kg, respectively. The maximum level of cadmium in food supplements is established as 1 mg/kg, except for food supplements exclusively or mainly consisting of dried seaweed, products derived from seaweed, or dried bivalve mollusks—3 mg/kg. The maximum levels of arsenic are set only for infant or baby products and, depending on the product, should not exceed 0.010–0.020 mg/kg. The maximum levels of As in food supplements have not been identified [39]. There is limited data on the heavy metal content of C-PC, but studies on the determination of heavy metals in algae products were found. Al-Dhabi N.A. evaluated the content of six heavy metals, Ni, Zn, Hg, Pt, Mg, and Mn, in *Spirulina* food products for human consumption. All tested metals were within the daily intake levels. The content of Hg ranged from 0.002 mg/kg dw to 0.028 mg/kg dw [22]. Sandaruber F. and others determined heavy metal concentrations in 15 commercially available microalgae, including *S. platensis* and *A. flos-aquae* powders. The concentrations of heavy metals (means and standard deviations) varied within the following wide limits: from 0.89 (0.14) μg/100 g to 799.2 (14.8) μg/100 g in *S. platensis* and 60.37 (0.05) μg/100 g in *A. flos-aquae* for As, from 0.54 (0.26) μg/100 g to 9.61 (1.56) μg/100 g in *S. platensis* and 0.58 (0.30) μg/100 g in *A. flos-aquae* for Cd, from 0.25 (0.07) μg/100 g to 4.91 (1.02) μg/100 g in *S. platensis* and 0.3835 (0.0001) μg/100 g in *A. flos-aquae* for Hg, and from 4.25 (5.31) μg/100 g to 22.7 (16.06) μg/100 g in *S. platensis* and 4.98 (6.33) μg/100 g in *A. flos-aquae* for Pb. The concentrations of Cd, Hg, and Pb in the tested *S. platensis* and *A. flos-aquae* products did not exceed the maximum levels specified in Regulation EU 2023/015. The highest concentrations of Hg and As among all the different tested algal powders were determined in *S. platensis*. However, one product from *S. platensis* had the lowest concentrations of all the four determined heavy metals combined. Notably, the highest concentrations of heavy metals were found in products from China, where the regulations for heavy metals were only set for macroalgae but not microalgae. Therefore, the legislation on food supplements varies between the EU, the US, and Asian countries. Even in the cultivation of algae, an impure cultivation medium can cause the contamination with heavy metals [40].

3.4.2. Cosmetic Products

The manufacturing of cosmetic products must also adhere to good manufacturing practices. According to Regulation (EC) No. 1223/2009, heavy metals, such as arsenic, cadmium, lead, and mercury (with some exceptions), and their compounds are included in the list of substances prohibited in cosmetic products. If preservatives, such as thiomersal or phenylmercuric salts, are used in cosmetic products, the maximum allowable mercury concentration is 0.007% of the ready-to-use preparation [41]. If the cosmetic product contains traces of prohibited substances, the evidence must be provided that such traces were technically unavoidable. The safety assessor must decide whether the trace level is toxicologically acceptable and whether the product is safe [42].

3.4.3. Medical Devices

Arsenic, lead, cadmium, mercury, and their compounds are included in the list of substances that are carcinogenic, mutagenic, or toxic to reproduction (CMR). Thus, according to Regulation 2017/745, the concentration of these substances in medical devices must not exceed 0.1% by mass (*w*/*w*), with some exceptions provided in this Regulation when a higher amount of such substances must be justified. It is important to consider whether the intended device will be used to treat children, pregnant or lactating women, or other patient groups considered particularly vulnerable to such agents [43,44].

3.4.4. Medicines

The European Medicines Agency categorizes the elements Cd, As, Pb, and Hg as Class 1 substances based on their toxicity to humans. They should not be used in the manufacturing of pharmaceuticals, and their usage must be strictly limited. The ICH guidelines on elemental impurities establishes the permitted daily exposure (PDE) of each element of toxicological concern. The oxidation state of the element in the drug product, the route of administration, relevant animal and human studies, and safety data are the factors considered in the safety assessment of these elements. Established PDE and recalculated permitted concentrations of these elemental impurities in drug products, drug substances, and excipients with daily doses of not more than 10 g per day for oral, parental, inhalation, and cutaneous exposure are provided in Table 1. This guideline applies to newly developed drug products, including products with proteins and polypeptides, but does not apply to herbal products [45].

Table 1. Maximum allowed levels for heavy metals in food supplements, cosmetic products, medical devices, and medicines.

Products	Maximum Levels for Heavy Metals				References
	Pb	Cd	As	Hg	
Food supplements	3 mg/kg	1 mg/kg (3 mg/kg) [1]	Not identified	0.10 mg/kg	Regulation (EU) 2023/915 [38]
Cosmetic products	Prohibited [2]	Prohibited [2]	Prohibited [2]	0.007% of ready-to-use preparation [3]	Regulation 1223/2009 [41]
Medical devices	≤0.1% by mass (*w*/*w*) [4]	≤0.1% by mass (*w*/*w*) [4]	≤0.1% by mass (*w*/*w*) [4]	≤0.1% by mass (*w*/*w*) [4]	Regulation 2017/745 [42]
Medicines [5]					
Oral	5 µg/day (0.5 µg/g)	5 µg/day (0.5 µg/g)	15 µg/day (1.5 µg/g)	30 µg/day (3 µg/g)	ICH guideline Q3D (R2) on elemental impurities [44]
Parental	5 µg/day (0.5 µg/g)	1.7 µg/day (0.2 µg/g)	15 µg/day (1.5 µg/g)	3 µg/day (0.3 µg/g)	
Inhalation	50 µg/day (5 µg/g)	3 µg/day (0.3 µg/g),	1.9 µg/day (0.2 µg/g)	1.2 µg/day (0.1 µg/g),	
Cutaneous	50 µg/day (5 µg/g)	20 µg/day (2 µg/g)	30 µg/day (3 µg/g)	30 µg/day (3 µg/g)	

[1] For food supplements exclusively or mainly consisting of dried seaweed, products derived from seaweed, or dried bivalve mollusks. [2] The safety assessor must decide whether the trace level of the prohibited substances is toxicologically acceptable and whether the product is safe. [3] In the case of using preservatives, such as thiomersal or phenylmercuric salts. [4] Concentration in mass percent (weight by weight). [5] Established PDE and recalculated permitted concentrations of elemental impurities in drug products, drug substances, and excipients with daily doses of not more than 10 g/day are given in the parentheses.

Therefore, the purification process is critically important for ensuring the safety of the natural source material. In this study, our aim was to assess the residual heavy metal content after the purification of C-PC. According to the determined content of heavy metals,

C-PC isolated from the cyanobacterial biomasses collected in nature could be used in the development of cosmetics, medical devices, or pharmaceutical products. However, other ingredients may also contain heavy metal impurities and heavy metals may enter the product during manufacturing. Thus, it is essential to consider the permitted concentrations of these heavy metals in the final product.

4. Materials and Methods

4.1. Collection of Cyanobacterial Biomass

The biomass of cyanobacteria was collected with a plankton net (with a mesh size of 20 μm) from the Kaunas Lagoon during cyanobacteria bloom in September–October 2019, 2020, and 2022. The collected biomass was frozen and stored at −20 °C in a freezer. In addition, phytoplankton samples were taken from the surface water layer (0.10–0.30 m) for microscopic analyses using a Ruttner water sampler to examine the bloom-forming species. Samples were preserved with 4% (*v*/*v*) formaldehyde solution. Microscopic analysis revealed that species of the genus *Aphanizomenon*, especially *A. flos-aquae*, dominated in the year 2019 (constituting up to 99% of the total phytoplankton biomass), while species of the genus *Microcystis* prevailed in the years 2020 and 2022 (up to 98%).

4.2. C-PC Extraction and Purification

Phycocyanin extraction and purification were conducted using wild cyanobacterial biomass following the method described by Khazi et al. (2018), with some modifications [46].

C-PC was extracted using one freeze-thaw cycle (freezing at −20 °C and thawing at 20 ± 2 °C). The supernatant for purity was collected after centrifugation at 8000× *g* for 10 min and precipitated with a 50% saturated ammonium sulfate solution overnight at +4 °C. The ammonium sulfate-precipitated solution was centrifuged at 10,000× *g* for 10 min and the precipitate was resuspended with 10 mM Na-phosphate buffer (pH 7.0). Desalting was performed via diafiltration using a membrane with a pore size of 10 kDa. Gel filtration chromatography on a Sephadex G-25 column was used to purify C-PC from biomass with dominant *Microcystis* spp. The column was pre-equilibrated and eluted with 10 mM Na-phosphate buffer (pH 7.0), with the flow rate set at 0.5 mL/min. Purification of C-PC from the biomass with dominant *A. flos-aquae* was carried out through ion exchange chromatography on a Q-Sepharose XL column. After pre-equilibration of the column with 10 mM Na-phosphate buffer (pH 7.0), elution was performed using a linear gradient with 0.5 M NaCl and the same buffer at a flow rate of 0.5 mL/min. The purified C-PC extract was freeze-dried after desalting.

4.3. Materials: C-PC Partially Purified from S. platensis

C-PC partially purified from *S. platensis* was purchased from Sigma-Aldrich (St. Louis, MO, USA).

4.4. Purity Assessment of Phycocyanin

The purity of C-PC was determined spectrophotometrically, according to the following formula (Bennett, Bogodar, 1973) [47]:

$$\text{C-PC purity} = \text{OD620/OD280}, \quad (1)$$

where OD280 indicates the absorbance of total proteins and OD620 indicates the absorbance of phycocyanin. The experiment was repeated three times.

4.5. C-PC Sample Collection

Heavy metals were determined in four lyophilized phycocyanin samples, summarized in Table 2. The first sample (S1) of C-PC was isolated from cyanobacterial biomass collected in the Kaunas Lagoon (Lithuania) in 2019. *A. flos-aquae* was dominated in this biomass. Ion exchange chromatography was used to purify C-PC. The second (S2) and the third (S3)

samples were isolated from cyanobacterial biomass collected in the Kaunas Lagoon in the years 2020 and 2022, respectively. The genus of *Microcystis* dominated these biomasses. Gel filtration chromatography was used for the purification of C-PC. The fourth sample (S4) was C-PC isolated from cultivated *S. platensis* (Sigma-Aldrich). This sample was taken as a reference for C-PC isolated from naturally collected cyanobacterial biomass.

Table 2. C-PC samples for heavy metal determination.

Sample Code	Substance	Source	Purification Method	Year
S1	C-PC, lyophilized powder	Cyanobacterial biomass, Kaunas Lagoon, Lithuania (*A. flos-aquae*)	Ion exchange chromatography	2019
S2	C-PC, lyophilized powder	Cyanobacterial biomass, Kaunas Lagoon, Lithuania (*Microcystis* spp.)	Gel filtration chromatography	2020
S3	C-PC, lyophilized powder	Cyanobacterial biomass, Kaunas Lagoon, Lithuania (*Microcystis* spp.)	Gel filtration chromatography	2022
S4	C-PC, lyophilized powder	Cultivated *S. platensis*, (Sigma-Aldrich)	Unknown	Unknown

4.6. Inductively Coupled Plasma-Mass Spectrometry

The concentrations of the heavy metals—lead (Pb), cadmium (Cd), arsenic (As), chromium (Cr), and mercury (Hg)—were analyzed using an inductively coupled plasma mass spectrometer NexION™ 300 D (PerkinElmer, Shelton, CT, USA) equipped with nickel cones and a quartz cyclonic spray chamber as a sample introduction system and using the standard mode (STD). The optimized instrument conditions and measurement parameters are listed in Table 3.

Table 3. Instrumental operating conditions of the ICP-MS system.

ICP-MS Parameter	Operation Conditions
Spray chamber	Quartz cyclonic
Sample introduction	MEINHARD® nebulizer
RF [1] power	1300 W
Plasma Ar [2] flow	18 L/min
Nebulizer Ar flow	1.02 L/min
Auxiliary Ar low	1.20 L/min
Mode	STD
Helium flow for KED [3]	5.3 mL/min
Dwell time	50 ms
Replicates	3

[1] Radio frequency, [2] argon gas, and [3] kinetic energy discrimination.

The calibration solutions for ICP-MS analysis were prepared using the Pure Plus 10 mg/L Multi-Element calibration standard 3 (PerkinElmer, Shelton, CT, USA) and the 10 mg/L Hg (PerkinElmer, Shelton, CT, USA) calibration standard. Germanium (Ge) was added as an internal standard to the samples.

Calibration graphs for the determinations of lead, cadmium, arsenic, and mercury in samples using ICP-MS were prepared in the concentration range from 0 to 2 μg/L. Correlation coefficients for lead, cadmium, arsenic, and mercury were 0.9999, 0.9999, 0.9999, and 0.9986, respectively. Data of the limits of detection (LOD) and limits of quantification (LOQ) for these four trace elements are presented in Table 4.

Table 4. Data of the limits of detection (LOD) and limits of quantification (LOQ) for lead, cadmium, arsenic, and mercury.

Heavy Metal	LOD (µg/L)	LOQ (µg/L)
Pb	0.002	0.008
Cd	0.002	0.006
As	0.001	0.004
Hg	0.005	0.016

To determine trace elements—Pb, Cd, As, Cr, and Hg—a closed quartz vessel and the microwave oven Multiwave 3000 (Anton Paar GmbH, Graz, Austria) digestion procedure were employed. A 100 mg of C-PC sample was accurately weighed into quartz digestion vessels and 1 mL of 65% HNO_3, and 1 mL of H_2O_2 were added to the digestion vessels and digested through following the microwave program: 60 bar pressure, 200 °C temperature, and 800 W microwave power. The digests were transferred into pre-cleaned polyethylene containers and diluted with ultra-purified water. Heavy metal concentrations were expressed as micrograms per gram of C-PC on a dry weight basis. The experiment was repeated four times.

4.7. Statistical Analysis

These data were statistically calculated and analyzed using SPSS V29.0. Metal concentrations and purity coefficients of the C-PC samples were expressed as means. The one-way ANOVA and Bonferroni test (with equal variances assumed) was employed to determine the statistical significance ($p < 0.05$) of concentrations of the individual elements among the C-PC samples and purity coefficients of the C-PC samples, while Dunnett's T3 test (with equal variances not assumed) was employed to determine the statistical significances ($p < 0.05$) of different metal concentrations in the same C-PC sample.

5. Conclusions

ICP-MS analysis of heavy metals revealed higher levels of the most investigated heavy metals in C-PC isolated from the biomass with the dominant *Microcystis* spp. compared to C-PC isolated from the biomass with the predominant *A. flos-aquae*. Additionally, C-PC isolated from cultivated *S. platensis* exhibited lower concentrations of As and Pb compared to C-PC isolated from naturally collected cyanobacterial biomass. However, it had significant concentrations of Cd and Hg. These results could have been influenced by several factors, such as the dominant algal species, which, due to their structural features, have different capacities to attract heavy metals, as well as the purification method and the purity grade of C-PC.

Author Contributions: Conceptualization, N.S. and D.G.; methodology, D.B., R.N., J.K., D.M., J.Š., I.K. and A.S.; software, D.G.; validation, N.S., D.G. and R.N.; formal analysis, D.G.; investigation, D.B., D.G. and N.S.; resources, J.K., D.M. and R.N.; data curation, D.G.; writing—original draft preparation, D.G.; writing—review and editing, G.B.-M. and N.S.; visualization, D.G. and G.B.-M.; supervision, N.S.; project administration, N.S.; funding acquisition, N.S. and A.S. All authors have read and agreed to the published version of the manuscript.

Funding: This research received no external funding.

Data Availability Statement: The data supporting the findings of this study are available from the corresponding author [D.G.] upon reasonable request.

Conflicts of Interest: The authors declare that there are no conflicts of interest regarding the publication of the present article.

References

1. Chen, L.; Giesy, J.; Adamovsky, O.; Svirčev, Z.; Meriluoto, J.; Codd, G.A.; Mijovik, B.; Shi, T.; Xun, T.; Li, S.C.; et al. Challenges of using blooms of *Microcystis* spp. in animal feeds: A comprehensive review of nutritional, toxicological and microbial health evaluation. *Sci. Total Environ.* **2021**, *764*, 142319.
2. Wright, L.P.; Zhang, L.; Cheng, I.; Aherne, J.; Wentworth, G.R. Impacts and Effects Indicators of Atmospheric Deposition of Major Pollutants to Various Ecosystems—A Review. *Aerosol Air Qual. Res.* **2018**, *18*, 1953–1992. [CrossRef]
3. Chi, Z.; Hong, B.; Tan, S.; Wu, Y.; Li, H.; Lu, C.H.; Li, W. Impact Assessment of heavy metal cations to the characteristics of photosynthetic phycocyanin. *J. Hazard. Mater.* **2020**, *391*, 122225. [CrossRef] [PubMed]
4. Rahman, Z.; Singh, V.P. The relative impact of toxic heavy metals (THMs) (arsenic (As), cadmium (Cd), chromium (Cr)(VI), mercury (Hg), and lead (Pb)) on the total environment: An overview. *Environ. Monit. Assess.* **2019**, *191*, 419. [PubMed]
5. Shanab, S.; Essa, A.; Shalaby, E. Bioremoval capacity of three heavy metals by some microalgae species (Egyptian Isolates). *Plant Signal. Behav.* **2012**, *7*, 392–399. [CrossRef] [PubMed]
6. Mehta, S.K.; Gaur, J.P. Use of Algae for Removing Heavy Metal Ions from Wastewater: Progress and Prospects. *Crit. Rev. Biotechnol.* **2005**, *25*, 113–152. [PubMed]
7. Xia, W.; Chen, L.; Deng, X.; Liang, G.; Giesy, J.P.; Rao, Q.; Wen, Z.; Wu, Y.; Chen, J.; Xie, P. Spatial and interspecies differences in concentrations of eight trace elements in wild freshwater fishes at different trophic levels from middle and eastern China. *Sci. Total Environ.* **2019**, *672*, 883–892. [CrossRef]
8. Raulinaitis, M.; Ignatavičius, G.; Sinkevičius, S.; Oškinis, V. Assessment of heavy metal contamination and spatial distribution in surface and surface sedimental layers in the northern part of Lake Babrukas. *Ekologija* **2012**, *58*, 33–43. [CrossRef]
9. Tchounwou, P.B.; Yedjou, C.G.; Patlolla, A.K.; Sutton, D.J. Heavy Metal Toxicity and the Environment. Environmental Toxicology. In *Molecular, Clinical and Environmental Toxicology*, 1st ed.; Lunch, A., Ed.; Springer: New York, NY, USA, 2012; Volume 3, pp. 133–164.
10. Yadav, S.; Prajapati, R.; Atri, N. UV-B-Heavy Metal Interaction: Comparative Evaluation on Photosynthetic Properties of Three Cyanobacteria. *Curr. Microbiol.* **2016**, *73*, 739–746. [CrossRef]
11. Jia, Y.; Chen, W.; Zuo, Y.; Lin, L.; Song, L. Heavy metal migration and risk transference associated with cyanobacterial blooms in eutrofic freshwater. *Sci. Total Environ.* **2018**, *613–614*, 1324–1330. [CrossRef]
12. Bellamy-Carter, J.; Sound, J.K.; Leney, A.C. Probing heavy metal binding to phycobiliproteins. *FEBS J.* **2022**, *289*, 4646–4656. [CrossRef]
13. Minkova, K.M.; Tchernov, A.A.; Tchorbadjieva, M.I.; Fournadjieva, S.T.; Antova, R.E.; Busheva, M.C. Purification of C-phycocyanin from *Spirulina (Arthrospira) fusiformis*. *J. Biotechnol.* **2003**, *102*, 55–59. [CrossRef] [PubMed]
14. Kauno Marios Regional Park. Available online: https://kaunomarios.lt/gamta,p2#Hidrologija (accessed on 15 April 2023).
15. The Environmental Protection Agency. Available online: https://aaa.lrv.lt/lt/veiklos-sritys/vanduo/upes-ezerai-ir-tvenkiniai/upiu-ezeru-ir-tvenkiniu-bukle/upiu-ezeru-ir-tvenkiniu-chemine-bukle (accessed on 17 April 2023).
16. Apibendrinta Lietuvos Aplinkos Būklės ir Jos Pokyčių Ataskaita 2022, Aplinkos Apsaugos Agentūra. Available online: https://aaa.lrv.lt/uploads/aaa/documents/files/leidinys%20ataskaita_SPAUDA11(1).pdf (accessed on 19 April 2023).
17. Rossen, B.P. Biochemistry of arsenic detoxification. *FEBS Lett.* **2002**, *529*, 86–92. [CrossRef] [PubMed]
18. Mathema, V.B.; Thakuri, B.C.; Sillanpää, M. Bacterial mer operon-mediated detoxification of mercurial compounds: A short review. *Arch. Microbiol.* **2011**, *193*, 837–844. [CrossRef]
19. Cires, S.; Ballot, A. A review of the phylogeny, ecology, and toxin production of bloom- forming *Aphanizomenon* spp. and related species within the *Nostocales* (cyanobacteria). *Harmful Algae* **2016**, *54*, 21–43. [PubMed]
20. Chen, J.Z.; Tao, X.C.; Xu, J.; Zhang, T.; Liu, Z.L. Biosorption of lead, cadmium, and mercury by immobilized *Microcystis aeruginosa* in a column. *Process Biochem.* **2005**, *40*, 3675–3679. [CrossRef]
21. Sun, R.; Mo, Y.; Feng, X.; Zhang, L.; Jin, L.; Li, Q. Effects of typical species (*Aphanizomenon fosaquae* and *Microcystis aeruginosa*) on photoreduction of Hg^{2+} in water body. *J. Environ. Sci.* **2019**, *85*, 9–16. [CrossRef]
22. Al-Dhabi, N.A. Heavy metal analysis in commercial *Spirulina* products for human consumption. *Saudi J. Biol. Sci.* **2013**, *20*, 383–388. [CrossRef] [PubMed]
23. Gelagutashvili, E. Interaction of Heavy Metal Ions with C-Phycocyanin: Binding Isotherms and Cooperative Effects. Available online: https://arxiv.org/abs/0707.3019 (accessed on 10 March 2023).
24. Park, W.S.; Kim, H.J.; Li, M.; Lim, D.H.; Kim, J.; Kwak, S.S.; Kang, C.M.; Ferruzzi, M.G.; Ahn, M.J. Two Classes of Pigments, Carotenoids and C-Phycocyanin, in *Spirulina* Powder and Their Antioxidant Activities. *Molecules* **2018**, *23*, 2065. [CrossRef]
25. Glazer, A.N. Phycobilisome: A macromolecular complex optimized for light energy transfer. *Biochim. Biophys. Acta* **1984**, *768*, 29–51. [CrossRef]
26. Silva, E.F.; Figueira, F.S.; Lettnin, A.P.; Carrett-Dias, M.; Filgueira, D.M.V.B.; Kalil, S.; Trindade, G.S.; Votto, A.P.S. C-Phycocyanin: Cellular targets, mechanisms of action and multi drug resistance in cancer. *Pharmacol. Rep.* **2017**, *70*, 75–80. [CrossRef]
27. Tan, S.; Tan, X.; Chi, Z.; Zhang, D.; Li, W. In vitro assessment of the toxicity of lead (Pb^{2+}) to phycocyanin. *Chemosphere* **2018**, *192*, 171–177. [CrossRef]
28. Chi, Z.; Tan, S.; Tan, X.; Zhong, L.; Li, W. The toxicity of cadmium ion (Cd^{2+}) to phycocyanin: An in vitro spectroscopic study. *Environ. Sci. Pollut. Res.* **2018**, *25*, 14544–14550. [CrossRef] [PubMed]

29. Ashaolu, T.J.; Samborska, K.; Lee, C.C.; Tomas, M.; Capanoglu, E.; Tarhan, O.; Taze, B.; Jafari, S.M. Phycocyanin, a super functional ingredient from algae; properties, purification characterization, and applications. *Int. J. Biol. Macromol.* **2021**, *193*, 2320–2331.
30. Patel, A.; Mishra, S.; Pawar, R.; Ghosh, P.K. Purification, and characterization of C-PC from cyanobacteria species of marine and freshwater habitat. *Protein Expr. Purif.* **2005**, *40*, 248–255. [CrossRef]
31. Jungbauer, A.; Hahn, R. Ion-Exchange Chromatography. In *Methods in Enzymology*, 1st ed.; Jungbauer, A., Hahn, R., Eds.; Elsevier: Amsterdam, The Netherlands, 2009; Volume 463, pp. 349–371.
32. Moraes, C.C.; Kalil, S.J. Strategy for a protein purification design using C-phycocyanin extract. *Bioresour. Technol.* **2009**, *100*, 5312–5317. [CrossRef]
33. Silveira, S.T.; Quines, L.K.M.; Burkert, C.A.V.; Kalil, S.J. Separation of phycocyanin from *Spirulina platensis* using ion exchange chromatography. *Bioprocess Biosyst. Eng.* **2008**, *31*, 477–482. [CrossRef]
34. Patil, G.; Chethana, S.; Sridevi, A.S.; Raghavarao, K.S.M.S. Method to obtain C-phycocyanin of high purity. *J. Chromatogr. A* **2006**, *1127*, 76–81. [CrossRef]
35. Pierre, G.; Delattre, C.; Dubessay, P.; Jubeau, S.; Vialleix, C.; Cadoret, J.P.; Probert, I.; Michaud, P. What is in Store for EPS Microalgae in the Next Decade? *Molecules* **2019**, *24*, 4296. [CrossRef] [PubMed]
36. Adjali, A.; Clarot, I.; Chen, Z.; Marchioni, E.; Boudier, A. Physicochemical degradation of phycocyanin and means to improve its stability: A short review. *J. Pharm. Anal.* **2022**, *12*, 406–414. [PubMed]
37. Yu, P.; Wu, Y.; Wang, G.; Jia, T.; Zhang, Y. Purification and bioactivities of phycocyanin. *Crit. Rev. Food Sci. Nutr.* **2017**, *57*, 3840–3849. [PubMed]
38. Council Regulation (EEC) No 315/93 of 8 February 1993 Laying Down Community Procedures for Contaminants in Food. Available online: https://eur-lex.europa.eu/legal-content/EN/TXT/?uri=CELEX%3A01993R0315-20090807 (accessed on 25 May 2023).
39. Commission Regulation (EU) 2023/915 of 25 April 2023 on Maximum Levels for Certain Contaminants in Food and Repealing Regulation (EC) No 1881/2006. Available online: https://eur-lex.europa.eu/legal-content/EN/ALL/?uri=celex%3A32006R1881 (accessed on 25 May 2023).
40. Sandgruber, F.; Gielsdorf, A.; Baur, A.C.; Schenz, B.; Müler, S.M.; Schwerdtle, T.; Stangl, G.I.; Griehl, C.; Lorkowski, S.; Dawczynski, C. Variability in Macro- and Micronutrients of 15 Commercially Available Microalgae Powders. *Mar. Drugs* **2021**, *19*, 310. [PubMed]
41. Regulation (EC) No 1223/2009 of the European Parliament and of the Council of 30 November 2009 on Cosmetic Products. Available online: https://eur-lex.europa.eu/legal-content/EN/TXT/?uri=CELEX%3A02009R1223-20221217 (accessed on 25 May 2023).
42. 2013/674/EU: Commission Implementing Decision of 25 November 2013 on Guidelines on Annex I to Regulation (EC) No 1223/2009 of the European Parliament and of the Council on Cosmetic Products. Available online: https://eur-lex.europa.eu/legal-content/EN/TXT/?uri=CELEX%3A32013D0674 (accessed on 25 May 2023).
43. Regulation (EU) 2017/745 of the European Parliament and of the Council of 5 April 2017 on Medical Devices, Amending Directive 2001/83/EC, Regulation (EC) No 178/2002 and Regulation (EC) No 1223/2009 and Repealing Council Directives 90/385/EEC and 93/42/EEC. Available online: https://eur-lex.europa.eu/legal-content/EN/ALL/?uri=CELEX%3A32017R0745 (accessed on 25 May 2023).
44. Regulation (EC) No 1272/2008 of the European Parliament and of the Council of 16 December 2008 on Classification, Labelling and Packaging of Substances and Mixtures, Amending and Repealing Directives 67/548/EEC and 1999/45/EC, and Amending Regulation (EC) No 1907/2006. Available online: https://eur-lex.europa.eu/legal-content/EN/TXT/?uri=CELEX%3A02008R1272-20230420 (accessed on 25 May 2023).
45. ICH Guideline Q3D (R2) on Elemental Impurities. EMA/CHMP/ICH/353369/2013, Committee of Medicinal Products for Human Use. 2 May 2022. Available online: https://www.ema.europa.eu/en/documents/scientific-guideline/international-conference-harmonisation-technical-requirements-registration-pharmaceuticals-human-use_en-16.pdf (accessed on 25 May 2023).
46. Khazi, M.I.; Demirel, Z.; Liaqat, F.; Dalay, M.C. Analytical Grade Purification of Phycocyanin from Cyanobacteria. In *Biofuels from Algae. Methods in Molecular Biology*, 1st ed.; Spilling, K., Ed.; Springer: New York, NY, USA, 1980; pp. 173–179.
47. Bennett, A.; Bogorad, L. Complementary chromatic adaption in a filamentous blue-green alga. *J. Cell Biol.* **1973**, *58*, 419–435. [PubMed]

Paper 3

Title: *In Vitro* Study of Cyano-Phycocyanin Release from Hydrogels and *Ex Vivo* Study of Skin Penetration

Authors: Galinytė, Daiva; Bernatonienė, Jurga; Žilius, Modestas; Rysevaitė-Kyguolienė, Kristina; Savickas, Arūnas; Karosienė, Jūratė; Briedis, Vitalis; Pauža, Dainius Haroldas; Savickienė, Nijolė

Pharmaceuticals, 17, 9 (2024)

pharmaceuticals

MDPI

Article

In Vitro Study of Cyano-Phycocyanin Release from Hydrogels and Ex Vivo Study of Skin Penetration

Daiva Galinytė [1,*], Jurga Bernatoniene [2], Modestas Žilius [3], Kristina Rysevaitė-Kyguolienė [4], Arūnas Savickas [2], Jūratė Karosienė [5], Vitalis Briedis [3], Dainius Haroldas Pauža [4] and Nijolė Savickienė [1]

[1] Department of Pharmacognosy, Faculty of Pharmacy, Academy of Medicine, Lithuanian University of Health Sciences, Sukilėlių av. 13, 50162 Kaunas, Lithuania; nijole.savickiene@lsmu.lt
[2] Department of Drug Technology and Social Pharmacy, Faculty of Pharmacy, Academy of Medicine, Lithuanian University of Health Sciences, Sukilėlių av. 13, 50162 Kaunas, Lithuania; jurga.bernatoniene@lsmu.lt (J.B.); arunas.savickas@lsmu.lt (A.S.)
[3] Department of Clinical Pharmacy, Faculty of Pharmacy, Academy of Medicine, Lithuanian University of Health Sciences, Sukilėlių av. 13, 50162 Kaunas, Lithuania; modestas.zilius@lsmu.lt (M.Ž.); vitalis.briedis@lsmu.lt (V.B.)
[4] Institute of Anatomy, Faculty of Medicine, Academy of Medicine, Lithuanian University of Health Sciences, Mickevičiaus St. 9, 44307 Kaunas, Lithuania; kristina.rysevaite@lsmu.lt (K.R.-K.); dainius.pauza@lsmu.lt (D.H.P.)
[5] Laboratory of Algology and Microbial Ecology, Nature Research Centre, Akademijos St. 2, 08412 Vilnius, Lithuania; jurate.karosiene@gamtc.lt
* Correspondence: daiva.galinyte@stud.lsmu.lt

Abstract: Background: This study explored the most suitable materials for incorporating cyano-phycocyanin (C-PC) into hydrogels, focusing on maintaining the C-PC's long-term structural integrity and stabilityNext, the release of C-PC from the hydrogels and its skin penetration were investigated. Methods: A series of 1% (w/w) C-PC hydrogels was prepared using various gelling agents and preservatives. Spectrophotometric measurements compared the amount of C-PC in the hydrogels to the initially added amount. After selecting the most suitable gelling agent and preservative, two C-PC hydrogels, with and without propylene glycol (PG) (Sigma-Aldrich, St. Louis, MO, USA), were produced for further testing. In vitro release studies utilized modified Franz-type diffusion cells, while ex vivo skin-permeation studies employed Bronaugh-type cells and human skin. Confocal laser scanning microscopy analyzed C-PC accumulation in the skin. Results: The findings demonstrated that sodium alginate (Sigma-Aldrich, St. Louis, MO, USA), hydroxyethyl cellulose (HEC) (Sigma-Aldrich, St. Louis, MO, USA), and Soligel^{TM} (Givaudan, Vernier, Switzerland) are effective biopolymers for formulating hydrogels while maintaining C-PC stability. After 6 h, C-PC release from the hydrogel containing PG was approximately 10% or 728.07 ($\pm$19.35) $\mu g/cm^2$, significantly higher than the nearly 7% or 531.44 ($\pm$26.81) $\mu g/cm^2$ release from the hydrogel without PG ($p < 0.05$). The ex vivo qualitative skin-permeation study indicated that PG enhances C-PC penetration into the outermost skin layer. Conclusion: PG's ability to enhance the release of C-PC from the hydrogel, coupled with its capacity to modify the skin barrier ex vivo, facilitates the penetration of C-PC into the stratum corneum.

Keywords: cyano-phycocyanin; hydrogel; sodium alginate; propylene glycol; in vitro drug release; ex vivo skin penetration

Citation: Galinytė, D.; Bernatoniene, J.; Žilius, M.; Rysevaitė-Kyguolienė, K.; Savickas, A.; Karosienė, J.; Briedis, V.; Pauža, D.H.; Savickienė, N. In Vitro Study of Cyano-Phycocyanin Release from Hydrogels and Ex Vivo Study of Skin Penetration. *Pharmaceuticals* **2024**, *17*, 1224. https://doi.org/10.3390/ph17091224

Academic Editors: Katalin Kristó and Tamás Sovány

Received: 20 August 2024
Revised: 2 September 2024
Accepted: 11 September 2024
Published: 17 September 2024

1. Introduction

C-PC is a supramolecular protein–chromophore complex present in all cyanobacterial species [1,2]. Recent studies have increasingly highlighted C-PC's potential for treating various skin conditions due to its ability to promote tissue regeneration, enhance wound healing, and exhibit antioxidant, antimicrobial, and anti-inflammatory properties [3]. For instance, in vivo wound-healing research confirmed that incorporating C-PC into hydrogels

enhances the antioxidant capacity, reduces the levels of inflammatory markers (IL-6, IL-1β, TNF-α), and accelerates the wound-healing process [4]. Additionally, C-PC demonstrated significant anti-photoaging effects in UVB-induced mouse skin by preventing collagen-fiber degradation, enhancing antioxidant enzyme activity, and reducing inflammatory factor expression [5]. Subcutaneous injections of C-PC in melanoma-induced mice increased the absolute number of T lymphocytes and myeloid cells, showing a positive immunomodulatory effect and reducing tumor tissue [6]. Both in vitro and in vivo studies suggested that C-PC can increase the activation of pro-apoptotic genes and suppress anti-apoptotic genes, indicating its potential as a treatment for skin cancer [3].

C-PC applications are dependent upon its purity, measured by the absorbance ratio A620/A280, where A620 is the absorbance of C-PC at 620 nm, and A280 is the absorbance of other proteins at 280 nm [7]. C-PC with a purity greater than 0.7 is suitable for food, greater than 1.5 for cosmetics, and greater than 4.0 for therapeutic treatments [8]. However, the unique structure of C-PC presents challenges to developing effective topical formulations, as various factors, such as temperature, pH, and excipients, can affect its stability during manufacturing [9,10]. The C-PC consists of a heterodimeric monomer composed of α and β subunits, where each α subunit is bound to one bilin chromophore and each β subunit is associated with two bilin chromophores. These monomers formed a ring-shaped trimer $(\alpha\beta)_3$, which further assembles into hexameric structures $[(\alpha\beta)_3]_2$ [11,12]. Phycocyanobilins are responsible for C-PC's distinctive blue color. In vitro, C-PC solutions usually contain various oligomeric states, such as trimers, hexamers, and occasionally, monomers, with molecular weights ranging from approximately 44 to 260 kDa [1,13]. Compounds that interact with the tetrapyrrole structure, such as oxygen, free radicals, and acids, can accelerate C-PC degradation. Alterations in the chromophore's structure can fade color and reduce therapeutic activity. [12]. Therefore, the preservation of C-PC's structural stability is essential when developing topical applications with this promising natural material.

Hydrogels, which are three-dimensional polymeric materials with high water content, are an excellent medium for incorporating hydrophilic substances like C-PC [14,15]. Suitable gelling agents that do not compromise C-PC stability are critical in these formulations. Synthetic polymers such as crosslinked polyacrylic acid, commercially available as Carbopol® (The Lubrizol Corporation, Wickliffe, OH, USA) and Pemulen™ (The Lubrizol Corporation, Wickliffe, OH, USA) are commonly used due to their properties, including viscosity, transparency, and bioadhesion [16–19]. Poloxamer 407 (Sigma-Aldrich, St. Louis, MO, USA), a copolymer of ethylene oxide and propylene oxide, can also be used to create thermosensitive hydrogels that are suitable for localized therapy and enhanced drug permeation. [20–22]. Biopolymers, like sodium alginate, cellulose, and chitosan, are valued for their biocompatibility, biodegradability, and environmental sustainability [23]. Sodium alginate, obtained from brown seaweeds or microbial fermentation, is composed of β-d-mannuronic acid and α-l-guluronic acid units [24]. Its characteristics, including rapid gelation, outstanding biocompatibility, and low cost, vary depending on the algal species from which it is derived. [23,25–27]. Cellulose is a natural polymer composed of glucose monomers, forming the fundamental structural component in plant cell walls, and is found in fibers like flax and cotton. It can also be of bacterial origin (e.g., Acetobacter xylinum). Water-soluble cellulose derivatives are typically produced by etherifying cellulose, reacting its hydroxyl groups with organic compounds such as methyl and ethyl groups [28]. Chitosan, a biopolymer obtained from the skeletal structures of crustaceans, insect cuticles, and fungal cell walls, is composed of copolymers of glucosamine and N-acetylglucosamine. Chitosan enhances epithelialization and exhibits both wound healing and antimicrobial properties [15,23,29]. However, its application is limited by its low solubility in neutral and basic pH conditions, so it is frequently employed in the form of hydrogels prepared by dissolving chitosan in an acidic solution [29,30]. Soligel™, a biopolymer produced biotechnologically using Rhizobium sp., is a branched polysaccharide consisting of a sequence of monomer units that includes six neutral sugars (three

glucose and three galactose molecules) in the pyranose form, along with one glucuronic acid and a pyruvyl substituent [31].

After applying the hydrogel to the skin, the drug must first be released from its vehicle and then partitioned into the outermost layer of the skin, the stratum corneum, which serves as the primary rate-limiting step for its delivery. For pharmaceuticals, the skin presents both a challenge as a barrier and an opportunity due to its large surface area for drug delivery [32,33]. For passive absorption and permeation through the stratum corneum, the substance must possess specific physicochemical characteristics, such as a molecular weight of less than 500 kDa, moderate lipophilicity, and suitable solubility in both lipids and water [34]. Thus, another challenge for topical formulations with C-PC is high molecular weight and hydrophilicity. Enhancing the skin permeation of drugs is a crucial focus in pharmaceutical research [35,36]. PG, a chemical penetration enhancer commonly used in topical formulations, can overcome these barrier properties and facilitate drug transport across the skin by disrupting the diffusional pathways within the skin, thereby increasing drug permeability [37,38] However, there have been no studies on the ability of PG to promote the skin penetration of C-PC.

In pursuit of a versatile biomaterial platform, this investigation explored the most suitable material compositions for fabricating a hydrogel that could integrate C-PC, with a steadfast emphasis on ensuring its structural integrity and stability. Additionally, the research sought to evaluate the release of C-PC from the formulated hydrogel and assess the extent of C-PC penetration into the skin.

2. Results

2.1. Selection of Gelling Agent

In this study, C-PC was isolated from cyanobacterial biomass collected from the Kaunas Lagoon (Kaunas, Lithuania), with a purity of 1.5 (0.006). To identify the most suitable gelling agent, the research team prepared a series of 1% (*w*/*w*) C-PC hydrogels using a variety of polymeric materials as the primary structural components. The gelling agents and their concentrations were selected for this study based on information from the literature sources and technical data sheets provided by the manufacturers. The study focused on three synthetic polymers at the following concentrations: Carbopol® Ultrez 21 (Lubrizol Corporation, Wickliffe, OH, USA)- 0.8% (*w*/*w*) [18,29], Pemulen™ (Lubrizol Corporation, Wickliffe, OH, USA)—0.5% (*w*/*w*) [19], and Poloxamer 407 (Sigma-Aldrich, St. Louis, MO, USA)—15% (*w*/*w*) [22]. Additionally, seven biopolymers were studied, including sodium alginate (Sigma-Aldrich, St. Louis, MO, USA)—3.5% (*w*/*w*) [39,40], hydroxyethyl cellulose (HEC) (Sigma-Aldrich, St. Louis, MO, USA)—5.5% (*w*/*w*) [41], sodium carboxymethyl cellulose (NaCMC) (Sigma-Aldrich, St. Louis, MO, USA)—5% (*w*/*w*) [42], hydroxy-propyl methylcellulose (HPMC) (Sigma-Aldrich, St. Louis, MO, USA)—15% (*w*/*w*) [41,43], hydroxyethyl methylcellulose (HEMC) (Sigma-Aldrich, St. Louis, MO, USA)—3% (*w*/*w*) [44], chitosan 80/1000 molecular weight (chitosan) (Sigma-Aldrich, St. Louis, MO, USA)—3% (*w*/*w*) [29], and Soligel™ (Givaudan, Vernier, Switzerland)—1.5% (*w*/*w*) [31]. The stabilities of the C-PC in these hydrogels were evaluated spectrophotometrically by measuring the C-PC content in the prepared hydrogels and comparing it with the initial amount of C-PC added. The hydrogels were stored at +4 °C for 48 h before analysis. As depicted in Figure 1, the results indicated that C-PC remained structurally stable in hydrogels containing sodium alginate, Soligel™, HEC, NaCMC, or HEMC, with no statistically significant decrease in C-PC concentration observed ($p > 0.05$). However, in the formulations with Poloxamer 407 and chitosan, the C-PC content decreased by 12.20% and 12.00%, respectively ($p < 0.05$). The most significant instability was observed in hydrogels with Carbopol® Ultrez 21, where the C-PC content was 71.80% lower than the initial amount ($p < 0.05$), and with Pemulen™, which showed a decrease of 50.30% ($p < 0.05$). A visible fading of the hydrogels' color accompanied the decrease in C-PC concentration.

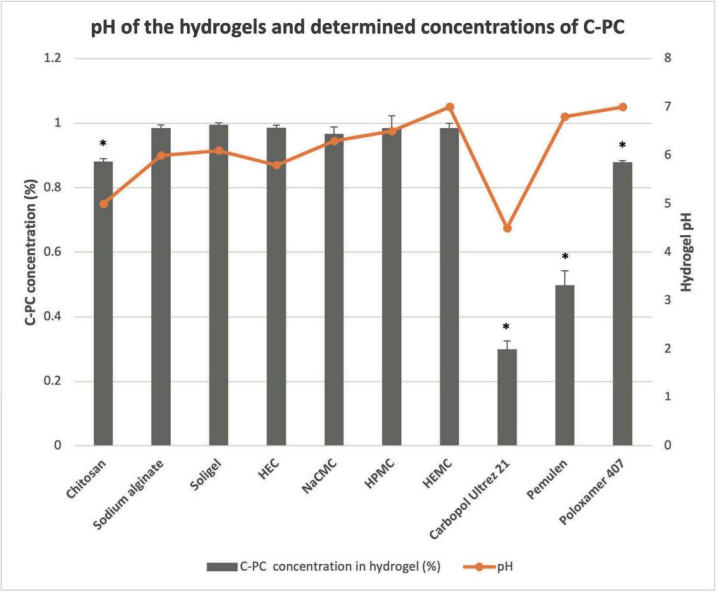

Figure 1. pH of hydrogels and determined concentrations of C-PC in the produced hydrogels with different gelling agents. An asterisk (*) indicates statistically significant differences between the added and determined concentrations of C-PC ($p < 0.05$), evaluated using a paired-sample *t*-test. The means and standard deviations are presented. The experiment was repeated three times.

Based on these findings, six polysaccharide-based biopolymers—sodium alginate, Soligel™, HEC, NaCMC, HPMC, and HEMC—were selected for further research, as no statistically significant changes in C-PC concentration were observed with these gelling agents.

2.2. Selection of Preservative for C-PC Hydrogels

The next phase of the study involved screening to identify the most suitable preservative system for the C-PC-containing hydrogels. Eighteen C-PC hydrogels were prepared using in the biopolymers selected in the previous stage—sodium alginate, Soligel™, HEC, NaCMC, HPMC, and HEMC—and three environmentally friendly preservatives, namely SharoSENSE™ Plus 184 (SHARON Laboratories, Ashdod, Israel) (maltol, didecyldimonium chloride), SharoSENSE™ Plus 785 (SHARON Laboratories, Ashdod, Israel) (maltol, sorbic acid, sodium benzoate), and Sharomix™ 721 (SHARON Laboratories, Ashdod, Israel) (dehydroacetic acid, benzyl alcohol, water). The hydrogels were stored at +4 °C for 48 h before undergoing spectrophotometric analysis. The stability of the C-PC in these hydrogels was assessed by measuring the C-PC content spectrophotometrically and comparing it with the initial amount of C-PC added during the formulation. The changes in C-PC concentrations across the hydrogels containing different preservative systems are illustrated in Figure 2.

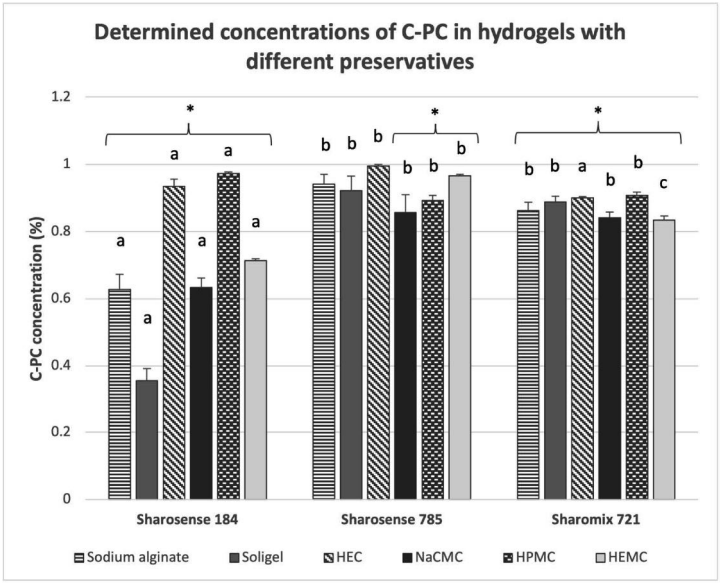

Figure 2. Determined concentrations of C-PCs in hydrogels with different preservatives. Different letters denote statistically significant differences ($p < 0.05$) in the C-PC concentrations among hydrogels containing the same gelling agent but different preservatives, as assessed using Bonferroni's test. An asterisk (*) indicates statistically significant differences ($p < 0.05$) between the initially added and the determined C-PC concentrations, evaluated using a paired-sample *t*-test. The means and standard deviations are presented. The experiment was repeated three times.

When SharoSENSE Plus^{TM} 184 was used with gelling agents, such as sodium alginate, Soligel ^{TM}, HEC, NaCMC, and HEMC, the C-PC concentration was significantly lower ($p < 0.05$) compared to hydrogels containing SharoSENSE^{TM} Plus 785 and Sharomix^{TM} 721. Depending on the gelling agent, the C-PC concentration decreased by 6.60% to 64.40% in combination with SharoSENSE Plus^{TM} 184, with visual color changes observed in the hydrogels. In contrast, the combination of SharoSENSE Plus^{TM} 184 with HPMC resulted in a higher C-PC concentration than the other hydrogels containing HPMC but different preservative systems ($p < 0.05$). Hydrogels containing SharoSENSE^{TM} Plus 785 and Sharomix^{TM} 721 showed smaller reductions in their C-PC concentration compared to those with SharoSENSE PlusTM 184. Specifically, Sharomix^{TM} 721 resulted in a C-PC concentration decrease of 9.30% to 16.60%, while SharoSENSE^{TM} Plus 785 caused a reduction of 0.5% to 14.30%, depending on the specific gelling agent used. The smallest reductions in C-PC concentration were observed with SharoSENSE^{TM} Plus 785 compared to the other preservative systems. A statistically significant difference ($p < 0.05$) in C-PC reduction was found when using SharoSENSE Plus^{TM} 184 and Sharomix^{TM} 721 with all tested gelling agents. However, no statistically significant difference ($p > 0.05$) was observed with SharoSENSE^{TM} Plus 785 in combination with sodium alginate, Soligel^{TM}, or HEC.

Therefore, based on the structural stability of C-PC in hydrogels with different preservatives, the combinations of sodium alginate, Soligel^{TM}, and HEC with SharoSENSE^{TM} Plus 785 were selected for further investigation.

2.3. Microbiological Evaluation of C-PC Hydrogels

Three different C-PC hydrogels were formulated for microbiological analysis using selected gelling agents, namely sodium alginate, Soligel™, and HEC, combined with the preservative SharoSENSE™ Plus 785 (maltol, sorbic acid, and sodium benzoate). The formulations were as follows:

- I C-PC gel: C-PC (1% *w*/*w*), glycerol (Sigma-Aldrich, St. Louis, MO, USA) (5% *w*/*w*), sodium alginate (3.5% *w*/*w*), and Sharosense 785 (0.05% *w*/*w*);
- II C-PC gel: C-PC (1% *w*/*w*), glycerol (5% *w*/*w*), Soligel (1.5% *w*/*w*), and Sharosense 785 (0.05% *w*/*w*);
- III C-PC gel: C-PC (1% *w*/*w*), glycerol (5% *w*/*w*), HEC (5.5% *w*/*w*), and Sharosense 785 (0.05% *w*/*w*).

Glycerol did not significantly impact the stability of C-PC in the hydrogels.

The microbiological evaluation of C-PC hydrogels was performed at the Kaunas Department of the National Public Health Care Laboratory (Kaunas, Lithuania).

The results, presented in Table 1, indicated that the pathogens *Staphylococcus aureus*, *Pseudomonas aeruginosa*, *Candida albicans*, and *Escherichia coli* were not detected in the C-PC hydrogels. The count of aerobic mesophilic bacteria was less than 1.0×10^1 CFU/g. These findings confirm the excellent antimicrobial properties of SharoSENSE™ Plus 785 in all tested C-PC hydrogels.

Table 1. Results of microbiological evaluation of C-PC hydrogels.

Microorganisms	Hydrogel Samples		
	I C-PC Hydrogel	**II C-PC Hydrogel**	**III C-PC Hydrogel**
Candida albicans	Not detected	Not detected	Not detected
Escherichia coli	Not detected	Not detected	Not detected
Pseudomonas aeruginosa	Not detected	Not detected	Not detected
Staphylococcus aureus	Not detected	Not detected	Not detected
Number of aerobic mesophilic bacteria CFU */g	$<1.0 \times 10^1$	$<1.0 \times 10^1$	$<1.0 \times 10^1$

* The number of microorganisms or colony-forming units of a group of microorganisms in a certain unit of volume or mass.

2.4. In Vitro Evaluation of C-PC Release from Experimental Hydrogels

Based on the structural stability of C-PC and the microbiological evaluation of the C-PC hydrogels, the combinations of sodium alginate, Soligel™, and HEC with SharoSENSE™ Plus 785 were identified as suitable formulations for C-PC hydrogels development. Among these, sodium alginate was selected for further investigation as the gelling agent due to its shared origin with C-PC, with both being derived from algae. For the in vitro release study, two semisolid formulations were prepared, with their composition and pH shown in Table 2. The objective of this study was to assess the influence of PG on the release of C-PC from the hydrogel matrix. The C-PC hydrogel without PG served as the control.

The release of C-PC from the PG-containing hydrogel was detected after 30 min and became quantitatively significant at 2 h, with 3.25% (258.304 (36.959) μg/cm^2) of C-PC released. In comparison, the C-PC release from the hydrogel without PG was observed at 30 min but was quantitatively significant only after 3 h, with 3.59% (286.490 (7259) μg/cm^2) of C-PC released (Figure 3). The determination coefficient ($R^2 = 0.9995$) indicates an excellent fit of the linear model to the experimental data, suggesting a nearly perfect linear release of C-PC over time under the tested conditions. The slope values of the equations (120.48 for the PG hydrogel and 89.447 for the hydrogel without PG) represent the rate of C-PC release from the hydrogels per unit of time, with the higher slope in the PH hydrogel indicating a faster release compared to the control. After 6 h, the release data showed a statistically significant difference ($p < 0.05$) between the two formulations. The C-PC gel

with PG released nearly 10% of the C-PC, amounting to 728.07 ± 19.35 μg/cm^2, whereas the hydrogel without PG released approximately 7%, or 531.44 ± 26.81 μg/cm^2.

Table 2. Composition and pH of experimental C-PC hydrogels.

	Excipient	C-PC Hydrogel without PG (C-PC Hydrogel) (%, *w*/*w*)	C-PC Hydrogel with PG (C-PC PG Hydrogel) (%, *w*/*w*)
Composition of Experimental Hydrogels	Purified water	90	75
	Sodium alginate	3.5	3.5
	C-PC	1	1
	Glycerol	5	5
	PG	-	15
	SharoSENSE^{TM} Plus 785	0.5	0.5
Determined pH		5.0 (0.03)	4.8 (0.01)

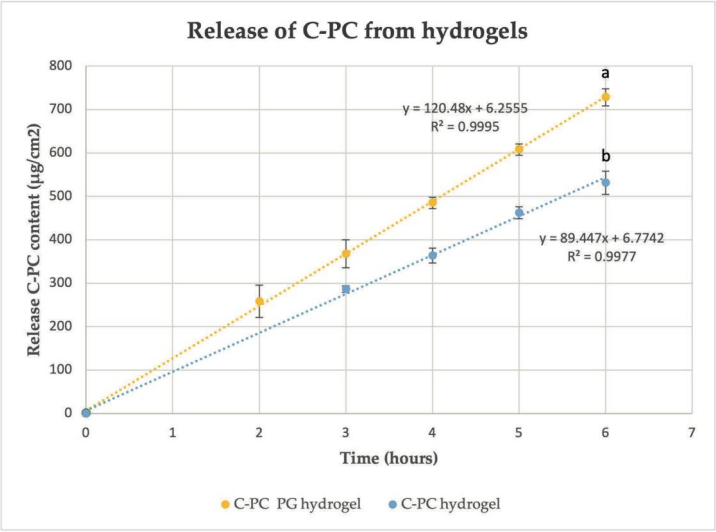

Figure 3. The release of C-PC from hydrogels: C-PC PG hydrogel and C-PC hydrogel without PG (control). Different letters indicate statistically significant differences ($p < 0.05$) determined by independent-samples *t*-test. Means and standard deviations are presented. The experiment was repeated 3 times.

These findings indicate that the presence of PG significantly enhances the release rate of C-PC from the hydrogel, suggesting that the PG-containing formulation may be more suitable for applications requiring a quicker C-PC delivery. Conversely, the hydrogel without PG provides a more controlled, slower release, which could be advantageous for sustained-release applications. Further detailed studies are necessary to elucidate the exact mechanism by which PG facilitates C-PC release.

2.5. Ex Vivo Qualitative Assessment of C-PC Skin Permeation from Experimental Hydrogels

In this pilot study, we qualitatively evaluated the influence of the penetration enhancer PG on the penetration of the high molecular weight hydrophilic protein C-PC into the skin. Two semisolid C-PC formulations, one containing PG and one without, were utilized for this investigation (Table 2).

The results of the ex vivo qualitative skin-penetration study are presented in Figure 4. The skin that was not treated with any hydrogel formulation served as the control (Figure 4, row Control). The fluorescent properties of C-PC were employed for qualitative assessment, with skin autofluorescence being excluded from the analysis (Figure 4, column C-PC channel).

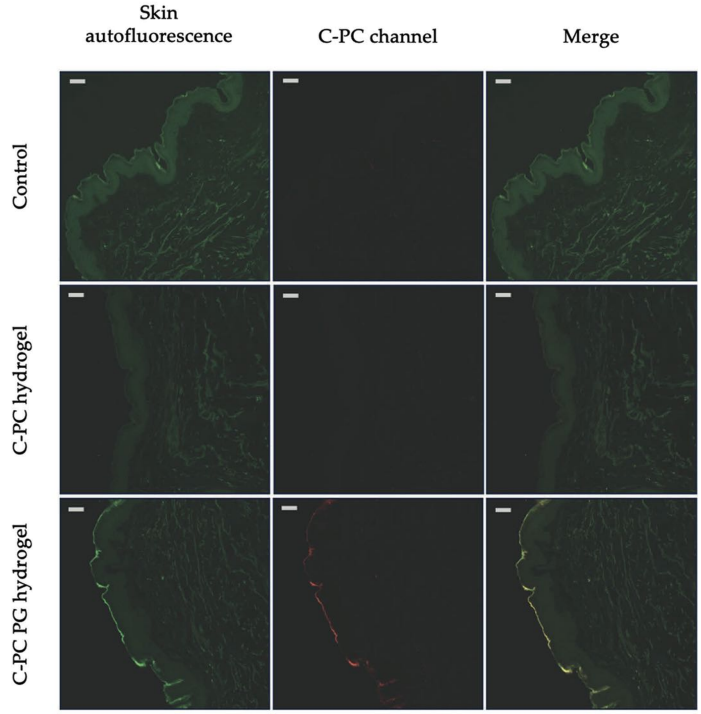

Figure 4. Confocal images of human skin autofluorescence (control) and human skin section after treatment with C-PC hydrogel and C-PC PG hydrogel. Scale bar 50 µm. The experiment was repeated 3 times.

In the C-PC hydrogel row, significant skin autofluorescence is observed (Figure 4, column skin autofluorescence), but no fluorescence is detected in the C-PC channel, indicating that the C-PC did not penetrate the skin. This observation is consistent with the notion that C-PC, due to its high molecular weight and hydrophilic nature, does not penetrate the outermost layer of the skin—the stratum corneum—which is composed predominantly of ceramides, cholesterol, and fatty acids that contribute to its hydrophobic properties [45]. Conversely, the C-PC PG hydrogel formulation exhibited visible fluorescence in the C-PC channel (red color), indicating the presence of C-PC within the stratum corneum.

Thus, the ex vivo skin-penetration study demonstrated that, within 24 h, C-PC was not detected in skin samples treated with the C-PC hydrogel lacking PG. In contrast, the C-PC from the C-PC PG hydrogel was predominantly localized in the stratum corneum, suggesting that the penetration-enhancer PG facilitates the penetration of C-PC into the skin.

3. Discussion

3.1. The Influence of Gelling Agents and Hydrogel Production Technology on the C-PC Stability

In this study, we aimed to identify the most suitable gelling agents for the production of C-PC hydrogel, with a focus on maintaining C-PC stability. Our investigation into C-PC stability within semi-solid formulations revealed that C-PC remained structurally stable in most formulations containing polysaccharide-based biopolymers, including sodium alginate, HEC, NaCMC, HPMC, HEMC, and Soligel™. Studies conducted by other researchers have suggested that the incorporation of polysaccharides can effectively enhance C-PC stability. A common approach to improve protein stability is through glycation, a process wherein covalent cross-links form between the carbonyl groups of reducing sugars and the amino groups of the protein. The reaction can optimize the physicochemical properties of protein–sugar conjugates. For example, the glycation of C-PC has been shown to enhance its functionality. Polysaccharides with negatively charged functional groups, such as carboxyl or sulfate groups, can engage in electrostatic interactions with the positively charged amino acid residues on the surfaces of C-PC proteins, thereby improving the overall stability and functionality of the C-PC molecules [2]. However, a decrease in C-PC concentration was observed in the hydrogel containing chitosan. The heating of the chitosan hydrogel during manufacturing may have affected C-PC stability, despite careful monitoring to ensure the temperature did not exceed 40 °C. Previous research has indicated that C-PC stability significantly declines when the temperature surpasses the critical range of 45–47 °C, with the degradation rates increasing rapidly at higher temperatures [2,46]. These degradation reactions are likely associated with changes in the C-PC's secondary, tertiary, and quaternary structures due to elevated temperatures [12]. Heat treatment has been shown to induce aggregation of C-PC subunits, contributing to its degradation and a noticeable reduction in the intensity of its characteristic blue coloration [2,46]. Additionally, a visible color fade was observed in hydrogels containing Carbopol® Ultrez 21, Pemulen™, and Poloxamer 407. The use of acetic acid in chitosan hydrogels, sodium hydroxide in Carbopol® Ultrez 21 formulations, and triethanolamine in Pemulen™ formulations may contribute to a reduction in C-PC stability. The pH values of the C-PC hydrogels containing chitosan, Poloxamer 407, Carbopol® Ultrez 21, and Pemulen™ were measured at 5.0, 7.0, 4.5, and 6.8, respectively. According to previous studies, C-PC exhibits optimal stability within a pH range of 5.5 to 6.0 [47]. These findings indicate that C-PC is sensitive to variations in both temperature and pH, and it is crucial to carefully monitor and maintain these parameters within optimal limits when producing formulations with C-PC.

3.2. Identifying an Efficient Preservative for C-PC Hydrogels

Preservatives are a diverse group of chemical compounds commonly incorporated into cosmetic and pharmaceutical formulations to prevent microbial contamination and ensure product integrity. Despite their antimicrobial benefits, preservatives in skincare or treatment products can elicit adverse reactions, such as skin irritation or contact dermatitis [48]. The primary objective of this study was to identify an effective preservative system that is clean, safe, non-toxic, possesses a long shelf-life, and does not adversely impact the stability of C-PC. Three environmentally friendly preservatives were evaluated, namely SharoSENSE™ Plus 184 (maltol, didecyldimonium chloride), SharoSENSE™ Plus 785 (maltol, sorbic acid, sodium benzoate), and Sharomix™ 721 (dehydroacetic acid, benzyl alcohol, and water). SharoSENSE™ Plus 785 was selected for further use in preserving C-PC hydrogels due to its minimal impact on C-PC stability.

The chosen preservative system, SharoSENSE™ Plus 785, comprises three active ingredients, namely maltol, sorbic acid, and sodium benzoate. Benzoic acid ($C_7H_6O_2$) is an

aromatic carboxylic acid characterized by a carboxyl group (-COOH) directly attached to a benzene ring. It occurs naturally in various plant species, including fruits, vegetables, and fungi, with its concentration influenced by factors such as plant species, growing conditions, and environmental interactions [49]. Industrially synthesized benzoic acid and its derivates are commonly used as antibacterial and antifungal agents, as well as flavoring agents in food, cosmetics, and pharmaceuticals. While benzoic acid and its salts are generally considered safe within established limits, human exposure may occasionally exceed regulatory standards, and various absorption routes may be involved [50]. The preservative composition also includes sorbic acid, another organic acid with a broad-spectrum antimicrobial activity. Sorbic acid and sodium benzoate operate through similar mechanisms, inhibiting microorganisms by disrupting nutrient uptake, particularly by affecting the proton motive force (PMF) across microbial cell membranes. This disruption impairs the cell's ability to maintain pH balance and transport essential molecules, leading to inhibited growth or cell death. Both sorbate and benzoate are particularly effective at low pH levels, with sorbic acid demonstrating greater efficacy between pH 4.0 and 6.0 compared to sodium benzoate [51]. Maltol, known as 3-hydroxy-2-methyl-4-pyrone, is a naturally occurring compound found in various plant sources, including *Larix deciduas*, *Evodiopanax innovans*, *Cercidiphyllum japonicum*, and *Panax ginseng*. It can also be produced by certain bacteria and molds. Maltol is widely used in the food industry as a flavoring agent due to its sweet aroma and is also used as a food additive and preservative. Although maltol's antimicrobial activity is considered limited, requiring high concentrations (around 4000 ppm) to effectively inhibit microbial growth, it is regarded as non-toxic and generally recognized as safe (GRAS) for use in food and other consumer products [52].

Therefore, the SharoSENSE^{TM} Plus 785 preservative system serves as an effective bridge between natural and synthetic substances. The combination of its components may enhance the antimicrobial spectrum and potentially reduce the quantity of preservatives required, thereby minimizing the risk of adverse reactions in consumers.

3.3. Contextualizing the Microbiological Results of C-PC Hydrogels

To ensure the microbial safety of cosmetics and other topical products, it is essential to identify skin pathogens such as *Staphylococcus aureus*, *Pseudomonas aeruginosa*, and *Candida albicans*, as these can cause skin or eye infections. Additionally, detecting other microorganisms, including fecal contamination indicators like *Escherichia coli*, is crucial for verifying hygienic handling during the manufacturing process and ensuring high-quality production [53]. According to the European Standard EN ISO 17516:2014 [53], cosmetic products must be free from *Staphylococcus aureus*, *Pseudomonas aeruginosa*, and *Candida albicans*. The total count of aerobic mesophilic microorganisms should not exceed 1×10^2 CFU per gram or milliliter for products intended for children under three years of age, for use around the eyes, or for application to mucous membranes, and should not exceed 1×10^3 CFU per gram or milliliter for other cosmetic products [53].

3.4. Analysis and Implications of C-PC Release Profiles in Experimental Hydrogels

Topical formulations face additional challenges, with the critical factor being the release of the active substances before their penetration through the stratum corneum to exert a local or systemic effect [54]. In vitro studies involving the release of active substances through semipermeable synthetic membranes are conducted to evaluate the release process from semisolid formulations. The release of a drug before it penetrates the skin is a crucial consideration. Studies indicate that utilizing solvents to enhance drug release from the delivery system can significantly boost the drug's skin-penetration capabilities, primarily due to the establishment of a higher concentration gradient [54]. Our in vitro C-PC-release study revealed that PG significantly promoted the faster release of C-PC from the hydrogel ($p < 0.05$). Several studies by other authors have also demonstrated the ability of PG to increase drug release from the formulation. Yang D. and other studies showed that PG significantly enhanced the release percent of Loxoprofen from polymer matrices consisting

of an acrylic pressure-sensitive adhesive (PSA) containing a carboxyl group [55]. Wang Z. and others revealed that PG significantly increased the release of licochalcone A (a flavonoid compound extracted from the roots of *Glycyrrhiza glabra* L.) from a Carbomer 940 hydrogel by occupying the licochalcone A and Carbomer 940 binding site [56]. Thus, PG plays a crucial role in enhancing the release of active ingredients, such as C-PC, in in vitro experiments through several mechanisms. First, PG functions as a co-solvent, improving the solubility of both hydrophilic and lipophilic compounds within the hydrogel matrix. This increased solubility is critical because it can enhance the thermodynamic activity of the active ingredient, thereby driving its diffusion from the hydrogel into the surrounding medium [57]. In the specific context of this study, the inclusion of PG in the sodium alginate hydrogel formulation resulted in a statistically significant acceleration of C-PC release compared to the hydrogel without PG. This can be explained by PG's ability to disrupt intermolecular interactions within the hydrogel matrix. Sodium alginate, a polysaccharide, forms a gel network that can effectively trap active ingredients like C-PC. However, PG is capable of weakening these interactions—possibly by interfering with hydrogen bonding or by occupying the binding sites between the C-PC molecules and the alginate chains. This disruption reduces the energy barrier for the diffusion of C-PC molecules, facilitating their release from the hydrogel [58]. Furthermore, PG may also influence the structural dynamics of the hydrogel matrix itself. It can cause partial swelling or plasticization of the polymer network, which increases the pore size within the gel, thereby creating additional pathways for the diffusion of the active ingredient [58]. The observed increase in the rate of C-PC release in the presence of PG aligns with previous findings in pharmaceutical research, where PG has been shown to enhance the release profiles of various drugs from polymeric carriers by modifying both the drug–polymer interactions and the physical structure of the carrier [58]. Moreover, sodium alginate is a gelling agent with a controlled release function [27]. The study on the release of C-PC from polylactic acid/phycocyanin–alginate composite cosmetic patches showed that the release of C-PC also depends on the ratio of C-PC to alginate. As this ratio decreases, the ability to release C-PC also decreases [59]. In our study, the concentration of C-PC in the gel was only 1%, so it is likely that, by increasing the concentration of C-PC and the ratio of C-PC to alginate, it would be possible to achieve a higher percentage of released C-PC.

Thus, the multifaceted action of PG not only promotes faster release but also contributes to a more consistent and predictable release profile, which is essential for achieving the desired therapeutic outcomes in topical drug delivery systems. Overall, the inclusion of PG in the hydrogel formulation is a key factor that modulates the release kinetics of C-PC, making it a critical component in the design of effective topical formulations.

3.5. Insights into Ex Vivo C-PC Skin Permeation from Experimental Hydrogels

Cosmetic or pharmaceutical products applied topically face significant challenges in delivering active components into the deeper layers of the skin, as the stratum corneum, the outermost layer, serves as a highly effective barrier against the permeation of most compounds [60]. Our ex vivo qualitative skin-penetration study confirmed that high molecular weight and hydrophilic molecules, such as C-PC, have limited penetration ability into the stratum corneum. However, the presence of PG enhanced the penetration of C-PC into this outer layer. The correlation between the in vitro release of C-PC facilitated by PG and its subsequent ex vivo permeation through the stratum corneum warrants careful consideration. PG is well-established as a penetration enhancer, primarily due to its ability to modify both the physicochemical properties of the drug and the skin barrier, thereby contributing to improved permeation [35,54]. To fully understand whether the ex vivo permeation observed is directly related to the effective drug release seen in vitro, it is essential to explore the mechanisms by which PG operates in both contexts. In vitro, PG enhances the release of C-PC by disrupting the hydrogel matrix, as discussed earlier. This increased release rate results in a higher concentration of C-PC available at the skin surface, which is a critical factor for initiating permeation through the stratum corneum.

The elevated concentration gradient established by the more efficient release of C-PC is likely a significant driver for its enhanced ex vivo permeation [37]. However, the ex vivo environment introduces additional complexities that influence drug permeation. The stratum corneum serves as the primary barrier to drug penetration, and PG facilitates permeation by interacting with the lipid matrix within this layer. PG's ability to fluidize lipids in the stratum corneum and increase its permeability is a key mechanism that must be considered. This interaction not only facilitates the entry of C-PC into the skin but also enhances its retention within the stratum corneum, as observed in ex vivo studies [35,37,54]. A study by Kis N. et al. demonstrated that PG increases lipid mobility within the stratum corneum, although the majority of the lipids remain in a solid phase even after treatment. PG significantly enhanced the mobility of amino acids in both keratin filaments and the natural moisturizing factor (NMF) free amino acids, acting similarly to NMF by replacing water in the stratum corneum [61]. In summary, the effective in vitro release of C-PC facilitated by PG is a critical precursor to its ex vivo permeation. The concentration of C-PC at the skin surface, modulated by PG in vitro, is pivotal for its subsequent diffusion into and through the stratum corneum. Without effective release, the availability of C-PC for permeation would be significantly reduced, leading to suboptimal therapeutic outcomes. Thus, the enhanced in vitro release of C-PC, driven by PG, correlates strongly with the observed ex vivo permeation results. PG not only promotes C-PC release from the hydrogel but also prepares the skin barrier for more efficient drug penetration. These dual roles of PG—in enhancing both release and permeation—create a synergistic effect that underlies the successful delivery of C-PC through the skin.

In conclusion, the effective in vitro release of C-PC in the presence of PG is indeed a critical factor that contributes to the observed ex vivo permeation. The mechanistic link between these two phenomena lies in PG's ability to simultaneously enhance the solubility and diffusion of C-PC in vitro and modify the skin barrier ex vivo, thereby ensuring efficient drug delivery.

4. Materials and Methods

4.1. Materials

C-PC was isolated from cyanobacteria biomass collected in Kaunas Lagoon (Kaunas, Lithuania). SharoSENSE Plus™ 184 (maltol, didecyldimonium chloride), SharoSENSE™ Plus 785 (maltol, sorbic acid, sodium benzoate), and Sharomix™ 721 (dehydroacetic acid, benzyl alcohol, water) were received from SHARON Laboratories (Ashdod, Israel). Soligel™ (a polysaccharide consisting of monomer units that include three glucose and three galactose molecules in the pyranose form, along with one glucuronic acid and a pyruvyl substituent) was received from Givaudan (Vernier, Switzerland). Carbopol® Ultrez 21 (C10-30 alkyl acrylate crosspolymer) and Pemulen™ (C10-30 alkyl acrylate crosspolymer) were received from The Lubrizol Corporation (Wickliffe, OH, USA). Poloxamer 407 (poly(oxyethylene)-poly(oxypropylene)-poly(oxyethylene) triblock copolymer), sodium alginate, hydroxyethyl cellulose, sodium carboxymethyl cellulose, hydroxy-propyl methyl-cellulose, methyl 2-hydroxyethyl cellulose, chitosan 80/1000, glycerol, and propylene glycol were purchased from Sigma-Aldrich (St. Louis, MO, USA). All reagents and solvents were of analytical grade. Purified deionized water was obtained using a Milli-Q® water purification system (Millipore, Burlington, MA, USA).

4.2. Collection of Cyanobacterial Biomass

The biomass of cyanobacteria was collected with a plankton net (with a mesh size of 20 μm) from the Kaunas Lagoon (Kaunas, Lithuania) during a cyanobacteria bloom in September–October 2022. The collected biomass was frozen and stored at −20 °C in a freezer. In addition, phytoplankton samples were taken from the surface water layer (0.10–0.30 m) for microscopic analyses using a Ruttner water sampler to examine the bloom-forming species. Samples were preserved with a 4% (*v*/*v*) formaldehyde solution.

Microscopic analysis revealed that species of the genus *Microcystis* prevailed in the samples collected in 2022 (up to 98%).

4.3. C-PC Extraction and Purification

C-PC extraction and purification were conducted using wild-collected cyanobacterial biomass following the method described by Khazi et al. (2018), with some modifications [62]. C-PC was extracted using one freeze–thaw cycle (freezing at −20 °C and thawing at 20 ± 2 °C). The supernatant for purity assessment was collected after centrifugation at 8000× *g* for 10 min and precipitated with a 50% saturated ammonium sulfate solution overnight at +4 °C. The ammonium sulfate-precipitated solution was centrifuged at 10,000× *g* for 10 min, and the precipitate was resuspended with 10 mM sodium phosphate buffer (pH 7.0). Desalting was performed via diafiltration using a membrane with a 10 kDa pore size. Gel filtration chromatography on a Sephadex G-25 column was used to purify the C-PC from the biomass with a dominant presence of *Microcystis* spp. The column was pre-equilibrated and eluted with 10 mM sodium phosphate buffer (PBS), pH 7.0, at a flow rate of 0.5 mL/min. The purified C-PC solution was rapidly frozen at −40 °C and then freeze-dried using a VaCo 2 freeze dryer (Zirbus Technology, Bad Grund, Harz, Germany) at a vacuum pressure of about 0.05 mbar for approximately 24–36 h. The freeze-dried C-PC powder was stored at −20 °C.

4.4. Purity Assessment of C-PC

The purity of C-PC was determined spectrophotometrically, according to the following formula (Bennett, Bogodar, 1973) [63]:

$$\text{C-PC purity} = \text{OD620/OD280},$$

where OD280 indicates the absorbance of total proteins and OD620 indicates the absorbance of C-PC. The experiment was repeated three times.

4.5. Production of Experimental C-PC Hydrogels

The 1% (*w*/*w*) C-PC gels were prepared using various gelling agents, including chitosan (3% *w*/*w*), sodium alginate (3.5% *w*/*w*), Soligel™ (1.5% *w*/*w*), HEC (5.5% *w*/*w*), NaCMC (5% *w*/*w*), HPMC (15% *w*/*w*), HEMC (3% *w*/*w*), Carbopol® Ultrez 21 (0.8% *w*/*w*), Pemulen™ (0.5% *w*/*w*), and poloxamer 407 (15% *w*/*w*). Lyophilized C-PC powder was dissolved in purified water. The appropriate amount of gelling agent was added and mixed using an IKAMAG® C-MAG HS7 magnetic stirrer with a heated surface (IKA-Werke GmbH & Co. KG, Staufen, Germany). The mixture was stored at +4 °C until swelling occurred. For the preparation of the chitosan hydrogel, chitosan and purified water were heated to +30 °C. Acetic acid was added drop by drop until the chitosan dissolved and a transparent hydrogel formed. Lyophilized C-PC powder dissolved in purified water was homogeneously mixed with the prepared chitosan gel. For Carbopol® Ultrez 21, the mixture was neutralized with an 18% sodium hydroxide solution to achieve the desired pH value (5.5–7.5) and stirred until a homogeneous hydrogel was obtained. In the production of the poloxamer 407 hydrogel, triethanolamine was used for neutralization, and the mixture was stirred until a homogeneous hydrogel formed. When producing hydrogels with glycerol, PG, and preservatives (SharoSENSE PlusTM 184, Sharosense 785, and Sharomix 721), these substances were dissolved in purified water together with lyophilized C-PC powder. C-PC hydrogels were stored at +4 °C for 48 h prior to spectrophotometric analysis.

4.6. Spectrophotometric Analysis

The amount of C-PC in the produced hydrogels was determined using the spectrophotometric method. The calibration curve ($y = 1.8673x - 0.0043$; $R^2 = 0.9998$) was produced using C-PC solutions in PBS of a 0.1–0.6 mg/mL concentration ($n = 11$) with 3 replicates. The absorbance of the solutions was measured at a wavelength of 620 nm.

The C-PC hydrogel was placed into PBS (pH 7.4) and stirred at 100 rpm for 30 min, then centrifuged at 10,000× *g* rpm for 10 min at 25 °C. In this way, the gel matrix was broken, resulting in a clear C-PC solution in the PBS. The amount of C-PC determined spectrophotometrically was compared with the amount initially added to formulate the hydrogel. The repeatability of each spectrophotometric experiment, during which the amount of C-PC in the hydrogel formulation was determined, was assessed over three trials.

4.7. Microbiological Analysis

The microbiological examination of C-PC hydrogels was conducted at the Kaunas Department of the National Public Health Care Laboratory (Kaunas, Lithuania) to evaluate the microbiological contamination. The microorganisms tested were selected based on the Scientific Committee on Consumer Safety Notes of Guidance for the Testing of Cosmetic Ingredients and Their Safety Evaluation [53]. The microbiological methods used to examine the presence of *Candida albicans*, *Escherichia coli*, *Pseudomonas aeruginosa*, *Staphylococcus aureus*, and the total count of aerobic mesophilic bacteria were chosen according to international standards, as detailed in Table 3.

Table 3. Methods of microbiological testing of C-PC hydrogels.

Microorganisms	Method for Detecting Microorganisms
Candida albicans	LST EN ISO 18416:2016 except ISO 18416:2015/Amd1:2022 (N) [64]
Escherichia coli	LST EN ISO 21150:2016 except ISO 21150:2015/Amd1:2022 (N) [65]
Pseudomonas aeruginosa	LST EN ISO 22717:2016 except ISO 22717:2015/Amd1:2022 (N) [66]
Staphylococcus aureus	LST EN ISO 22718:2016 except ISO 22718:2015/Amd1:2022 (N) [67]
Number of aerobic mesophilic bacteria CFU */g	LST EN ISO 21149:2017 except ISO 21149:2017/Amd1:2022 (N) [68]

* The number of microorganisms or colony-forming units of a group of microorganisms in a certain unit of volume or mass.

4.8. Determination of pH of Experimental C-PC Hydrogels

The pH of the C-PC experimental formulations (n = 3) was assessed using a pH-Meter 766 Calimatic (Knick Elektronische Messgeräte GmbH & Co, Berlin, Germany).

4.9. In Vitro Study of C-PC Release from Experimental C-PC Hydrogels

In vitro release studies were carried out in triplicate (n = 3) using modified Franz-type diffusion cells [69–71]. An infinite dose of the donor phase (~1.00 g) was loaded into the cell with a polyvinylidene difluoride (PVDF) 0.22 µm dialysis membrane Durapore® (Merck KGaA, Darmstadt, Germany). The diffusion area was 1.33 cm^2. The experimental conditions did not limit the solubility and dissolution of C-PC in the PBS acceptor medium (the volume of the acceptor medium was 5 mL) during the diffusion process. The acceptor medium was mixed using an IKAMAG® C-MAG HS7 magnetic stirrer with a heated surface (IKA-Werke GmbH & Co.KG, Staufen, Germany) and maintained at 32 ± 0.1 °C. Acceptor medium samples (1.0 mL) were taken after 0.5, 1, 2, 3, 4, 5, and 6 h. The amount of C-PC released was evaluated using the spectrophotometric method. The C-PC flux was expressed as the amount of C-PC released per cm^2 per unit of time.

4.10. Ex Vivo Skin-Permeation Study of C-PC

Ex vivo skin-permeation studies of C-PC were performed using Bronaugh-type flow-through diffusion cells following the method described by Žilius M. et al. with some modifications [72]. The study was carried out using Caucasian women's abdominal skin obtained from the Department of Plastic and Reconstructive Surgery, Hospital of the Lithuanian University of Health Sciences, after cosmetic surgery. The Kaunas Region Bioethical Committee has approved the use of human skin for transdermal penetration studies, with ethical approval code BE-2-42 (3 May 2023). The effective diffusion area in the

cells was 0.64 cm^2. The skin samples (n = 3 per formulation) were pre-equilibrated in a PBS solution at +25 °C for 12 h before the experiments. After equilibration, an infinite dose of the donor phase was applied to the skin cells, approximately 500 mg of hydrogel. The cells were sealed with Parafilm and covered with aluminum foil to protect them from light. The ex vivo skin-penetration tests were carried out for 24 h. At the end of the experiment, the skin specimens were gently washed with PBS solution and placed in a 4% (v/v) formalin solution for 3 h. Then, the skin samples were washed with a PBS solution and placed in a 30% (v/v) sucrose solution for 12 h.

The skin was embedded in a Shandon Cryomatrix compound (Thermo Fisher Scientific, Waltham, MA, USA) and frozen at −60 °C on a cooling stage. The frozen skin samples were sectioned at 20µm using a cryostat microtome (Microm HM 560, Leica, Wetzlar, Germany), then examined by confocal laser scanning microscopy (CLSM) (LSM 700, ZEISS, Oberkochen, Germany). C-PC was detected using a 639 nm diode laser. Using a Plan-Apochomat 20x objective with a numerical aperture (NA) of 0.55, images with a field size of 2048 µm × 2048 µm were generated. Transverse skin-section images were collected using ZEN 2010 software, and the z-stack method was applied to evaluate the accumulation of C-PC in the skin. C-PC was excited at 651 nm and detected at 670 nm. A Cy3 filter was utilized to isolate tissue autofluorescence and digitally assign the emission to a green color channel.

4.11. Statistical Analysis of Data

The research results were statistically calculated and analyzed using IBM SPSS Statistics version 29.0. (SPSS Inc., Chicago, IL, USA). The results were expressed as the mean and standard deviation. A paired-sample t-test was used to compare two dependent samples, while an independent samples t-test was used to compare two independent samples ($p < 0.05$). Bonferroni's test was applied to the comparison of more than two independent samples ($p < 0.05$).

5. Conclusions

The study demonstrated that polysaccharide biopolymers, such as sodium alginate, hydroxyethyl cellulose, and SoligelTM, are effective at formulating C-PC hydrogels while preserving the stability of C-PC. The preservative SharoSENSETM Plus 785 exhibited excellent antimicrobial properties and compatibility with C-PC in the semisolid formulation. An in vitro release study indicated that, after 6 h, C-PC release from the sodium alginate hydrogel containing PG was approximately 10%, or 728.07 (±19.35) µg/cm^2, which was significantly higher than the nearly 7%, or 531.44 (±26.81) µg/cm^2, release from the hydrogel without PG ($p < 0.05$). Furthermore, an ex vivo qualitative skin-permeation study revealed that PG enhanced the penetration of C-PC into the outer layer of the skin, the stratum corneum. However, for C-PC to exert its effective antioxidant and anti-inflammatory effects on the skin, mere penetration into the stratum corneum may not be sufficient. Therefore, it is advisable to further develop technological formulations that can encapsulate C-PC molecules and improve drug delivery.

Author Contributions: Conceptualization, D.G., N.S. and J.B.; methodology, D.G., N.S., J.B., M.Ž., K.R.-K., D.H.P., J.K., V.B. and A.S.; software, D.G.; validation, N.S., D.G. and M.Ž.; formal analysis, D.G. and M.Ž.; investigation, D.G. and N.S.; resources, J.K., V.B. and J.B.; data curation, D.G.; writing—original draft preparation, D.G.; writing—review and editing, N.S.; visualization, D.G. and N.S.; supervision, N.S.; project administration, N.S.; funding acquisition, N.S. All authors have read and agreed to the published version of the manuscript.

Funding: This research received no external funding.

Institutional Review Board Statement: The study was conducted in accordance with the Declaration of Helsinki and approved by the Institutional Review Board (or Ethics Committee) of the Kaunas Region Bioethical Committee (protocol code BE-2-42, date of approval: 3 May 2023).

Informed Consent Statement: Not applicable.

Data Availability Statement: The data supporting the findings of this study are available from the corresponding author [D.G.] upon reasonable request.

Conflicts of Interest: The authors declare no conflicts of interest.

References

1. Osman, A.; Salama, A.; Ghany, A.A.; Sitohy, M. Antibacterial activity and mechanism of action of phycocyanin extracted from an Egyptian strain of *Anabaena oryzae* SOS13. *Zagazig J. Agric. Biochem. Appl.* **2015**, *42*, 30–321.
2. Yuan, B.; Li, Z.; Shan, H.; Dashnyam, B.; Xu, W.; McClements, D.J.; Zhang, B.; Tan, M.; Wang, Z.; Cao, C. A review of recent strategies to improve the physical stability of phycocyanin. *Curr. Res. Food Sci.* **2022**, *5*, 2329–2337. [PubMed]
3. Dranseikienė, D.; Balčiūnaitė- Murzienė, G.; Karosienė, J.; Morudov, D.; Juodžiukynienė, N.; Hudz, N.; Gerbutavičienė, R.J.; Savickienė, N. Cyano-Phycocyanin: Mechanisms of Action on Human Skin and Future Perspectives in Medicine. *Plants* **2022**, *11*, 1249. [CrossRef] [PubMed]
4. Alka; Singh, P.; Pal, R.R.; Mishra, N.; Singh, N.; Verma, A.; Saraf, S.S. Development of pH-Sensitive hydrogel for advanced wound healing: Graft copolymerization of locust bean gum with acrylamide and acrylic acid. *Int. J. Pharm.* **2024**, *661*, 124450. [PubMed]
5. Zhou, Y.; Bai, R.; Huang, Y.; Li, W.; Chen, J.; Cheng, Z.; Wu, X.; Diao, Y. The anti- photoaging effect of C-phycocyanin on ultraviolet B- irradiated BALB/c-nu mouse skin. *Front. Bioeng. Biotechnol.* **2023**, *11*, 1229387.
6. Salgado, M.T.S.F.; Silva, M.C.S.; Fratelli, C.; Braga, A.R.C.; Lopes, T.B.G.; Ferreira, E.; Silva, I.L.D.; Paiva, L.S.; Souza Votto, A.P. Bioactive C-phycocyanin exerts immunomodulatory and antitumor activity in mice with induced melanoma. *Toxicol. Appl. Pharmacol.* **2024**, *484*, 116874.
7. Fernandes, R.; Campos, J.; Serra, M.; Fidalgo, J.; Almeida, H.; Casas, A.; Toubarro, D.; Barros, A.I.R.N.A. Exploring the Benefits of Phycocyanin: From Spirulina Cultivation to Its Widespread Applications. *Pharmaceuticals* **2023**, *16*, 592. [CrossRef]
8. Sala, L.; Moraes, C.C.; Kalil, S.J. Cell Pretreatment with Ethylenediaminetetraacetic Acid for Selective Extraction of C-Phycocyanin with Food Grade Purity. *Biotechnol. Prog.* **2018**, *34*, 1261–1268.
9. Guo, J.W.; Jee, S.H. Strategies to develop a suitable formulation for inflammatory skin disease treatment. *Int. J. Mol. Sci.* **2021**, *22*, 6078. [CrossRef]
10. Hsieh-Lo, M.; Castillo, G.; Ochoa-Becerra, M.A.; Mojica, L. Phycocyanin and phycoerythrin: Strategies to improve production yield and chemical stability. *Algal Res.* **2019**, *42*, 101600.
11. Ciccone, L.; Vandooren, J.; Nencetti, S.; Orlandini, E. Natural Marine and Terrestrial Compounds as Modulators of Matrix Metalloproteinases-2 (MMP-2) and MMP-9 in Alzheimer's Disease. *Pharmaceuticals* **2021**, *14*, 86. [CrossRef] [PubMed]
12. Jaeschke, D.P.; Teixeira, I.R.; Marzak, L.D.F.; Mercali, G.D. Phycocyanin from Spirulina: A review of extraction methods and stability. *Food Res. Int.* **2021**, *143*, 110314.
13. Eisenberg, I.; Harris, D.; Levi- Kalisman, Y.; Yochelis, S.; Shemesh, A.; Ben-Nissan, G.; Sharon, M.; Raviv, U.; Adir, N.; Keren, N.; et al. Concentration- based self-assembly of phycocyanin. *Photosynth. Res.* **2017**, *134*, 39–49. [PubMed]
14. Wang, T.; Yi, W.; Zhang, Y.; Wu, H.; Fan, H.; Zhao, J.; Wang, S. Sodium alginate hydrogel containing platelet- rich plasma for wound healing. *Colloids Surf. B Biointerfaces* **2023**, *222*, 113096.
15. Peng, W.; Li, D.; Dai, K.; Wang, Y.; Song, P.; Li, H.; Tang, P.; Zhang, Z.; Li, Z.; Zhou, Y.; et al. Recent progress of collagen, chitosan, alginate and other hydrogels in skin repair and wound dressing applications. *Int. J. Biol. Macromol.* **2022**, *208*, 400–408.
16. Knoos, P.; Onder, S.; Pedersen, L.; Lennart, P.; Ulvenlund, S.; Wahlgren, M. Surfactants modify the release from tablets made of hydrophobically modified poly (acrylic acid). *Results Pharma Sci.* **2013**, *3*, 7–14.
17. Calixto, G.; Yoshii, A.C.; Roxha e Silva, H.; Curry, B.S.F.; Chorilli, M. Polyacrilic acid polymers hydrogels intended to topical drug delivery: Preparation and characterization. *Pharm. Dev. Technol.* **2014**, *20*, 490–496.
18. Grip, J.; Engstad, R.E.; Skjæveland, I.; Škalko- Basnet, N.; Holsæter, A.M. Sprayable Carbopol hydrogel with soluble beta-1,3/1,6-glucan as an active ingredient for wound healing—Development and *in-vivo* evaluation. *Eur. J. Pharm. Sci.* **2017**, *107*, 24–31.
19. Katakam, P.; Chary, N. Formulation Development and Physico Chemiical Evaluation of Topical Formulation of Acetofenac Using Pemulen. *J. Pharm. Sci. Res.* **2015**, *7*, 640–642.
20. Dumortier, G.; Grossiord, J.L.; Agnely, F.; Chaumeil, J.C. A review of poloxamer 407 pharmaceutical and pharmacological characteristics. *Pharm. Res.* **2006**, *23*, 2709–2728.
21. Dios-Perez, I.; Gonzalez-Garcinuno, A.; Tabernero, A.; Blanco-Lopez, M.; Garcia-Esteban, J.A.; Moreno-Rodilla, V.; Curto, B.; Perez-Esteban, P.; Valle, E.M.M. Development of a thermosensitive hydrogel based on Polaxamer 407 and gellan gum with inclusion complexes (Sulfobutylated-β-cyclodextrin–Farnesol) as a local drug delivery system. *Eur. J. Pharm. Sci.* **2023**, *191*, 106618. [PubMed]
22. Gonzalez-Paredes, A.; Clares-Naveros, B.; Ruiz-Martinez, M.A.; Durban-Fornieles, J.J.; Ramos-Cormenzana, A.; Monteoliva-Sanchez, M. Delivery systems for natural antioxidant compounds: Archaeosomes and archaeosomal hydrogels characterization and release study. *Int. J. Pharm.* **2011**, *421*, 321–331. [PubMed]
23. Yuan, N.; Shao, K.; Chen, C. Chitosan, alginate, hyaluronic acid and other novel multifunctional hydrogel dressings for wound healing: A review. *Int. J. Biol. Macromol.* **2023**, *240*, 124321.

24. Guo, X.; Wang, Y.; Qin, Y.; Shen, P.; Peng, Q. Structures, properties and application of alginic acid: A review. *Int. J. Biol. Macromol.* **2020**, *162*, 618–628. [PubMed]
25. Terescenso, D.; Benali, L.H.; Canivet, F.; Gelebart, M.B.; Hucher, N.; Gore, E.; Picard, C. Bio-sourced polymers in cosmetic emulsions: A hidden potential of the alginates as thickeners and gelling agents. *Int. J. Cosmet. Sci.* **2021**, *43*, 573–587.
26. Shafei, S.; Khanmohammadi, M.; Heidari, R.; Ghanbari, H.; Nooshabadi, V.T.; Farzamfar, S.; Akbariqomi, M.; Sanikhani, N.S.; Absalan, M.; Tavoosidana, G. Exosome loaded alginate hydrogel promotes tissue regeneration in full- thickness skin wounds, An in vivo study. *J. Biomed. Mater. Res. Part A* **2020**, *108*, 545–556.
27. Zhang, M.; Zhang, Q.; Chen, X.; Jiang, T.; Song, P.; Wang, B.; Zhao, X. Mussel- inspired nanocomposite hydrogel based on alginate and antimicrobial peptide for infected wound repair. *Int. J. Biol. Macromol.* **2022**, *219*, 1087–1099.
28. Kabir, S.M.F.; Sikdar, P.P.; Haque, B.; Bhuiyan, M.A.R.; Ali, A.; Islam, M.N. Cellulose- based hydrogel materials: Chemistry, properties and their prospective applications. *Prog. Biomater.* **2018**, *7*, 153–174.
29. El-Kased, R.F.; Amer, R.I.; Attia, D.; Elmaraz, M.M. Honey- based hydrogel: In vitro and comparative In vivo evaluation for wound healing. *Sci. Rep.* **2017**, *7*, 9692.
30. Freitas, E.D.; Moura, C.F., Jr.; Kerwald, J.; Beppu, M.M. An Overview of Current Knowledge on the Properties, Synthesis and Applications of Quaternary Chitosan Derivatives. *Polymers* **2020**, *12*, 2878. [CrossRef]
31. Product File Soligel 01/2012. Available online: www.soliance.com (accessed on 19 August 2024).
32. Menon, G.K. New insights into skin structure: Scratching the surface. *Adv. Drug Deliv. Rev.* **2002**, *54*, S3–S17. [PubMed]
33. Bouwstra, J.A.; Honeyell-Nguyen, P.L. Skin structure and mode of action of vesicles. *Adv. Drug Deliv. Rev.* **2002**, *54*, S41–S55. [PubMed]
34. Quan, T. Molecular insights of human skin epidermal and dermal aging. *J. Dermatol. Sci.* **2023**, *112*, 48–53.
35. Lane, M.E. Skin penetration enhancers. *Int. J. Pharm.* **2013**, *447*, 12–21. [PubMed]
36. Patil, U.K.; Saraogi, R. Natural products as potential drug permeation enhancer in transdermal drug delivery system. *Arch. Dermatol. Res.* **2014**, *306*, 419–426. [PubMed]
37. Mistry, J.; Notman, R. Mechanisms of the Drug Penetration Enhancer Propylene Glycol Interacting with Skin Lipid Membranes. *J. Phys. Chem.* **2024**, *128*, 3885–3897.
38. Fiume, M.M.; Bergfeld, W.F.; Belsito, D.V.; Hill, R.A.; Klaassen, C.D.; Liebler, D.; Marks, J.G., Jr.; Shank, R.C.; Slaga, T.J.; Snyder, P.W.; et al. Safety Assessment of Propylene Glycol, Tripropylene Glycol, and PPGs as Used in Cosmetics. *Int. J. Toxicol.* **2012**, *31*, 2455–2605.
39. Wang, X.; Guan, S.; Zhang, K.; Li, J. Benlysta-Loaded Sodium Alginate Hydrogel and Its Selective Functions in Promoting Skin Cell Growth and Inhibiting Inflammation. *ASC Omega* **2020**, *5*, 10395–10400.
40. Dananjaya, S.H.S.; Bandara, N.; Molagoda, I.N.; Sandamalika, W.M.G.; Kim, D.; Ganepola, N.; Attanayake, A.P.; Choi, D. Multifunctional alginate/ polydeoxyribonucleotide hydrogels for promoting diabetic wound healing. *Int. J. Biol. Macromol.* **2024**, *257*, 128367.
41. Chang, R.Y.K.; Okamoto, Y.; Morales, S.; Kutter, E.; Chan, K. Hydrogel formulations containing non-ionic polymers for topical delivery of bacteriophages. *Int. J. Pharm.* **2021**, *605*, 120850.
42. Enoch, K.; Somasundaram, A.A. Rheological insights on Carboxymethyl cellulose hydrogels. *Int. J. Biol. Mecromolecules* **2023**, *253*, 127481.
43. Natori, N.; Shibano, Y.; Hiroki, A.; Taguchi, M.; Miyajima, A.; Yoshizawa, K.; Kawano, Y.; Hanawa, T. Preparation and Evaluation of Hydrogel Film Containing Tramadol for Reduction of Peripheral Neuropathic Pain. *J. Pharm. Sci.* **2023**, *112*, 132–137. [PubMed]
44. Kovacevic, B.; Jones, M.; Wagle, S.R.; Ionescu, C.M.; Fostes, T.; Danic, M.; Mikov, M.; Mooranian, A.; Al-Salami, H. The effect of deoxycholic acid-based hydrogels on hepatic, muscle and pancreatic beta cells. *Ther. Deliv.* **2024**, *15*, 41–54.
45. Phatale, V.; Vaiphei, K.K.; Jha, S.; Patil, D.; Agrawal, M. Overcoming skin barriers through advanced transdermal drug delivery approaches. *J. Control. Release* **2022**, *351*, 361–380.
46. Huo, Y.; Hou, X.; Yu, Y.; Wen, X.; Ding, Y.; Li, Y.; Wang, Z. Improving the Thermal and Oxidative Stability of Food-Grade Phycocyanin from *Arthrospira platensis* by Addition of Saccharides and Sugar Alcohols. *Foods* **2022**, *11*, 1752. [CrossRef]
47. Chaiklahan, R.; Bunnag, B.; Chirasuwan, N. Stability of phycocyanin extracted from Spirulina sp.: Influence of temperature, pH and preservatives. *Process Biochem.* **2012**, *47*, 659–664.
48. Głaz, P.; Rosinska, A.; Wozniak, S.; Boguszewska-Czubara, A.; Biernasiuk, A.; Matosiuk, D. Effect of Commonly Used Cosmetic Preservatives on Healthy Human Skin Cells. *Cells* **2023**, *12*, 1076. [CrossRef]
49. Long, M.C.; Nagegowda, D.A.; Kaminaga, Y.; Ho, K.K.; Kish, C.M.; Schnepp, J.; Sherman, D.; Weiner, H.; Rhodes, D.; Dudareva, N. Involvement of snapdragon benzaldehyde dehydrogenase in benzoic acid biosynthesis. *Plant J. Cell Mol. Biol.* **2009**, *59*, 256–265.
50. Olmo, A.; Calzada, J.; Nuñez, M. Benzoic acid and its derivatives as naturally occurring compounds in foods and as additives: Uses, exposure, and controversy. *Crit. Rev. Food Sci. Nutr.* **2017**, *57*, 3084–3103.
51. Jay, J.M.; Loessner, M.J.; Golden, D.A. *Modern Food Microbiology*, 7th ed.; Springer Science+ Business Media, INC: New York, NY, USA, 2005; pp. 301–305.
52. Ziklo, N.; Bibi, M.; Salama, P. The Antimicrobial Mode of Action of Maltol and Its Synergistic Efficacy with Selected Cationic Surfactants. *Cosmetics* **2021**, *8*, 86. [CrossRef]

53. *The SCCS Notes of Guidance for the Testing of Cosmetic Ingredients and Their Safety Evaluation*; 9th Revision; Scientific Committee on Consumer Safety (SCCS); European Commission: Brussels, Belgium. 2016. Available online: https://ec.europa.eu/health/scientific_committees/consumer_safety/docs/sccs_o_190.pdf (accessed on 19 August 2024).
54. Yu, H.L.; Goh, C.F. Glycols: The ubiquitous solvent for dermal formulations. *Eur. J. Pharm. Biopharm.* **2024**, *196*, 114182.
55. Yang, D.; Liu, C.; Quan, P.; Fang, L. A systematic approach to determination of permeation enhancer action efficacy and sites: Molecular mechanism investigated by quantitative structure–activity relationship. *J. Controll. Release* **2020**, *322*, 1–12.
56. Wang, Z.; Xue, Y.; Zhu, Z.; Hu, Y.; Zeng, Q.; Wu, Y.; Wang, Y.; Shen, C.; Jiang, C.; Liu, L.; et al. Quantitative Structure-Activity Relationship of Enhancers of Licochalcone A and Glabridin Release and Permeation Enhancement from Carbomer Hydrogel. *Pharmaceutics* **2022**, *14*, 262. [CrossRef] [PubMed]
57. Carrer, V.; Alonso, C.; Pont, M.; Zanuy, M.; Cordoba, M.; Espinosa, S.; Barba, C.; Oliver, M.A.; Marti, M.; Coderch, L. Effect of propylene glycol on the skin penetration of drugs. *Arch. Dermatol. Res.* **2020**, *312*, 337–352.
58. Tran, H.N.; Kim, I.G.; Kim, J.H.; Bhattacharyya, A.; Chung, E.J.; Noh, I. Incorporation of Cell-Adhesive Proteins in 3D-Printed Lipoic Acid- Maleic Acid- Poly (Propylene Glycol)- Based Tough Gel Ink for Cell- Supportive Microenvironment. *Macromol. Biosci.* **2023**, *23*, 2300316.
59. Adli, S.A.; Ali, F.; Azmi, A.S.; Anuar, H.; Nasir, N.A.M.; Hasham, R.; Idris, M.K.D. Development of Biodegradable Cosmetic Patch Using a Polylactic Acid/Phycocyanin-Alginate Composite. *Polymers* **2020**, *12*, 1669. [CrossRef]
60. Kis, N.; Gunnarsson, M.; Berko, S.; Sparr, E. The effects of glycols on molecular mobility, structure, and permeability in stratum corneum. *J. Controll. Release* **2022**, *343*, 755–764.
61. Minghetti, P.; Cilurzo, F.; Casiraghi, A.; Montanari, L.; Fini, A. Ex vivo study of transdermal permeation of four diclofenac salts from different vehicles. *J. Pharm. Sci.* **2007**, *96*, 814–823.
62. Khazi, M.I.; Demirel, Z.; Liaqat, F.; Dalay, M.C. Analytical Grade Purification of Phycocyanin from Cyanobacteria. In *Biofuels from Algae. Methods in Molecular Biology*, 1st ed.; Spilling, K., Ed.; Springer: New York, NY, USA, 1980; pp. 173–179.
63. Bennett, A.; Bogorad, L. Complementary chromatic adaption in a filamentous blue-green alga. *J. Cell Biol.* **1973**, *58*, 419–435.
64. *LST EN ISO 18416:2016*; Cosmetics–Microbiology–Detection of Candida albicans. European Committee for Standardization (CEN): Brussels, Belgium, 2016.
65. *LST EN ISO 21150:2016*; Cosmetics–Microbiology–Detection of Escherichia coli. European Committee for Standardization (CEN): Brussels, Belgium, 2016.
66. *LST EN ISO 22717:2016*; Cosmetics–Microbiology–Detection of Pseudomonas aeruginosa. European Committee for Standardization (CEN): Brussels, Belgium, 2016.
67. *LST EN ISO 22718:2016*; Cosmetics–Microbiology–Detection of Staphylococcus aureus. European Committee for Standardization (CEN): Brussels, Belgium, 2016.
68. *LST EN ISO 21149:2017*; Cosmetics–Microbiology–Enumeration and detection of aerobic mesophilic bacteria. European Committee for Standardization (CEN): Brussels, Belgium, 2017.
69. Marquele-Oliveira, F.; Fonseca, Y.M.; de Freitas, O.; Fonseca, M.J. Development of topical functionalized formulations added with propolis extract: Stability, cutaneous absorption and in vivo studies. *Int. J. Pharm.* **2007**, *342*, 40–48.
70. Marquele, F.D.; Oliveira, A.R.; Bonato, P.S.; Lara, M.G.; Fonseca, M.J. Propolis extract release evaluation from topical formulations by chemiluminescence and HPLC. *J. Pharm. Biomed. Anal.* **2006**, *41*, 461–468. [PubMed]
71. Olejnik, A.; Goscianska, J.; Nowak, I. Active compounds release from semisolid dosage forms. *J. Pharm. Sci.* **2012**, *101*, 4032–4045. [PubMed]
72. Žilius, M.; Ramanauskienė, K.; Briedis, V. Release of propolis phenolic acids from Semisolid formulations and their penetration into the human skin in vitro. *Evid.-Based Complement. Altern. Med.* **2013**, *2013*, 958717.

Paper 4

Title: Cyano-phycocyanin Loaded Enriched Transfersomes for Enhanced Topical Skin Delivery and Antioxidant Protection

Authors: Galinytė, Daiva; Aroffu, Matteo; Manconi, Maria; Žilius, Modestas; Rysevaitė-Kyguolienė, Kristina; Karosienė, Jūratė; Koreivienė, Judita; Briedis, Vitalis; Pauža, Dainius Haroldas; Savickas, Arūnas; Escribano Ferrer, Elvira; Manca, Maria Letizia; Savickienė, Nijolė

International Journal of Pharmaceutics, 683, 126079 (2025)

International Journal of Pharmaceutics 683 (2025) 126079

Contents lists available at ScienceDirect

International Journal of Pharmaceutics

journal homepage: www.elsevier.com/locate/ijpharm

Cyano-phycocyanin loaded enriched transfersomes for enhanced topical skin delivery and antioxidant protection

Daiva Galinytė [a,1,*], Matteo Aroffu [b,1], Maria Manconi [b], Modestas Žilius [c], Kristina Rysevaitė-Kyguolienė [d], Jūratė Karosienė [e], Judita Koreivienė [e], Vitalis Briedis [c], Dainius Haroldas Pauža [d], Arūnas Savickas [f], Elvira Escribano Ferrer [g], Maria Letizia Manca [b], Nijolė Savickienė [a]

[a] Department of Pharmacognosy, Faculty of Pharmacy, Academy of Medicine, Lithuanian University of Health Sciences, Sukilėlių Av. 13, 50162 Kaunas, Lithuania
[b] Department of Life and Environmental Sciences, University of Cagliari, University Campus, S.P.Monserrato-Sestu Km 0.700, 09042 Cagliari, Italy
[c] Department of Clinical Pharmacy, Faculty of Pharmacy, Academy of Medicine, Lithuanian University of Health Sciences, Sukilėlių Av. 13, 50162 Kaunas, Lithuania
[d] Institute of Anatomy, Faculty of Medicine, Academy of Medicine, Lithuanian University of Health Sciences, Mickeviciaus St. 9, 44307 Kaunas, Lithuania
[e] Laboratory of Algology and Microbial Ecology, Nature Research Centre, Akademijos St. 2, 08412 Vilnius, Lithuania
[f] Department of Drug Technology and Social Pharmacy, Faculty of Pharmacy, Academy of Medicine, Lithuanian University of Health Sciences, Sukilėlių Av. 13, 50162 Kaunas, Lithuania
[g] Biopharmaceutics and Pharmacokinetics Unit, Institute for Nanoscience and Nanotechnology, University of Barcelona, Barcelona, Spain

ARTICLE INFO

Keywords:
Cyano-phycocyanin
Phospholipid vesicles
Transfersomes
HaCaT cells
Ex vivo skin penetration

ABSTRACT

This study aimed to develop and evaluate cyano-phycocyanin (C-PC)-loaded enriched transfersomes for topical application, improved skin delivery, and antioxidant protection. The main objective was to overcome the limitations associated with C-PC's instability and poor skin permeability due to its high molecular weight and hydrophilicity. Six formulations were prepared using an organic solvent-free two-step method: glycerol-enriched transfersomes (Gly-transfersomes), glycerol and cholesterol-enriched transfersomes (Gly-chol-transfersomes), hyaluronate-enriched transfersomes (Hyal-transfersomes), hyaluronate and cholesterol-enriched transfersomes (Hyal-chol-transfersomes), glycerol and hyaluronate-enriched transfersomes (Hyal-gly-transfersomes), and a combination of all three (Hyal-gly-chol-transfersomes). Empty vesicles were prepared via direct sonication, then C-PC was gently loaded using mild sonication in a temperature-controlled ultrasonic bath. All formulations demonstrated properties suitable for skin delivery, with mean diameters <115 nm, polydispersity indexes <0.2, and zeta potential below −30 mV. Cryo- transmission electron microscopy confirmed spherical, unilamellar or oligolamellar morphology. Gly- and Gly-chol-transfersomes exhibited the highest encapsulation efficiency (~52 %) and remained stable for up to 8 months at 4 °C. Antioxidant activity of C-PC (~23–27 μmol TE/g of dry C-PC) was confirmed via DPPH assay. Biological tests on HaCaT cells exposed to H_2O_2-induced oxidative stress showed ~80 % cell viability after treatment with C-PC formulations, compared to ~60 % in untreated cells, indicating cytoprotective activity. *Ex vivo* skin penetration studies revealed significantly higher C-PC accumulation in the epidermis especially for Gly- and Gly-chol-transfersomes versus aqueous C-PC. These findings confirm the potential of enriched transfersomes as effective carriers to improve the skin delivery and bioactivity of C-PC in antioxidant skin care formulations.

* Corresponding author.
E-mail addresses: daiva.galinyte@stud.lsmu.lt (D. Galinytė), matteo.aroffu@unica.it (M. Aroffu), manconi@unica.it (M. Manconi), modestas.zilius@lsmu.lt (M. Žilius), kristina.rysevaite@lsmu.lt (K. Rysevaitė-Kyguolienė), jurate.karosiene@gamtc.lt (J. Karosienė), judita.koreiviene@gamtc.lt (J. Koreivienė), vitalis.briedis@lsmu.lt (V. Briedis), dainius.pauza@lsmu.lt (D.H. Pauža), arunas.savickas@lsmu.lt (A. Savickas), eescribano@ub.edu (E.E. Ferrer), mlmanca@unica.it (M.L. Manca), nijole.savickiene@lsmu.lt (N. Savickienė).
[1] These authors contributed equally to this work.

https://doi.org/10.1016/j.ijpharm.2025.126079
Received 12 May 2025; Received in revised form 24 July 2025; Accepted 13 August 2025
Available online 14 August 2025

1. Introduction

The term "phycocyanin" is derived from the Greek words *phyco* meaning "algae" and *cyanos* meaning "blue", reflecting both the origin of this compound and its distinctive color (Andonova et al., 2024). C-PC, a phycobiliprotein present in all cyanobacterial species- commonly known as blue-green algae- plays a crucial role in photosynthesis by capturing light energy. Beyond its photosynthetic function, C-PC is notable for its biological properties and therapeutic potential (Adjali et al., 2022). An increasing number of studies have demonstrated its beneficial effects in treating various skin disorders, including skin cancer. As a potent antioxidant, C-PC neutralizes reactive oxygen species (ROS), thereby mitigating oxidative stress-related cellular damage and reducing pathological conditions such as inflammation and carcinogenesis (Adjali et al., 2022). It may also delay or prevent skin aging by minimizing UVB-induced skin damage and wrinkle formation. This protective effect is attributed to its ability to downregulate matrix metalloproteinases (MMPs) and ROS production while maintaining the expression of essential skin barrier proteins such as involucrin, filaggrin, and loricrin (Jang and Kim, 2021). Further studies have demonstrated C-PC's capacity to scavenge ROS and repair radiation-induced damage in skin cells (Dong et al., 2025). It has also shown promising synergistic effects when combined with anti-inflammatory drugs like piroxicam or anticancer agents such as topotecan and doxorubicin, particularly in multidrug-resistant cells (Adjali et al., 2022). C-PC is therefore considered a promising anti-tumor candidate for melanoma therapy, acting on multiple cellular pathways without damaging non-tumoral cells (Saldago et al., 2022). Its administration has been associated with reduced tumor growth and increased levels of B cells, T lymphocytes, and myeloid cells in the inguinal lymph nodes, indicating both anti-tumor and immunomodulatory effects (Saldago et al., 2024). In addition to its antioxidant and anti-cancer properties, C-PC also exhibits wound-healing and antimicrobial activity, further supporting its potential in dermatological applications (Dahmen et al., 2024; Alka et al., 2024).

Despite its promising bioactivity, topical formulations of C-PC present significant challenges, primarily due to its high molecular weight and instability under various environmental conditions (Li et al., 2022). Structurally, C-PC consists of α and β subunits (each ~17–19 kDa), which form (αβ) monomers that assemble into trimers and hexamers. Each subunit is covalently linked to phycocyanobilins- chromophores responsible for the blue color and light-absorbing properties of C-PC (Adjali et al., 2022). This complex structure contributes to its sensitivity to temperature, pH, and light, which can lead to degradation and loss of bioactivity (Adjali et al., 2022; Li et al., 2022). Thus, formulation development and storage conditions must account for these vulnerabilities. In addition, C-PC's high molecular weight and hydrophilicity hinder its ability to penetrate the skin barrier. Passive permeation through the stratum corneum- the outermost skin layer – requires compounds to possess favorable physicochemical properties, including a molecular weight below 500 Da, moderate lipophilicity, and balanced solubility in both lipophilic and aqueous environments (Quan, 2023).

Various methods have been developed to enhance skin delivery by disrupting or weakening the stratum corneum. Chemical permeation enhancers such as azones, glycols, ethanol, and terpenes are commonly used to compromise the skin barrier, but they may cause irritation or long-term skin damage. Physical techniques like sonophoresis, electroporation, magnetophoresis, microneedles, thermal ablation, microdermabrasion, and iontophoresis can be effective, but are often painful, expensive, and reduce patient compliance (Akl et al., 2024). Nanotechnology offers a promising alternative to overcome these limitations (Zewail et al., 2025). Among nanocarriers, vesicular systems, such as invasomes or transethosomes, have demonstrated enhanced skin penetration and biological activity of active compounds (Zafar et al., 2024; Aodah et al., 2023; Kumari et al., 2023).

Recent studies have shown that phospholipid-based vesicular systems can effectively encapsulate C-PC (Castangia et al., 2016; Castangia et al., 2016; Manconia et al., 2009). These include liposomes, hyalurosomes, santosomes, ethosomes, and penetration enhancer-containing vesicles (PEVs). However, to date, no studies have investigated the use of transfersomes for topical delivery of C-PC. Transfersomes are elastic, deformable phospholipid vesicles containing edge activators – surfactants or bilayer- modifying molecules – that enhance flexibility and facilitate penetration (Allaw et al., 2020). These systems improve the stability and properties of active compounds, enhance solubility, promote skin partitioning, and fluidize the lipid barrier (Akl et al., 2024). Transfersomes have been used to deliver various proteins or hydrophilic biomolecules, including enzymes, growth factors, and antigens (Modi and Pharadia, 2012; Matharoo et al., 2024). For instance, Sapkota and colleagues encapsulated papain in transfersomes, reducing superficial skin damage in animal models (Sapkota et al., 2023). Doustvaghe et al. delivered recombinant human epidermal growth factor in transferosomes achieving improved skin deposition (Doustvaghe et al., 2024). Recently, Aroffu and colleagues developed transfersomes enriched with glycerol, hyaluronic acid, or their combination (so-called enriched transfersomes) resulting in long-lasting formulations (9 months) capable of enhancing ovalbumin deposition in both the epidermis and dermis (Aroffu et al., 2024).

Based on these findings, enriched transfersomes were selected for the topical delivery of C-PC. The concentration of sodium deoxycholate, used as an edge activator, was optimized to account the large molecular size and aggregation tendency of C-PC. A small amount of cholesterol was added in selected formulations to assess its impact on a) encapsulation efficiency, b) stability and c) skin permeation. Six different C-PC-loaded enriched transfersomes (Gly-transfersomes, Gly-chol-transfersomes, Hyal-transfersomes, Hyal-chol-transfersomes, Hyal-gly-transfersomes, Hyal-gly-chol-transfersomes) were prepared and characterized in terms of vesicle size (mean diameter, MD), polydispersity index (PI), zeta potential (ZP), and encapsulation efficiency (EE). Their stability was monitored and evaluated over a period of 8 months under light-protected conditions, while being stored at 4 °C in a refrigerator. Biological properties (biocompatibility and ability to counteract H_2O_2-induced oxidative stress) were evaluated *in vitro* using human keratinocytes (HaCaT) as the most representative cells of the outermost skin strata. The two most promising formulations were further tested in *ex vivo* skin penetration studies to compare their performance against C-PC in PBS and C-PC in PBS with propylene glycol (PG), a known penetration enhancer.

To the best of our knowledge, this is the first report on enriched transfersomes for C-PC skin delivery, using a two-step, solvent-free method specifically adapted to preserve the structural integrity and biological activity of this sensitive protein.

2. Materials and methods

2.1. Materials

C-PC was isolated from cyanobacterial biomass collected from the Kaunas Reservoir (Kaunas, Lithuania) and the Simnas fishpond (Simnas, Lithuania). Lipoid S75 (S75), a mixture of phospholipids from soy (70 % phosphatidylcholine, 9 % phosphatidylethanolamine, and 3 % lysophosphatidylcholine) was purchased from Lipoid GmbH (Ludwigshafen, Germany). Sodium hyaluronate (low molecular weight, hyal), glycerol (gly), and sodium chloride were obtained from Galeno (Potenza, Italy). Sodium deoxycholate (SDC), cholesterol (chol), and other chemicals were supplied by Sigma-Aldrich (St. Louis, MO, USA). All materials were of analytical grade. High-purity deionized water was prepared using a Milli-Q® water purification system (Millipore, Burlington, MA, USA). Cell medium, fetal bovine serum, penicillin, streptomycin, Fungizone, and all the other reagents used for cell studies were purchased from Thermo-Fisher Scientific Inc (Waltham, Massachusetts, USA).

2.2. Collection of cyanobacterial biomass

Cyanobacterial biomass was collected from the Kaunas Reservoir (Kaunas, Lithuania) and the Simnas fishpond (Simnas, Lithuania) during a cyanobacteria bloom during August –October 2023 using a cyanobacteria harvesting prototype AS-LAND (Algae – economy based ecological service of aquatic ecosystems. Layman's Report, 2023).

The collected biomass was frozen and stored at −20 °C. Additionally, phytoplankton samples were obtained from the surface water layer (0.10–0.30 m) using a Ruttner water sampler for microscopic analysis to identify bloom-forming species. Additionally, the collected biomass was tested for cyanotoxins by the enzyme-linked immunosorbent assay (ELISA) using the Beacon Analytical Systems (Saco, ME, USA) and Eurofins Abraxis (Warminster, PA, USA) ELISA tests according to the manufacturer's instruction. For C-PC isolation, non-toxic biomass with dominance of *Aphanizomenon flos-aquae* (>95 % total phytoplankton biomass) was selected.

2.3. C-PC extraction and purification

C-PC extraction and purification were performed following the method outlined by Khazi et al. (2018) with slight modifications (Khazi et al., 1980). Extraction involved a single freeze–thaw cycle (freezing at −20 °C and thawing at 20 ± 2 °C). The supernatant for C-PC purification was collected after centrifugation at 8,000 × g for 10 min and precipitated overnight at + 4 °C with a 50 % saturated ammonium sulfate solution. The precipitate was centrifuged at 10,000 × g for 10 min, and the pellet was resuspended in 10 mM Na-phosphate buffer (pH 7.0). Desalting was performed via diafiltration using a 10 kDa pore-size membrane.

C-PC was further purified by ion exchange chromatography using a Q-Sepharose XL resin. The column was pre-equilibrated with 10 mM Na-phosphate buffer (pH 7.0). Elution was carried out with a linear gradient of 0.5 M NaCl in the same buffer at a flow rate of 0.5 mL/min. The purified C-PC solution was rapidly frozen at −40 °C and freeze-dried using a VaCo 2 freeze dryer (Zirbus Technology, Bad Grund, Harz, Germany) at an approximately 0.05 mbar for 24–36 h. The freeze-dried C-PC powder was stored at −20 °C.

2.4. Purity assessment of C-PC

The purity of C-PC was determined spectrophotometrically, using the following formula (Bennett and Bogorad, 1973):

$$\text{C-PC purity} = OD_{620}/OD_{280},$$

where OD_{280} represents the absorbance of total proteins and OD_{620} represents the absorbance of C-PC. The experiment was performed in triplicate.

2.5. Vesicle preparation

C-PC-loaded enriched transfersomes were prepared using a two-step preparation process, avoiding the use of organic solvents. First, S75 (120 mg), sodium deoxycholate (20 mg), and optionally cholesterol (10 mg) were weighed into a glass vial and hydrated with 2 mL of: 1) 10 % glycerol in saline solution to obtain Gly-transfersomes, 2) 0.1 % sodium hyaluronate in saline solution to obtain Hyal-transfersomes, or 3) their combination (10 % glycerol, 0.1 % sodium hyaluronate in saline solution) to obtain Hyal-gly-transfersomes. The dispersions were sonicated using a high-intensity ultrasonic disintegrator (Soniprep 150, MSE Crowley, London, UK) with 2 repetitions of 15 cycles (4 s on, 2 s off) at a probe amplitude of 14 μm. To prevent overheating, samples were allowed to cool down after each sonication repetition. During the second step, C-PC (20 mg) was added to the preformed empty transfersomes, and the mixture underwent additional sonication in an ultrasonic bath (Bandelin Sonorex RK 512H) for 6 cycles of 5 min each, at 25–30 °C. The detailed compositions of the samples are provided in Table 1.

2.6. Transfersome characterization

The average particle size (mean diameter, MD), polydispersity index (PI), and zeta potential (ZP) of transfersomes were determined at 25 °C using a Zetasizer Ultra (Malvern Panalytical, Worcestershire, UK), after diluting each sample 1:100 with water to ensure optical clarity.

Transfersome formation and morphology were assessed by cryogenic transmission electron microscopy (cryo-TEM). A volume of 3 μL from each sample was applied to a glow-discharged holey carbon grid. Excess liquid was removed by gentle blotting with filter paper to produce a thin aqueous film. The grids were then vitrified by rapid plunge-freezing into liquid ethane maintained at its melting point, using a Vitrobot (FEI Company, Eindhoven, The Netherlands). This step was performed at room temperature and 100 % relative humidity. Vitrified specimens were transferred to a Tecnai F20 transmission electron microscope (FEI Company) using a Gatan cryotransfer system (Gatan, Pleasanton, CA, USA) and imaged under low-dose conditions. Micrographs were acquired at an accelerating voltage of 200 kV and a specimen temperature of approximately −173 °C, using an Eagle CCD camera (FEI Company).

2.7. Encapsulation efficiency

The encapsulation efficiency (EE) of the transfersomes was evaluated using the dialysis method (Fulgheri et al., 2023). 1 mL of each sample were placed in Spectra/Por 300 kDa (Biotech) dialysis membranes and dialyzed against 1L of high-purity deionized water at 25 °C for 24 h to remove unincorporated C-PC. Encapsulation efficiency (EE) was calculated by comparing the C-PC content before and after dialysis. To determine the C-PC content, transfersomes were disrupted using a 2 % (w/v) Triton™ X-100 solution, and the C-PC concentration was measured spectrophotometrically at a wavelength of 620 nm.

EE (%) was calculated according to the following formula:

$$EE(\%) = \frac{\text{C} - \text{PC content after dialysis}}{\text{C} - \text{PC content before dialysis}} \times 100$$

2.8. Stability studies

Transfersome stability was evaluated by monitoring variations in mean diameter, polydispersity index, and zeta potential during 8 months of storage at 4 °C, under refrigerated and light-protected conditions. All measurements were conducted in triplicate.

2.9. DPPH assay

The DPPH assay followed the protocol described by Agrawal and colleagues, with minor modifications (Agrawal et al., 2021). 100 μL of sample (C-PC in solution or loaded in enriched transfersomes) or blank (milli-Q water) were mixed with 400 μL of milli-Q water and 500 μL of DPPH methanolic solution (40 μg/mL). Milli-Q water was necessary to prevent C-PC precipitation. After 30 min of incubation in the darkness and at room temperature, the absorbance was read at 517 nm with a multi-plate reader (BioTek Epoch-SN, Agilent, USA). The antioxidant activity was calculated according to the following equation (Eq. (1)):

$$\text{Antioxidant activity } \% = (\text{A blank} - \text{A sample})/\text{A blank} \times 100.$$

A calibration curve was built using Trolox (6-hydroxy-2,5,7,8-tetramethylchroman-2-carboxylic acid) in the range of 7.8–125 μg/mL. Further calculations were made according to the equations of Rumpf and colleagues, and results were expressed as μmol of Trolox equivalent/g of dry extract (Rumpf et al., 2023; Allaw et al., 2020). All the experiments were performed in triplicate.

Table 1
Composition of C-PC-loaded enriched transfersomes.

	Gly-transfersomes	Gly-chol-transfersomes	Hyal-transfersomes	Hyal-chol-transfersomes	Hyal-gly-transfersomes	Hyal-gly-chol-transfersomes
Phospholipid S75 (mg)	120	120	120	120	120	120
Sodium deoxycholate (mg)	20	20	20	20	20	20
Cyano- phycocyanin (mg)	20	20	20	20	20	20
Cholesterol (mg)	—	10	—	10	—	10
Glycerol 10 % (w/v), sodium chloride 0.9 % (w/v) (mL)	2	2	—	—	—	—
Sodium hyaluronate 0.1 % (w/v), sodium chloride 0.9 % (w/v) (mL)	—	—	2	2	—	—
Sodium hyaluronate 0.1 % (w/v), glycerol 10 % (w/v), sodium chloride 0.9 % (w/v) (mL)	—	—	—	—	2	2

2.10. In vitro cytocompatibility and protective effect against oxidative damages

Human keratinocytes (HaCaT, ATCC collection, Manassas, VA, US) were grown as monolayers under 100 % humidity and 5 % CO_2 at 37 °C in Dulbecco Modified Eagle medium containing 10 % fetal bovine serum, 1 % penicillin/streptomycin, and Fungizone. To assess the viability, cells were seeded in 96-well plates ($1x10^4$ cells/well) and incubated in the previous culture conditions for 24 h. Thereafter, the medium was withdrawn and replaced with C-PC in solution or loaded in enriched transfersomes, properly diluted with fresh medium at final C-PC concentrations of 1000, 100, 10, and 1 μg/mL. Untreated cells were used as positive control. After 24 h, media were discarded and replaced with 100 μL of MTT solution (0.5 mg/mL, final concentration), and cells were incubated for an additional 3 h. MTT solution was then removed, dimethyl sulfoxide (DMSO) was added, and absorbance was measured at 570 nm with a microplate reader (BioTek Epoch-SN, Agilent, USA). Cell viability was calculated as a percentage of live cells versus untreated control cells (100 % viability).

To assess the efficacy of the formulations in counteracting hydrogen peroxide-induced cell death, 24 h after seeding, cells were stressed with hydrogen peroxide (0.25 mM) and subsequently treated for 4 h with samples (C-PC in solution or loaded in enriched transfersomes) adjusted to a final concentration of 10 μg/mL of C-PC in the medium. Lastly, the MTT solution (0.5 mg/mL, final concentration) was added, and absorbance was measured at 570 nm (BioTek Epoch-SN, Agilent, USA) 3 h later after adding DMSO. Untreated cells (100 % viability) were used as a positive control, while those stressed with hydrogen peroxide and not treated with C-PC samples were used as a negative control.

2.11. Ex vivo skin-permeation study of C-PC

Ex vivo skin permeation studies of C-PC were performed using Bronaugh-type flow-through diffusion cells, following a previously described method (Galinytė et al., 2024).

Abdominal skin samples from Caucasian women were obtained from the Department of Plastic and Reconstructive Surgery at the Hospital of the Lithuanian University of Health Sciences after cosmetic procedures, with ethical approval from the Kaunas Region Bioethical Committee (approval code BE-2-42, 3 May 2023). The effective diffusion area of the cells was 0.64 cm^2. Skin samples ($n = 3$ per formulation) were pre-equilibrated in PBS solution at 25 °C for 12 h before applying 0.5 mL of C-PC (10 mg/mL) in solution or loaded in transfersomes in the donor compartment. A C-PC solution containing 15 % (v/v) of propylene glycol (PG) was used as a positive control due to the well-known penetration enhancer properties of PG (Mistry and Notman, 2024). The diffusion cells were sealed with Parafilm and covered with aluminum foil to prevent light exposure. The tests were performed for 24 h at 37 °C.

Following the experiment, the skin specimens were rinsed with PBS, fixed in 4 % (v/v) formalin for 3 h, washed with PBS, and incubated in 30 % (w/v) sucrose for 12 h. The skin samples were embedded in Shandon Cryomatrix compound (Thermo Fisher Scientific, Waltham, MA, USA), frozen at −60 °C, sectioned at 20 μm using a cryostat microtome (Microm HM 560, Leica, Wetzlar, Germany), and analyzed via confocal laser scanning microscopy (CLSM) (LSM 700, ZEISS, Oberkochen, Germany). C-PC was detected using a 639 nm diode laser, with excitation at 651 nm and emission at 670 nm. Tissue auto-fluorescence was filtered using Cy3 filter, and emission was digitally assigned to the green channel. Images with a field size of 2048 μm × 2048 μm were captured with a Plan-Apochromat 20× objective (numerical aperture, NA = 0.55). Transverse skin-section images were collected using ZEN 2010 software, and the z-stack method was employed to evaluate C-PC accumulation in the skin.

2.12. Statistical analysis of data

Statistical analysis was performed using IBM SPSS Statistics version 29.0 (SPSS Inc., Chicago, IL, USA). Results were presented as mean and standard deviation. One-way ANOVA was applied for independent sample comparisons, whereas repeated-measure ANOVA was used for dependent sample comparisons. A significance level of $p < 0.05$ was considered statistically significant.

3. Results

3.1. Vesicle preparation and characterization

Enriched transfersomes were formulated to deliver C-PC, extracted from cyanobacterial biomass to the skin. The purified C-PC used in this study exhibited a high purity of 3.227 ± 0.045. Sodium deoxycholate was combined with the phospholipid S75 to formulate basic transfersomes, which were further enriched with glycerol, sodium hyaluronate, or their combination to ensure the formation of highly deformable vesicles suitable for cutaneous application. All nanosystems were prepared either with or without cholesterol (chol) to evaluate its role in modulating the accumulation and penetration of C-PC into and through the skin. To preserve the structural stability of C-PC- particularly in the presence of organic solvents or under stressful conditions (i.e., high temperatures), which are often required for proper phospholipid vesicle assembly- C-PC was loaded using an active approach, also known as remote drug loading (Pisani et al., 2023). This method involves loading

the active compound after the production of empty liposomes and is typically based on diffusion across the surface of the liposomes (gradient loading) (Antimisiaris, 2021). Accordingly, empty transfersomes were first prepared via direct sonication. C-PC was then incorporated into the pre-formed empty transfersomes at a concentration of 10 mg/mL using ultrasonic bath sonication.

The structure and morphology of C-PC-loaded transfersomes were visualized using cryo-TEM (Fig. 1). Gly-transfersomes (Fig. 1a) and Gly-chol-transfersomes (Fig. 1b) appeared small, spherical, unilamellar, and homogeneously dispersed. In contrast, Hyal-transfersomes (Fig. 1c) and Hyal-chol-transfersomes (Fig. 1d) were slightly larger, with visible bi- and oligo-lamellar structures. The larger size of these vesicles is likely attributable to sodium hyaluronate, which may influence vesicle assembly, hydration, and swelling properties (Elsheikh et al., 2023). Hyal-gly-transfersomes (Fig. 1e) and Hyal-gly-chol-transfersomes (Fig. 1f) were also slightly larger than Gly- and Gly-chol-transfersomes, with moderate dispersity and some lamellar structures, likely related to the presence of sodium hyaluronate. Additionally, the combination of glycerol and sodium hyaluronate likely enhances hydration and alters the assembly of the components, thereby contributing to the observed changes in vesicle size.

Dynamic laser light scattering (DLS) measurements further corroborated these findings, revealing that the particle size of the enriched transfersomes ranged from ~90 nm for Hyal-gly-chol-transfersomes to ~115 nm for Hyal-gly-transfersomes (Table 2). The inclusion of cholesterol slightly reduced vesicle size, likely due to its role in stabilizing and tightening the bilayer structure (Chakraborty et al., 2020).

The polydispersity index values ranged from ~0.07 for Hyal-transfersomes to ~0.17 for Gly-transfersomes and Gly-chol-transfersomes, indicating a high degree of homogeneity across all formulations. These narrow PI values were consistent with the uniformly dispersed vesicles observed in the cryo-TEM images.

Zeta potential measurements ranged from ~−33 mV for Gly-transfersomes to ~−44 mV for Hyal-chol-transfersomes. All formulations exhibited a high negative surface charge (less than −30 mV), suggesting systems with sufficient electrostatic repulsion. Overall, cholesterol-containing formulations displayed more negative ZP values, which may lead to enhanced stability (Honary and Zahir, 2013).

Table 2
Mean diameter (MD), polydispersity index (PI), zeta potential (ZP) and encapsulation efficiency (EE) of C-PC-loaded enriched transfersomes. Mean values and standard deviations are reported (n = 3). The same letter within the same column indicates values that are not statistically different ($p > 0.05$), while different letters denote statistically significant differences ($p < 0.05$).

	MD (nm)	PI	ZP (mV)	EE (%)
Gly-transfersomes	101.92 ± 25.92[a]	0.17 ± 0.04[a]	−32.98 ± 4.33[a]	51.56 ± 4.41[a]
Gly-chol-transfersomes	96.80 ± 11.91[a]	0.17 ± 0.04[a]	−36.44 ± 3.23[a]	51.51 ± 4.78[a]
Hyal-transfersomes	108.13 ± 1.45[a]	0.07 ± 0.02[a]	−34.98 ± 0.95[a]	36.31 ± 3.00[b]
Hyal-chol-transfersomes	101.60 ± 18.81[a]	0.13 ± 0.06[a]	−43.69 ± 0.95[b]	37.14 ± 4.05[b]
Hyal-gly-transfersomes	115.15 ± 12.05 [a]	0.16 ± 0.02[a]	−39.12 ± 0.26[b]	32.92 ± 2.52[b]
Hyal-gly-chol-transfersomes	90.08 ± 12.22[a]	0.13 ± 0.03[a]	−37.41 ± 0.76[a]	35.42 ± 3.24[b]

Encapsulation efficiency of C-PC varied significantly among the formulations after purification (Spectra/Por 300 kDa). The highest EE were observed for Gly-transfersomes (51.56 ± 4.41 %) and Gly-chol-transfersomes (51.51 ± 4.78 %), in contrast to the other formulations, which ranged from ~33 % to ~37. Cholesterol did not appear to have a substantial effect on this parameter.

Characterization results indicated that Gly-transfersomes and Gly-chol-transfersomes were the most promising formulations due to their superior C-PC encapsulation, highly negative superficial charge, uniform size, and narrow polydispersity. Cryo-TEM supported the successful formation of the nanosystems, revealing their structure as

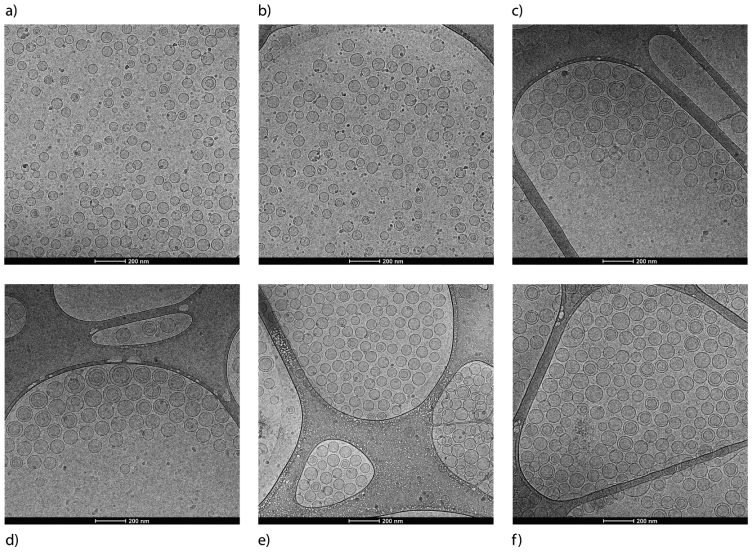

Fig. 1. Representative cryo-TEM images of C-PC- loaded enriched transfersomes: (a) Gly-transfersomes; (b) Gly-chol-transfersomes; (c) Hyal-transfersomes; (d) Hyal-chol-transfersomes; (e) Hyal-gly-transfersomes; (f) Hyal-gly-chol-transfersomes.

spherical, unilamellar, or oligolamellar vesicles.

3.2. Stability of C-PC-loaded transfersomes

The stability of transfersomes was assessed by measuring their mean diameter, polydispersity index, zeta potential at 30-day intervals over an 8-month storage period at 4 °C, under refrigerated and light-protected conditions.

No changes in the color of any transfersome formulation were observed throughout the storage period. While all formulations consistently exhibited negative zeta potential values, significant variations in mean diameter and polydispersity index were observed depending on the composition. Particle size analysis revealed that Gly-transfersomes, Gly-chol-transfersomes, Hyal-gly-transfersomes, and Hyal-gly-chol-transfersomes were the most stable, showing no substantial changes in mean diameter compared to the initial time point (t0) (Fig. 2). In contrast, Hyal-transfersomes and Hyal-chol-transfersomes exhibited marked increases in particle size starting from the 4th to 5th month, suggesting aggregation and vesicle fusion, and indicating limited long-term stability. Along with the size, the polydispersity index of these formulations increased from values <0.2 to values ≥0.3, indicating the formation of heterogeneous vesicle populations with varying sizes-consistent with the observed increase in mean diameter. Overall, glycerol appeared to play a key role in enhancing formulation stability by mitigating hyaluronate-related fusion processes, even in the systems containing both components (i.e., Hyal-gly-transfersomes and Hyal-gly-chol-transfersomes).

3.3. Antioxidant activity of C-PC-loaded enriched transfersomes with respect to the solution

The scavenging of C-PC, in solution or loaded in enriched transfersomes, was measured by DPPH assay and expressed as both Antioxidant Activity (AA) and Trolox Equivalent Antioxidant Capacity (TEAC) (Table 3).

Table 3
Antioxidant activity (AA, expressed as %) and Trolox Equivalent Antioxidant Capacity (TEAC, expressed as μmol of Trolox Equivalents (TE)/g of dry C-PC) of C-PC in solution or loaded in enriched transfersomes. The same letter within the same column indicates statistically different values ($p < 0.05$) from those of the C-PC solution.

	AA (%)	TEAC (μmol TE/g)
Gly-transfersomes	42.1 ± 2.1[a]	26.8 ± 1.3[a]
Gly-chol-transfersomes	41.9 ± 4.0[a]	26.6 ± 2.4[a]
Hyal-transfersomes	37.8 ± 1.9[a]	24.2 ± 1.1
Hyal-chol-transfersomes	39.2 ± 1.5[a]	25.0 ± 1.0
Hyal-gly-transfersomes	40.8 ± 4.5[a]	25.9 ± 2.7[a]
Hyal-gly-chol-transfersomes	41.7 ± 2.9[a]	26.5 ± 1.7[a]
C-PC solution	36.4 ± 1.8	23.3 ± 1.1

The C-PC solution's Antioxidant Activity was ~36 %, which corresponds to 23.3 μmol of Trolox Equivalents (TE)/g of dry C-PC. These values were slightly lower than those provided by the enriched transfersomes, which ranged from ~38 % to ~42 % for the Antioxidant Activity and from ~24 μmol TE/g to ~27 μmol TE/g for the Trolox Equivalent Antioxidant Capacity. These small differences might be due to the weak intrinsic antioxidant activity of transfersomes, whose main phospholipid – S75 – contains phosphatidylcholine and traces of α-tocopherol, as reported elsewhere (De Leo et al., 2018). Nonetheless, these results demonstrate that the encapsulation of C-PC in enriched transfersomes did not alter its antioxidant activity, thus highlighting the suitability of both the preparation method and the systems for the encapsulation of C-PC.

3.4. In vitro studies with HaCaT cells

Keratinocytes were used as the main representative cells of the outermost skin layer. Biocompatibility was assayed by adding C-PC in

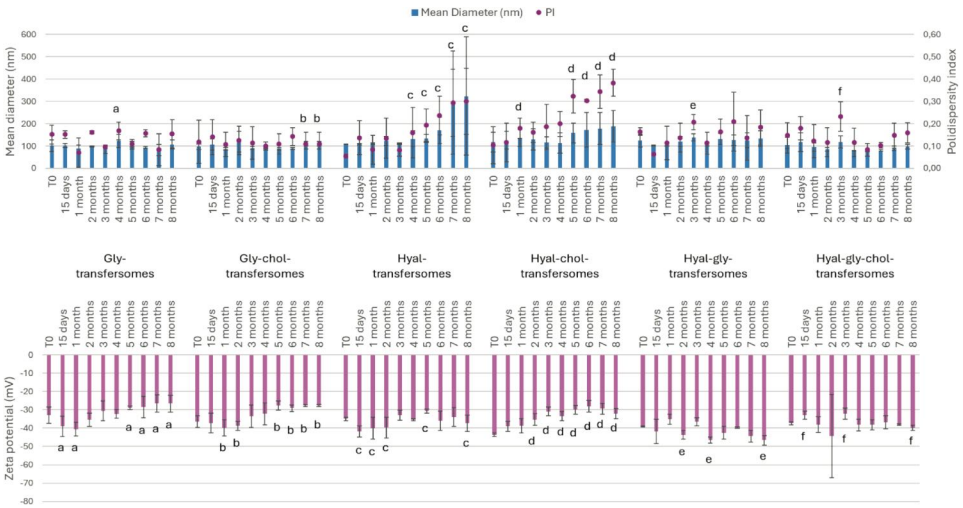

Fig. 2. Mean diameter (MD), polydispersity index (PI), and zeta potential (ZP) of enriched transfersomes containing C-PC during 8 months of storage at 4 °C under light-protected conditions. Mean values and standard deviations of at least three replicates are reported. Within each formulation group (Gly-transfersomes, Gly-chol-transfersomes, Hyal-transfersomes, Hyal-chol-transfersomes, Hyal-gly-transfersomes, or Hyal-gly-chol-transfersomes), the same letter indicates a statistically significant difference ($p < 0.05$) from the corresponding t_0 value for mean diameter and zeta potential.

solution or loaded into enriched transfersomes after dilution with cell medium to final concentrations of 1000, 100, 10, and 1 μg/mL (Fig. 3, a). The highest dose tested (1000 μg/mL) was clearly cytotoxic, as cell viability dropped below 45 % for all the enriched transfersomes, regardless of the composition. Cell viability was lower for enriched transfersomes than the solution possibly due to the carrier composition and the very high dose tested. Nonetheless, also the C-PC solution, at the same dose, reduced cell viability to ~45 %. Notably, Gly-transfersomes and Gly-chol-transfersomes provided higher viability than Hyal-gly-transfersomes and Hyal-gly-chol-transfersomes. At a 100 μg/mL dose, viability was ~80 %, with no differences between encapsulated and unencapsulated C-PC. Similarly, no differences were detected when testing the 10 and 1 μg/mL concentrations, which yield cell viability >90 % and >100 %, respectively.

The 10 μg/mL dose was selected to evaluate the protective effects against H_2O_2-induced oxidative stress on the same cell line, finding a compromise between cell viability and DPPH results (Fig. 3, b). When cells were only treated with H_2O_2, cell viability decreased to ~60 %. On the contrary, when C-PC was added in solution or loaded into enriched transfersomes, cell viability increased to ~80 % with no substantial differences between the formulations. No differences were also detected between encapsulated and unencapsulated C-PC. These results further confirm the suitability of the preparation method and nanosystems in preserving the antioxidant activity of C-PC, thus also reinforcing the DPPH assay results.

3.5. *Ex vivo qualitative assessment of C-PC skin permeation from experimental formulations*

Based on the characteristics, stability and biocompatibility data, Gly-transfersomes and Gly-chol-transfersomes were selected as the most promising candidates for an *ex vivo* skin penetration study. This study compared the accumulation and penetration of C-PC into and through the skin from the selected enriched transfersomes with those of a C-PC solution in PBS and a C-PC solution in PBS containing 15 % (v/v) propylene glycol (PG), a well-known penetration enhancer used as a positive control (Fig. 4). All formulations were tested at the same C-PC concentration of 10 mg/mL, exploiting the intrinsic fluorescence of C-PC for qualitative assessment (Fig. 4, **C-PC channel**). Skin autofluorescence was excluded from the analysis (Fig. 4, **Skin autofluorescence**).

C-PC in PBS solution exhibited limited skin penetration, likely due to its high molecular weight and hydrophilic nature, with fluorescence being nearly undetectable in the C-PC channel. As expected, the addition of PG to the PBS solution slightly enhanced C-PC penetration into the outermost skin layer, as indicated by the appearance of a narrow fluorescent band. In contrast, the enriched transfersomes significantly improved C-PC penetration and accumulation within the upper skin layers, as evidenced by more pronounced fluorescent signal across the skin surface compared to both the PBS solution and the positive control. Among the transfersomes, those lacking cholesterol exhibited slightly more intense and broader fluorescence than the Gly-chol-transfersomes, likely due to their more flexible bilayer structure.

4. Discussion

In this study, enriched transfersomes were selected to enhance the accumulation and penetration of C-PC into and through the skin, leveraging the unique properties of these vesicular systems for cutaneous administration of large, sensitive, and hydrophilic molecules. To the best of our knowledge, this is the first report describing the use of such systems for the topical administration of C-PC. Recent research has highlighted the advantages of transfersomes over conventional liposomes, especially in terms of elasticity and deformability, which enable them to cross the skin barrier structures, such as the stratum corneum, and reach the deeper layers of the epidermis and dermis (Akl et al., 2024; Sapkota et al., 2023). These vesicles exhibit self-regulating and adaptive properties under mechanical stress, facilitating efficient passage through skin pores with minimal energy input (Kumbhar et al., 2024). Structurally, transfersomes consist of phospholipids and edge activators, typically used at concentrations ranging from 10 to 25 % w/v (Kumbhar et al., 2024; Phatale et al., 2022). In this study, sodium deoxycholate was selected as the edge activator due to its biocompatibility and its ability to destabilize the lipid bilayer, reduce interfacial tension, increase fluidity and elasticity, and enhance the ability of

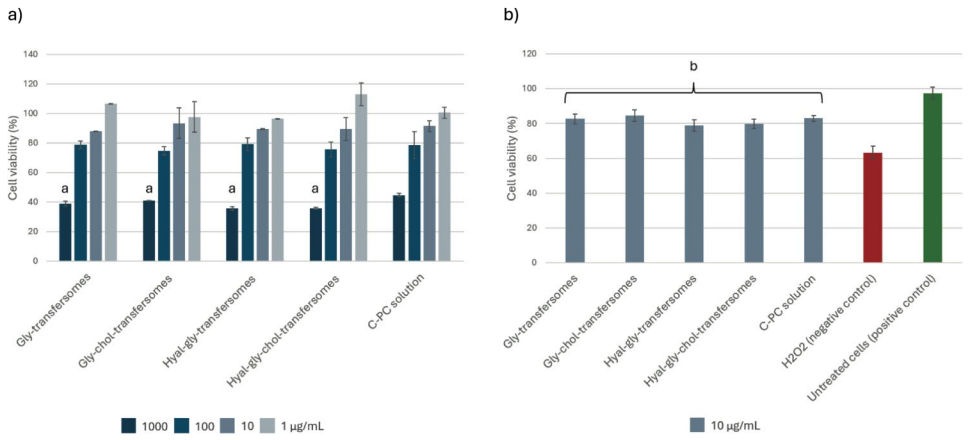

Fig. 3. a) Viability (%) of HaCaT cells incubated for 24 h with C-PC in solution or loaded into enriched transfersomes at final concentrations of 1000, 100, 10, and 1 μg/mL. Untreated cells were used as a positive control and represent 100 % viability. The same letter indicates statistically different values ($p < 0.05$) from those of the C-PC solution. b) Viability (%) of HaCaT cells stressed with H_2O_2 0.25 mM and treated with C-PC in solution or loaded into enriched transfersomes at 10 μg/mL concentration. Untreated cells were used as a positive control, whereas cells stressed with H_2O_2 served as a negative control. Mean values ± standard deviations are reported ($n = 8$). The same letter indicates statistically different values ($p < 0.05$) from those stressed with H_2O_2 (negative control).

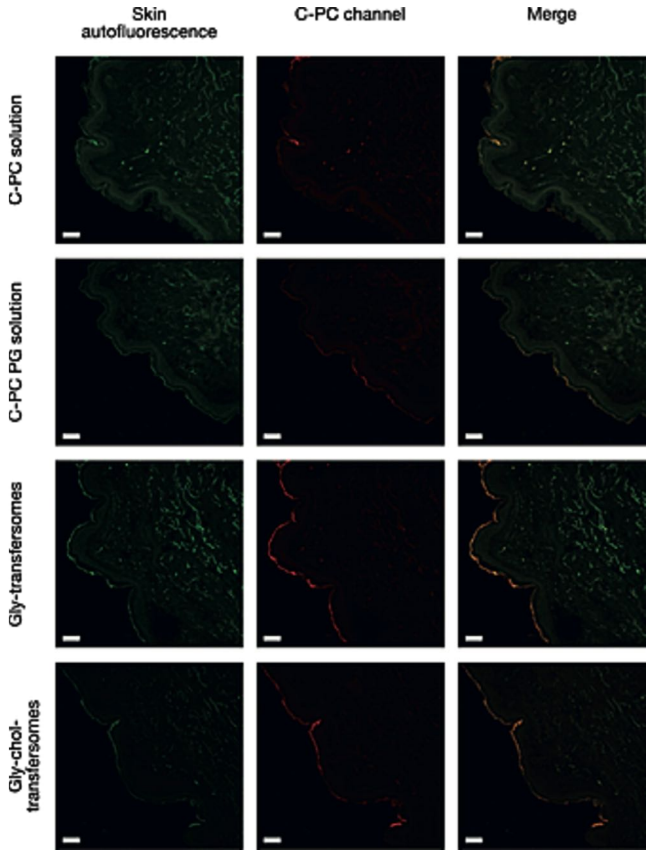

Fig. 4. Confocal images of human skin sections after treatment with C-PC in PBS solution (upper panel), in PBS solution with 15 % (v/v) propylene glycol (medium upper panel, positive control), loaded in Gly-transfersomes (medium lower panel), and loaded in Gly-chol-transfersomes (lower panel). Scale bar: 50 μm. The experiment was performed in triplicate.

vesicles to adapt to the narrow skin pores (Akl et al., 2024; Guillot et al., 2023). Soy lecithin was chosen as the primary phospholipid component for its ability to improve transfersome stability compared to egg lecithin (Kumbhar et al., 2024). To further enhance deformability and skin spreadability, glycerol, sodium hyaluronate, or both were incorporated into the formulations, resulting in enriched systems such as Gly-transfersomes, Hyal-transfersomes, and Hyal-gly-transfersomes, respectively. Glycerol was included for its humectant and penetration-enhancing properties as well as its ability to improve vesicle stability and flexibility (Sapkota et al., 2023; Manca et al., 2016; Alam et al., 2023). Additionally, it increases formulation viscosity, facilitating topical application (Manca et al., 2017; Zhu et al., 2022). Sodium hyaluronate was included for its well-known hydrating and skin regenerating properties (Zhu et al., 2020). Hyaluronic acid-based vesicles, known as hyalurosomes, have demonstrated efficacy in delivering bioactive compounds, such as curcumin or licorice extract, while also promoting skin restoration and providing effective protection against oxidative stress (Manca et al., 2015; Castangia et al., 2015). Furthermore, C-PC-loaded hyalurosomes have been shown to enhance its antioxidant activity in stressed human keratinocytes and promote deeper skin deposition compared to C-PC in solution (Castangia et al., 2016). In another study, Aroffu et al. showed that enriched transfersomes containing glycerol, hyaluronic acid or both promoted protein accumulation in the epidermis and dermis (Aroffu et al., 2024). Based on this, enriched transfersomes were selected as carriers for C-PC, with additional cholesterol introduced in selected formulations (Gly-chol-transfersomes, Hyal-chol-transfersomes, and Hyal-gly-chol-transfersomes) to evaluate its effects on the main physico-chemical, technological and biological properties of these nanosystems. Although cholesterol is known to stabilize vesicle membranes by increasing rigidity and reducing drug leakage, no significant differences were observed in our study regarding stability or encapsulation efficiency (Akl et al., 2024; Kumbhar et al., 2024; Manca et al., 2017; Shah et al., 2020). Higher concentrations of cholesterol may improve stability but may also reduce vesicle deformability and impair penetration (Duangjit et al., 2011).

All enriched transfersomes were prepared using a two-step method to ensure uniformity and avoid the use of organic solvents. This approach was essential for preserving the structural integrity of C-PC, a highly temperature-sensitive protein. Previous studies have reported that C-PC stability decreases significantly at temperatures exceeding 45–47 °C, with accelerated degradation at higher temperatures (Yuan et al., 2022; Huo et al., 2022). In preliminary experiments, direct sonication of C-PC with transfersome-forming agents resulted in approximately 20–60 % degradation of C-PC (data not shown). To prevent this, C-PC was added to preformed empty transfersomes and gently sonicated in an ultrasonic bath at a controlled temperature of 25–30 °C. This method was developed combining different approaches described in the literature to prepare vesicles encapsulating C-PC (Castangia et al., 2016; Manconi et al., 2010). Notably, the DPPH assay confirmed the suitability of this method in preserving the structural integrity of C-PC as Antioxidant activity and Trolox Equivalent Antioxidant Capacity values were comparable regardless of whether C-PC had undergone the preparation process.

To achieve efficient penetration of C-PC into the skin, lipid vesicles must possess key properties, including mean diameter, polydispersity index, zeta potential, encapsulation efficiency, and stability (Guillot et al., 2023). The enriched transfersomes obtained were small, with an average size ranging from ~90 nm to ~115 nm, and uniformly dispersed, with PI values <0.2, thus suitable for skin delivery. Indeed, homogeneous phospholipid vesicles with a diameter of 300 nm or smaller are reported to partially deliver their contents into deeper skin layers, especially when they are flexible (Danaei et al., 2018). Unilamellar structures were predominant in glycerol-based formulations (Gly-transfersomes and Gly-chol-transfersomes) whereas oligolamellar structures were observed in hyaluronate- containing systems (Mistry and Notman, 2024). Generally, oligolamellar and multilamellar vesicles are larger due to multiple aqueous compartments and may exhibit extended-release profiles, making them beneficial for sustained release. In contrast, unilamellar vesicles are more commonly associated with the rapid release of encapsulated material (Rumpf et al., 2023). Hydrophilic compounds are generally associated with lower encapsulation efficiencies (10–50 %) due to their tendency to remain in the aqueous phase rather than integrate into the vesicular structure (Guillot et al., 2023). In this study, Gly-transfersomes and Gly-chol-transfersomes exhibited the highest encapsulation efficiencies (~52 %), thus in line with the literature. Cholesterol did not significantly affect encapsulation efficiency. By contrast, the addition of sodium hyaluronate resulted in lower encapsulation efficiencies (~33–37 %), suggesting that fewer components may lead to higher encapsulation. Such a trend was not observed by Aroffu et al., who's enriched transfersomes featured only 5 mg/mL of sodium deoxycholate, suggesting a contribution of this compound in the decrease of encapsulation efficiencies in the case of C-PC-loaded Hyal-transfersomes (Aroffu et al., 2024). Nevertheless, preliminary data from our study indicated that a concentration of 10 mg/mL sodium deoxycholate was more suitable for formulating enriched transfersomes with appropriate characteristics to deliver large, aggregation-prone proteins such as C-PC (data not shown).

Since temperature plays a crucial role in vesicle stability, the enriched transfersomes were stored at 4 °C in a refrigerator and protected from light for 8 months. Their main physicochemical parameters (i.e., MD, PI, and ZP) were monitored every 30 days. The formulations containing glycerol (Gly-transfersomes, Gly-chol-transfersomes, Hyal-gly-transfersomes, and Hyal-gly-chol-transfersomes) exhibited the highest stability as all parameters remained unchanged throughout the observation period. This is likely due to glycerol's stabilizing effect on phospholipid bilayers, which helps maintain vesicle structure during storage (Sapkota et al., 2023; Manca et al., 2016; Alam et al., 2023). In contrast, formulations lacking glycerol but containing sodium hyaluronate (Hyal- transfersomes and Hyal-chol-transfersomes) showed significant increases in particle size and PI after 4–5 months, indicating instability. These were therefore excluded from subsequent *in vitro* studies.

Cytotoxicity studies, conducted on human keratinocytes, revealed similar responses to both free C-PC and the C-PC-loaded enriched transfersomes (Gly-transfersomes, Gly-chol-transfersomes, Hyal-gly-transfersomes, and Hyal-gly-chol-transfersomes) when tested at a concentration of 1000 μg/mL. Comparable cytotoxic effects at similar concentrations were previously reported for free C-PC by Puglisi et al. (Puglisi et al., 2022). At lower concentrations (1 and 10 μg/mL), all formulations were non-cytotoxic, aligning with published data (Jang and Kim, 2021). The C-PC concentration of 10 μg/mL was selected to evaluate protection against H_2O_2-induced oxidative stress. Exposure to H_2O_2 reduced cell viability by ~40 %, whereas treatment with C-PC in solution or loaded in vesicles restored cell viability to ~80 %, demonstrating a protective effect against oxidative stress. These results are consistent with those reported by Castangia et al., confirming that the encapsulation method did not impair the biological activity of C-PC (Castangia et al., 2016).

Considering the outcomes of physicochemical characterization, stability, and biological studies, Gly-transfersomes and Gly-chol-transfersomes were selected to evaluate C-PC skin accumulation *ex vivo*. A comparison was made between a) C-PC-loaded enriched transfersomes, b) C-PC in PBS, and c) C-PC in PBS with 15 % (v/v) of PG (positive control). The latter was selected as a positive control due to its previously demonstrated ability to enhance C-PC delivery into the stratum corneum (Galinytė et al., 2024). As expected, when applied as a plain solution, C-PC failed to penetrate the stratum corneum and was nearly undetectable. PG improved C-PC deposition in the stratum corneum, though its effect was limited. In contrast, C-PC delivered via Gly-transfersomes and Gly-chol-transfersomes showed significantly higher accumulation, as evidenced by stronger fluorescent signals. Direct comparison between studies is difficult due to methodological differences, including the use of varying skin models and experimental conditions. Nevertheless, overall findings seem to support the superior performance of vesicular carriers, especially when modified. For instance, C-PC-loaded PEG-hyalurosomes applied to newborn pig skin resulted in detectable protein accumulation in both the epidermis and dermis after 8 h (Castangia et al., 2016). In contrast, liposomal formulations tested on human skin failed to achieve transdermal permeation, with only limited accumulation in the upper layers and approximately 3 % of the applied dose retained (Manconia et al., 2009). In this study, the observed higher accumulation of C-PC in the stratum corneum may indicate the formation of a surface reservoir, from which the active compound could be gradually released to the deepest skin layers over time. This accumulation may be particularly useful for cosmetic or preventive dermatological applications where antioxidant protection is desired (i.e., UV radiation and environmental pollutants) (Castangia et al., 2016; Manconia et al., 2009; Sapkota et al., 2023).

5. Conclusions

This study demonstrated the successful development of enriched transfersomes for C-PC skin delivery. Gly-transfersomes and Gly-chol-transfersomes exhibited the highest encapsulation efficiency and stability, outperforming sodium hyaluronate-enriched formulations. The gentle two-step preparation approach was effective in preserving the delicate structure of C-PC, as confirmed by DPPH assay and biological tests. *Ex vivo* studies demonstrated the superior ability of Gly-transfersomes and Gly-chol-transfersomes to enhance C-PC accumulation in the stratum corneum compared to the C-PC solution, regardless of the presence of a penetration enhancer such as PG. Considering the protective effects observed at a cellular level, enriched transfersomes carrying C-PC hold strong potential for preventive skin care applications against ROS inducers such as UV radiation and environmental pollutants. Nonetheless, further studies are needed to quantitatively evaluate the deposition of C-PC in the skin via these enriched transfersomes.

Funding: This research did not receive any specific grant from

funding agencies in the public, commercial, or not-for-profit sectors.

Institutional Review Board Statement: The study was conducted in accordance with the Declaration of Helsinki and approved by the Institutional Review Board (or Ethics Committee) of the Kaunas Region Bioethical Committee (protocol code BE-2–42, date of approval: 3 May 2023).

CRediT authorship contribution statement

Daiva Galinytė: Writing – original draft, Visualization, Validation, Software, Methodology, Investigation, Formal analysis, Data curation, Conceptualization. **Matteo Aroffu:** Writing – review & editing, Validation, Software, Methodology, Investigation, Formal analysis. **Maria Manconi:** Writing – review & editing. **Modestas Žilius:** Validation, Methodology, Formal analysis. **Kristina Rysevaitė-Kyguolienė:** Methodology. **Jūratė Karosienė:** Resources, Methodology, Formal analysis. **Judita Koreivienė:** Resources. **Vitalis Briedis:** Resources. **Dainius Haroldas Pauža:** Resources. **Arūnas Savickas:** Methodology. **Elvira Escribano Ferrer:** Methodology, Formal analysis. **Maria Letizia Manca:** Writing – review & editing, Validation, Supervision, Resources, Methodology, Investigation, Conceptualization. **Nijolė Savickienė:** Writing – review & editing, Visualization, Validation, Supervision, Project administration, Methodology, Investigation, Conceptualization.

Declaration of competing interest

The authors declare that they have no known competing financial interests or personal relationships that could have appeared to influence the work reported in this paper.

Data availability

The data supporting the findings of this study are available from the corresponding author [D.G.] upon reasonable request.

References

Adjali, A., Clarot, I., Chen, Z., Marchioni, E., Boudier, A., 2022. Physicochemical degradation of phycocyanin and means to improve its stability: a short review. J. Pharm. Anal. 12, 406–414.

Agrawal, M., Bansal, S., Chopra, K., 2021. Evaluation of the in vitro and in vivo antioxidant potentials of food grade Phycocyanin. J. Food Sci. Technol. 58, 4382–4390.

Akl, M.A., Eldeen, M.A., Kassem, A.M., 2024. Beyond skin deep: phospholipid- based nanovesicles as game- changers in transdermal drug delivery. AAPS PharmSciTech 25 (6), 184.

Alam, M.S., Sultana, N., Rashid, M.A., Alhamhoom, Y., Ali, A., Waheed, A., Ansari, M.S., Aqil, M., Mujeeb, M., 2023. Quality by design-optimized glycerosomes- enabled nanosunscreen gel of rutin hydrate. Gels 9, 752.

Algae – economy based ecological service of aquatic ecosystems. Layman's Report. 2023. https://algaeservice.gamtostyrimai.lt/wp-content/uploads/2023/12/Laymans-report-EN-2023-12-06.pdf (accessed on 5 Feb 2025).

Alka, Singh, P., Pal, R.R., Mishra, N., Singh, N., Verma, A., Saraf, S.S., 2024. Development of pH-sensitive hydrogel for advanced wound healing: Graft copolymerization of locust bean gum with acrylamide and acrylic acid. Int. J. Pharm. 661, 124450.

Allaw, M., Pleguezuelos-Villa, M., Manca, M.L., Caddeo, C., Aroffu, M., Nacher, A., Díez-Sales, O., Ruiz Saurí, A., Escribano Ferrer, E., Fadda, A.M., Manconi, M., 2020. Innovative strategies to treat skin wounds with mangiferin: fabrication of transfersomes modified with glycols and mucin. Nanomedicine 15 (17), 1671–1685.

Allaw, M., Pleguezuelos- Villa, M., Manca, M.L., Caddeo, C., Aroffu, M., Nacher, A., Diez-Sales, O., Sauri, A.R., Ferrer, E.E., Fadda, A.M., Manconi, M., 2020. Innovative strategies to treat skin wounds with magniferin: fabrication of transfersomes modified with glycols and mucin. Nanomedicine (Lond.) 15 (17), 1671–1685.

Andonova, V., Nikolova, K., Iliev, I., Georgieva, S., Petkova, N., Feizi-Dehnayebi, M., Nikolova, S., Gerasimova, A., 2024. Spectral characteristics, in silico perspectives, density functional theory (DFT), and therapeutic potential of green- extracted phycocyanin from spirulina. Int. J. Mol. Sci. 25, 9170. https://doi.org/10.3390/ijms25179170.

Antimisiaris, S.G. (Ed.), 2021. Liposomes in Drug Delivery: What, Where, How and When to Deliver, first ed. Academic Press, Cambridge, MA, USA, pp. 101–120.

Aodah, H.A., Hashmi, S., Akhtar, N., Ullah, Z., Zafar, A., Zaki, R.M., Khan, S., Ansari, M. J., Jawaid, T., Alam, A., Ali, M.S., 2023. Formulation development, optimization by box–behnken design, and in vitro and ex vivo characterization of hexatriacontane–loaded transethosomal gel for antimicrobial treatment for skin infections. Gels 9, 322.

Aroffu, M., Abi Rached, R., Castangia, I., Italiani, P., D'Apice, L., Fernández-Busquets, X., Nacher, A., Manconi, M., Pedraz, J.L., Manca, M., 2024. A preliminary investigation on hydrogel disks imbibed with enriched transfersomes as a promising tool to promote the cutaneous deposition of vaccine antigens. J. Drug Delivery Sci. Technol. 102, 106399.

Bennett, A., Bogorad, L., 1973. Complementary chromatic adaption in a filamentous blue-green alga. J. Cell Biol. 58, 419–435.

Castangia, I., Caddeo, C., Manca, M.L., Casu, L., Latorre, A.C., Diez-Sales, O., Ruiz-Sauri, A., Fadda, B.G., Manconi, A.M., 2015. Delivery of liquorice extract by liposomes and hyalurosomes to protect the skin against oxidative stress injuries. Carbohydr. Polym. 134, 657–663.

Castangia, I., Manca, M.L., Catalan-Latorre, A., Maccioni, A.M., Fadda, A.M., Manconi, M., 2016. Phycocyanin- encapsulating hyalurosomes as carrier for skin delivery and protection from oxidative stress damage. J. Mater. Sci. – Mater. Med. 27, 75.

Castangia, I., Manca, M.L., Caddeo, C., Bacchetta, G., Pons, R., Demurtas, D., Diez-Sales, O., Fadda, A.M., Manconi, M., 2016. Santosomes as natural and efficient carriers for the improvement of phycocyanin reepithelising ability in vitro and in vivo. Eur. J. Pharm. Biopharm. 2016 (103), 149–158.

Chakraborty, S., Doktorova, M., Molugu, T.R., Heberle, F.A., Scott, H.L., Dzikovski, B., Nagao, M., Stingaciu, L.-R., Standaert, R.F., Barrera, F.N., Katsaras, J., Khelashvili, G., Brown, M.F., Ashkar, R., 2020. How cholesterol stiffens unsaturated lipid membranes. PNAS 117 (36), 21896–21905. https://doi.org/10.1073/pnas.2004807117.

Dahmen, I., Chtourou, H., Hadrich, F., Baccar, N., Sayadi, S., Ayadi, H., Chamkha, M., 2024. Phormidium versicolor PC skin cream evaluation for its stability and biological activities. Appl. Microbiol. Biotechnol. 108, 541. https://doi.org/10.1007/s00253-024-13359-0.

Danaei, M., Dehghankhold, M., Ataei, S., Hasanzadeh Davarani, F., Javanmard, R., Dokhani, A., Khorasani, S., Mozafari, M.R., 2018. Impact of particle size and polydispersity index on the clinical applications of lipidic nanocarrier systems. Pharmaceutics 10, 57.

De Leo, V., Milano, F., Mancini, E., Comparelli, R., Giotta, L., Nacci, A., Longobardi, F., Garbetta, A., Agostiano, A., Catucci, L., 2018. Encapsulation of curcumin-loaded liposomes for colonic drug delivery in a pH-responsive polymer cluster using a pH-driven and organic solvent-free process. Molecules 23, 739.

Dong, J., Lang, Y., He, J., Cui, J., Liu, X., Yuan, H., Li, L., Zhou, M., Wang, S., 2025. Phycocyanin- based multifunctional microspheres for treatment of infected radiation- induced skin injury. Biomaterials 317, 123061. https://doi.org/10.1016/j.biomaterials.2024.123061.

Doustvaghe, Y.K., Haeri, A., Sisakht, M.M., Amirkhani, M.A., Vatanpour, H., 2024. Recombinant human epidermal growth factor- loaded liposomes and transferosomes for dermal delivery: development, characterization, and cytotoxicity evaluation. Drug Dev. Res. 85 (5), e22234.

Duangjit, S., Opanasopit, P., Rojanarata, T., Ngawhirunpat, T., 2011. Characterization and in vitro skin permeation of meloxicam-loaded liposomes versus transfersomes. J. Drug Deliv. 2011, 418316.

Elsheikh, M.A., Gaafar, P.M.E., Khattab, M.A., Helwah, M.K.A., Noureldin, M.H., Abbas, H., 2023. Dual-effects of caffeinated hyalurosomes as a nano-cosmeceutical gel counteracting UV-induced skin ageing. Int. J. Pharm.: X 5, 100170. https://doi.org/10.1016/j.ijpx.2023.100170.

Fulgheri, F., Aroffu, M., Ramírez, M., Román-Álamo, L., Peris, J.E., Usach, I., Nacher, A., Manconi, M., Fernàndez-Busquets, X., Manca, M.L., 2023. Curcumin or quercetin loaded nutriosomes as oral adjuvants for malaria infections. Int. J. Pharm. 643, 123195.

Galinytė, D., Bernatoniene, J., Žilius, M., Rysevaitė- Kyguolienė, K., Savickas, A., Karosienė, J., Briedis, V., Pauža, D.H., Savickienė, N., 2024. In vitro study of cyanophycocyanin release from hydrogels and ex vivo study of skin penetration. Pharmaceuticals 17, 1224.

Guillot, A.J., Martinez-Navarrete, M., Garrigues, T.M., Melero, A., 2023. Skin drug delivery using lipid vesicles: a starting guideline for their development. J. Control. Release 355, 624–654.

Honary, S., Zahir, F., 2013. Effect of zeta potential on the properties of nano-drug delivery systems – a review (Part 2). Trop. J. Pharm. Res. 12, 265–273. https://doi.org/10.4314/tjpr.v12i2.20.

Huo, Y., Hou, X., Yu, Y., Wen, X., Ding, Y., Li, Y., Wang, Z., 2022. Improving the thermal and oxidative stability of food-grade phycocyanin from arthrospira platensis by addition of saccharides and sugar alcohols. Foods 11, 1752.

Jang, Y.A., Kim, B.A., 2021. Protective effect of spirulina-derived C-phycocyanin against ultraviolet B-induced damage in HaCaT cells. Medicina 57, 273.

Khazi, M.I., Demirel, Z., Liaqat, F., Dalay, M.C., 1980. Analytical grade purification of phycocyanin from cyanobacteria, first ed. Springer, New York, NY, USA, pp. 173–179.

Kumari, S., Alsaidan, O.A., Mohanty, D., Zafar, A., Das, S., Gupta, J.K., Khalid, M., 2023. Development of soft luliconazole invasomes gel for effective transdermal delivery: optimization to in–vivo antifungal activity. Gels 9, 626.

Kumbhar, P.S., Kamble, V., Vishwas, S., Kumbhar, P., Kolekar, K., Gupta, G., Veiga, F., Paiva-Santos, A.C., Goh, B.H., Singh, S.K., Dua, K., Disouza, J., Patravale, V., 2024. Unravelling the success of transfersomes against skin cancer: journey so far and road ahead. Drug Deliv. Transl. Res. 14, 2325–2344.

Li, Y., Zhang, Z., Abbaspourrad, A., 2022. Improved pH stability, heat stability, and functionality of phycocyanin after PEDylation. Int. J. Biol. Macromol. 222, 1758–1767.

Manca, M.L., Castangia, I., Zaru, M., Nacher, A., Valenti, D., Fernandez-Busquets, X., Fadda, A.M., Manconi, M., 2015. Development of curcumin loaded sodium hyaluronate immobilized vesicles (hyalurosomes) and their potential on skin inflammation and wound restoring. Biomaterials 71, 100–109.
Manca, M.L., Cencetti, C., Matricardi, P., Castangia, I., Zaru, M., Sales, O.D., Nacher, A., Valenti, D., Maccioni, A.M., Fadda, A.M., Manconi, M., 2016. Glycerosomes: use of hydrogenated soy phosphatidylcholine mixture and its effect on vesicle features and diclofenac skin penetration. Int. J. Pharm. 511, 198–204.
Manca, M.L., Manconi, M., Zaru, M., Valenti, D., Peris, J.E., Matricardi, P., Maccioni, A. M., Fadda, A.M., 2017. Glycerosomes: Investigation of role of 1,2-dimyristoyl-sn-glycero-3- phosphatidycholine (DMPC) on the assembling and skin delivery performances. Int. J. Pharm. 532, 401–407.
Manconi, M., Mura, S., Manca, M.L., Fadda, A.M., Dolz, M., Hernandez, M.J., Casanovas, A., Díez-Sales, O., 2010. Chitosomes as drug delivery systems for C-phycocyanin: preparation and characterization. Int. J. Pharm. 392, 92–100.
Manconia, M., Pendas, J., Ledon, N., Moreira, T., Sinico, C., Saso, L., Fadda, A.M., 2009. Phycocyanin liposomes for topical anti-inflammatory activity: in vitro in vivo studies. J. Pharm. Pharmacol. 61, 423–430.
Matharoo, N., Mohd, H., Michniak- Kohn, B., 2024. Transferosomes as a transdermal drug delivery system: dermal kinetics and recent developments. Wiley Interdiscip. Rev. Nanomed. Nanobiotechnol. 16 (1), e1918.
Mistry, J., Notman, R., 2024. Mechanisms of the drug penetration enhancer propylene glycol interacting with skin lipid membranes. J. Phys. Chem. B 128, 3885–3897.
Modi, C.D., Pharadia, P.D., 2012. Transferosomes: new dominants for transdermal drug delivery. Am J Pharm Tech Res 3, 1–13.
Phatale, V., Vaiphei, K.K., Jha, S., Patil, D., Agrawal, M., Alexander, A., 2022. Overcoming skin barriers through advanced transdermal drug delivery approaches. J. Control. Release 351, 361–380.
Pisani, S., Di Martino, D., Cerri, S., Genta, I., Dorati, R., Bertino, G., Benazzo, M., Conti, B., 2023. Investigation and comparison of active and passive encapsulation methods for loading proteins into liposomes. Int. J. Mol. Sci. 24, 13542. https://doi.org/10.3390/ijms241713542.
Puglisi, R., Biazzi, E., Gesmundo, D., Vanni, R., Tava, A., Cenadelli, S., 2022. The antioxidant activity of a commercial and a fractionated phycocyanin on human skin cells in vitro. Molecules 27, 5276.
Quan, T., 2023. Molecular insights of human skin epidermal and dermal aging. J. Dermatol. Sci. 112, 48–53.
Rumpf, J., Burger, R., Schulze, M., 2023. Statistical evaluation of DPPH, ABTS, FRAP, and Folin-Ciocalteu assays to assess the antioxidant capacity of lignins. Int. J. Biol. Macromol. 233, 123470.
Saldago, M.T.S.F., Silva, E.F., Matsumoto, A.M., Mottozo, F.H., Amarante, M.C.A., Kalil, S.J., Votto, A.P.S., 2022. C-phycocyanin decreases proliferation and migration of melanoma cells: In silico and in vitro evidence. Bioorg. Chem. 122, 105757. https://doi.org/10.1016/j.bioorg.2022.105757.
Saldago, M.T.S.F., Silva, M.C.S., Fratelli, C., Braga, A.R.C., Lopes, T.B.G., Ferreira, E., Silva, I.L.D., Paiva, L.S., Votto, A.P.S., 2024. Bioactive C-phycocyanin exerts immunomodulatory and antitumor activity in mice with induced melanoma. Toxicol. Appl. Pharmacol. 484, 116874.
Sapkota, R., Munt, D.J., Kincaid, A.E., Dash, A.K., 2023. Liposomes and transfersomes in the delivery of papain for the treatment of keloids and hypertrophic scars. PLoS One 18 (12), e0290224. https://doi.org/10.1371/journal.pone.0290224.
Shah, S., Dhawan, V., Holm, R., Nagarsenker, M.S., Perrie, Y., 2020. Liposomes: Advancements and innovation in the manufacturing process. Adv. Drug Deliv. Rev. 154–155, 102–122.
Yuan, B., Li, Z., Shan, H., Dashnyam, B., Xu, W., McClements, D.J., Zhang, B., Tan, M., Wang, Z., Cao, C., 2022. A review of recent strategies to improve the physical stability of phycocyanin. Curr. Res. Food Sci. 5, 2329–2337.
Zafar, A., Yasir, M., Singh, L., Jafar, M., Warsi, M.H., Panda, D.S., 2024. Luteolin–loaded invasomes gel for transdermal delivery: development, optimization, in–vitro, and preclinical evaluation. J. Oleo Sci. 73 (9), 1221–1240.
Zewail, M., Gaafar, P.M.E., Abou Youssef, N.A.H., Ali, M.E., Ragab, M.F., Kamal, M.F., Noureldin, M.H., Abbas, H., 2025. Novel Spirulina platensis bilosomes for combating UVB induced skin damage. Pharmaceuticals 16, 36.
Zhu, J., Tang, X., Jia, Y., Ho, C.T., Huang, Q., 2020. Applications and delivery mechanisms of hyaluronic acid used for topical/transdermal delivery- a review. Int. J. Pharm. 578, 119127.
Zhu, C., Zhang, Y., Wu, T., He, Z., Guo, T., Feng, N., 2022. Optimizing glycerosome formulations via orthogonal experimental design to enhance transdermal triptolide delivery. Acta Pharm. 72, 135–146.

Paper 5

Title: Topical C-Phycocyanin-Loaded Transfersomes Attenuate Early Proinflammatory Epidermal Remodelling in a DMBA/TPA-Induced Mouse Model of Skin Dysplasia

Authors: Galinytė, Daiva; Juodžiukynienė, Nomeda; Balnytė, Ingrida; Zigmantaitė, Vilma; Karosienė, Jūratė; Bernatonienė, Jurga; Savickienė, Nijolė

Pharmaceutics, 18, 5, 600 *(2026)*

pharmaceutics

MDPI

Article

Topical C-Phycocyanin-Loaded Transfersomes Attenuate Early Proinflammatory Epidermal Remodelling in a DMBA/TPA-Induced Mouse Model of Skin Dysplasia

Daiva Galinytė [1,*], Nomeda Juodžiukynienė [2], Ingrida Balnytė [3], Vilma Zigmantaitė [4,5], Jūratė Karosienė [6], Jurga Bernatoniene [7] and Nijolė Savickienė [1]

[1] Department of Pharmacognosy, Faculty of Pharmacy, Academy of Medicine, Lithuanian University of Health Sciences, Sukilėlių av. 13, 50162 Kaunas, Lithuania; nijole.savickiene@lsmu.lt
[2] Department of Veterinary Pathobiology, Faculty of Veterinary, Academy of Veterinary, Lithuanian University of Health Sciences, Tilžės St. 18, 47181 Kaunas, Lithuania; nomeda.juodziukyniene@lsmuni.lt
[3] Department of Histology and Embryology, Faculty of Medicine, Academy of Medicine, Lithuanian University of Health Sciences, A. Mickevičiaus St. 9, 44307 Kaunas, Lithuania; ingrida.balnyte@lsmu.lt
[4] Biological Research Centre, Lithuanian University of Health Sciences, Tilžės St. 18, 47140 Kaunas, Lithuania; vilma.zigmantaite@lsmu.lt
[5] Laboratory of Membrane Biophysics, Institute of Cardiology, Lithuanian University of Health Sciences, Sukilėlių av. 15, 47181 Kaunas, Lithuania
[6] Laboratory of Algology and Microbial Ecology, State Scientific Research Institute, Nature Research Centre, Akademijos St. 2, 08412 Vilnius, Lithuania; jurate.karosiene@gamtc.lt
[7] Department of Drug Technology and Social Pharmacy, Faculty of Pharmacy, Academy of Medicine, Lithuanian University of Health Sciences, Sukilėlių av. 13, 50162 Kaunas, Lithuania; jurga.bernatoniene@lsmu.lt
* Correspondence: daiva.galinyte@stud.lsmu.lt

Abstract

Background/Objectives: Cutaneous squamous cell carcinoma (cSCC) develops through inflammation-driven preneoplastic alterations characterized by epidermal hyperplasia, dysplasia, and increased proliferative activity. C-phycocyanin (C-PC) possesses antioxidant and anti-inflammatory properties; however, its topical potential to attenuate a tumour-promoting cutaneous microenvironment is limited by poor skin penetration. This study evaluated the effects of C-PC-loaded transfersomes in a 7,12-dimethylbenz[*a*]anthracene (DMBA)/12-O-tetradecanoylphorbol-13-acetate (TPA)-induced mouse model of skin carcinogenesis. **Methods**: Male BALB/c mice were assigned to six groups (n = 10 per group). Carcinogenesis was initiated with a single topical application of DMBA, followed by twice-weekly TPA application for 16 weeks. C-PC-loaded transfersomes (1 mg/mL or 10 mg/mL) were applied topically. Histopathological assessment included epidermal thickness, rete ridge depth, mitotic activity, mast cell density, and semi-quantitative scoring of hyperplasia, dysplasia, and inflammation. Ki-67 immunohistochemistry was used to evaluate basal and suprabasal proliferation. **Results**: Carcinogen exposure induced marked epidermal thickening, severe dysplasia, increased mitotic activity, elevated Ki-67 expression, and pronounced dermal inflammation. Treatment with C-PC-loaded transfersomes significantly reduced epidermal thickness, rete ridge depth, mast cell density, mitotic counts, and suprabasal Ki-67 index. The 1 mg/mL concentration demonstrated the most consistent attenuation of dysplasia severity and inflammatory changes. No adverse histopathological alterations were observed in internal organs. **Conclusions**: These findings indicate that transfersome-mediated topical delivery of C-PC attenuates early inflammation-driven epidermal remodelling and tumour-promoting alterations in experimental skin carcinogenesis, supporting its potential as a topical preventive strategy.

Academic Editor: Montse Mitjans Arnal

Received: 16 April 2026
Revised: 7 May 2026
Accepted: 12 May 2026
Published: 14 May 2026

Keywords: c-phycocyanin; transfersomes; topical delivery; skin cancerogenesis; DMBA/TPA model; cutaneous squamous cell carcinoma; chemoprevention; Ki-67 proliferation index

1. Introduction

cSCC is one of the most common non-melanoma skin cancers and represents a growing public health concern due to its steadily increasing incidence worldwide [1]. The disease originates from an uncontrolled proliferation of atypical epidermal keratinocytes and is generally considered the result of a prolonged intraepidermal dysplastic process [2]. cSCC typically develops through a multistep progression from actinic keratosis (AK), a precancerous lesion characterized by dysplastic keratinocytes, to invasive carcinoma [2]. Ultraviolet radiation (UVR)-induced DNA damage, chronic inflammation, and local immunosuppression are central drivers of this process, leading to genetic and epigenetic alterations that disrupt epidermal homeostasis and promote pathological keratinocyte proliferation. Major risk factors include advanced age, cumulative UVR exposure, fair skin, male sex, immunosuppression, smoking, and genetic susceptibility, while human papillomavirus infection may further contribute to the development of the specific anatomical sites [1,2]. Despite advances in surgical and non-surgical management, cSCC incidence and associated morbidity continue to rise, underscoring the importance of preventive strategies targeting early, preinvasive stages of disease development.

Given that cSCC arises from a prolonged precancerous phase characterized by oxidative stress, chronic inflammation, and progressive disruption of the epidermal microenvironment, therapeutic intervention at early stages is particularly attractive. However, current preventive approaches, including UVR protection, provide only partial efficacy and are often limited by compliance, tolerability, or inconsistent clinical benefit [1]. Therefore, increasing attention has been directed toward identifying safe, biologically active compounds that can modulate key pathogenic mechanisms before irreversible malignant transformation occurs.

Natural compounds with antioxidant and anti-inflammatory properties are particularly promising in this context. Various phytochemicals, including plant polyphenols such as resveratrol, curcumin, catechins, quercetin, and honokiol have been widely investigated as chemopreventive agents against skin carcinogenesis due to their antioxidant, anti-inflammatory, DNA-protective, and antiproliferative properties [3]. However, despite promising preclinical findings, their clinical applications remain limited by poor bioavailability, rapid metabolism, and insufficient skin penetration, necessitating the development of advanced delivery strategies, including nanoengineered delivery systems to enhance their pharmacokinetic features. Moreover, there is still insufficient clinical evidence to confirm their efficacy and long-term safety [3,4]. Among existing chemopreventive approaches, retinoids represent one of the most extensively studied and clinically applied classes of agents for non-melanoma cancers, including cSCC. These compounds regulate key processes in carcinogenesis, including cell proliferation, differentiation, and inflammation. However, their clinical use remains limited due to adverse effects, including hepatotoxicity and metabolic disturbances, as well as emerging evidence of resistance development in cancer cells [5].

In this context, C-PC, a bioactive phycobiliprotein derived from cyanobacteria, has attracted increasing attention for its multifunctional biological activity. C-PC has demonstrated potent antioxidant, anti-inflammatory, and anticancer effects in multiple experimental models [6,7]. Accumulating evidence indicates that C-PC exerts protective effects against various skin disorders through its strong antioxidant capacity, enabling efficient

https://doi.org/10.3390/pharmaceutics18050600

scavenging of reactive oxygen species (ROS) and attenuation of oxidative stress-driven inflammation and carcinogenic processes [8,9]. In addition, C-PC has been shown to mitigate UVB-induced skin damage and delay photoaging by suppressing matrix metalloproteinase activity while preserving the expression of key epidermal barrier proteins, including involucrin, filaggrin, and loricrin [10]. Furthermore, C-PC inhibits melanoma cell proliferation and migration by modulating key regulators of tumour progression, including MAPK-associated signalling pathways, cell cycle regulators (CDK4/6), the angiogenic factor VEGF, the cell adhesion molecule N-cadherin, and matrix metalloproteinase MMP-9. Importantly, these effects are predominantly cytostatic and do not compromise the viability of non-tumorigenic cells [11]. Collectively, these findings suggest that C-PC can interfere with early tumour-promoting pathways by limiting cell proliferation and migration through modulation of signalling molecules involved in cell cycle regulation, angiogenesis, and extracellular matrix remodelling, while maintaining a favourable safety profile [11–13]. However, despite these promising properties, the topical preventive potential of C-PC against cSCC development remains largely unexplored, particularly in vivo. Moreover, due to its high molecular weight, topical formulations containing C-PC face significant challenges in achieving adequate skin penetration. Transfersomal systems are particularly suited to overcoming this limitation due to their high membrane elasticity, which enables passage through intercellular skin pathways that are smaller than their vesicle diameter. Importantly, the biological performance of such systems depends not only on drug loading but also on the vesicle deformability, physicochemical stability, and skin deposition properties. In our previous study, we developed C-PC-loaded glycerol-transfersomes designed to enhance epidermal delivery of this bioactive compound and demonstrated their cytocompatibility and cytoprotective effects against oxidative stress in HaCaT keratinocytes, thereby providing a rationale for subsequent in vivo evaluation [14]. We hypothesized that improved topical delivery of C-PC protects against early-stage cSCC by reducing oxidative stress, inflammation, and pathological epidermal proliferation. To test this hypothesis, the present study employed a DMBA/TPA-induced mouse model of skin carcinogenesis, which distinguishes between tumour initiation and promotion phases and is widely used to evaluate chemopreventive strategies [15]. Importantly, DMBA/TPA-induced tumours show similarities to human cSCC, including alterations in oncogenic signalling pathways and the involvement of inflammation-driven tumour progression [16,17].

2. Materials and Methods

2.1. Materials

C-PC was isolated from non-toxic cyanobacterial biomass harvested from the Kaunas Reservoir (Kaunas, Lithuania) and the Simnas fishpond (Simnas, Lithuania), characterized by the dominance of *Aphanizomenon flos-aquae* (>95% of total phytoplankton biomass), as previously described by Galinytė et al. [14]. The purity of the obtained C-PC was 3.227 ± 0.045 (OD620/OD280) [14].

C-PC-loaded glycero-transfersomes (T-PC) were prepared and characterized as previously described by Galinytė et al. [14]. The selected formulation was characterized by a nanoscale vesicle size (~100 nm), a narrow polydispersity index (<0.2), a high negative zeta potential (≤ -30 mV), high C-PC encapsulation efficiency (~50%), and predominantly spherical unilamellar vesicles confirmed by cryo-transmission electron microscopy [14].

DMBA, TPA and Mayer's hematoxylin were purchased from Sigma-Aldrich (St. Louis, MO, USA). Anti-Ki67 antibody (ab16667, clone SP6) was purchased from Abcam (Cambridge, UK). DCS LabLine Antibody Dilution Buffer (AL120R100), DCS DetectionLine SUPERVision-2 Polymer-Reagent (HRP, LD521R125), citrate buffer (pH 6, CL009C500),

https://doi.org/10.3390/pharmaceutics18050600

and DCS LabLine IHC Wash Buffer (WL583C2500) were obtained from DCS Innovative Diagnostik-Systeme (Hamburg, Germany).

2.2. In Vivo Experimental Design

The DMBA/TPA-induced mouse skin tumorigenesis protocol was performed as previously described by Li et al. [17]. The potential of topical C-PC-loaded transfersomes to modulate a tumour- promoting cutaneous microenvironment was evaluated.

In vivo experiments were performed in 2025 at the Lithuanian University of Health Sciences Biological Research Centre (Kaunas, Lithuania). All animal experiments were approved by the State Food and Veterinary Service of the Republic of Lithuania (approval No. G2-236) and conducted in accordance with national and European Union legislation.

Male BALB/c albino mice (*Mus musculus*), aged 8–12 weeks, were obtained from the Lithuanian University of Health Sciences Vivarium (Kaunas, Lithuania). Animals were acclimatized for 3 days before the study and housed under controlled environmental conditions (ambient temperature of 21 ± 2.5 °C and relative humidity of 50–55%; 12 h light/12 h dark cycle), with *ad libitum* access to water and food (standard pelleted rodent diet).

Animals were randomly assigned to six groups (n = 10 per group). The dorsal skin was shaved once per week using an electric clipper. The experimental protocol consisted of an initiation–promotion scheme using DMBA and TPA. Skin carcinogenesis was initiated by a single topical application of DMBA (50 µg in acetone). One week later, tumour promotion was carried out by topical application of TPA (5 µg in acetone or PEG/acetone solution) twice per week for 16 weeks. Topical treatment with C-PC-loaded transfersomes (T-PC) or empty transfersomes was applied twice per week, 2 h after each TPA application. All formulations were applied at a fixed dose of 200 µL per animal to a defined dorsal skin area (2 × 2 cm). All carcinogen-exposed groups received identical DMBA/TPA treatment and differed only in the type of topical formulation applied (C-PC-loaded transfersomes at different concentrations, empty transfersomes, or no additional treatment). In addition, separate non-carcinogen groups were included; these were not exposed to DMBA/TPA and received topical application of C-PC-loaded transfersomes at different concentrations. The detailed treatment protocol is presented in Table 1. The selected concentrations of C-PC (1 and 10 mg/mL) were based on previously published studies reporting wide ranges of effective concentrations, depending on the experimental model and route of administration. For example, topical C-PC formulations at ~2.5 mg/mL have been shown to exert protective effects in UVB-induced skin damage models, while concentrations of 2–6 mg/mL demonstrated biological activity in wound healing models [18,19]. Considering this variability and the limited skin penetration of high-molecular-weight compounds, a relatively broad concentration range was selected to evaluate potential dose-dependent effects.

Table 1. Experimental groups and treatment schedule.

Treatment	Group I	Group II	Group III	Group IV	Group V	Group VI
Group description	Non-carcinogen+ T-PC 1 mg/mL	Non-carcinogen+ T-PC 10 mg/mL	Carcinogen control	Carcinogen+ empty transfersomes	Carcinogen+ T-PC 1 mg/mL	Carcinogen+ T-PC 10 mg/mL
T-PC 1 mg/mL, (200 µL)	Twice/week	_	_	_	Twice/week	_
T-PC 10 mg/mL, (200 µL)	_	Twice/week	_	_	_	Twice/week

https://doi.org/10.3390/pharmaceutics18050600

Table 1. *Cont.*

Treatment	Group I	Group II	Group III	Group IV	Group V	Group VI
Empty transfersomes (200 μL)	–	–	–	Twice/week	–	–
DMBA (50 μg in acetone, 200 μL)	–	–	Single dose	Single dose	Single dose	Single dose
TPA (5 μg in acetone or PEG/acetone, 200 μL)	–	–	Twice/week	Twice/week	Twice/week	Twice/week

Animals were weighed twice weekly, and routine clinical observations were performed throughout the study. After 16 weeks, animals were euthanized by cervical dislocation, in accordance with institutional and European Union guidelines. Skin and internal organ samples were collected and fixed in 10% neutral buffered formalin for further analysis.

2.3. Histotechnique

Skin and internal organ specimens (liver, spleen, lungs, heart, kidneys, brain, testes, mesenteric lymph node) from each animal were collected for histopathological examination. The samples were fixed in 10% neutral-buffered formalin at room temperature. Paraffin blocks were prepared using a Shandon Pathcentre embedding system (Thermo Fisher Scientific, Waltham, MA, USA) and a TES 99 tissue processor (Medite Medizintechnik GmbH, Bergdorf, Germany). Serial 4-μm sections from each sample were cut using a Sakura Accu-Cut SRM microtome (Sakura Finetek, Torrance, CA, USA) and stained with routine hematoxylin and eosin (H&E).

2.4. Histopathological Examination

Histological slides were evaluated, and image analysis was performed using a light microscope (Olympus BX41, Olympus Corporation, Tokyo, Japan) equipped with a DP72 digital camera and CellSens Dimension software version 1.16 (Olympus Corporation, Tokyo, Japan). A predefined set of epidermal and dermal histomorphological parameters was assessed. Epidermal criteria included epidermal thickness, rete ridge depth, hyperplasia, dysplastic alterations, mitotic activity, and spongiosis, whereas dermal criteria comprised inflammatory infiltrate, circulatory changes, and mast cell density. Semiquantitative alterations were graded on a 4-point scale (0 = absent, 1 = mild, 2 = moderate, 3 = severe), while quantitative parameters were expressed as measurements (μm) or absolute counts per standardized area (2.37 mm^2).

Histopathological evaluation was performed to assess the potential systemic toxicity of the tested formulations. Organ-specific histomorphological examination was conducted in the heart, liver, kidneys, spleen, lungs, testes, and mesenteric lymph nodes to identify degenerative, necrotic, inflammatory, adaptive, and neoplastic alterations.

2.5. Immunohistochemistry: Ki-67

Immunohistochemistry for Ki-67 was performed on all skin samples. Formalin-fixed, paraffin-embedded tissue sections were mounted on poly-L-lysine-coated slides (Thermo Fisher Scientific, Branchburg, NJ, USA). Heat-induced antigen retrieval was carried out in citrate buffer (pH 6) (CL009C500; DCS Innovative Diagnostik-Systeme, Hamburg, Germany) for 30 min at 110 °C using a pressure cooker (Thermo Fisher Scientific, Branchburg, NJ, USA). The Shandon CoverPlate System (Thermo Fisher Scientific, Branchburg, NJ, USA) was used for staining. Endogenous peroxidase activity was quenched with 3% hydrogen peroxide solution (Valentis, Kaunas, Lithuania) and then further blocked with Hydrogen Peroxide Blocking Reagent (AB64218; Abcam, Cambridge, UK). Primary Rb mAb to Ki67

https://doi.org/10.3390/pharmaceutics18050600

antibody (ab16667, clone SP6; Abcam, Cambridge, UK) was applied at a 1:200 dilution and incubated overnight at 4 °C. DCS LabLine Antibody Dilution Buffer (AL120R100; DCS Innovative Diagnostik-Systeme, Hamburg, Germany) was used for antibody dilution. Slides were subsequently incubated with DCS DetectionLine SUPERVision-2 Polymer-Enhancer (LD511R125; DCS Innovative Diagnostik-Systeme, Hamburg, Germany) for 30 min at room temperature, followed by the DCS DetectionLine SUPERVision-2 Polymer-Reagent (HRP) (LD521R125; DCS Innovative Diagnostik-Systeme, Hamburg, Germany) for 30 min at room temperature. Immunoreactivity was visualized using DCS ChromoLine DAB concentrate (DC136C007; DCS Innovative Diagnostik-Systeme, Hamburg, Germany) diluted in DCS ChromoLine DAB substrate buffer (PC137R125; DCS Innovative Diagnostik-Systeme, Hamburg, Germany) at a ratio of 1 drop per 1 mL, applied for 4 min at room temperature. DCS LabLine IHC Wash-Buffer (WL583C2500; DCS Innovative Diagnostik-Systeme, Hamburg, Germany) was used after each step. Slides were counterstained with Mayer's hematoxylin solution (Sigma -Aldrich, Taufkirchen, Germany), dehydrated and mounted.

Ki-67 expression was evaluated separately in the basal and suprabasal (parabasal) layers of the epidermis. For each animal, 10 non-overlapping digital images at 200× magnification were analysed in the most representative hyperplastic or dysplastic areas, avoiding ulcerated and heavily crusted regions. In each image, all basal and parabasal keratinocytes were counted, and the number of Ki-67-positive nuclei was recorded. The Ki-67 index was calculated as the percentage of positive cells relative to the total number of basal or parabasal cells, respectively.

2.6. Statistical Analysis

Statistical analysis was performed using IBM SPSS Statistics version 29.0 (IBM, Armonk, NY, USA). Data distribution normality was assessed using the Shapiro–Wilk test. Homogeneity of variances was evaluated using Levene's test.

For normally distributed data with homogeneous variances, one-way ANOVA followed by Tukey's post hoc test was applied. When the homogeneity of variance assumptions were violated, Welch's ANOVA followed by the Games–Howell post hoc test was used. Non-normally distributed variables and ordinal data (e.g., hyperplasia, dysplasia, inflammation scores) were analysed using the Kruskal–Wallis test with Bonferroni-adjusted pairwise comparisons.

Correlation analyses between proliferative indices and histopathological parameters were performed using Spearman's rank correlation coefficient (ρ). A p-value < 0.05 was considered statistically significant.

3. Results

3.1. General Observations on the Effects of C-PC-Loaded Transfersomes on Skin Tumour Development and Animal Well-Being

Topical application of DMBA followed by repeated TPA treatment induced visible skin alterations in mice, including erythema, hyperkeratosis, and papilloma-like lesions, indicating early-stage activation of the tumorigenesis process.

Animals were monitored daily for health and welfare status and twice weekly for body weight and general clinical condition, using predefined animal welfare scoring criteria. During the initial tumour promotion phase (weeks 1–5), TPA was administered in acetone as a vehicle, resulting after approximately 4–5 weeks in pronounced local skin irritation in all TPA-treated groups. Increased scratching behaviour led to superficial skin lesions predominantly located in areas accessible to scratching or grooming rather than at the direct application site.

https://doi.org/10.3390/pharmaceutics18050600

To reduce animal discomfort and comply with animal welfare requirements, the TPA acetone vehicle was modified to a TPA PEG/acetone solution from the 6th to the 12th week of treatment. This modification markedly alleviated skin irritation scores and reduced self-inflicted skin lesions. During the final experimental phase (weeks 13–16), TPA in acetone was reintroduced to further enhance carcinogenesis promotion; however, despite the intensified promotion protocol and adherence to animal welfare requirements, fully developed squamous cell carcinoma could not be induced.

Throughout the experimental period, animals remained active, with normal posture and locomotion, and no signs of impaired respiration, systemic distress, or treatment-related mortalities were observed.

Body weight analysis demonstrated a significant effect of time on body weight ($p < 0.001$), reflecting normal growth (Figure 1), as well as significant time × group interaction ($p = 0.004$) and group effects ($p = 0.001$); however, body weight values remained within physiological ranges, with no signs of systemic toxicity.

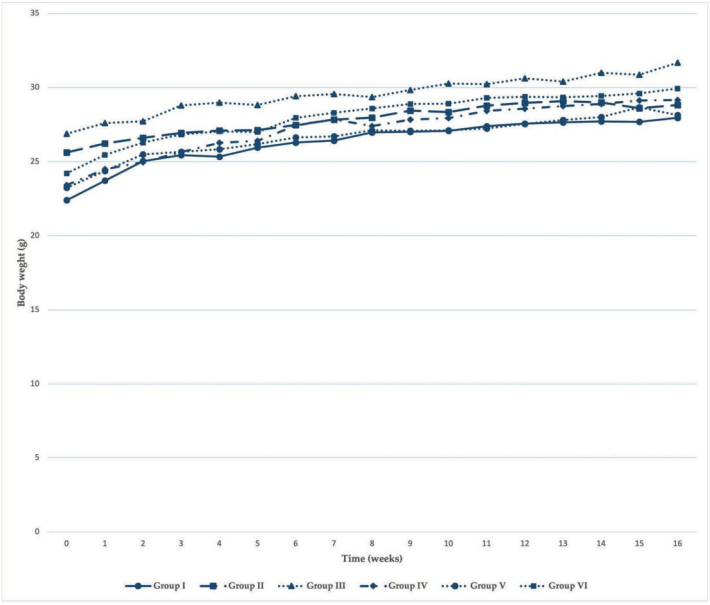

Figure 1. Body weight monitoring during the experimental period.

Visually assessed composite skin irritation scores (including erythema, hyperpigmentation, dryness, formation of skin lesions, oedema, and inflammation) differed significantly between experimental groups throughout all three experimental phases (Kruskal–Wallis test, $p < 0.001$).

In experimental groups treated exclusively with T-PC and not exposed to the carcinogen (Groups I–II), the formulation was well tolerated on intact skin, with no clinically relevant irritation observed even at the higher C-PC concentration.

During Phase I, the carcinogen control group (Group III) exhibited significantly higher skin irritation scores than both the T-PC-only groups (Groups I and II) and the T-PC-treated carcinogen groups (Groups V and VI) (adjusted $p < 0.05$). In Phase II, after modifying the

https://doi.org/10.3390/pharmaceutics18050600

TPA from an acetone vehicle to PEG/acetone, intergroup differences persisted but were less pronounced. The carcinogen control group (Group III) remained significantly different from the non-carcinogen groups, while no statistically significant differences were observed among the carcinogen-treated groups. In Phase III, the reintroduction of TPA in acetone led to a renewed increase in skin irritation severity, with the carcinogen control group (Group III) again exhibiting higher scores and significantly differing from the T-PC-treated carcinogen group (Group V).

Representative macroscopic images of dorsal skin from all experimental groups at study termination (week 16) are presented in Figure 2.

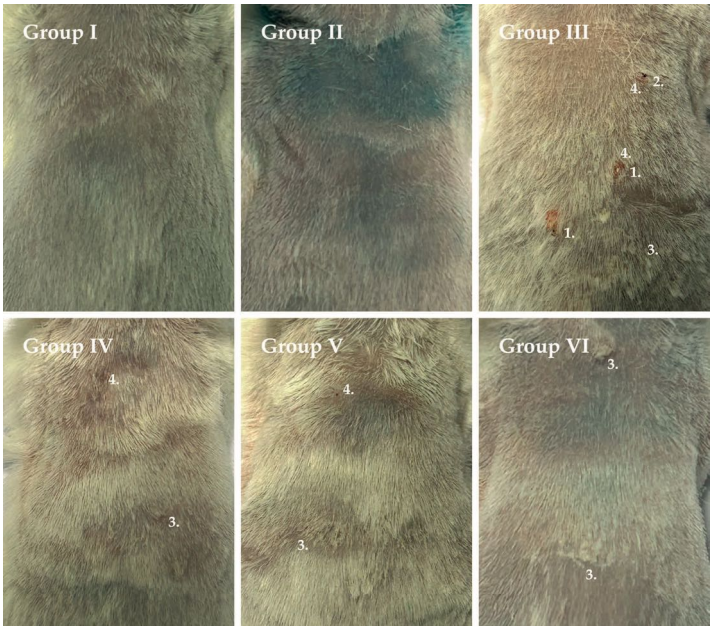

Figure 2. Representative macroscopic images of dorsal skin condition in mice from all experimental groups at the end of the study (week 16). (1) Papilloma-like lesions; (2) wound formation; (3) dryness and flaking; (4) signs of inflammation.

At study termination, only a limited number of animals in the carcinogen control group (Group III) developed small superficial papilloma-like lesions, whereas the predominant macroscopic phenotype was inflammatory and irritative skin damage. Notably, carcinogen-treated groups receiving transfersome-based formulations exhibited visually improved skin condition compared to the carcinogen control group.

3.2. Histopathological Evaluation of Skin Tissue

3.2.1. Epidermal Alterations

In this study, the primary focus was on evaluating epidermal alterations, including epidermal thickening, dysplasia, hyperplasia, oedema, and mitotic activity, as the development of fully established squamous cell carcinoma was not achieved in compliance with animal welfare regulations.

https://doi.org/10.3390/pharmaceutics18050600

In Groups I and II, animals were not exposed to the carcinogen, and these groups were intended to demonstrate that T-PC, when applied topically to the skin, does not induce epidermal hyperplasia, dermal inflammation, or increased proliferative activity and, therefore, may be considered safe in the context of carcinogenesis modulation.

Epidermal thickness and rete ridge depth differed among the experimental groups (Figure 3a,b). The lowest values were observed in the control groups not exposed to the carcinogen (Groups I and II), in which epidermal architecture remained close to physiological conditions, with epidermal thickness ranging from 10 to 20 μm. In these groups, rete ridges were short and uniform, consistent with normal skin architecture (rete ridge depth 0–10 μm, predominantly flat rete ridges with a height of 3–4 nuclei).

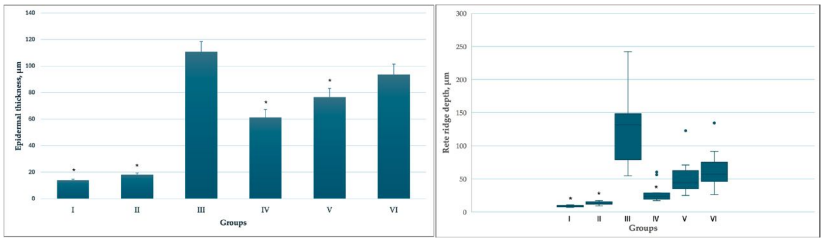

(**a**) (**b**)

Figure 3. (**a**) Distribution of epidermal thickness across different experimental groups. Data are presented as mean and SD. * $p < 0.05$ compared with the carcinogen-only group (Group III), Games–Howell post hoc test following Welch's ANOVA. (**b**) Distribution of rete ridge depth across different experimental groups. Data are shown as box-and-whisker plots displaying the median, interquartile range (IQR), and range; outliers are shown as individual points. Statistical analysis was performed using the Kruskal–Wallis test followed by Bonferroni-adjusted pairwise comparisons. * $p < 0.05$ versus the carcinogen-only group (Group III).

In all carcinogen-exposed groups (Groups III, IV, V, and VI), a marked increase in epidermal thickness was observed, indicating proliferative and hyperplastic alterations of the epidermis. The greatest epidermal thickness was recorded in the carcinogen-alone group (Group III) and in the carcinogen combined with transfersomes containing a higher concentration of C-PC (Group VI). Although epidermal thickness in Groups IV and V was increased compared with the non-carcinogen control groups (Groups I and II), it was significantly lower than in the carcinogen-only group (Group III).

Analysis of rete ridge depth revealed a similar pattern. Carcinogen-exposed groups exhibited significant elongation of rete ridges, particularly in Group III, where deep epidermal invaginations into the dermis were observed. These changes indicate active remodelling of epidermal architecture characteristic of preneoplastic processes. Notably, rete ridge depth in Group IV was significantly lower than in the carcinogen-only group (Group III).

Epidermal dysplasia. The distribution of epidermal dysplasia grades differed among the experimental groups (Figure 4a). No epidermal dysplasia was detected in the groups not exposed to the carcinogen (Groups I and II), accounting for 0% of all cases (Figure 4c,d). In these groups, epidermal morphology was comparable to that of untreated mice maintained under identical conditions (Figure 4b). The epidermis remained close to physiological conditions, appearing very thin and composed of 2–3 layers of keratinocytes. Keratinocyte nuclei were regularly arranged, the stratum spinosum layer was minimal, and the stratum corneum was thin and compact, without evidence of hyperkeratosis or spongiosis. No epidermal oedema was observed.

https://doi.org/10.3390/pharmaceutics18050600

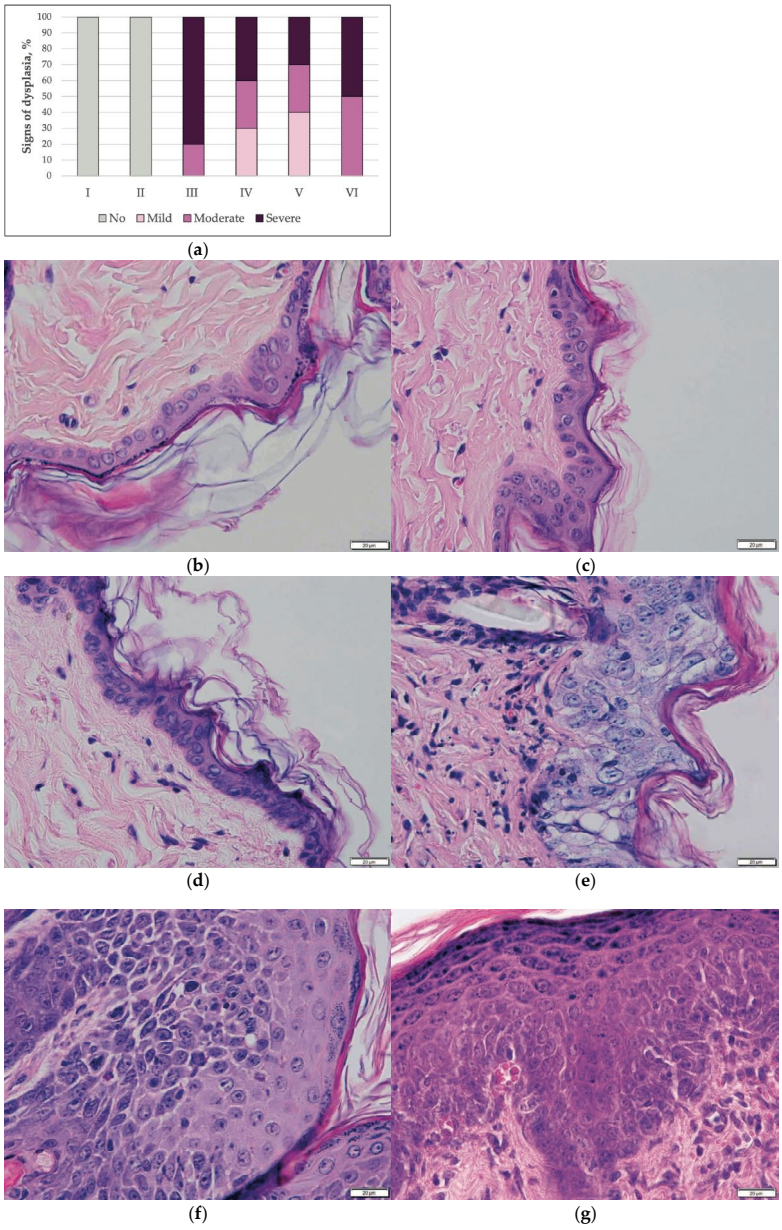

Figure 4. (**a**) Distribution of epidermal dysplasia grades across experimental groups. The percentage distribution of epidermal dysplasia grades is presented for each experimental group. (**b**) Histological

https://doi.org/10.3390/pharmaceutics18050600

appearance of the non-treated epidermis. H&E, ×200. (**c**) Histological appearance of the epidermis, T-PC 1 mg/mL (Group I). H&E, ×400. (**d**) Histological appearance of the epidermis, T-PC 10 mg/mL (Group II). H&E, ×400. (**e**) Histological appearance of the epidermis showing severe epidermal dysplasia (Group III): marked nuclear pleomorphism, hyperchromasia, and an increased nuclear-to-cytoplasmic (N/C) ratio are observed not only in the basal layer but also in the suprabasal layers; cellular differentiation is disrupted, cells are arranged irregularly, and the normal epidermal architecture is disturbed; no evidence of invasion through the basement membrane is observed. H&E, ×400. (**f**) Histological appearance of the epidermis showing moderate epidermal dysplasia (Group IV): pronounced nuclear pleomorphism is observed, characterized by variably sized, irregular, hyperchromatic nuclei and an increased nuclear-to-cytoplasmic ratio. Mitotic figures are present, some of which are observed not only in the basal layer. Epidermal layer differentiation is disturbed, with indistinct boundaries between the basal and parabasal layers and irregular arrangement of keratinocytes. However, cells with nuclear atypia are not yet present throughout all epidermal layers, and cells in the upper layers remain fully differentiated. H&E, ×400. (**g**) Histological appearance of the epidermis: mild epidermal dysplasia (Group V). Some keratinocyte nuclei are variably sized, irregularly shaped, and hyperchromatic. Mild disturbance of cellular polarity is observed in the lower epidermal layers, with an increased nuclear-to-cytoplasmic (N/C) ratio in some cells. Disruption of maturation is more pronounced in the lower third of the epidermis, while mature, well-differentiated cells are observed in the upper layers. H&E, ×400.

In the group treated with the carcinogen in combination with empty transfersomes (Group IV), a mixed spectrum of dysplasia was observed, with mild dysplasia accounting for approximately 30%, moderate dysplasia for approximately 30%, and severe dysplasia for approximately 40%. In the group treated with the carcinogen together with T-PC at a concentration of 1 mg/mL (Group V), mild dysplasia accounted for approximately 40% of all cases, while the proportion of severe dysplasia decreased from approximately 80% to around 30% compared with the carcinogen-only group. In the group treated with the carcinogen combined with T-PC at a concentration of 10 mg/mL (Group VI), severe dysplasia accounted for approximately 50% of cases.

In contrast, in the group treated with the carcinogen alone (Group III), severe dysplasia predominated, accounting for approximately 80% of all cases, whereas moderate dysplasia was observed in only approximately 20% of animals. Representative histological examples of different grades of epidermal dysplasia are shown in Figure 4e–g.

Both epidermal thickness and rete ridge depth showed strong positive correlations with dysplasia grade (Spearman's $\rho = 0.828$ and 0.834, respectively, $p < 0.001$; Figure 5). A clear trend of increasing epidermal thickness with increasing dysplasia severity was observed, with lower dysplasia grades associated with a thinner epidermis, whereas higher-grade dysplasia was characterized by marked epidermal thickening. This relationship indicates that increased epidermal thickness represents a consistent feature of dysplastic progression and reflects structural remodelling of the epidermis accompanying preneoplastic processes.

Further analysis of rete ridge depth in relation to dysplasia grade demonstrated a similarly strong positive association, with increasing dysplasia severity corresponding to progressively elongated rete ridges. Higher-grade dysplasia was associated with deep, irregularly distributed rete ridges extending into the deeper dermal layers.

Hyperplasia. In the control groups (Groups I and II), no epidermal hyperplasia was observed (Figure 6a). In the group treated with the carcinogen alone (Group III), moderate-to-severe epidermal hyperplasia predominated. In animals treated with the carcinogen in combination with empty transfersomes (Group IV), epidermal hyperplasia was most frequently classified as mild or moderate.

https://doi.org/10.3390/pharmaceutics18050600

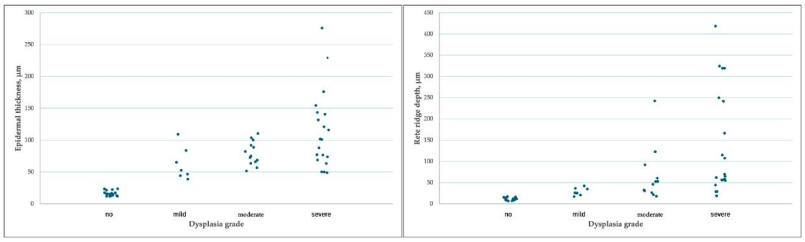

(**a**) (**b**)

Figure 5. (**a**) Distribution of epidermal thickness across dysplasia grades. (**b**) Distribution of rete ridge depth across dysplasia grades. Dots represent individual measurements. A strong positive correlation with dysplasia grade was observed (Spearman's ρ = 0.828 and 0.834, respectively; $p < 0.001$).

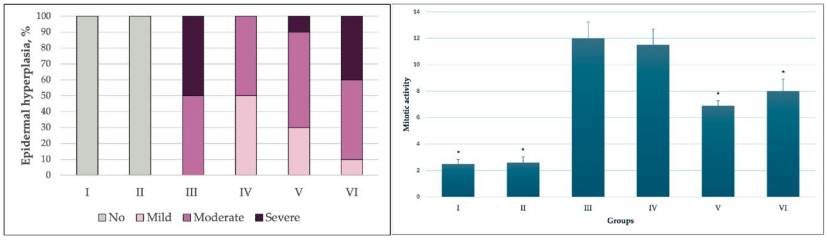

(**a**) (**b**)

Figure 6. (**a**) Distribution of epidermal hyperplasia severity across experimental groups. The percentage distribution of epidermal hyperplasia grades is presented for each experimental group. (**b**) Distribution of epidermal mitotic activity (number of mitoses per 2.37 mm^2) across experimental groups. Data are presented as mean and SD. * $p < 0.05$ compared with the carcinogen-only group (Group III), one-way ANOVA followed by Tukey's post hoc test.

When the carcinogen was applied together with T-PC at a concentration of 1 mg/mL (Group V), a reduced proportion of severe hyperplasia was observed, with mild and moderate hyperplasia predominating. In the group treated with the carcinogen combined with T-PC at 10 mg/mL (Group VI), moderate and severe epidermal hyperplasia still predominated; however, the overall severity was slightly lower than in the carcinogen-only group. The superior effect observed at the lower C-PC concentration may reflect formulation-dependent factors rather than purely pharmacological activity. Higher loading levels may reduce vesicle deformability or promote partial encapsulation saturation, potentially limiting dermal penetration efficiency. These findings indicate that treatment with transfersomes was associated with a reduction in the intensity of epidermal hyperplasia, although it did not eliminate hyperplastic changes.

Mitotic activity. Evaluation of mitotic activity, expressed as the number of mitoses per 2.37 mm^2, revealed minimal proliferative activity in the control groups (Groups I and II), with an average of 2–3 mitoses per 2.37 mm^2 (Figure 6b). In contrast, groups exposed to the carcinogen exhibited markedly increased mitotic activity, reaching up to approximately 12 mitoses per 2.37 mm^2. Application of T-PC resulted in significantly lower mitotic activity compared with the carcinogen-only group and the group treated with the carcinogen combined with empty transfersomes.

https://doi.org/10.3390/pharmaceutics18050600

Epidermal oedema (spongiosis) was detected exclusively in the carcinogen-exposed groups and showed considerable variability both between and within the groups (Figure 7). In the group treated with the carcinogen alone (Group III), marked epidermal oedema predominated, characterized by widened intercellular spaces between keratinocytes and disruption of normal epidermal architecture.

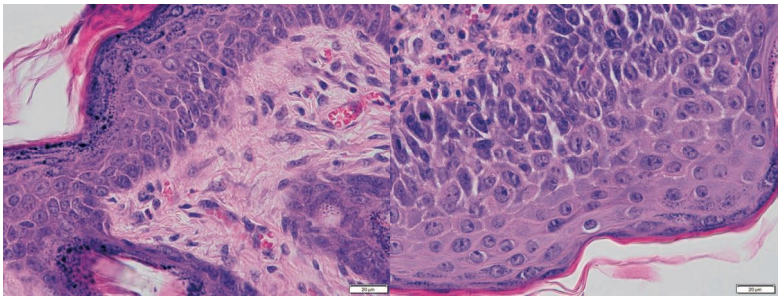

(**a**) (**b**)

Figure 7. (**a**) Histological appearance of the epidermis showing mild oedema: slightly widened intercellular spaces between keratinocytes are visible, particularly within the stratum spinosum; keratinocytes remain normally interconnected (carcinogen + T-PC, Group V). H&E, ×400. (**b**) Histological appearance of the epidermis showing marked (moderate) oedema: clearly widened intercellular spaces between keratinocytes are observed, particularly within the stratum spinosum; however, keratinocytes remain interconnected (carcinogen group, Group III). H&E, ×400.

In groups treated with T-PC and the carcinogen, epidermal oedema intensity ranged from mild to severe but did not show a consistent association with proliferative activity or dysplasia grade. No epidermal oedema was observed in the control groups.

The presence of both intercellular oedema (spongiosis) and intracellular oedema in histological sections suggests that the oedematous changes observed in this model most likely reflect acute carcinogen-induced tissue injury and an inflammatory response rather than a direct component of preneoplastic transformation.

3.2.2. Dermal Alterations

Inflammation. The distribution of dermal inflammation severity differed markedly among the experimental groups (Figure 8a).

No inflammatory changes were observed in the control groups (Groups I–II). In contrast, the group treated with the carcinogen alone (Group III) exhibited predominantly severe dermal inflammation (Figure 8e), accounting for the majority of cases (70%), with the remaining samples showing moderate inflammation. In the group treated with the carcinogen in combination with empty transfersomes (Group IV), the inflammatory response was more heterogeneous. While moderate and severe inflammation remained prevalent, some samples exhibited mild or no inflammation, suggesting partial attenuation of the inflammatory response compared with the carcinogen-only group. In the groups treated with the carcinogen together with T-PC (Groups V and VI), a clear shift toward lower inflammation severity was observed. In Group V (Figure 8g), mild inflammation predominated, with fewer cases of moderate and severe inflammation. Similarly, in Group VI, although moderate and severe inflammation remained present, their proportions were reduced compared with the carcinogen-only group, and mild inflammation accounted for a substantial fraction of cases.

https://doi.org/10.3390/pharmaceutics18050600

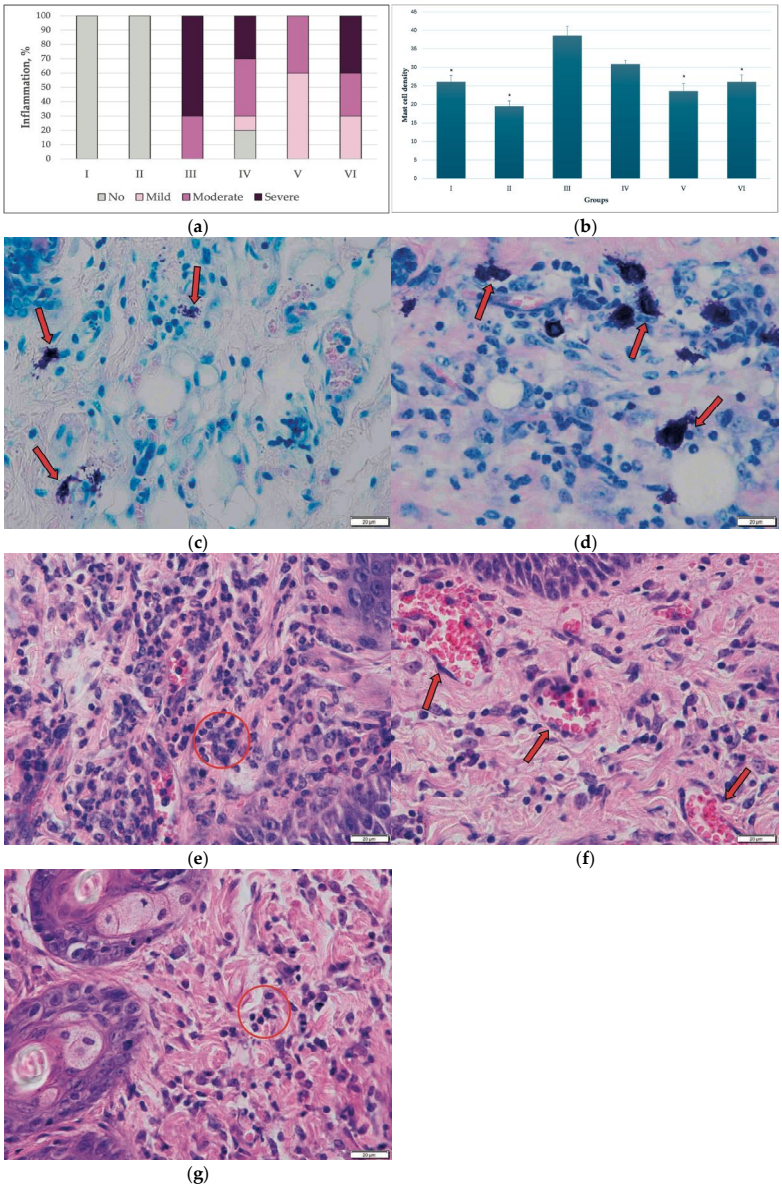

Figure 8. (**a**) Distribution of inflammation grades across different experimental groups, presented as percentage values. (**b**) Mast cell density (number of mast cells per 2.37 mm^2) in the dermis of different experimental groups. Values are expressed as mean and SD. Statistical differences among

https://doi.org/10.3390/pharmaceutics18050600

groups were analysed using one-way ANOVA followed by Tukey's multiple comparisons test (* $p < 0.05$ versus Group III). (**c**) Sparse mast cells (red arrows) in the dermis, Giemsa staining (Group V). (**d**) Numerous mast cells (red arrows) in the dermis, Giemsa staining (Group III). (**e**) Marked dermal inflammation characterized by abundant neutrophils (outlined in red), many exhibiting reactive (band-shaped) nuclei (Group III). (**f**) Pronounced dermal hyperemia associated with severe inflammation, showing dilated and blood-filled vessels (erythrocytes indicated by red arrows) (Group III). (**g**) Significantly reduced inflammatory response in the dermis, neutrophils outlined in red (Group V).

Overall, these findings indicate that application of C-PC, particularly when delivered via transfersomes at a concentration of 1 mg/mL (Group V), was associated with a reduction in the intensity of dermal inflammation, shifting the inflammatory profile from predominantly severe toward milder forms, although inflammation was not completely abolished.

Hyperaemia was detected exclusively in the carcinogen-exposed groups (Figure 8f) and was closely associated with the intensity of the inflammatory infiltrate. No hyperaemia was observed in the control groups treated with T-PC only (Groups I and II). In the group treated with the carcinogen alone (Group III), moderate to severe hyperaemia predominated, whereas in the groups treated with the carcinogen and T-PC (Groups V and VI), mild to moderate hyperaemia was more frequently observed.

Oedema was evaluated as a reactive change and a component of inflammation, particularly acute inflammation. No oedema was observed in the control groups treated with T-PC only (Groups I and II). In the group exposed to the carcinogen alone (Group III), oedema was most often moderate to severe. In the groups in which the carcinogen was applied together with transfersomes, either empty or in combination with C-PC (Groups IV, V, and VI), the oedema intensity was lower, with mild to moderate oedema predominating and severe oedema observed less frequently. In all carcinogen-exposed groups (Groups III, IV, V, and VI), oedema correlated with the intensity of inflammation and was interpreted as a secondary tissue response rather than an independent pathological process.

Mast cell density was lower in the groups not exposed to the carcinogen and differed significantly among the carcinogen-exposed groups (Figure 8b–d). The highest mast cell density was observed in the carcinogen-only group (Group III), indicating a pronounced activation of the dermal inflammatory microenvironment. In the groups treated with the carcinogen in combination with empty transfersomes (Group IV), mast cell density remained elevated but was lower than in the carcinogen-only group, suggesting partial attenuation of the inflammatory response. In the groups treated with the carcinogen together with T-PC (Groups V and VI), mast cell density was significantly reduced compared with the carcinogen-only group. Among these, Group V exhibited the lowest mast cell density, while Group VI showed slightly higher values, although still significantly lower than those observed in Group III.

Overall, these findings indicate that T-PC application was associated with reduced mast cell accumulation in the dermis, suggesting a potential modulatory effect of C-PC on the inflammatory microenvironment induced by the carcinogen.

A significant positive correlation was found between dermal inflammation severity and mast cell density (Spearman's $\rho = 0.438$, $p < 0.001$). Samples exhibiting more pronounced, diffuse inflammatory infiltrates showed higher mast cell counts, whereas in the control groups, only occasional lymphocytes were observed.

3.3. Immunohistochemical Assessment of Epidermal Proliferation and Its Association with Histopathological Parameters

Quantitative analysis of epidermal proliferation revealed significant differences in Ki-67 expression among the experimental groups (Figure 9a–g). In the basal epidermal

https://doi.org/10.3390/pharmaceutics18050600

layer, the Ki-67 index was significantly higher in the carcinogen-treated group (Group III) compared with the control groups (Groups I and II) ($p < 0.05$). Treatment with T-PC resulted in a partial reduction in basal proliferative activity, with significant differences observed between Group III and Group VI ($p < 0.05$), whereas differences between Group III, Group IV, and Group V were less consistent.

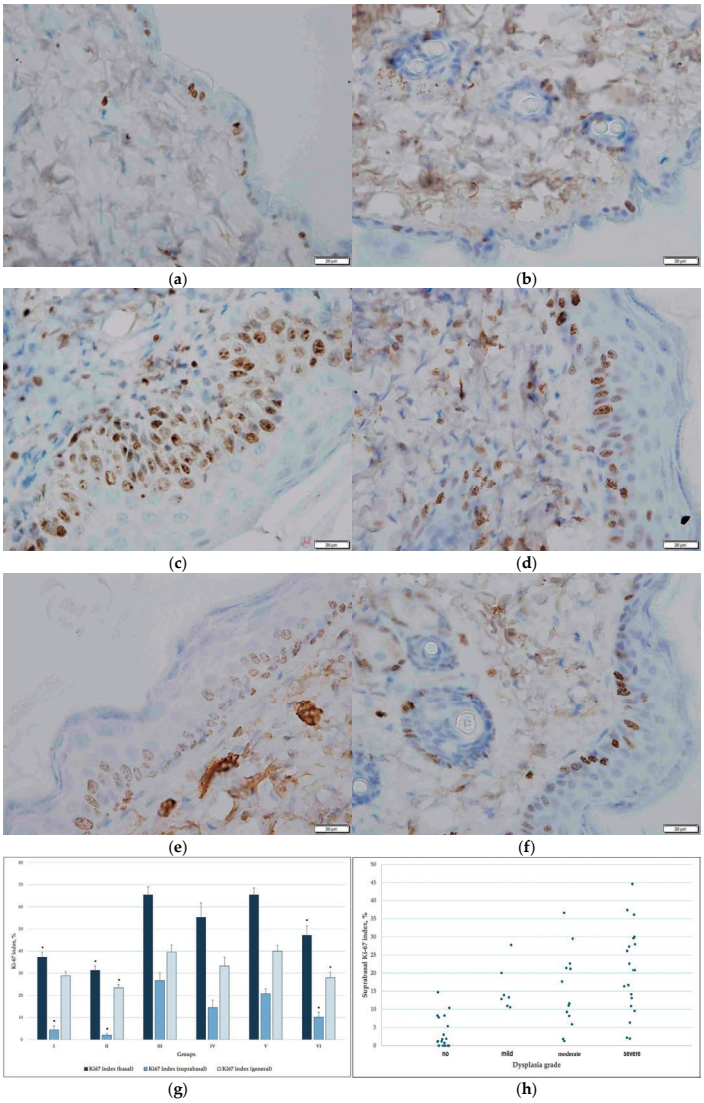

Figure 9. *Cont.*

https://doi.org/10.3390/pharmaceutics18050600

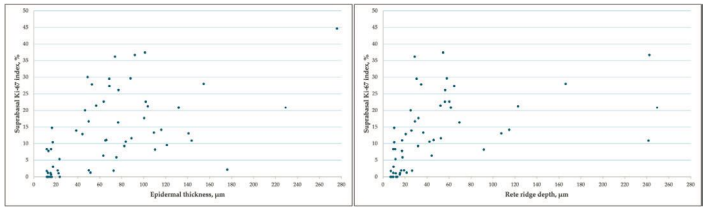

(**i**) (**j**)

Figure 9. (**a**–**f**) Representative immunohistochemical staining of Ki-67 expression in the epidermis of experimental groups: (**a**) Group I, (**b**) Group II, (**c**) Group III, (**d**) Group IV, (**e**) Group V, (**f**) Group VI. (**g**) Ki-67 proliferation index in the epidermis across experimental groups. Data are presented as mean and SD for basal, suprabasal, and total epidermal Ki-67 indices. Statistical analysis was performed using one-way ANOVA with Tukey's post hoc test for variables with homogeneous variances, and Welch's ANOVA followed by Games–Howell post hoc test for variables with unequal variances. * $p < 0.05$ compared with the carcinogen-only group (Group III). (**h**) Relationship between epidermal dysplasia grade and epidermal proliferative activity. The scatter plot shows the epidermal Ki-67 proliferation index (%) for individual animals by dysplasia grade (no dysplasia, mild, moderate, severe). A positive correlation was observed (Spearman's $\rho = 0.66$, $p < 0.05$). (**i**) Correlation between epidermal thickness and suprabasal Ki-67 index. The scatter plot illustrates the relationship between epidermal thickness and the suprabasal Ki-67 proliferation index (Spearman's $\rho = 0.64$, $p < 0.05$). (**j**) Correlation between rete ridge depth and suprabasal Ki-67 index. The scatter plot illustrates the relationship between rete ridge depth and the suprabasal Ki-67 proliferation index (Spearman's $\rho = 0.71$, $p < 0.05$).

Suprabasal Ki-67 index was markedly increased in the carcinogen-only group (Group III) compared with both control groups (Groups I and II) ($p < 0.05$). Application of empty transfersomes or T-PC reduced suprabasal proliferative activity, especially in Group VI relative to Group III ($p < 0.05$), although values remained elevated compared with the controls. These findings indicate that suprabasal Ki-67 expression is a particularly sensitive marker of pathological epidermal proliferation.

Analysis of the total epidermal Ki-67 index also revealed a statistically significant reduction in carcinogen and T-PC-treated group (Group VI) compared with the carcinogen-only group (Group III, ($p < 0.05$)), while the other carcinogen-and transfersomes-treated groups did not show statistical significance. Overall, the total Ki-67 index was less sensitive to intergroup differences than separate analyses of the basal and suprabasal epidermal layers.

Although occasional Ki-67-positive cells were observed in the suprabasal layer of the control groups treated with T-PC-only, this finding likely reflects physiological epidermal regeneration and mild mechanical or chemical irritation associated with topical application, animal scratching behaviour, or minor microtrauma due to the skin shaving process, rather than pathological proliferative activity.

As the suprabasal Ki-67 index was identified as a more sensitive marker of pathological proliferation, correlation analysis was performed between suprabasal Ki-67 expression and selected histopathological parameters, including dysplasia grade, epidermal thickness, and rete ridge depth.

The strongest statistically significant positive association was observed between epidermal proliferative activity and rete ridge depth (Spearman's $\rho = 0.71$, $p < 0.05$, Figure 9j). A positive correlation between the Ki-67 indexes and epidermal thickness was also found (Spearman's $\rho = 0.64$, $p < 0.05$, Figure 9i). Epidermal thickness and rete ridge depth reflect structural alterations in epidermal architecture that develop during carcinogenesis, not

https://doi.org/10.3390/pharmaceutics18050600

only because of increased basal-layer proliferation, but also because proliferative activity expands into the suprabasal epidermal layers. A positive correlation between epidermal dysplasia grade and epidermal proliferative activity (Spearman's $\rho = 0.66$, $p < 0.05$, Figure 9h) indicated that higher dysplasia severity in this experimental model was associated with increased epidermal proliferative activity.

Immunohistochemical analysis of proliferation marker (Ki-67) showed extensive nuclear positivity in basal and suprabasal epidermal layers in the carcinogen group (Group III). In contrast, C-PC treatment significantly reduced the number of Ki-67–positive cells in a dose-dependent manner, indicating suppressed epidermal cell proliferation.

3.4. Histopathological Assessment of Internal Organs

Histological evaluation of internal organs, including liver, spleen, lungs, heart, kidneys, brain, testes, and mesenteric lymph nodes, revealed no treatment-related pathological alterations in any experimental group.

All examined organs maintained normal histoarchitecture, with no evidence of degenerative, necrotic, inflammatory, or neoplastic changes, confirming the systemic safety of topically applied C-PC-loaded transfersomes.

4. Discussion

The present study was designed as a proof-of-concept investigation to evaluate the preventive potential of C-PC-loaded transfersomes in the early stages of skin carcinogenesis using the widely established DMBA/TPA mouse model proposed by Li et al. [17]. A single application of DMBA induces oncogenic mutations—most commonly in *Hras*—whereas repeated TPA treatment promotes inflammation-driven clonal expansion and progression toward squamous cell carcinoma. Importantly, this mouse model exhibits genomic similarities to several subtypes of human SCC, supporting its translational relevance [17,20].

In the present study, carcinogenesis was initiated by a single topical application of DMBA, followed by twice-weekly application of TPA to promote tumour development. TPA is considered one of the most powerful skin tumour promoters and exerts its effects by profoundly reshaping molecular pathways involved in tumour promotion. By stimulating clonal expansion of initiated cells, TPA induces a strong inflammatory response while suppressing programmed cell death, thereby creating a microenvironment favourable for tumour progression. At the molecular level, TPA-induced upregulation of ornithine decarboxylase (ODC), cyclooxygenase-2 (COX-2), and interleukin-6 (IL-6), together with activation of the IL-6/STAT3 signalling axis and suppression of transglutaminase-2 (TG2), plays a central role in epidermal hyperproliferation, inflammation, and tumour promotion [21].

Although the DMBA/TPA model is widely used to induce cSCC, progression to fully developed invasive cSCC was not achieved under the present experimental conditions in accordance with animal welfare requirements. Therefore, this study focused primarily on early tumour-promoting and preneoplastic epidermal alterations rather than on overt tumour burden or malignant progression. Importantly, these early inflammation-driven changes represent a biologically relevant stage of carcinogenesis, during which modulation of the epidermal microenvironment may critically influence subsequent malignant transformation.

Consistent with this concept, pronounced precancerous histopathological alterations were observed in the carcinogen control group (Group III). The observed changes were characteristic of inflammation-driven tumour promotion in the DMBA/TPA model, including pathways associated with COX-2–IL-6–STAT3 signalling. Group III exhibited predominantly severe dermal inflammation (70% of cases), accompanied by hyperaemia, oedema,

https://doi.org/10.3390/pharmaceutics18050600

and increased mast cell density, indicating marked activation of the dermal inflammatory microenvironment. In parallel, substantial epidermal remodelling was evident, including pronounced epidermal thickening, increased rete ridge depth, and a predominance of moderate-to-severe hyperplasia. Severe epidermal dysplasia was detected in 80% of samples, with the remaining cases showing moderate dysplasia. These structural alterations were further supported by significantly elevated proliferative activity, as demonstrated by increased mitotic counts (up to ~12 mitoses per 2.37 mm^2) and a markedly elevated Ki-67 index.

Cutaneous squamous cell carcinoma develops through a well-recognized multistep process characterized by progressive architectural and molecular alterations of the epidermis. Disease progression typically evolves from actinic keratosis (AK) and intraepidermal dysplasia toward invasive carcinoma, accompanied by increasing keratinocyte proliferation, impaired differentiation, and chronic inflammation. Approximately 70% of cSCC cases are estimated to arise from pre-existing AK lesions, highlighting AK as a clinically relevant precursor stage [1,2]. Histologically, AK represents a continuous dysplastic spectrum ranging from basal-layer atypia to a full-thickness intraepidermal disorder consistent with SCC in situ, frequently associated with hyperkeratosis and dyskeratosis [1]. The epidermal disorganization, keratinocyte atypia, and hyperproliferative features observed in the present study are consistent with these early carcinogenic stages rather than fully developed invasive carcinoma. Given that cSCC arises through progressive precancerous stages, early intervention aimed at attenuating inflammation-and proliferation-driven events represents a rational preventive strategy, particularly in high-risk populations. Algae-derived bioactive compounds have attracted increasing attention in this context. Notably, extracts of *Limnospira platensis* (formerly *Spirulina platensis*), rich in C-PC, have demonstrated inhibitory effects in experimental models of chemically induced carcinogenesis [20]. Therefore, this study evaluated whether C-PC-loaded transfersomes could interfere with early tumour-promoting alterations in the skin.

Based on our previous ex vivo skin penetration studies, the free C-PC solution showed undetectable fluorescence within the skin layers, indicating limited skin penetration due to its high molecular weight and hydrophilic nature. In contrast, C-PC-loaded transfersomes significantly enhanced epidermal accumulation of C-PC [14]. Therefore, the present in vivo study was designed to evaluate the biological effects of the optimized transfersomal formulation, while groups treated with empty transfersomes were included to distinguish the effects of the carrier system from those of the encapsulated active compound. Evaluation of the study results demonstrated that transfersomes, when used with the carcinogen, markedly improved histopathological conditions in mouse skin by attenuating the development of hyperplasia and dysplasia, reducing epidermal thickening, and suppressing inflammatory and proliferative processes. Notably, even empty transfersomes (without C-CP) exerted a protective effect: severe hyperplasia was completely prevented, severe dysplasia was reduced by up to 40% compared with the carcinogen-only group, and the proportion of severe inflammation decreased from 70% to 30%. This suggests that transfersomes may modulate cutaneous responses not only through active compound delivery but also through carrier-dependent mechanisms, such as improved stratum corneum hydration, modulation of the lipid microenvironment, and barrier stabilization. Recent studies demonstrated that improved barrier integrity, together with modulation of inflammatory pathways, contributes to overall treatment outcomes [22]. In this context, the carrier-dependent effects observed in the present study may similarly support the therapeutic response.

Glycerol, a component of the transfersomal formulation, may contribute to the observed biological effects not only through its well-established role as a humectant but also

https://doi.org/10.3390/pharmaceutics18050600

via anti-inflammatory mechanisms. In an imiquimod-induced murine model of psoriasiform dermatitis, topical glycerol significantly reduced erythema, inflammation, and epidermal thickness [23]. Moreover, glycerol may indirectly support skin homeostasis by modulating the cutaneous microbiome, as commensal bacteria can ferment glycerol into bioactive metabolites, such as lactic acid, that inhibit pathogenic species, including *Staphylococcus aureus*, and upregulate genes associated with barrier function [24]. Glycerol plays a central role in maintaining epidermal hydration and barrier integrity, with high concentrations present in the stratum corneum. Glycerol generated through lipolysis and transported via AQP3 in the basal and spinous layers is essential for maintaining these elevated levels, whereas altered AQP3 expression has been linked to psoriasis, nonmelanoma skin cancer, and atopic eczema [25]. Thus, exogenous glycerol delivered via transfersomes may support barrier stabilization and, by indirect mechanisms, attenuate inflammation-driven epidermal hyperproliferation observed in the DMBA/TPA model.

When discussing the effects of C-PC, it is essential to consider that in Groups I and II, where T-PC was applied to intact skin without carcinogen exposure, the formulation was well tolerated and did not induce clinically relevant irritation, even at the higher C-PC concentration. Histopathological analysis revealed preserved epidermal architecture with physiological thickness, short, uniform rete ridges, and normally arranged keratinocytes. No epidermal hyperplasia, dysplasia, spongiosis, oedema, hyperaemia, or inflammatory infiltrates were observed. These findings indicate that topical T-PC does not induce structural or proliferative alterations in healthy skin and may be considered safe under non-carcinogenic conditions.

Previous studies demonstrate that C-PC suppresses TPA-induced skin carcinogenesis pathways in a dose-dependent manner by reducing ODC, COX-2, and IL-6 expression and inhibiting STAT3 phosphorylation, while simultaneously inducing TG-2 expression, which is associated with differentiation and apoptosis [21]. In vivo studies further showed that C-PC significantly inhibits DMBA-induced skin tumour development by decreasing tumour incidence and size, delaying tumour onset, and modulating key regulators of the cell cycle and apoptosis, including mutant p53, Cdc25A, Bcl-2, and p27 [13]. Beyond its anti-proliferative effects, C-PC exhibits pronounced antioxidant and anti-inflammatory properties, including inhibition of NF-κB activation, suppression of NADPH oxidase, and activation of the Nrf2/HO-1 pathway [26,27]. While systemic anti-inflammatory effects are largely attributed to hepatic metabolites such as phycocyanorubin, topical delivery models indicate that C-PC also exerts local antioxidant and anti-inflammatory actions. Indeed, recent evidence demonstrates that topically administered C-PC directly suppresses NF-κB signalling, reduces pro-inflammatory cytokine expression, attenuates oxidative stress, and promotes M2 macrophage polarization within the skin microenvironment [9,27]. Modulation of the tumour microenvironment represents a critical component of cutaneous squamous cell carcinoma (CSCC) progression [28]. Chronic inflammation, COX-2 overexpression, stromal activation, and immune cell infiltration contribute to tumour promotion and angiogenesis [29].

In the present study, C-PC-loaded transfersomes—particularly at 1 mg/mL—markedly reduced skin inflammation and structural epidermal alterations, including epidermal thickness and rete ridge depth. The more pronounced effect observed at the lower concentration may indicate that optimal biological performance depends on preserving vesicle elasticity rather than maximal drug loading. Higher C-PC content may alter membrane packing and reduce transfersome flexibility, thereby limiting penetration efficiency. Both C-PC concentrations significantly decreased mast cell density. Previous studies have shown that mast cells are key regulators of the tumour microenvironment. Upon activation, they release a wide range of pro-inflammatory and pro-angiogenic mediators, including

https://doi.org/10.3390/pharmaceutics18050600

vascular endothelial growth factor (VEGF), fibroblast growth factor-2 (FGF-2), tumour necrosis factor α (TNF-α), transforming growth factor-β, interleukins (IL1, IL3, IL4, IL5, IL6 IL8, IL10), and matrix metalloproteinases, which contribute to angiogenesis, extracellular matrix remodelling, and tumour progression [30–32]. Moreover, mast cell density has been shown to increase during disease progression from dysplasia to SCC [32]. These findings are in line with previous reports from DMBA/croton oil-induced mouse models of skin tumorigenesis, where mast cell density was significantly increased in carcinogen-treated animals, whereas treatment with C-type natriuretic peptide, alone or in combination with cisplatin, reduced mast cell infiltration [33]. Therefore, the observed reduction in mast cell density in C-PC-loaded transfersome-treated groups may contribute to the suppression of inflammation-driven epidermal remodelling. However, this interpretation remains indirect, as angiogenic markers and specific inflammatory mediators were not directly assessed in the present study. Furthermore, both C-PC concentrations significantly reduced mitotic activity, while the higher concentration (10 mg/mL) additionally decreased basal and suprabasal Ki-67 proliferation indexes. Taken together, the observed effects likely result from the combined effects of enhanced dermal delivery and carrier-mediated modulation of the skin microenvironment. Collectively, these findings support the role of C-PC-loaded transfersomes in attenuating inflammation-driven epidermal remodelling and suppressing early tumour-promoting events.

Despite the promising findings, several limitations of the present study should be acknowledged. First, only male animals were included in the experimental design. Since sex-related differences in skin physiology, hormonal regulation, and inflammatory responses may influence carcinogenesis and treatment outcomes, future studies including both sexes would further strengthen the generalizability of these findings. Furthermore, the present study focused exclusively on the protective effects of C-PC-loaded transfersomes during early stage of cSCC development. In later stages of tumour progression, the tumour microenvironment becomes increasingly complex, with enhanced angiogenesis, immune evasion, and invasive behaviour [2]. Given that C-PC has been reported to promote pro-apoptotic signalling while suppressing anti-apoptotic pathways, it may also possess therapeutic potential in more advanced stages of cSCC development [34]. Therefore, additional investigations evaluating the effects of C-PC-loaded transfersomes during later stages of carcinogenesis, including advanced dysplastic lesions and invasive squamous cell carcinoma, are warranted. In addition, the formulation was not directly compared with an established standard topical therapeutic agent, which should be addressed in future studies to further evaluate its relative efficacy and clinical potential.

5. Conclusions

The present study demonstrates that topical C-PC-loaded transfersomes attenuate early carcinogenesis-associated epidermal and dermal alterations in the DMBA/TPA mouse model. C-PC delivery significantly reduced inflammation severity, mast cell accumulation, mitotic activity, and basal and suprabasal Ki-67 expression, indicating suppression of pathological proliferation and tumour-promoting epidermal remodelling. These findings further suggest that transfersomal systems may modulate early tumour-promoting events not only by enhancing the delivery of C-PC but also, potentially, through carrier-related physicochemical interactions with the cutaneous barrier.

Further studies investigating molecular signalling pathways and long-term tumour incidence are warranted to validate the potential clinical applicability of C-PC-loaded transfersomes.

Author Contributions: Conceptualization, D.G., N.J. and N.S.; methodology, D.G., N.S., N.J., V.Z., J.K. and I.B.; validation, D.G., N.S., N.J. and I.B.; formal analysis, D.G., investigation, D.G., N.J.,

I.B.; resources, J.K., V.Z., N.J. and I.B.; data curation, D.G.; writing—original draft preparation, D.G.; writing—review and editing, N.J., J.K., N.S., I.B., V.Z. and J.B.; visualization, D.G. and N.J.; supervision, N.S.; project administration, N.S. All authors have read and agreed to the published version of the manuscript.

Funding: This research received no external funding.

Institutional Review Board Statement: The study was approved by the State Food and Veterinary Service of the Republic of Lithuania (approval No. G2-236, 22 February 2023).

Informed Consent Statement: Not applicable.

Data Availability Statement: The data supporting the findings of this study are available from the corresponding author (D.G.) upon reasonable request.

Conflicts of Interest: The authors declare no conflicts of interest.

References

1. Li, Z.; Lu, F.; Zhou, F.; Song, D.; Chang, L.; Liu, W.; Yan, G.; Zhang, G. From actinic keratosis to cutaneous squamous cell carcinoma: The key pathogenesis and treatments. *Front. Immunol.* **2025**, *16*, 1518633. [CrossRef]
2. Fania, L.; Didona, D.; Di Pietro, F.R.; Verkhovskaia, S.; Morese, R.; Paolino, G.; Donati, M.; Ricci, F.; Coco, V.; Candi, E.; et al. Cutaneous squamous cell carcinoma: From pathophysiology to novel therapeutic approaches. *Biomedicines* **2021**, *9*, 171. [CrossRef]
3. Liu, H.M.; Cheng, M.Y.; Xun, M.H.; Zhao, Z.W.; Zhang, Y.; Tang, W.; Cheng, J.; Ni, J.; Wang, W. Possible Mechanisms of Oxidative Stress-Induced Skin Cellular Senescence, Inflammation, and Cancer and the Therapeutic Potential of Plant Polyphenols. *Int. J. Mol. Sci.* **2023**, *24*, 3755. [CrossRef]
4. Bastos, M.; Saraiva, L.; Marques, A.C.; Amaral, M.H. Skin cancer chemoprevention: An overview. *Drug Discov. Today* **2025**, *30*, 104493. [CrossRef]
5. Ramchatesingh, B.; Martínez Villarreal, A.; Arcuri, D.; Lagacé, F.; Setah, S.A.; Touma, F.; Al-Badarin, F.; Litvinov, I.V. The Use of Retinoids for the Prevention and Treatment of Skin Cancers: An Updated Review. *Int. J. Mol. Sci.* **2022**, *23*, 12622. [CrossRef]
6. Aoki, J.; Sasaki, D.; Asayama, M. Development of a method for phycocyanin recovery from filamentous cyanobacteria and evaluation of its stability and antioxidant capacity. *BMC Biotechnol.* **2021**, *21*, 40. [CrossRef] [PubMed]
7. Jiang, L.; Wang, Y.; Liu, G.; Liu, H.; Zhu, F.; Ji, H.; Li, B. C-Phycocyanin exerts anticancer effects via the MAPK signaling pathway in MDA-MB-231 cells. *Cancer Cell Int.* **2018**, *18*, 12.
8. Adjali, A.; Clarot, I.; Chen, Z.; Marchioni, E.; Boudier, A. Physicochemical degradation of phycocyanin and means to improve its stability: A short review. *J. Pharm. Anal.* **2022**, *12*, 406–414. [PubMed]
9. Dong, J.; Lang, Y.; He, J.; Cui, J.; Liu, X.; Yuan, H.; Li, L.; Zhou, M.; Wang, S. Phycocyanin-based multifunctional microspheres for treatment of infected radiation-induced skin injury. *Biomaterials* **2025**, *317*, 123061. [PubMed]
10. Jang, Y.A.; Kim, B.A. Protective effect of *spirulina*-derived C-phycocyanin against ultraviolet B-induced damage in HaCaT cells. *Medicina* **2021**, *57*, 273. [CrossRef]
11. Salgado, M.T.S.F.; Silva, E.F.E.; Matsumoto, A.M.; Mattozo, F.H.; de Amarante, M.C.A.; Kalil, S.J.; Votto, A.P.S. C-Phycocyanin decreases proliferation and migration of melanoma cells: In silico and in vitro evidences. *Bioorg. Chem.* **2022**, *122*, 105757. [CrossRef]
12. Dibaei, F.; Fazilati, M.; Moenzadeh, F.; Kefayat, A.H.; Jazayeri, N.; Talebi, A. Anti-angiogenesis effects of C-phycocyanin of *Spirulina platensis* on B16-F10 melanoma tumors in C57BL/6 mouse. *Pathobiol. Res.* **2018**, *21*, 141–146.
13. Gupta, N.K.; Gupta, K.P. Development of mouse skin tumors by 7,12-dimethylbenz(a)anthracene and its prevention by C-phycocyanin involve regulators of cell cycle and apoptosis. *Integr. Pharmacol. Toxicol. Genotoxicol.* **2015**, *1*, 61–67.
14. Galinytė, D.; Aroffu, M.; Manconi, M.; Žilius, M.; Rysevaitė-Kyguolienė, K.; Karosienė, J.; Koreivienė, J.; Briedis, V.; Pauža, D.H.; Savickas, A.; et al. Cyano-phycocyanin loaded enriched transfersomes for enhanced topical skin delivery and antioxidant protection. *Int. J. Pharm.* **2025**, *683*, 126079. [CrossRef] [PubMed]
15. Surien, O.; Masre, S.F.; Basri, D.F.; Ghazali, A.R. Chemopreventive Effects of Oral Pterostilbene in Multistage Carcinogenesis of Skin Squamous Cell Carcinoma Mouse Model Induced by DMBA/TPA. *Biomedicines* **2022**, *10*, 2743. [CrossRef]
16. Schwarz, M.; Münzel, P.A.; Braeuning, A. Non-melanoma skin cancer in mouse and man. *Arch. Toxicol.* **2013**, *87*, 783–798. [CrossRef]
17. Li, H.; Brakebusch, C. Analyzing skin tumor development in mice by the DMBA/TPA model. *Methods Cell Biol.* **2021**, *163*, 113–121.
18. Zhou, Y.; Bai, R.; Huang, Y.; Li, W.; Chen, J.; Cheng, Z.; Wu, X.; Diao, Y. The anti-photoaging effect of C-phycocyanin on ultraviolet B-irradiated BALB/c-nu mouse skin. *Front. Bioeng. Biotechnol.* **2023**, *11*, 1229387. [CrossRef] [PubMed]

https://doi.org/10.3390/pharmaceutics18050600

19. Qu, J.; Geng, X.; Qin, S.; Li, J.; Li, W. The utilization of TGase-crosslinked phycocyanin-collagen hydrogels for the purpose of facilitating skin wound healing. *Int. J. Biol. Macromol.* **2025**, *320*, 145932. [CrossRef]
20. Grawish, M.E.; Zaher, A.R.; Gaafar, A.I.; Nasif, W.A. Long-term effect of *Spirulina platensis* extract on DMBA-induced hamster buccal pouch carcinogenesis. *Med. Oncol.* **2010**, *27*, 20–28. [CrossRef]
21. Gupta, N.K.; Gupta, K.P. Effects of C-phycocyanin on representative genes of tumor development in mouse skin exposed to 12-O-tetradecanoyl-phorbol-13-acetate. *Environ. Toxicol. Pharmacol.* **2012**, *34*, 941–948. [CrossRef]
22. Yang, J.; Zhu, J.; Lu, S.; Qin, H.; Zhou, W. Transdermal psoriasis treatment inspired by tumor microenvironment-mediated immunomodulation and advanced by exosomal engineering. *J. Control Release* **2025**, *382*, 113664. [CrossRef]
23. Choudhary, V.; Kaddour-Djebbar, I.; Custer, V.E.; Uaratanawong, R.; Chen, X.; Cohen, E.; Yang, R.; Ajebo, E.; Hossack, S.; Bollag, W.B. Glycerol improves skin lesion development in the imiquimod mouse model of psoriasis. *Int. J. Mol. Sci.* **2021**, *22*, 8749. [CrossRef]
24. Salgaonkar, N.; Kadamkode, V.; Kumaran, S.; Mallemala, P.; Christy, E.; Appavoo, S.; Majumdar, A.; Mitra, R.; Dasgupta, A. Glycerol fermentation by skin bacteria generates lactic acid and upregulates genes associated with skin barrier function. *Exp. Dermatol.* **2022**, *31*, 1364–1372. [CrossRef]
25. Madiraju, S.R.; Possik, E.; Al-Mulla, F.; Nolan, C.J.; Prentki, M. Glycerol and glycerol-3-phosphate: Multifaceted metabolites in metabolism, cancer, and other diseases. *Endocr. Rev.* **2026**, *47*, 93–120. [CrossRef] [PubMed]
26. Ramos, S.D.P.; Bürck, M.; Costa, S.F.F.; Assis, M.; Braga, A.R.C. *Spirulina* as a key ingredient in the evolution of eco-friendly cosmetics. *BioTech* **2025**, *14*, 41. [CrossRef]
27. Liu, R.; Qin, S.; Li, W. Phycocyanin: Anti-inflammatory effect and mechanism. *Biomed. Pharmacother.* **2022**, *153*, 113362. [CrossRef] [PubMed]
28. Corchado-Cobos, R.; Garcia-Sancha, N.; González-Sarmiento, R.; Pérez-Losada, J.; Canueto, J. Cutaneous squamous cell carcinoma: From biology to therapy. *Int. J. Mol. Sci.* **2020**, *21*, 2956. [CrossRef]
29. Combalia, A.; Carrera, C. Squamous cell carcinoma: An update on diagnosis and treatment. *Dermatol. Pract. Concept.* **2020**, *10*, e2020066. [PubMed]
30. Sakalauskaitė, S.; Riškevičienė, V.; Šengaut, J.; Juodžiukynienė, N. Association of mast cell density, microvascular density and endothelial area with clinicopathological parameters and prognosis in canine mammary gland carcinomas. *Acta Vet. Scand.* **2022**, *64*, 14. [CrossRef]
31. Alda, S.; Ceausu, R.A.; Gaje, P.N.; Raica, M.; Cosoroaba, R.M. Mast Cell: A Mysterious Character in Skin Cancer. *Vivo* **2024**, *38*, 58–68. [CrossRef]
32. Ribatti, D.; Tamma, R.; Annese, T.; Crivellato, E. The role of mast cells in human skin cancers. *Clin. Exp. Med.* **2021**, *21*, 355–360. [CrossRef]
33. Dhanusu Sivakalai, S.; Sowndhar Rajan, B.; Vellaichamy, E. C-type natriuretic peptide (CNP) inhibits 7,12-Dimethylbenz[a]anthracene (DMBA)/Croton oil-induced skin tumor growth by modulating inflammation in Swiss albino mice. *J. Biochem. Mol. Toxicol.* **2023**, *37*, e23423. [CrossRef] [PubMed]
34. Dranseikienė, D.; Balčiūnaitė-Murzienė, G.; Karosienė, J.; Morudov, D.; Juodžiukynienė, N.; Hudz, N.; Gerbutavičienė, R.J.; Savickienė, N. Cyano-Phycocyanin: Mechanisms of Action on Human Skin and Future Perspectives in Medicine. *Plants* **2022**, *11*, 1249. [CrossRef] [PubMed]

https://doi.org/10.3390/pharmaceutics18050600